EFFECT OF AMPHIPHILIC DIBLOCK COPOLYMERS ON P-GLYCOPROTEIN SUBSTRATE PERMEABILITY IN CACO-2 CELLS

By

Jason Zastre

B.Sc. (Pharm), University of Manitoba, 1994
M.Sc. (Pharm), University of Manitoba, 1998

A THESIS SUBMITTED IN PARTIAL FULFILMENT OF THE REQUIREMENTS FOR THE DEGREE OF

DOCTOR OF PHILOSOPHY

in

THE FACULTY OF GRADUATE STUDIES

Pharmaceutical Sciences

We accept this thesis as conforming
to the required standard

THE UNIVERSITY OF BRITISH COLUMBIA

August 2004

ABSTRACT

A series of short block length methoxypoly(ethylene glycol)-*block*-poly(caprolactone) (MePEG-*b*-PCL) diblock copolymers were synthesized, characterized and evaluated for enhancing the permeability of P-gp substrates in an intestinal epithelial cell line, caco-2. Altering MePEG:caprolactone feed weight ratios produced diblocks composed of varying PCL lengths, with MePEG of MW 550, 750 or 2000. The diblocks formed micelles above the critical micelle concentration (CMC) values and hydrophobicity, solubility, CMC, and micelle size, were dependent on the block lengths of the diblock copolymers.

Caco-2 cellular accumulation studies with two homologous P-glycoprotein substrates, rhodamine 123 (R-123) and rhodamine 6G (R-6G), showed that accumulation of the relatively hydrophilic P-gp substrate, R-123, was enhanced at high concentrations of MePEG-*b*-PCL diblock copolymers above their CMC with little activity below the CMC. Whereas, cellular accumulation with the relatively hydrophobic substrate, R-6G, was maximally enhanced over a wide range of diblock concentrations, lower or close to the CMC and which also corresponded to an 8-25 fold reduction in diblock concentration compared to R-123. Diblocks with intermediate to high HLB values were more effective at enhancing R-123 accumulation, while all diblocks were shown to enhance R-6G accumulation. Similar accumulation enhancement profiles with MePEG-*b*-PCL were observed with two additional P-gp substrates, doxorubicin and paclitaxel, which have large differences in their relative hydrophobicities. At high diblock copolymer concentrations, R-123 and R-6G accumulation decreased and was likely due to substantial partitioning of R-123 and R-6G into micelles, reducing the free fraction available for cellular uptake. A substantially different rate of

substrate accumulation with MePEG-*b*-PCL was observed depending upon the hydrophobicity of the P-gp substrate. MePEG-*b*-PCL diblocks increased the rate and extent of R-123 accumulation, but not the rate of accumulation of R-6G.

The difference in MePEG-*b*-PCL diblock composition and concentrations required to enhance the accumulation of P-gp substrates with different relative hydrophobicities suggests that additional pathways may be involved besides a reduction of P-gp mediated efflux. To determine the cellular uptake pathways contributing to enhanced caco-2 cellular accumulation of P-gp substrates by MePEG-*b*-PCL block copolymers, the effects of endocytosis inhibitors, ATP depletion conditions, and directional transepithelial flux experiments were performed. For the hydrophilic R-123, $MePEG_{17}$-*b*-PCL_5 enhanced the cellular accumulation of R-123 at high concentrations of diblock above the CMC, which did not appear to involve endocytosis of micellized R-123. This suggests that $MePEG_{17}$-*b*-PCL_5 micelles may provide a 'depot' for free unimer to interact with the cell membrane and contribute either to enhanced passive transmembrane diffusion of R-123 through membrane permeability changes, or inhibition of P-gp mediated efflux, or both. In the secretory direction, diblock was capable of reducing the efflux of both R-123 and R-6G. However, $MePEG_{17}$-*b*-PCL_5 greatly enhanced the cellular accumulation of R-123 in the transepithelial directional flux studies in the absence of an increase in the absorptive flux. It is proposed that the basolateral membrane permeability of R-123 may limit the absorptive flux. In contrast, $MePEG_{17}$-*b*-PCL_5 was able to enhance the absorptive flux of the hydrophobic R-6G. ATP depletion studies demonstrated that $MePEG_{17}$-*b*-PCL_5 increased the accumulation of R-123 possibly through a membrane permeabilization effect. Erythrocyte hemolysis studies also provided evidence that

$MePEG_{17}$-*b*-PCL_5 caused membrane perturbation effects, which could result in enhanced transmembrane diffusion of R-123.

TABLE OF CONTENTS

LIST OF FIGURES

LIST OF TABLES

LIST OF SCHEMES

LIST OF ABBREVIATIONS

λ_{EM}	Emission wavelength
λ_{EX}	Excitation wavelength
ABC	ATP-Binding Cassette
AEF	Accumulation Enhancement Factor
AP	Apical
AM	Acetoxymethyl ester
ANOVA	Analysis of Variance
ATP	Adenosine triphosphate
BBB	Blood Brain Barrier
BL	Basolateral
BSEP	Bile Salt Export Protein
$CDCL_3$	Deuterated chloroform
cDNA	Complementary Deoxyribonucleic acid
CFTR	Cystic fibrosis transmembrane regulator
CL	6-caprolactone monomer
CMC	Critical micelle concentration
CNS	Central Nervous System
CNT	Concentrative nucleoside transporter
CSA	Cyclosporin A
CSF	Cerebrospinal fluid
CSM	Cysteine-scanning mutagenesis

DMEM	Dulbecco's modified eagle's media
DMPC	Dimyristoylphosphatidylcholine
DOX	Doxorubicin
DPH	1,6,-diphenyl-1,3,5-hexatriene
DPM	Disintegrations per minute
DPN	Degree of polymerization
DPPC	Dipalmitylphoshatidylcholine
FBS	Fetal bovine serum
ΔG	Gibbs free energy
GI	Gastrointestinal
GLUT	Glucose transporter
GPC	Gel permeation chromatography
HBSS	Hanks balanced salt solution
Hepes	*N*-(2-hydroxyethyl)piperazine-*N'*-2-ethanesulfonate
HLB	Hydrophilic-Lipophilic balance
HVC	Hydrophobic vacuum cleaner
JAM	Junction adhesion molecule
kDa	Kilodalton
Kpart	Partition coefficient
LDH	Lactate dehydrogenase
MCT	Monocarboxylate transporter
MDCK	Madin Darby canine kidney
MDR	Multidrug resistance

MePEG	Methoxypoly(ethylene glycol)
$MePEG_x$	Methoxypoly(ethylene glycol) with X number of ethylene glycol units
MePEG-*b*-PCL	Methoxypoly(ethylene glycol)-*block*-poly(caprolactone)
M/I	Monomer:Initiator ratio
$\overline{M}_n$	Number average molecular weight
MRP	Multidrug resistance-asscociated protein
$\overline{M}_w$	Weight average molecular weight
MW	Molecular weight
NBD	Nucleotide binding domain
NMR	Nuclear magnetic resonance spectroscopy
PBS	Phosphate buffered saline
PC	Phosphatidylcholine
PCL	Poly(caprolactone)
PCL_x	Poly(caprolactone) with X number of caprolactone repeat units
PCS	Photon correlation spectroscopy
PDI	Polydispersity index
PDLLA	Poly(D,L-lactide)
PE	Phosphatidylethanolamine
PEG	Poly(ethylene glycol)
PEO	Poly(ethylene oxide)
PEPT	Peptide transporter
P-gp	P-glycoprotein
PPO	Poly(propylene oxide)

PTX	Paclitaxel
R-123	Rhodamine 123
R-6G	Rhodamine 6G
RES	Reticuloendothelial system
R_f	Retention factor
RT-PCR	Reverse transcription polymerize chain reaction
SD	Standard deviation
SEM	Standard error of the mean
SGLT	Sodium dependent glucose transporter
$Sn(Oct)_2$	Stannous 2-ethylhexanoate
TM	Transmembrane
TMR	Tetramethylrosamine
TPGS	d-alpha-Tocopheryl Polyethylene Glycol-1000 Succinate
UWL	Unstirred water layer

ACKNOWLEDGEMENT

First and foremost, I am grateful to have had such an excellent supervisor, Dr. Helen Burt. Helen has provided me with a stimulating lab environment in which to grow and learn in and an unwavering commitment to the success of this project and my Ph.D studies. I feel extremely fortunate to have her as my mentor and friend. My sincere gratitude also goes to John Jackson, who always is a welcoming presence in the lab and whose valuable discussions were insightful and helpful during my studies.

My sincere thanks go out to my committee for their effort and thoughtful discussions and suggestions: Drs. Colin Fyfe, Stelvio Bandiera, Lawerence Mayer, and Thomas Chang. Special thanks goes to Dr Kristina Sachs-Barrable for valuable assistance with Western blotting, Jie Chen her expertise with RT-PCR, and Dr Wayne Vogl for help with confocal microscopy work. To all my past and present lab mates; Dr. Christine Allen, Kevin Letchford, Chris Springate, Ruiwen Shi, Linda Liang, Wes Wong, Tobi Higo, Karen Long, Jingfang Wang and past lab alumni, Drs. Richard Liggins and Chuck Winternitz, I thank you all for your friendship, support, and encouragement throughout this work. I also want to say thanks to Mike Borslein, Catherine Cheung, Famida Iqbal, and Mandeep Bajwa for working hard during your summertime and making a significant contribution to this work.

I want to dedicate this work to my two beautiful children, Halie and Taven, and my wife Bobbi-Lynn. You three have unselfishly sacrificed so much to allow me to pursue my dreams, my aspirations, and my passion. Through the good times and the bad, we achieved this together.

I am also extremely grateful for the contributions of Angiotech Pharmaceuticals Inc. and the Canadian Institutes of Health Research for financial support of this project. I am also

very appreciative to the Science Council of British Columbia for awarding me with the GREAT Scholarship.

CHAPTER 1

BACKGROUND

1.1. INTRODUCTION

Active drug efflux transporters belonging to the ATP binding cassette (ABC) family of proteins can have a major impact on the pharmacokinetics and pharmacological activity of many drugs (Ayrton and Morgan, 2001; Schinkel and Jonker, 2003). In particular, the action of an 170 kDa transmembrane efflux transporter, called P-glycoprotein (P-gp), can serve as an absorption barrier to limit the oral availability of susceptible drugs from the gastrointestinal tract, limit entry of drugs to target tissues such as the brain, and increase drug bilary and intestinal clearance (Hunter and Hirst, 1997; Sparreboom *et al.*, 1997). The overexpression of P-gp is also associated with the development of multidrug resistance (MDR) in tumor cells and presents a major problem in terms of reduced clinical responsiveness to chemotherapy of various human malignancies (Krishna and Mayer, 2000).

Inhibition of P-gp can be achieved using agents (frequently termed modulators or chemosensitizers) that can reduce P-gp drug efflux leading to an overall increase in drug permeability and improved cytotoxicity against tumors. Various pharmacological agents have been discovered to possess this chemosensitizing effect. They include nifedipine, verapamil, cyclosporin A, cyclosporin derivative SDZ PSC 833, forskolin derivatives, trifluoperazine, and progesterone (Ford and Hait, 1990; Hunter *et al.*, 1991b; Zacherl *et al.*, 1994; Van Asperen *et al.*, 1998). These agents primarily work by either competitively or non-competitively blocking the binding of a substrate to the P-gp drug-binding domain (Ayesh *et al.*, 1996). However, the majority of these compounds exhibit other pharmacological activities that can result in unwanted toxicities, particularly the first generation compounds

such as verapamil and cyclosporin A. The development of second and third generation compounds was based on improving potency and reducing toxicity (Krishna and Mayer, 2000). Another class of compounds demonstrating an ability to inhibit drug efflux transporters are nonionic surfactants such as polysorbate 80 and Cremophor EL® (Schinkel and Jonker, 2003). The majority of these compounds are pharmaceutically acceptable materials with no pharmacological activity and are primarily utilized in enteral and parenteral formulations as stabilizing and solubilizing excipients. Although the mechanism of P-gp inhibition by surfactants remains poorly understood, it has been suggested that surfactants may exert their effect by a non-specific mechanism involving structural perturbations in the lipid phase of the membrane leading to altered membrane fluidity and inducing protein conformational changes that can inhibit P-gp ATPase activity (Woodcock *et al.*, 1992; Drori *et al.*, 1995; Rege *et al.*, 2002; Kabanov *et al.*, 2002b).

Recently, amphiphilic triblock copolymers composed of poly(ethylene oxide)-*b*-poly(propylene oxide)-*b*-poly(ethylene oxide) also known as Pluronic® block copolymers, have been shown to enhance cellular accumulation, membrane permeability, and to modulate multidrug resistance of numerous P-gp substrates (Paradis *et al.*, 1994; Alakhov *et al.*, 1996; Miller *et al.*, 1997; Batrakova *et al.*, 1998a; Batrakova *et al.*, 1998b; Batrakova *et al.*, 1999; Batrakova *et al.*, 1999). Amphiphilic block copolymers have been increasingly utilized in drug delivery and typically have an A-B diblock or A-B-A / B-A-B triblock structure, where the A is the hydrophilic block such as polyethylene glycol and the B is the hydrophobic block such as poly(D,L-lactide). In an aqueous environment, amphiphilic block copolymers can form micelles with the hydrophobic block forming the core, surrounded by a shell of hydrophilic polymer. Polymeric micelles have been utilized for the solubilization and

delivery of drugs such as paclitaxel, indomethacin, amphotericin B, adriamycin, and dihydrotestosterone (Zhang *et al.*, 1996b; Yu *et al.*, 1998; Kim *et al.*, 1998; Yokoyama *et al.*, 1998a; Burt *et al.*, 1999; Allen *et al.*, 2000). When used for drug delivery, the core forming block is generally composed of biodegradable polymers such as poly(caprolactone), poly(β-benzyl L-asparate) and poly(D,L-lactide).

To our knowledge, no studies have been carried out to determine whether A-B type amphiphilic diblock copolymers possess an ability to reduce P-gp mediated efflux of drugs. Therefore, this work describes the synthesis and characterization of a novel series of low molecular weight amphiphilic diblock copolymers based on the hydrophilic methoxy(polyethylene glycol) (MePEG) and hydrophobic poly(caprolactone) (PCL), denoted as MePEG-*b*-PCL. The human colon adenocarcinoma cell line, caco-2, was utilized as an intestinal epithelial cell line model. Caco-2 cells undergo spontaneous enterocytic differentiation displaying well-organized cellular polarity, including microvilli and functional transporters including P-glycoprotein (Hidalgo and Jibin, 1996). This thesis investigates the effect of MePEG-*b*-PCL with varying block lengths on P-gp mediated efflux of substrates. P-gp substrates varying in relative hydrophobicity were evaluated and include the fluorescent rhodamine 123 (R-123) and rhodamine 6G (R-6G), and the chemotherapeutic drugs paclitaxel and doxorubicin.

1.2. DRUG PERMEATION

Systemic absorption of a drug from any absorption site, such as nasal, buccal, rectal, dermal, or intestinal, requires that a drug pass through one or more layers of cells in order to enter the systemic circulation. Drug entry or absorption into a cell requires drug transport through the cell membrane in a process termed *permeation*. Drug permeation involves

transport processes that contribute to the net influx of drug into the cell. However, several processes can counterbalance this influx and reduce the extent of drug permeating the membrane and ultimately traversing the cell.

1.2.1. Drug transport processes

Depending upon the intended site of action for a drug, a series of drug transport processes may be required to reach the target site. At an absorption site such as the intestinal epithelia, a drug must cross this cellular barrier to enter the general circulation. Once in the circulation, drug must cross the capillary endothelial barrier to reach the target tissue. In the tissue, drug can either interact with the surface of the cell to elicit the pharmacological activity or may be required to further permeate the cells in the tissue to access an intracellular target for activity. Drugs can permeate cell membranes either by passive diffusion, facilitated diffusion, or active transport processes. The passage of a drug molecule across epithelia or endothelia can be either by passing directly through cells termed *transcellular* flux, or passing between cells termed *paracellular* flux (Macheras et al., 1995). The pathway(s) used by a drug will be dependent upon the physicochemical properties of the drug and on the physiological properties of the cellular barrier.

At absorptive sites, the movement of drug is typically from the apical surface to the basolateral surface where the drug can then enter the general circulation or tissue compartment. However, movement is not restricted to one direction and can occur in the basolateral to apical direction. For transcellular flux, two routes of drug movement across the cell have been described (Camenisch *et al.*, 1996; Ho *et al.*, 2000). The cytoplasmic route involves drug partitioning and diffusion across the apical membrane into the cytoplasm of the cell, followed by diffusion across the basolateral membrane and then into the blood or

tissue compartment. Alternatively, a drug can enter the membrane and diffuse laterally within the membrane, around the cell and exit on the basolateral side. The latter is generally suggested to occur for very lipophilic drugs or drugs that resemble membrane components, such as aliphatic carboxylic acids (Cho *et al.*, 1990; Raub *et al.*, 1993; Sawada *et al.*, 1994).

Drugs which are either not recognized by carrier processes, or are hydrophilic and cannot enter the cell directly through the membrane, may be absorbed through paracellular flux. The presence of tight junctions and the lower absorptive surface area tends to limit the diffusion of drugs via this route. However, the absorption of large hydrophilic molecules may be enhanced through modulation of the tight junction integrity and increased paracellular flux (Daugherty and Mrsny, 1999a; Ward *et al.*, 2000).

1.2.1.1. Passive diffusion

The lipid nature of the cell membrane allows it to function as a selective permeability barrier to limit entry of some substances and allow others to pass through. Small unionized drug molecules that are relatively lipophilic can readily enter the lipid membrane bilayer and pass through the membrane by diffusion. Passive diffusion does not require the expenditure of energy, but rather is driven by the random motion of molecules down a concentration gradient. Movement of drug across the membrane is characterized by a solubility/diffusion model involving three steps (Stein, 1986): 1) Partitioning of the drug into the interfacial region of the bilayer; 2) Diffusion of the drug through the lipid bilayer interior; 3) Desorption of the drug from the internal membrane leaflet into the aqueous intracellular milieu. Fick's first law mathematically describes the diffusion of molecules from a vehicle across a barrier or membrane (Equation 1.1).

$$\frac{dQ}{dt} = \frac{DAK(Co - Ci)}{h} \qquad \text{Equation 1.1}$$

Where dQ/dt is the rate of diffusion across the membrane with a thickness (h), A is the surface area of the membrane available for diffusion and K is the partition coefficient of drug between the membrane and vehicle. The concentration gradient is the difference between the concentration of drug adjacent to the external membrane leaflet (Co) and internal leaflet (Ci), and D is the diffusion coefficient and reflects the resistance to the passage of diffusing molecules.

The solubility-diffusion model of permeation describes the permeability (P) of a molecule, that is, the velocity at which a molecule moves across a given area of the membrane, as being directly proportional to the ability of a molecule to dissolve in the membrane (measured by the partition coefficient, K) and to the ease with which it can diffuse across the membrane (measured by the diffusion coefficient, D) (Equation 1.2) (Lieb and Stein, 1986; Stein, 1986).

$$P = \frac{KD}{h} \qquad \text{Equation 1.2}$$

This model suggests that increasing the solubility of a drug in the lipid phase of the membrane will have a proportional increase in the permeability of the drug. Factors affecting the solubility of a drug in the lipid bilayer, such as, dipole moment, polarity, pKa and the pH of the environment will thus play an important role in determining the fraction of drug ionized and has led to the pH partition hypothesis, which states that only the unionized relatively hydrophobic species of a drug can partition and diffuse across membranes (Macheras et al., 1995).

The transverse or transmembrane movement of a drug will require the formation of suitable size 'holes' or free volume within the hydrocarbon chain interior of the bilayer to accommodate the molecular volume of the drug (Lieb and Stein, 1986). However, the

diffusing medium of the membrane contains lipids anchored together at their polar head region, which restricts the lipids ability to 'flow' around the diffusing solute (Lieb and Stein, 1986). The formation of 'holes' or free volume within the membrane will be the result of the fluid nature of the lipid bilayer allowing rotational and lateral movement of lipids (Stein, 1986). Therefore, the nature, composition and physical state of the lipid bilayer will greatly affect the diffusion of molecules across the membrane. Factors that increase or decrease the lipid ordering within the bilayer such as temperature (Xiang and Anderson, 1995; Xiang and Anderson, 1997; Xiang and Anderson, 1998) and lipid/cholesterol composition (Lande *et al.*, 1995; Xiang and Anderson, 1995; Xiang and Anderson, 1997) can change the extent of free volume within the bilayer and alter the permeability of a solute.

The presence of drug molecules within the membrane may also be a factor in disrupting the ordering of lipid bilayers. Drugs such as anesthetics are hydrophobic molecules which rapidly partition into lipid membranes and exert a fluidizing effect, which is attributed to their mechanism of action (Goldstein, 1984). Paclitaxel is hydrophobic and has also demonstrated a marked fluidization effect after partitioning into model phospholipid membranes (Balasubramanian and Straubinger, 1994). However, some compounds enter the membrane, increasing the lipid order within the bilayer and cause a 'rigidification' of the membrane. Doxorubicin, mitoxantrone, and aclarubicin have been shown to cause a decrease in the membrane fluidity of B14 and NIH 3T3 mouse fibroblast cells (Jedrzejczak *et al.*, 1999). The effect of drugs on membranes can also be concentration dependent, as observed for tamoxifen, which decreases membrane fluidity at low concentrations and increases fluidity at high concentrations (Severcan *et al.*, 2000). Surfactant molecules can act as permeation enhancers and following partitioning into model lipid membranes can disrupt

membrane order leading to increases in membrane fluidity and increased permeability of a drug through the membrane (Imanidis *et al.*, 1995; Nonaka *et al.*, 2002).

1.2.1.2. Facilitated diffusion

Many physiologically important substances such as glucose, nucleosides, and ions are too hydrophilic to passively diffuse across the cell membrane. However, specific carriers can transport these compounds across the membrane down their concentration gradient. This process is called facilitated diffusion and no net energy is consumed since the driving force is the solute concentration gradient (Macheras et al., 1995; Washington et al., 2001). Several facilitative transporters are known to be involved in drug permeation and they provide a means of enhancing drug permeation. One example is the glucose facilitative transporter GLUT (glucose transporter) which regulates the movement of glucose and other monosaccharides such as fructose and galactose between the extracellular and intracellular compartments (Olson and Pessin, 1996; Steffansen *et al.*, 2004). There are 7 known isoforms of GLUT, each with similar substrate specificity and overlapping tissue expression (Olson and Pessin, 1996; Oh and Amidon, 1999; Steffansen *et al.*, 2004). GLUT1 is primarily found in erythrocytes and capillary endothelia, GLUT2 is found in the liver and small intestine and GLUT5 is a fructose transporter found in the small intestine (Olson and Pessin, 1996; Oh and Amidon, 1999; Oh *et al.*, 1999; Steffansen *et al.*, 2004). Glucose derivatives of chlorambucil and tocopheryl both demonstrated improved erythrocyte permeation via the GLUT1 transporter (Bonina *et al.*, 1996; Halmos *et al.*, 1996).

Another facilitative transporter system shown to be important in drug permeation is the equilibrative nucleoside transporters or ENT. Currently three isoforms of ENT in humans have been identified and transport the hydrophilic purine and pyrimidine nucleosides

into cells (Hyde *et al.*, 2001). Both ENT1 and ENT2 are found extensively in the body, including the intestine, liver, capillary endothelia, and brain (Hyde *et al.*, 2001). The antiviral drugs ddC (2'3'-dideoxycytidine), ddI (2'3'-dideoxyinosine), and AZT (3'-azido-3'-deoxythymidine) and the anti-cancer drugs cytarabine and gemcitabine have been shown to be transported by ENT1 and ENT2 (Hyde *et al.*, 2001; Yao *et al.*, 2001; Steffansen *et al.*, 2004).

1.2.1.3. Active drug transport

Similar to facilitative transporters, active transport involves a carrier protein that selectively transports molecules or ions into the cell. However, active transport involves the movement of molecules or ions against their concentration gradient and thus requires the expenditure of energy (Macheras et al., 1995; Oh and Amidon, 1999; Washington et al., 2001). The energy utilized can be from the direct hydrolysis of ATP or indirectly supplied from the coupling of the transport of another molecule/ion down its concentration gradient (Washington et al., 2001). Active transporters utilizing ATP as an energy source typically involve ion transport such as the Na^+/K^+ ATPase that transports both Na^+ and K^+ against their concentration gradients and the H^+/K^+ ATPase that secretes H^+ into the stomach and moves K^+ into the cell (Oh and Amidon, 1999). Co-transport of molecules/ions involves the movement of one molecule down its concentration gradient and this supplies the energy needed to move another molecule/ion against its concentration gradient. The transport of both molecules/ions can be in the same direction, called *symport* or in the opposite directions termed *antiport* (Washington et al., 2001).

The majority of active transporters implicated in drug transport involve the uptake of specific nutrients, for example the sodium dependent glucose transporter (SGLT), sodium

dependent - concentrative nucleoside transporter (CNT), monocarboxylate transporters (MCT), and the peptide transporters (PEPT) (Steffansen *et al.*, 2004). Two isoforms of the peptide transporter (also called the oligopeptide transporter) have been isolated, termed PEPT1 and PEPT2 (Brodin *et al.*, 2002; Steffansen *et al.*, 2004). Although, both transporters are found in the kidney, PEPT1 is the only peptide transporter found in the apical membrane of the enterocytes and is primarily implicated in the absorption of di- and tripeptides (Brodin *et al.*, 2002). PEPT1 is a H^+ dependent symporter where the intracellular transport of oligopeptides is coupled with the uptake of H^+ from the lumen of the intestine into the cell. The proton gradient across the cell is maintained by the Na^+/H^+ exchanger which moves H^+ out of the cell and Na^+ inside, while the Na^+/K^+ ATPase maintains the Na^+ gradient (Adibi, 1997; Brodin *et al.*, 2002). Many peptidomimetic drugs such as the angiotensinogen converting enzyme (ACE) inhibitors enalapril, captopril, and fosinopril and amoxicillin and cephalexin have all been shown to be substrates for PEPT1 transporter in the intestinal epithelia which enhances their permeation (Dantzig, 1997; Yang *et al.*, 1999; Steffansen *et al.*, 2004).

1.2.2. Barriers to drug permeation

1.2.2.1. Biological membranes

The primary barrier limiting drug permeation is the cell membrane. The cell membrane acts as a semi-permeable barrier limiting the entry of substances into the cell while allowing others to freely move across. The fluid mosaic model of the membrane proposed by Singer and Nicolson describes the cell membrane as consisting of proteins interdispersed in a fluid lipid bilayer (Figure 1.1) (Singer and Nicolson, 1972). The hydrophobic nature of the membrane limits the entry of charged or hydrophilic substances

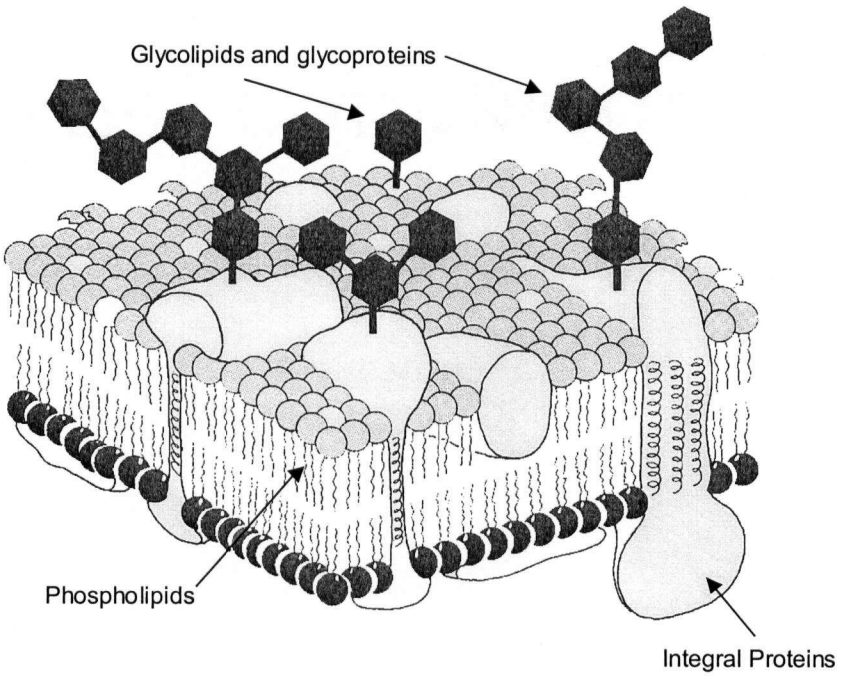

Phospholipid

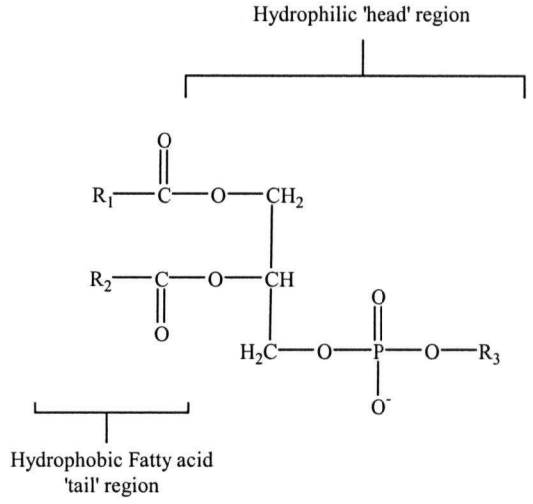

Cholesterol

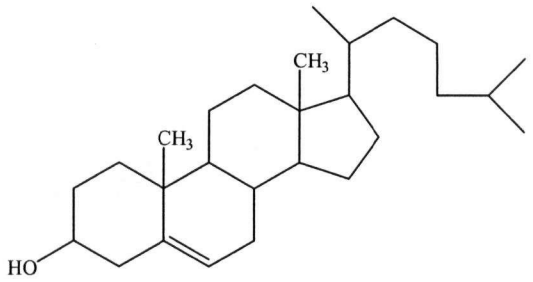

R_1 , R_2 = Saturated or Unsaturated C12 – C24 fatty acids
R_3 = Substituent group
Eg: Choline $-CH_2CH_2N^+(CH_3)_3$
Ethanolamine $-CH_2CH_2NH_3^+$

Figure 1.1. Fluid mosaic model of the plasma membrane adapted from (Cullis and Hope, 1991) and general structures of a phospholipid and cholesterol

while proteins within the membrane function as pores or channels that regulate the movement of small molecules such as water, ions, urea, and glucose through the membrane (Shargel and Yu, 1993).

The cell membrane is primarily composed of various phospholipids, proteins, and cholesterol. Phospholipids possess two discrete regions, a hydrophobic 'tail' section containing two long chain fatty acids (12-24 carbons in length), and a hydrophilic 'head' region consisting of various substituent groups (Figure 1.1). The relative balance of hydrophobic groups and hydrophilic groups in the phospholipid confers amphiphilicity to the molecule. This allows for the arrangement of the phospholipids into bilayer structures where the hydrophobic tails align into the interior and the hydrophilic head groups interact with the aqueous milieu (Figure 1.1). Within the fluid mosaic model, bilayer lipids are capable of rotational and lateral movement throughout the membrane (Andreoli et al., 1989). Dispersed throughout the membrane is cholesterol, which is anchored within the membrane by its single hydroxy group interacting with the hydrophilic head region of the phospholipids and the planar steroid ring structure associating with the lipid acyl chains (Andreoli et al., 1989). Within the membrane, cholesterol acts as a spacer between the phospholipid acyl chains, restricting acyl chain mobility within the bilayer, resulting in an increase in the membrane ordering and ultimately reducing the permeability of the membrane to hydrophilic substances (Andreoli et al., 1989; Cullis and Hope, 1991).

In general, eukaryotic membranes are composed of several phospholipids such as phosphatidylcholine, phosphatidylethanolamine, phosphatidylserine, phosphatidylinositol, as well as sphingolipids (Cullis and Hope, 1991). Phospholipids are also asymmetrically distributed within the two leaflets of the bilayer. Phosphatidylserine,

phosphatidylethanolamine, and phosphatidylinositol are primarily located in the inner leaflet of the membrane while phosphatidylcholine and sphingolipids are found in the outer leaflet (Cullis and Hope, 1991; Seydel, 2002). The importance of this lipid asymmetry is to maintain a proper lipid packing configuration which ensures a favorable bilayer curvature and protein conformations (Seydel, 2002). At physiological pH, the higher abundance of negatively charged phospholipids, such as phosphatidylserine, in the inner leaflet of the membrane results in a transmembrane electrical potential across the cell membrane (Cullis and Hope, 1991; Seydel, 2002). The charged surface of the cell membrane may further reduce the permeability of similarly charged molecules or may attract oppositely charged compounds. Alterations in the bilayer surface tension or lipid packing in the membrane either through abnormal lipid distribution or penetration of hydrophobic or amphiphilic drugs can change membrane permeability properties or protein function (Seydel, 2002). Furthermore, the exposure of phosphatidylserine on the cell surface has been associated with apoptosis and may play a significant role in cellular hemostasis and disease (Daleke, 2003). The slow transbilayer movement of phospholipids and the action of phospholipid flippases and floppases maintains the asymmetric distribution of lipids between the two membrane leaflets (Daleke, 2003).

1.2.2.2. Epithelia

Epithelia are sheets of cells bound tightly together that line all cavities and free surfaces of the body and function as a physical and chemical barrier to the external environment. Along with the functional barrier properties of the cell membrane, epithelia display a well-organized cellular polarity and specialized junctions connecting the cells together, which further contributes to the limited permeation of drugs (Washington et al.,

2001). Epithelial tissues are exploited for drug absorption into the systemic circulation including nasal, lung, buccal, ocular, skin, and intestinal epithelia, and each tissue has a distinct cellular histology, barrier properties, and permeability characteristics. The remainder of this discussion will focus on the intestinal epithelia and their barrier properties.

1.2.2.2.1. Intestinal epithelia

The gastrointestinal tract (GI tract) represents an extremely hostile environment as a site for efficient drug absorption. The wide variations in pH ranging from approximately 1.5 in the stomach to approximately 8.0 in the colon, extensive enzymatic activity, extraneous luminal contents (food substances and liquids), peristaltic activity of the GI tract reducing contact with absorptive surfaces, regional variation in cellular histology, and the presence of microorganisms, can all affect the rate and extent of drug absorption into the systemic circulation. Physiologically, the GI tract is well adapted for many absorptive processes to supply the body with essential nutrients while limiting entry of xenobiotics, toxins, and microorganisms. The primary regions of the GI tract responsible for absorption are the small intestine and the large intestine, with the small intestine being subdivided into the duodenum, jejunum, and ileum. Each region varies biochemically and histologically with regional variation in drug permeability being well established (Fagerholm *et al.*, 1997; Zheng *et al.*, 1999). The largest surface area available for absorption resides along the jejunum and ileum segments of the small intestine as a result of the extensive circular folding of the luminal surface and by further expansion into the finger-like projections called villi (Macheras et al., 1995). Lining the surface of the villi is a monolayer of mainly absorptive intestinal epithelial cells connected by tight junctional complexes (Figure 1.2). These specialized cellular interconnections bring the epithelial cells in close proximity to one another and prevent the

A

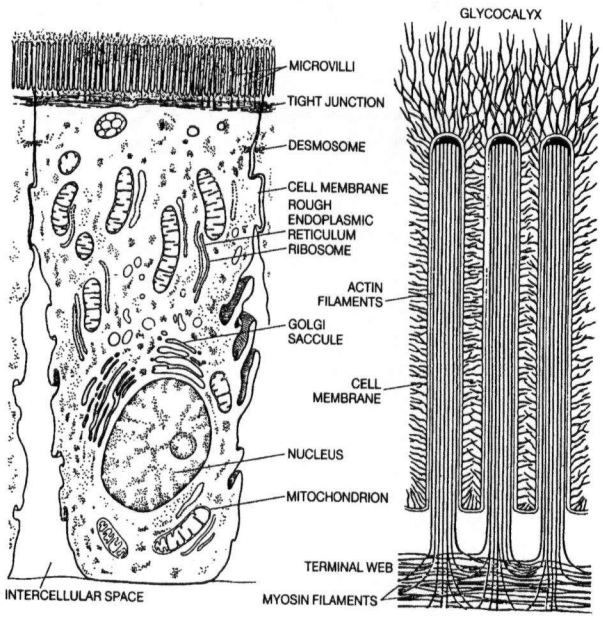

B

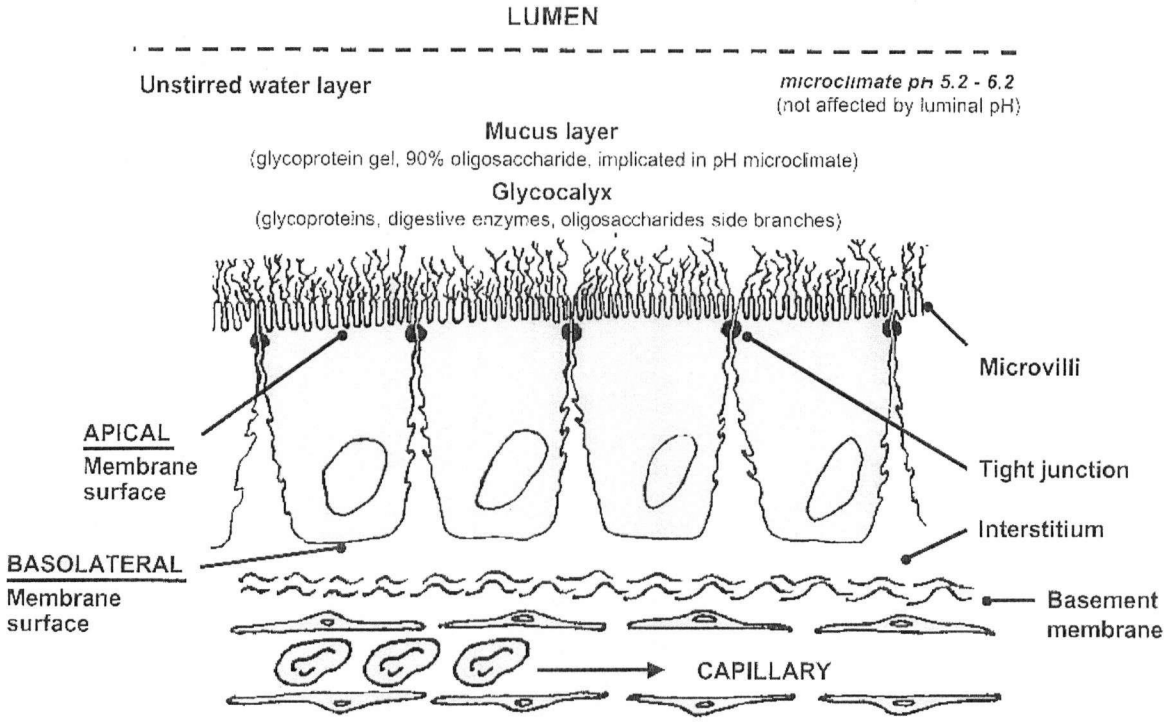

Figure 1.2. Schematic representations of (A) an intestinal enterocyte adapted from (Macheras et al., 1995) and (B) the intestinal epithelial barrier adapted from (Avdeef, 2003)

passage of luminal contents between cells. A family of transmembrane and cytosolic proteins such as occludin, claudin, and junction adhesion molecule (JAM), interact with each other between cells and with the cell cytoskeleton to form a rigid barrier (Daugherty and Mrsny, 1999a; Lapierre, 2000; Ward *et al.*, 2000). Modulation of these tight junctions, either pharmacologically or by chemically breaking them apart, is an attractive means for enhancing permeation of hydrophilic or high molecular weight drugs (Daugherty and Mrsny, 1999a; Ward *et al.*, 2000).

Absorptive intestinal epithelial cells, also called enterocytes, have an elongated columnar shape with a cellular polarity providing discrete apical (exposed to the intestinal lumen) and basolateral surfaces that are segregated by the tight junction (Figure 1.2). These surfaces differ structurally as well as biochemically in their protein content or protein function/activity and lipid composition (Morita *et al.*, 1989; Inui *et al.*, 1992; Oh *et al.*, 1999; Suzuki *et al.*, 2000). The apical membrane contains a higher proportion of cholesterol and is relatively less fluid than other cellular membranes (Swenson and Curatolo, 1992). The surface area for absorption is further increased through invagination of the apical membrane into microvilli (Figure 1.2). Glycolipids and glycoproteins within the apical membrane form a dense carbohydrate network extending outward into the intestinal lumen, termed the glycocalyx, which is chemically and structurally distinct from the basolateral membrane glycocalyx (Figure 1.3) (Morita *et al.*, 1989). The majority of these glycoproteins function as membrane bound enzymes such as disaccharidases, alkaline phosphatases, and aminopeptidases. Also embedded within the apical membrane are numerous membrane transporters that facilitate the directional absorptive influx of nutrients such as amino acids, peptides, sugars, nucleosides, and vitamins from the intestinal lumen into the systemic

circulation (Oh *et al.*, 1999). Additionally, several efflux transporters have been discovered which function to remove xenobiotics from within the enterocytes back out into the intestinal lumen and can effectively limit the permeation of xenobiotics, such as drugs, into the body (Hunter and Hirst, 1997; Oh *et al.*, 1999). Many drugs have been discovered to be substrates for these influx and efflux membrane transporters.

The intestinal epithelium contains goblet cells that secrete a layer of a high molecular weight glycoprotein and forms a mucus layer over the glycocalyx. Lipophilic drugs have demonstrated a reduced diffusion across this layer in comparison to hydrophilic drugs (Larhed *et al.*, 1997; Larhed *et al.*, 1998). Other specialized regions of the intestinal epithelia are the Peyer's patches. Cells in these regions are M cells, which are capable of engulfing macromolecules and playing an immunological role within the GI tract (Daugherty and Mrsny, 1999b). The ability of Peyer's patches to facilitate the absorption of large macromolecules or particulates has been exploited to deliver proteins such as insulin, which would not normally be able to cross the enterocytes (Haseto *et al.*, 1994; Jenkins *et al.*, 1994; Isoda *et al.*, 1997).

The layer directly adjacent to the intestinal epithelium is a unstirred water layer (UWL) through which nutrient or drug molecules must diffuse to contact the absorptive membrane surface. The thickness of the UWL ranges from 30-1000 μm depending on factors such as the method of measurement and efficiency of stirring in the bulk water (Thomson and Wild, 2001). Although this stagnant water layer has been considered to be a important diffusional barrier, its overall effect on limiting the permeability of drugs *in vivo* may be less significant (Chiou, 1994). The UWL extends through the mucus and glycocalyx

and possesses a pH lower than the bulk lumen. This acidic pH microclimate can range from 5.2-6.7 while the bulk pH is constant at 7.2 (Figure 1.2) (Shiau *et al.*, 1985).

1.2.2.3. Active secretion of drugs

The expression of drug efflux transporters throughout various excretory and barrier tissues such as the liver, kidney, intestine, and blood vessel endothelia, contributes to the formation of an effective barrier to limit drug permeation and absorption into cells or target tissues (Chan *et al.*, 2004). The importance of drug efflux transporters in reducing drug permeation was first shown by Juliano and Ling, where the over-expression of a membrane glycoprotein, termed P-glycoprotein, in Chinese hamster ovary cells resulted in reduced permeation of drugs across the cell membrane (Juliano and Ling, 1976). P-glycoprotein is just one example of an efflux transporter belonging to a superfamily of ATP-binding cassette (ABC) transporters found in bacteria, plants, fungi, and animal cells (Higgins, 1992). ABC transporters are transmembrane proteins sharing a high degree of sequence homology and organization, and are characterized by a highly conserved ATP binding domain located at the cytoplasmic face of the membrane (Higgins, 1992). Binding of ATP and subsequent hydrolysis, promotes the transport of a wide range of substrates across the membrane against the concentration gradient. Each ABC transporter is relatively specific for given substrates such as proteins, sugars, amino acids, ions, and peptides, and can function in a cellular influx or efflux direction (Higgins, 1992). For example, the cystic fibrosis transmembrane regulator (CFTR) found in the apical membrane of lung epithelia, functions to provide a pathway for Cl^- ion movement and regulates the rate of Cl^- ion flux (Sheppard and Welsh, 1999). Unlike other ABC transporters, those implicated in facilitating drug efflux possess broad substrate specificity. Although little is known about the cellular function of these drug efflux

transporters, their strategic location within the body and their ability to alter drug absorption, distribution, metabolism, and excretion characteristics and chemotherapeutic activity has led to the suggestion that they function in a protective role, preventing xenobiotics and metabolites from entering the body or accessing vital tissues.

1.2.2.3.1. P-glycoprotein

P-glycoprotein (P-gp) was the first efflux transporter identified and is the most widely studied and characterized. The over-expression of P-gp in human malignancies is associated with conferring multi-drug resistance (MDR). This cross-resistance of tumors to a chemically and mechanistically diverse group of chemotherapeutic agents presents a formidable challenge in anticancer therapy. Functionally, P-gp limits the permeation of cytotoxic drugs into the cell, reducing both the intracellular accumulation and therapeutic activity. However, other efflux transporters and non-transporter based mechanisms may also contribute to the MDR phenotype (Krishna and Mayer, 2000).

Numerous drugs have been characterized as being susceptible to P-gp mediated drug efflux to varying degrees. Compounds such as the anticancer drugs vinblastine and vincristine (Hunter *et al.*, 1991a; Hunter *et al.*, 1993b), paclitaxel (Van Asperen *et al.*, 1998), doxorubicin (Larrivee and Averill, 2000), and etoposide (Keller *et al.*, 1992); the cardiac drug digoxin (Drescher *et al.*, 2003); HIV drugs such as indinavir, saquinavir, and ritonavir (Aungst, 1999), and many others, have been shown to be substrates for P-gp. The wide variation of chemical species, mechanism of action, and physicochemical properties has limited the determination of clear structure activity relationships for P-gp. Although there are few conserved molecular elements that appear to be common between substrates, an important requirement for all substrates is a degree of hydrophobicity or amphiphilicity

within the molecule and the presence of hydrogen bonding acceptor groups (electron donating groups) for binding with P-gp (Seelig, 1998; Seelig and Landwojtowicz, 2000).

Based on sequence homology, human P-gp, also called MDR1 or ABCB1, belongs to the MDR/TAP (TAP = transporter associated with antigen processing) subfamily of ABC transporters, which also includes MDR3 (ABCB3) and BSEP (bile salt export pump) (Klein *et al.*, 1999). Both MDR3 and BSEP are found to be highly expressed in the canalicular membrane of the liver, acting as a phospholipid and bile salt transporter, respectively (Klein *et al.*, 1999; Chan *et al.*, 2004). MDR3 has been shown to selectively transport phosphatidylcholine within the membrane to maintain membrane lipid asymmetry (Daleke, 2003). Additionally, MDR1 has also been shown to transport phospholipids associated with its action as a hydrophobic molecule efflux transporter (Romsicki and Sharom, 2001). Although MDR3 has demonstrated the ability to transport several cytotoxic drugs, neither MDR3 nor BSEP have been implicated in multi-drug resistance or alterations in drug disposition (Chan *et al.*, 2004). In addition to expression in various malignancies, P-gp is constitutively expressed throughout normal human tissue. Immunohistochemistry studies have demonstrated expression and apical membrane localization of P-gp in numerous epithelial and endothelial tissues including lung, skin, liver, pancreas, prostate, adrenal gland, placenta, colon, intestine, and central nervous system endothelia (blood brain barrier or BBB) (Thiebaut *et al.*, 1987; Thiebaut *et al.*, 1989; Cordon-Cardo *et al.*, 1989; Cordon-Cardo *et al.*, 1990).

In the intestine, P-gp is localized in the apical brush border membrane of polarized epithelial cells (enterocytes), and its orientation facilitates the efflux of substrates from inside the cell back into the intestinal lumen (Thiebaut *et al.*, 1987; Cordon-Cardo *et al.*, 1990). P-

gp has been demonstrated to function as an absorption barrier, limiting the oral bioavailability of numerous drugs from the gastrointestinal tract. Sparreboom *et al.* showed that disruption of the MDR1a P-gp gene in mice led to an increase in the oral bioavailability of paclitaxel of 11% in wild type mice versus 35% when given to MDR1a(-/-) mice, suggesting that P-gp in the intestine limited the uptake of orally administered paclitaxel (Sparreboom *et al.*, 1997). Van Asperen *et al.* used the P-gp inhibitor SDZ PSC 833 and showed a substantial increase in AUC_{oral} in mice from 735 ng/h/mL^{-1} for paclitaxel alone to 8066 ng/h/mL^{-1} when given with SDZ PSC 833 (Van Asperen *et al.*, 1997). Oral bioavailability of paclitaxel in humans increased from 9.3% to 67% when paclitaxel was co-administered with the P-gp inhibitor cyclosporin A (Meerum Terwogt *et al.*, 1998). These findings suggest that drug efflux mediated by P-gp can reduce the oral absorption of susceptible drugs. Moreover, intestinal expression of P-gp has been linked to direct drug elimination from the blood. Removal of drug from the blood into the intestinal lumen occurs normally due to concentration gradients between the blood and the lumen (Arimori and Nakano, 1998). However, an increasing number of reports suggest that this route of drug elimination is in part mediated through basolateral to apical secretion by drug efflux transporters such as P-gp. Intestinal clearance of the fluoroquinolone antibiotic, grepafloxacin, was reduced by 51% when given IV together with the P-gp inhibitor, cyclosporin A (Yamaguchi *et al.*, 2002). Similarly, the intestinal clearance of the anthelmintic drug, ivermectin, was reduced by 28% using verapamil as a P-gp inhibitor (Laffont *et al.*, 2002). The presence of P-gp along the apical membrane of the hepatobiliary canalicular epithelia suggests a role in the enterohepatic circulation of drugs, and further supports the role of P-gp as a detoxifying transporter. Using MDR1a(-/-) knockout mice,

Van Asperen *et al.* demonstrated a reduction in doxorubicin biliary clearance from 13.3% of the administered dose in wild type mice, to 2.4% in mice lacking the MDR1a gene (Van Asperen *et al.*, 2000). Biliary clearance of grepafloxacin in rats was reduced by 40% with cyclosporin A treatment (Yamaguchi *et al.*, 2002).

The localization of P-gp in other tissues such as the placenta, testis, and the capillary endothelial lining of the BBB suggests a protective role of P-gp at blood-tissue interfaces to limit transfer of toxic substances, such as drugs, from the blood to vital organs (Schinkel and Jonker, 2003). At the BBB, drug transfer across the endothelial cells is primarily restricted to diffusion across the membrane due to the presence of tight junctions and the lack of fenestration between cells. Thus, the apical membrane localization of P-gp within these cells increases the barrier function by further limiting the entry of xenobiotics. Limited permeability of HIV drugs across the BBB due to the action of P-gp mediated efflux has been suggested to lead to the ability of HIV to reside in the brain unchallenged. Subsequently, the progressive viral replication in the CNS is linked with a loss of cognitive and motor functions, called AIDS dementia complex (Kim *et al.*, 1998; Polli *et al.*, 1999; Savolainen *et al.*, 2002).

1.2.2.3.2. Multidrug resistance-associated protein (MRP)

MRP was first isolated and characterized in a human lung cancer cell line which displayed a MDR phenotype not associated with overexpression of P-gp (Cole *et al.*, 1992). The MRP/CFTR subfamily of ABC transporters contains upwards of nine isoforms, labeled MRP1 through to MRP9, and CFTR (Klein *et al.*, 1999; Sun *et al.*, 2003; Chan *et al.*, 2004). Among the 9 MRP isoforms discovered to date, MRP1 and MRP2 are the most characterized and implicated in multidrug resistance and altered drug disposition.

MRP1 shares only 15% sequence homology with P-gp but can actively transport similar substrates. The anticancer drugs doxorubicin, etoposide, methotrexate, and vincristine are substrates for both P-gp and MRP1 (Chan *et al.*, 2004). Some drugs such as paclitaxel, cisplatin and indinavir are susceptible to P-gp efflux but are not as efficiently transported by MRP1 (Chan *et al.*, 2004). One major difference in substrate specificity between MRP1 and P-gp is that MRP1 can transport conjugated metabolites of drugs, including glutathione, glucuronate and sulfate derivatives (Jedlitschky *et al.*, 1996). Depletion of intracellular glutathione has been demonstrated to reverse the cellular resistance to several anticancer drugs, suggesting that the presence of glutathione within the cell is an important component to enable MRP1 efflux of drugs (Zaman *et al.*, 1995). Since these conjugates are large anionic compounds, it has been postulated that MRP1 may function as an organic anion transporter, where removal of non-anionic substrates from the cell is facilitated by forming anionic metabolites by conjugation with glutathione, followed by removal by MRP1 (Barrand *et al.*, 1997). However, some anticancer drugs that are not anionic, such as doxorubicin, have not demonstrated a glutathione conjugate dependence for MRP1 efflux, even though intracellular glutathione is still required for their transport by MRP1 (Barrand *et al.*, 1997; Borst *et al.*, 1999).

In normal tissue, MRP1 localization is on the basolateral surface of epithelia found in the intestine, brain, liver, testes, lung and kidney (Barrand *et al.*, 1997; Chan *et al.*, 2004). The basolateral localization results in transport of substrates from inside the cell towards the extracellular compartment. In contrast to P-gp where efflux promotes removal from the body, the direction of transport for MRP1 suggests that xenobiotics are transported into the body. However, some organs or tissue compartments are protected by basolateral surfaces,

for example the choroid plexus and seminiferous tubules of the testis. Surrounding the seminiferous tubules is a ring of Sertoli cells that are connected by tight junctions to form a protective permeability barrier. The apical surfaces of the Sertoli cells face the lumen of the tubule and the basolateral surfaces are adjacent to the interstitial space, containing the blood vessels. The high MRP1 expression found on the basolateral membranes of the Sertoli cells has been suggested to protect germ cells from xenobiotics/toxins from entering the lumen of the tubules (Wijnholds *et al.*, 1998; Borst *et al.*, 1999). By comparing the testes weight and histology between wild type and MRP1(-/-) knockout mice, a reduced testes weight and altered spermatogenesis were found in MRP1(-/-) knockout mice when treated with the anticancer drug, etoposide, suggesting a protective role for MRP1 localized on the blood-testis barrier (Wijnholds *et al.*, 1998). Similarly, the blood-cerebrospinal fluid (CSF) barrier is localized to the epithelium covering the choroid plexus in the brain with the apical surface facing the CSF and the basolateral surface adjacent to the perivascular space of the choroid plexus vasculature (Segal, 2000). The capillary endothelia within the choroid plexus lack tight junctions and are highly fenestrated and thus are relatively permeable to many compounds (Segal, 2000). However, the presence of MRP1 on the basolateral surface covering the choroid plexus has been demonstrated to be an effective permeability barrier preventing susceptible drugs from entering the CSF (Sugiyama *et al.*, 1999; Rao *et al.*, 1999; Wijnholds *et al.*, 2000).

The cellular localization and tissue expression of MRP2 is similar to P-gp. MRP2 is found on the apical membrane surface of epithelia in similar tissues to P-gp, such as liver, intestine, kidney, and brain capillary endothelia (Schinkel and Jonker, 2003; Chan *et al.*, 2004). MRP2 is an organic anion transporter, also called cMOAT (canalicular multispecific

organic anion transporter), and can efflux similar substrates as MRP1 including unconjugated and/or glutathione, glucuronate and sulfate conjugates (Chan *et al.*, 2004).

1.2.2.4. Enzymatic barriers

Presystemic biotransformation after oral administration of drugs has long been recognized as a significant event that can reduce the amount of parent drug from reaching the systemic circulation. Although not directly affecting drug permeation, enzymes located within the enterocytes of the intestinal epithelia and the liver can catalyze numerous phase I and phase II metabolic reactions and deactivate drugs. The primary enzymes responsible are the cytochrome P450 family, UDP-glucuronosyltransferases, and sulfotransferases, among others (Thummel *et al.*, 1997). Although the liver is a well known metabolizing organ, the intestinal epithelia are more recently being recognized as a significant site for drug presystemic metabolism.

The enterocytes of the intestine contain similar phase I and phase II catalyzing enzymes as the liver. In particular, a high concentration of cytochrome P450 isoform 3A4 (CYP3A4) is found in mature enterocytes of the small intestine (Thummel *et al.*, 1997; Wacher *et al.*, 2001). Other cytochrome P450 isoforms are also present in the enterocyte, such as CYP2D6 and CYP3A5 in addition to hydrolytic and phase II enzymes such as glutathione S-transferase (Thummel *et al.*, 1997; Wacher *et al.*, 2001). The effect of intestinal metabolism can be demonstrated via its effect on cyclosporin bioavailability. Initial views were that the low bioavailability was a function of the low solubility, membrane permeability and high molecular weight of cyclosporin (Wu *et al.*, 1995). Cyclosporin absorption was reported to be significant, with approximately 86% of the available drug absorbed, but intestinal and hepatic metabolism accounted for a 50% and a further 8%

reduction in cyclosporin absorption, respectively, resulting in an overall bioavailability of 27% (Wu *et al.*, 1995; Benet and Cummins, 2001). Other immunosuppressants such as tacrolimus (Floren *et al.*, 1997), and sirolimus (Lampen *et al.*, 1998), and drugs such as midazolam (Thummel *et al.*, 1996), and nifedipine (Grundy *et al.*, 1997) have also demonstrated significant presystemic metabolism by the intestinal enterocytes.

1.2.2.4.1. Drug efflux – metabolism alliance

Similar expression and localization patterns between CYP3A4 enzymes and drug efflux transporters within the intestine, liver, and kidney, together with overlapping substrate specificity suggests that these proteins may work synergistically to limit entry of xenobiotics/toxins into the body and to facilitate their removal (Wacher *et al.*, 1995). Furthermore, expression of P-gp and CYP3A4 can be up-regulated by similar substrates or modulators and may be co-regulated through the SXR (steroid and xenobiotic receptor) orphan nuclear receptor (Synold *et al.*, 2001). The apical localization of both P-gp and CYP3A4 enzymes in the enterocytes may result in these enzymes working in concert to form an efficient absorption barrier. One effect of this synergy is that the active efflux mediated by P-gp may increase the exposure of drugs to CYP3A4 metabolizing enzymes (Watkins, 1997). Upon entry into the cell of a drug that is susceptible to both P-gp efflux and CYP3A4 metabolism, a significant portion of the drug will be effluxed by P-gp back into the intestinal lumen and limit the amount that can cross into the blood, while some will be metabolized by CYP3A4. Drug that was effluxed out can then re-enter the cell and be re-exposed to metabolizing enzymes. This repetition of influx and efflux processes may prolong the intracellular residence time and result in an increase in the overall metabolism of the drug and a reduction in the amount of parent drug entering the blood. Hochman *et al.* compared

the ratio of the amount of major metabolite formed to the amount of parent drug transported across an intestinal cell line model and showed the effect of P-gp on indinivir metabolism (Hochman *et al.*, 2000). In the absorptive apical (AP) to basolateral (BL) direction, the ratio of metabolite formation to the amount transported across was 5 fold higher than in the BL to AP direction (Hochman *et al.*, 2000). Thus P-gp reduced the transport of indinivir when applied to the apical surface resulting in a greater extent of indinivir metabolism, whereas P-gp contributed to the increase in inidinivir transport across the cell in the BL to AP direction, which reduced the exposure to CYP3A4 and subsequent metabolite formation. This provided initial evidence that the effect of P-gp in reducing drug entry into and ultimately across the enterocyte could result in a greater extent of metabolism through the regulation of drug entry into the cell. Using a dual P-gp/CYP3A4 substrate, designated K77, and a substrate for CYP3A4 only, felodipine, Cummins *et al.* investigated the effect of P-gp on the extent of CYP3A4 metabolism of K77. K77 extraction ratio (equivalent to the metabolite formation/transport ratio) was 5 fold greater in the AP to BL direction compared to the BL to AP direction, and the ratio was the same for felodipine (Cummins *et al.*, 2002). P-gp inhibitors significantly reduced the extraction ratio in the AP to BL direction further supporting the regulatory role of P-gp in CYP3A4 intestinal metabolism (Cummins *et al.*, 2002).

Another proposed interplay between drug efflux transporters and metabolic enzymes is the P-gp mediated efflux of CYP3A4 metabolites. The metabolic conversion of a P-gp substrate by CYP3A4 to a higher affinity P-gp substrate or one with similar affinity, may promote biotransformation of the parent drug by reducing secondary metabolism of primary metabolites which are themselves CYP3A4 substrates (Watkins, 1997). Cummins and

Hochman *et al.* both showed a greater cellular removal of metabolite into the apical compartment, suggesting that the resulting metabolites may be substrates for P-gp (Hochman *et al.*, 2000; Cummins *et al.*, 2002). The interactions of several verapamil phase I metabolites with P-gp have been investigated to determine if the metabolites behaved as substrates or inhibitors (Pauli-Magnus *et al.*, 2000). However, there has been limited work to evaluate the substrate specificity of resulting metabolites of dual P-gp/CYP3A4 substrates to clarify this potential synergistic activity.

1.3. P-GLYCOPROTEIN

Sequence analysis has demonstrated that human P-gp is a 170 kDa protein comprised of 1280 amino acids organized into two homologous halves containing 610 amino acids each and connected by a 60 amino acid linker. Within each half there are 6 transmembrane (TM) spanning segments and a nucleotide-binding domain (NBD) for a total of 12 TM segments and 2 NBD's per P-gp transporter (Figure 1.3). The bilateral duplicates contain approximately 43% sequence homology and are labeled starting from the N-terminus as TM1-6/NBD1 and TM7-12/NBD2 with both NBD's located cytoplasmically (Figure 1.3). Three N-glycosylation branches are attached to the first extracellular loop between TM1 and TM2 (Schinkel *et al.*, 1993). Site directed mutagenesis studies demonstrated that N-glycosylation did not appear to affect transport activity of P-gp but could play an important role in membrane routing and stability (Schinkel *et al.*, 1993).

1.3.1. Current model for P-glycoprotein mediated drug efflux

The structural diversity of P-glycoprotein substrates has hampered progress in understanding how P-gp removes drugs from the cell. Standard ABC transporters typically function through classical pump mechanics where substrate interaction with the pump is via

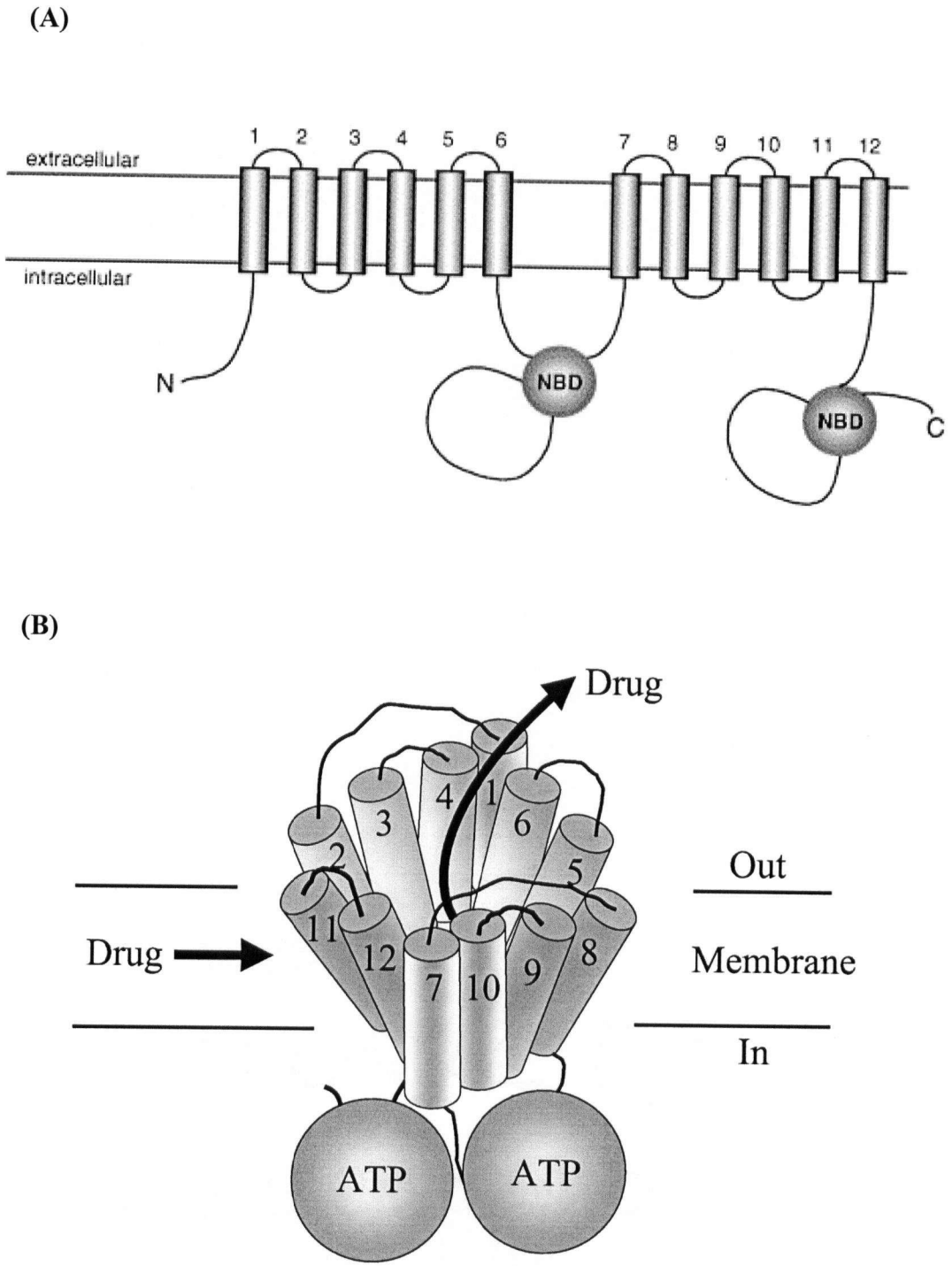

Figure 1.3. Topology models of P-gp. (A) Secondary structure of P-gp displaying the 12 transmembrane (TM) spanning segments labeled 1-12 and the two cytoplasmically located nucleotide binding domains (NBD) adapted from (Chan *et al.*, 2004). (B) Current proposed organization (tertiary structure) of P-gp within the cell membrane proposed by Loo *et al.*, demonstrating the 'funnel' shaped drug binding pocket formed by the TM segments (Loo *et al.*, 2004).

the aqueous domain (either cytoplasmic for an exporter or extracellular for an importer) with translocation through an aqueous channel or pore to the opposite side, for example the CFTR functioning to transport Cl^- ions (Higgins and Gottesman, 1992; Sheppard and Welsh, 1999). Although P-gp substrates are structurally diverse, a common feature is that they are relatively hydrophobic. This has led to the currently most accepted model for P-gp mediated efflux proposed by Gottesman *et al.*, called the Hydrophobic Vacuum Cleaner (HVC) model (Raviv *et al.*, 1990; Gottesman and Pastan, 1993). The HVC model postulates that drugs partition into the membrane due to their high partition coefficients, interact with P-gp directly within the lipid bilayer and then are translocated back out to the extracellular milieu. According to the HVC model, P-gp may function similar to a flippase, mediating the translocation of substrates from the inner cytoplasmic membrane leaflet to the outer membrane leaflet or directly into the extracellular milieu (Higgins and Gottesman, 1992). Direct evidence for this model has been demonstrated using P-gp expressing NIH-3T3 mouse fibroblasts and a lipophilic acetoxymethyl ester (AM) derivative of a fluorescent dye (Homolya *et al.*, 1993). The AM derivatives are non-fluorescent, lipophilic P-gp substrates that undergo rapid hydrolysis by cytoplasmic esterases within the cell back to the hydrophilic, non-P-gp substrate, fluorescent parent (calcein and fura-2) dye (Homolya *et al.*, 1993). Cellular accumulation studies using the AM derivatives showed a substantially reduced cellular fluorescence in P-gp expressing NIH-3T3 cells compared to the control wild type cells, suggesting that the AM derivatives were unable to reach the cytoplasmic milieu and be converted to the fluorescent dye (Homolya *et al.*, 1993). Furthermore, the cellular fluorescence of P-gp expressing NIH-3T3 cells was increased in the presence of P-gp inhibitors demonstrating that inhibition of P-gp increased the permeation of the AM

derivatives across the membrane into the cytoplasm (Homolya *et al.*, 1993). Additional support for the HVC model comes from transport studies uing a lipophilic fluorescent dye, Hoechst 33342. This P-gp substrate possesses strong fluorescence in a hydrophobic environment with negligible fluorescence in an aqueous environment (Shapiro *et al.*, 1997). Using isolated plasma membrane vesicles from a P-gp over-expressing cell line, a 50-60% drop in initial fluorescence was observed for Hoechst 33342 upon the addition of ATP to stimulate P-gp activity, suggesting that Hoechst 33342 was actively removed from the lipid membrane into an aqueous environment (Shapiro *et al.*, 1997). Upon addition of a P-gp inhibitor, re-equilibration of Hoechst 33342 within the membrane occurred, resulting in a return of the fluorescence intensity (Shapiro *et al.*, 1997).

The interaction of P-gp with substrates within the lipid bilayer suggests that the TM segments may be primarily responsible for substrate binding. Loo and Clarke have shown that deletion mutants of P-gp with both NBD's removed, still retained the ability to bind substrates, suggesting that the TM segments are responsible for binding and not the cytoplasmically located NBD regions (Loo and Clarke, 1999). Although the NBD deletion mutants were capable of binding to substrate, P-gp efflux activity was abolished, suggesting that the NBD groups are required for displacement of bound substrate (Loo and Clarke, 1999). If the TM segments are responsible for substrate interactions, then determining the number of binding sites and the specific TM segments responsible for binding is of value for the understanding of substrate structure activity relationships and for development of inhibitors. Initial work by Shapiro and Ling showed a positively cooperative binding pattern between two P-gp substrates, Hoechst 33342 and rhodamine 123. Compounds such as the anthracyclines were capable of stimulating Hoechst 33342 transport and inhibiting

rhodamine 123, while vinblastine and etoposide stimulated rhodamine 123 transport and inhibited Hoechst 33342 (Shapiro and Ling, 1997). This suggested that there were two or more possible distinct binding sites within the TM segments, which were termed the H and R binding site (Shapiro and Ling, 1997; Shapiro and Ling, 1998). To further define the substrate binding sites along the TM segments, Loo *et al.* utilized cysteine-scanning mutagenesis (CSM) in conjunction with cross-linking studies using thiol reactive substrates (Loo and Clarke, 1999). In brief, cysteine-scanning mutagenesis involves the removal or mutation of the seven endogenous cysteine residues in P-gp to alanine, followed by selective introduction of cysteine residues at desired locations and expression of the modified P-gp in a host cell line. The use of cross-linking studies between strategically placed cysteine residues can lead to an understanding of how P-gp folds within the membrane and which TM segments and amino acid residues are involved in drug binding (Loo and Clarke, 1999). Using CSM, verapamil was capable of protecting P-gp from inactivation through cross-linking by a thiol reactive verapamil derivative at amino acid residues along multiple TM segments from both domains, including TM's 4-6 and 9-12 (Loo and Clarke, 2001a; Loo *et al.*, 2004). Cysteine-scanning mutagenesis studies have also demonstrated that substrates may exhibit interactions between overlapping and/or distinct amino acid residues along different or similar TM segments, suggesting that a single drug binding pocket may be involved with multiple binding regions (Loo and Clarke, 2001a; Loo and Clarke, 2001b; Loo *et al.*, 2003a). Using a series of cross-linking reagents with spacer arms of various lengths, the measurements between the residues of the TM segments known to interact with substrates demonstrated a large binding pocket in a 'funnel' shape, with the TM regions closest to the cytoplasmic face in close proximity to each other and wider at the extracellular

face, ranging from approximately 50 Å in diameter at the top and 9-25 Å in the middle (Figure 1.3) (Loo and Clarke, 2001b). Electron microscopy on 2D crystals of P-gp have also demonstrated an aqueous chamber formed by the two TM domains of approximately 60-70 Å in diameter (Rosenberg *et al.*, 2001). This wide to narrow configuration suggests that substrates of varying size and shape are able to interact or 'fit' into the binding domain. These observations have led to the 'substrate induced fit' model for P-gp substrate interactions proposed by Loo and Clarke. This involves the mobility of P-gp drug binding pocket segments to accommodate a substrate through rotational or lateral movements of the TM segments to expose amino acid residues along the TM's for interaction (Loo and Clarke, 2001a). Evidence for the substrate induced fit model has been obtained by monitoring the oxidative cross-linking pattern of P-gp cysteine mutants in the presence and absence of substrates such as progesterone, cyclosporin A, and colchicine (Loo *et al.*, 2003c). Cross-linking patterns between TM segments differed in the absence or presence of substrate, suggesting that P-gp alters its conformation depending on the associating substrate (Loo *et al.*, 2003c). The interaction of verapamil with P-gp mutants with cysteine residues at amino acid 343 on TM6 and amino acid 982 on TM 12 promoted cross-linking between these amino acid residues with tris-(2-maleimidoethyl)amine (TMEA). In the absence of verapamil, no cross-linking was observed, demonstrating that verapamil interaction induced a conformational change in TM's which allowed cross-linking to occur (Loo *et al.*, 2003b).

Once bound to P-gp, how a substrate is then translocated out of the membrane and into the extracellular milieu involves the interactions of the NBD's and ATP hydrolysis. Unlike other ATP dependent transporters, P-gp maintains a constitutive ATPase activity in the absence of known substrates and this activity is found in highly purified P-gp

preparations containing endogenous or exogenous lipids (Sharom *et al.*, 1995; Sharom, 1997a). This basal level of ATPase activity may be the result of an unknown natural lipid soluble substrate or may be an intrinsic activity of the pump similar to the activity of MDR3 acting as a phospholipid flippase (Sharom *et al.*, 1995).

The current model for P-gp translocation of substrates involves an alternating cycle of ATP hydrolysis between both NBD's (Figure 1.4) (Sauna and Ambudkar, 2000; Sauna and Ambudkar, 2001). In the absence of a known substrate, Qu *et al.* have recently demonstrated that both NBD's in the resting state can be occupied with either ATP or ADP associated with P-gp's basal ATPase activity (Qu *et al.*, 2003). In the presence of a substrate, the binding of ATP with the NBD's and the substrate with the TM segments appear to be independent events, suggesting that binding is not coordinated and an ordered substrate/ATP binding pattern is not involved in the function of P-gp (Liu and Sharom, 1996). However, binding of the substrate increases the binding affinity of the NBD's for ATP and the catalytic cycle is promoted, possibly through conformational communication between the TM segments and the NBD's (Liu and Sharom, 1996; Qu *et al.*, 2003). Therefore, Step I in Figure 1.4 involves independent binding of substrate to the TM segments and ATP binding to one or both of the NBD's. Subsequent ATP hydrolysis from one NBD results in a conformational change in the TM segments, reducing the binding affinity for substrate and promoting release to the extracellular milieu (Step II and III in Figure 1.4) (Sauna and Ambudkar, 2001). Release of ADP from the first NBD initiates a second ATP hydrolysis event mediated through the second NBD (Steps IV-VI in Figure 1.4) (Sauna and Ambudkar, 2001). Both NBD's appear to have similar kinetic rates of ATP hydrolysis and thus are suggested to be recruited randomly in the catalytic cycle (Sauna and Ambudkar, 2001). The release of ADP from the

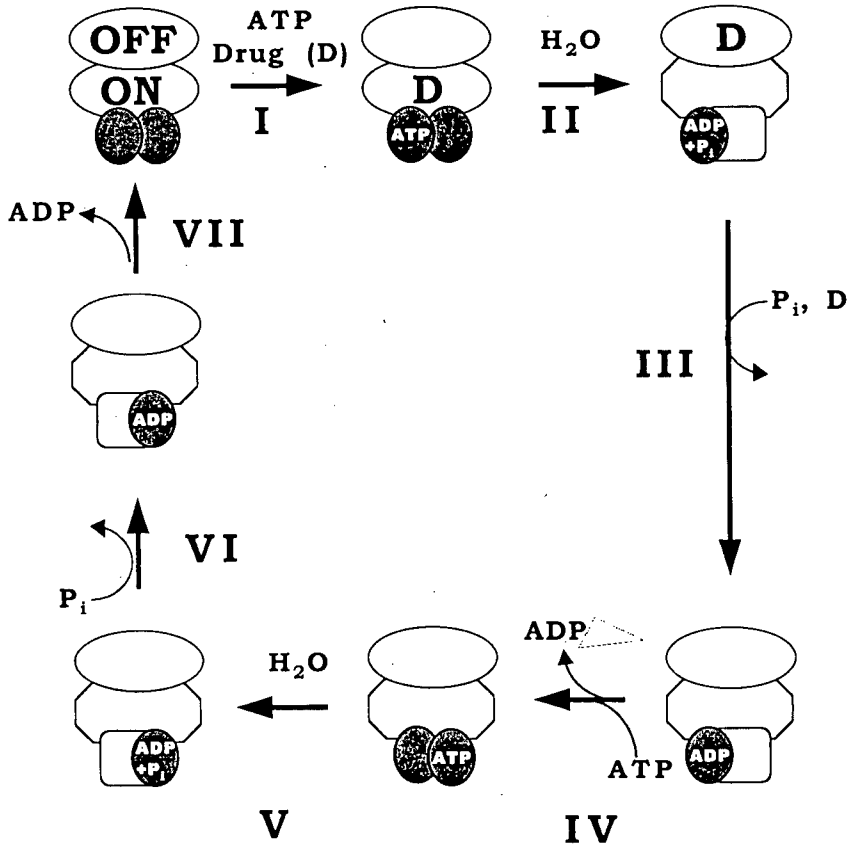

Figure 1.4. Alternating catalytic cycle of P-glycoprotein translocation of substrates adapted from (Sauna and Ambudkar, 2001). *Step I*: binding of substrate to the TM segments and ATP to one or both of the NBD's. *Step II-III*: ATP hydrolysis from one NBD with release of bound substrate. *Step IV-VII*: Second hydrolysis event on other NBD resulting in reconfiguration of P-gp to repeat the cycle.

second NBD allows for the reconfiguration of P-gp back to the 'resting' state for binding and translocation of another substrate molecule (Step VII in Figure 1.4) (Sauna and Ambudkar, 2001). Overall, translocation of substrate involves a 2:1 stoichiometry with hydrolysis of one ATP molecule promoting the release of substrate followed by the hydrolysis of a second ATP required to reset the conformation of P-gp (Sauna and Ambudkar, 2000). The extensive conformational changes within the TM domains during the catalytic cycle have been demonstrated by 2D crystal images of P-gp using electron microscopy (Rosenberg *et al.*, 2001).

1.3.2. Modulation of P-gp activity

The primary approach for either reversing the MDR phenotype for chemotherapy or enhancing drug bioavailability/disposition has been to co-administer P-gp inhibitors (also called modulators or chemosensitizers). The first generation P-gp modulators consisted of compounds already used clinically for other therapeutic applications, such as verapamil and cyclosporin A. Other first generation compounds included quinidine, tamoxifen, and progesterone (Robert and Jarry, 2003). Although these agents can effectively inhibit P-gp efflux activity *in vitro*, their use in patients is problematic due to intrinsic toxicities associated with their primary pharmacological activity (Krishna and Mayer, 2000). High doses are required to provide sufficient P-gp inhibition *in vivo* resulting in severe toxicity, such as cardiac toxicity by verapamil and renal toxicity and immunosupression with cyclosporin A (Sikic, 1997; Robert and Jarry, 2003). Derivatives of the first generation inhibitors were developed to improve the potency and to reduce the unwanted pharmacological activity. These second generation compounds included the less cardio-toxic R-enantiomer of verapamil, dexverapamil, and the non-immunosuppressive cyclosporin A

derivative, PSC 833 also called Valspodar. Further development of inhibitors has resulted in bi-functional inhibitors capable of modulating not just P-gp but also MRP or other efflux transporters. These compounds include Biricodar (VX-710) that is capable of inhibiting both P-gp and MRP1, GF-120918 (Elacridar) an acridone carboxamide that is active against P-gp and BCRP (breast cancer resistance protein) and LY 335979 (Zosuquidar) a high affinity inhibitor specific for P-gp (Robert and Jarry, 2003). Although clinical studies have demonstrated reversal of MDR with these inhibitors, toxicity problems and altered drug pharmacokinetics appears to be limiting the clinical effectiveness for many of these inhibitors (Krishna and Mayer, 2000). However, some third generation inhibitors, such as the anthranilic derivative, XR9576 (Tariquidar) have demonstrated minimal pharmacokinetic interactions and associated toxicity in combination with chemotherapeutic drugs (Robert and Jarry, 2003).

1.3.3. Relationship of P-glycoprotein activity with the lipid membrane environment

Substantial evidence now exists that demonstrates the interaction of P-gp and substrates within the lipid bilayer as postulated by the hydrophobic vacuum cleaner model. Since substrates must first partition into the membrane to gain access to the P-gp binding site, the physicochemical properties of the substrate and the membrane will influence the extent of this partitioning. Therefore, if the HVC model is valid, then the lipid bilayer composition and physical state of the lipids should affect P-gp-substrate interactions. Romsicki and Sharom explored the relationship of membrane lipids with P-gp-substrate binding affinity using highly purified P-gp that was labeled with a fluorophore (2-(4'-maleimidylanilino) naphthalene-6-sulfonic acid) on the NBD's and reconstituted with defined lipid compositions to form proteoliposomes (Romsicki and Sharom, 1999). Upon substrate binding to the

fluorophore-P-gp, conformational changes transferred from the TM segments to the NBD's resulted in quenching of the fluorescence, providing a measure of binding affinity (Liu and Sharom, 1996). Changing the lipid headgroup from egg PC (phosphatidylcholine) to egg PE (phosphatidylethanolamine) resulted in lower P-gp binding affinities for vinblastine, verapamil and daunorubicin (Romsicki and Sharom, 1999). A decrease in the binding affinity was also observed with respect to acyl chain saturation, where egg PC (unsaturated) demonstrated a higher binding affinity compared to the saturated DMPC (dimyristrlphosphatidylcholine; C14) or DPPC (dipalmitylphosphatidylcholine; C16) lipids (Romsicki and Sharom, 1999). Furthermore, the lipid-water partition coefficients of vinblastine, verapamil and daunorubicin were highest for egg PC followed by DMPC and DPPC liposomes. Hence, an increase in the partition coefficients resulted in an increase in the P-gp binding affinities of the drugs (Romsicki and Sharom, 1999). A similar correlation between lipid-water partition coefficients of substrates and their P-gp binding affinities was also demonstrated for a series of 11 known P-gp substrates (Seelig and Landwojtowicz, 2000).

A decrease in substrate affinity for P-gp was found in liposomes composed of lipids in the liquid-crystalline state compared to the gel state (Sharom, 1997b; Romsicki and Sharom, 1999; Lu *et al.*, 2001). The temperature dependence of the rate of P-gp transport of the fluorescent substrate, tetramethylrosamine, demonstrated an unpredictable pattern, where a constant and high rate of substrate transport was observed at temperatures below the lipid transition temperature ('rigid' gel state) and this decreased with increasing temperatures above the transition temperature ('fluid' liquid crystalline state) (Lu *et al.*, 2001). This atypical activity in a more rigid/ordered membrane environment was further demonstrated by

an increase in P-gp basal ATPase activity in proteoliposomes or isolated membrane vesicles that contained high proportions of cholesterol (Rothnie *et al.*, 2001; Garrigues *et al.*, 2002). In MDR presenting cells, P-gp has been demonstrated to be preferentially located within rigid/ordered microdomain regions in the membrane composed of a high proportion of cholesterol and sphingomylin lipid called 'lipid rafts' or caveolae (Lavie *et al.*, 1998; Luker *et al.*, 2000; Ghetie *et al.*, 2004). Caveolae have a function in both endocytotic processes and cholesterol efflux and the presence of P-gp in these rigid membrane microdomains may explain the requirement for a more ordered lipid environment for activity (Lavie *et al.*, 1998; Luker *et al.*, 2000). Although depletion of cholesterol within cell membranes resulted in a decrease in P-gp activity, the response appeared to be cell and substrate specific (Romsicki and Sharom, 1999; Luker *et al.*, 2000; Riou *et al.*, 2003; Troost *et al.*, 2004).

The importance of the membrane lipid environment has been further supported by the work of Sinicrope *et al.*, which demonstrated an approximately 5 fold reduction in P-gp transport of vinblastine and daunomycin across rat liver canalicular membrane vesicles in the presence of membrane fluidizers, such as benzyl alcohol (Sinicrope *et al.*, 1992). Drori *et al.* evaluated the membrane fluidizing effect of numerous standard P-gp inhibitors such as verapamil and cyclosporin A and found that many were capable of altering membrane lipid fluidity (either fluidizing or rigidifying) at concentrations that inhibited P-gp activity (Drori *et al.*, 1995). Since membrane fluidization may result in enhanced passive transmembrane permeability of a compound, Drori *et al.* postulated that P-gp inhibitors which affect membrane fluidity may enhance the passive permeability of a P-gp substrate in addition to possessing P-gp inhibitory activity (Drori *et al.*, 1995). Using proteoliposomes reconstituted with P-gp, Regev *et al.* showed that membrane fluidizers such as ether, chloroform, and

benzyl alcohol were capable of abolishing P-gp ATPase activity and increasing doxorubicin transmembrane movement rate by 2-fold (Regev *et al.*, 1999).

1.3.4. Differentiation between P-glycoprotein substrates and modulators

Modulators are able to bind to P-gp and act as competitive or non-competitive inhibitors to reduce the transport of a substrate (Ayesh *et al.*, 1996; Litman *et al.*, 1997). Although modulators act as antagonists, in many cases P-gp is apparently unable to transport the modulator and reduce its intracellular concentration as occurs for substrates. This contradiction in P-gp transport between substrate and modulator has been observed for the inhibitors, verapamil and progesterone. Verapamil was shown to be capable of inhibiting P-gp, resulting in an increased cellular accumulation of daunorubicin in the MDR Ehrlich ascites tumor cell line (EHR2/DNR+). However, no difference in verapamil accumulation under normal and ATP depletion conditions was found between wild type EHR2 cells and the MDR clone (Sehested *et al.*, 1990). Similarly, progesterone enhanced the cellular accumulation of vinblastine in a human colon carcinoma (SW-620) MDR clone, but the accumulation of progesterone was similar between the wild type SW-620 and the MDR clone suggesting that progesterone can inhibit P-gp but is not itself actively transported (Barnes *et al.*, 1996). Scala *et al.* evaluated 84 compounds known to bind with P-gp and attempted to classify them as either substrates or as antagonists (Scala *et al.*, 1997). Of the 84 compounds, 35 met the criteria for substrates and 42 met the criteria for antagonists while only 7 met both criteria, suggesting that substrate compounds are transported and have no antagonistic activity and antagonists are capable of inhibiting P-gp with no evidence of significant transport (Scala *et al.*, 1997).

Further complicating the differentiation between substrates and modulators is the

effect on P-gp ATPase activity and ATP hydrolysis. Although an increase in P-gp ATPase activity has been associated with substrate transport, both modulators and substrates have been found to stimulate ATPase activity (Scala *et al.*, 1997). Additionally, substrates and modulators have been shown to inhibit or have minimal effects on P-gp ATPase activity (Scala *et al.*, 1997; Sharom, 1997a; Shepard *et al.*, 1998; Romsicki and Sharom, 1999).

The differences in the ability of P-gp to transport modulators and substrates may be explained using the hydrophobic vacuum cleaner model. Substrate or modulator interactions with P-gp are considered to occur within the interior of the membrane. The extent of the interactions may be influenced by the ability of the substrate/modulator to partition into the membrane and also the rate of movement across the membrane. Eytan *et al.* compared the equilibrium transmembrane movement rates of P-gp substrates with well known P-gp modulators across multilamelar liposomes (Eytan *et al.*, 1996). Substrates for P-gp had slower equilibrium transmembrane movement rates (1-3 h) compared to modulators which exhibited rapid transmembrane movement rates across the lipid model membranes (5-10 min) (Eytan *et al.*, 1996). From these results Eytan *et al.* postulated that modulators were capable of binding and being transported by P-gp similar to substrates. However, the rapid transmembrane movement rate of the modulators intracellularly, overcame the outward efflux activity of P-gp leading to accumulation of the modulator inside the cell and resulting in an assumption that P-gp was unable to transport the modulator. In the case of substrates, the slow transmembrane movement rate resulted in effective retention of the substrate within the membrane, thus allowing sufficient time for P-gp to remove it back to the extracellular milieu (Eytan *et al.*, 1996).

Therefore, the efficiency of P-gp mediated efflux of substrates appears to depend on

the relative transmembrane movement rates of the substrates. Using a homologous series of rhodamine dyes, the efficiency of P-gp activity was measured by the extent of substrate accumulation in MDR Chinese hamster ovary cells and was found to depend on the passive transmembrane movement rates of the substrate dyes (Eytan *et al.*, 1997). Dyes that were effectively excluded from MDR overexpressing cells displayed the slowest transmembrane movement rate indicating that the rate of substrate diffusion was a major factor in determining the efficiency of P-gp efflux of a substrate (Eytan *et al.*, 1997). According to the solubility/diffusion model (see section 1.2.2.1), more lipophilic substrates should exhibit faster passive transmembrane diffusion rates and reduce the efficiency of P-gp efflux or, alternatively, exhibit modulator activity. This was confirmed by Lampidis *et al.* who showed that lipophilic anthracycline derivatives were capable of overcoming P-gp efflux and exhibited cytotoxicity to MDR overexpressing cells, whereas less lipophilic anthracyclines were effluxed by P-gp and were less cytotoxic (Lampidis *et al.*, 1997). Additionally, the more lipophilic anthracycline derivatives exhibited modulator activity, capable of increasing the cellular accumulation of the P-gp substrate rhodamine 123 (Lampidis *et al.*, 1997). These results were also observed with steroid derivatives, in which more lipophilic steroids had better modulator activity for enhancing vinblastine accumulation than relatively hydrophilic steroids (Barnes *et al.*, 1996).

1.3.5. Surfactants as P-gp inhibitors

Another class of agents found to inhibit P-gp mediated efflux are the natural and synthetic surfactants (Table 1.1). Surfactants have been employed as permeation enhancers to increase the permeability of drugs across many epithelial barriers including intestinal and dermal epithelia (Swenson and Curatolo, 1992; Endo *et al.*, 1996; Aungst, 2000). Surfactants

can partition into cell membranes causing membrane disorder and altering membrane integrity, which can result in an increase in drug permeability through the membrane (Swenson and Curatolo, 1992; Aungst, 2000). Given the importance of the lipid membrane environment on P-gp activity (see section 1.3.3) it is not surprising that surfactants have demonstrated an effect on P-gp efflux activity. Woodcock *et al.* were the first group to show that Cremophor EL®, a polyethoxylated castor oil surfactant, was capable of enhancing the cellular accumulation of daunorubicin into MDR resistant cell lines to levels comparable to the accumulation of daunorubicin in sensitive wild type cells (Woodcock *et al.*, 1990). An increase in the cellular accumulation and a concomitant decrease in the IC_{50} of doxorubicin and vincristine in MDR cells was also found using Cremophor EL® (Schuurhuis *et al.*, 1990). Woodcock *et al.* also demonstrated that other surfactants such as polysorbate 80 and Solutol HS15 were capable of increasing cellular accumulation of daunorubicin in MDR cell lines (Woodcock *et al.*, 1992). Studies using an MDR-overexpressing tumor bearing mouse model, showed that injection of Cremophor EL® with doxorubicin improved animal survival time (Woodcock *et al.*, 1992). In addition to reversing the MDR phenotype in tumors, several groups have demonstrated the potential of using surfactants to block the efflux of P-gp in the intestine to improve oral bioavailability. Using the caco-2 human colon adenocarcinoma cell line as a model for intestinal epithelia, Lo *et al.* found greater intracellular uptake of epirubicin in the presence of acacia or polysorbate surfactants compared to epirubicin alone or with the P-gp inhibitors verapamil and trifluoperizine (Lo *et al.*, 1998). Transport studies across caco-2 cells showed that polysorbate 80 and Cremophor EL® are both capable of reducing the basolateral to apical (BL to AP) permeability and increasing the AP to BL permeability of model peptides susceptible to P-gp efflux

Table 1.1: Surfactants demonstrated to modulate drug efflux transport

Structure	Reference
Polyethoxylated castor oil (Cremophor EL®) *A complex mixture containing a glycerol backbone with mono, di, or tri esters of 12-hydroxy-9-octadecenoic acid (ricinoleic acid) polyethoxylated to varying degrees and positions.* 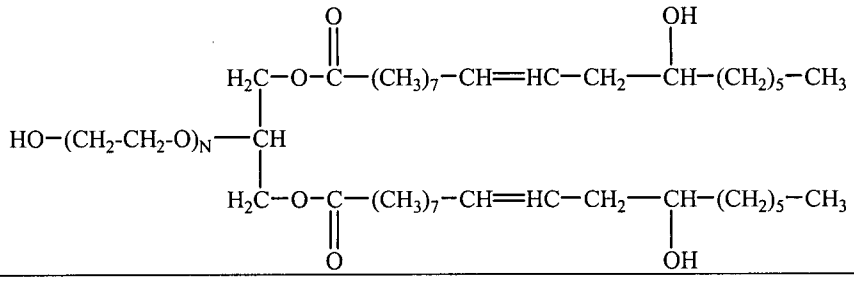	(Schuurhuis *et al.*, 1990) (Woodcock *et al.*, 1990) (Woodcock *et al.*, 1992) (Shono *et al.*, 2004) (Nerurkar *et al.*, 1996) (Nerurkar *et al.*, 1997)
Polyoxyethylene sorbitan esters (Polysorbate series) 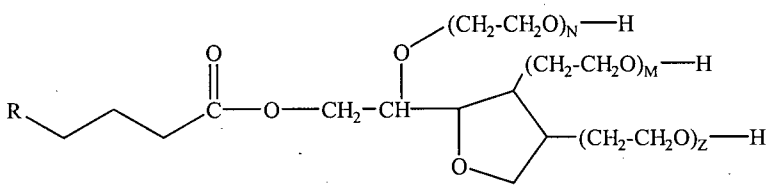	(Woodcock *et al.*, 1992) (Nerurkar *et al.*, 1996) (Nerurkar *et al.*, 1997) (Lo *et al.*, 1998)
D-alpha-tocopheryl polyethylene glycol –1000 succinate (Vitamin E TPGS®) 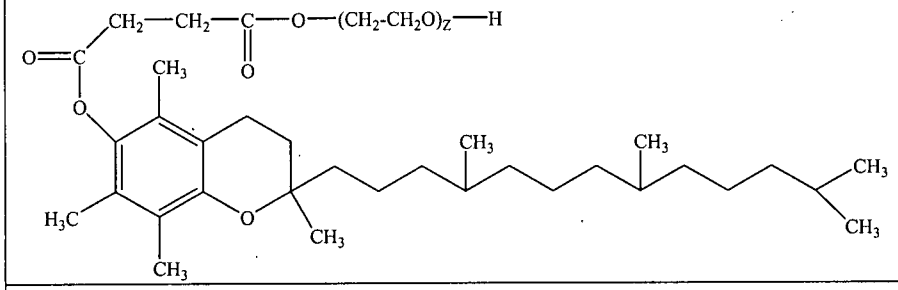	(Dintaman and Silverman, 1999) (Bogman *et al.*, 2003) (Yu *et al.*, 1999)
Polyoxyethylene ethers (Brij series) 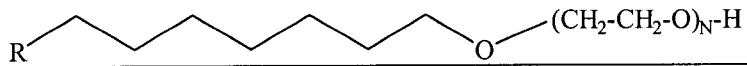	(Lo, 2003)
Polyoxyethylene esters of 12-hydroxystearic acid (Solutol HS15) 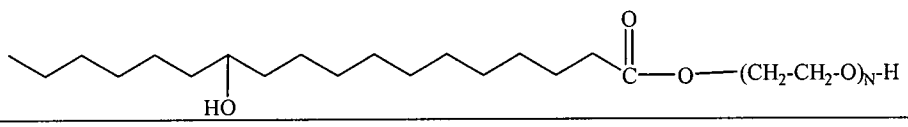	(Woodcock *et al.*, 1992) (Coon *et al.*, 1991)

(Nerurkar *et al.*, 1996). The amphiphilic polyethoxylated derivative of d-α-tocopherol (Vitamin E) was able to inhibit P-gp mediated efflux of amprenavir, paclitaxel, and the fluoresecent P-gp probe, rhodamine 123 from caco-2 cells (Dintaman and Silverman, 1999; Yu *et al.*, 1999).

Literature evidence to date indicates that a common feature for all surfactants demonstrating P-gp inhibition is that peak inhibition by surfactants occurs at a concentration equal to or below the CMC of the surfactant and that higher concentrations beyond the CMC result in a decrease in inhibitory activity (Nerurkar *et al.*, 1996; Nerurkar *et al.*, 1997). At concentrations below the CMC only unassociated surfactant molecules (also called unimers) will be present in solution. Therefore, Nerurkar *et al.* have suggested that the free surfactant unimers are primarily responsible for inhibiting P-gp activity (Nerurkar *et al.*, 1997). Higher concentrations of surfactant above the CMC will result in the formation of micelles into which the co-administered P-gp substrate may partition. Using equilibrium dialysis to separate 'free' from micellar 'bound' P-gp substrate, Nerurkar *et al.* found that an increase in micellar bound substrate at high surfactant concentrations correlated with the observed decrease in surfactant mediated inhibition of P-gp (Nerurkar *et al.*, 1996). This binding or sequestration of the P-gp substrate inside micelles will reduce the concentration of free substrate available to enter the cell, resulting in reduced substrate accumulation (Nerurkar *et al.*, 1997). Most P-gp substrates are hydrophobic in nature and will be readily solubilized within the hydrophobic core of micelles. If the surfactant concentration achieved at the target site for P-gp inhibition is high, sequestration of the P-gp substrate by surfactant micelles may reduce cellular uptake or permeability. Bardelmeijer *et al.* have shown that co-administration of Cremophor EL® with paclitaxel orally to mice at high surfactant

concentrations resulted in significant binding and a reduction in the plasma AUC (Bardelmeijer *et al.*, 2002). High concentrations of Cremophor EL® resulted in reduced cyclosporin A permeability across caco-2 monolayers in both the AP to BL and BL to AP directions (Chiu *et al.*, 2003).

A common method of surfactant classification is based on the hydrophilic/lipophilic balance (HLB) system developed by Griffin (Griffin, 1954). The HLB system, classifies surfactants not structurally, but rather on molecular proportions of the hydrophobic and hydrophilic groups comprising the surfactant. Low HLB value surfactants (1-7) are typically hydrophobic with a greater proportion of the hydrophobic segment and high HLB surfactants (12-20) are classified as hydrophilic with higher proportions of the hydrophilic segment. Using a structurally diverse series of surfactants ranging in HLB values, Lo investigated the relationship of surfactant HLB on reducing P-gp efflux and demonstrated that surfactants with intermediate HLB values (10-17) were most effective at enhancing epirubicin accumulation into caco-2 cells (Lo, 2003).

It has been suggested that the membrane-lipid environment may play an important role in the mechanism of surfactant inhibition of P-gp mediated efflux. Woodcock *et al.* determined that concentrations of Cremophor EL® capable of increasing intracellular daunorubicin accumulation in a P-gp overexpressing human leukaemic cell line correlated with an increase in membrane fluidity (Woodcock *et al.*, 1992). Using isolated membranes from an MDR human epidermoid carcinoma cell line (KB 8-5-11), Dudeja *et al.* showed that surfactants capable of inhibiting P-gp efflux (Cremophor EL®, polysorbate 40, Solutol HS15) produced a decrease in the membrane fluidity (rigidification), while surfactants that failed to inhibit P-gp (octylglucoside) had no effect on membrane fluidity (Dudeja *et al.*,

1995). Variability in both membrane fluidization effects and P-gp inhibitory activity by surfactants have been demonstrated using the caco-2 human colon adenocarcinoma cell line and an MDR clone of the Madin Darby canine kidney (MDCK) cells (Rege *et al.*, 2002; Hugger *et al.*, 2002b). Cremophor EL® and polysorbate 80 were found to inhibit P-gp activity in the caco-2 cell line but not in the MDR-MDCK cell line (Hugger *et al.*, 2002b). The differences in P-gp inhibition between the different cell types could not be explained by differences in membrane fluidity, since Cremophor EL® did not alter membrane fluidity in either cell line, while polysorbate 80 produced an increased membrane fluidity in the two cell lines, but at different concentrations (Hugger *et al.*, 2002b). Rege *et al.* found that at concentrations capable of inhibiting P-gp activity in caco-2 cells, Vitamin E TPGS® rigidized the caco-2 cell membrane while Cremophor EL® and polysorbate 80 fluidized the cell membrane (Rege *et al.*, 2002). It is apparent that both an increase or decrease in membrane fluidity may result from the influence of surfactants on the membrane and that the relationship of membrane fluidity to P-gp inhibition may be cell specific.

1.4. Amphiphilic block copolymers

Block copolymers are polymeric macromolecules comprised of two or more different polymers (homopolymer) connected together. Block copolymers can be classified into three types based on their homopolymer arrangement. Firstly, diblock copolymers are designated AB and are composed of one segment of homopolymer A and another segment of homopolymer B (Yokoyama, 1992). Secondly, triblock copolymers may be configured into ABA / BAB or ABC configurations (Yokoyama, 1992). Thirdly, multi-segment copolymers contain alternate repeats of homopolymer A and B many times throughout the copolymer, designated $(AB)_n$ (Yokoyama, 1992). Although these are general descriptive classifications

for copolymers, numerous permutations can be developed using a combination of several homopolymer blocks. Segmentation of the individual polymer blocks within the same macromolecule allows for compartmentalization of each polymer's chemical and physical functionality, providing the beneficial properties of both homopolymers in the same macromolecule (Yokoyama, 1992). Such is the case for amphiphilic block copolymers composed of blocks with different affinity for polar (hydrophilic block) and non-polar (hydrophobic block) solvents. The most widely used hydrophilic block is poly(ethylene glycol) or poly(ethylene oxide) (abbreviated as PEG, POE, or PEO) with the hydrophobic block being the most variable portion including blocks such as poly(D,L-lactide), poly(β-benzyl L-apartate), poly(caprolactone), and poly(propylene oxide) (Table 1.2). The hydrophobic portion of block copolymers is frequently composed of non-toxic monomers that are biodegradable, for example: poly(D,L-lactide) and poly(caprolactone).

1.4.1. Micelle formation

When placed in a solvent that selectively dissolves one of the blocks, the amphiphilic nature of these block copolymers allows for the formation of polymeric micelles. Polymeric micelles are association colloids formed, for example, in an aqueous solvent, from the self-association and phase separation of the hydrophobic blocks forming a core structure that is interfacially stabilized by a 'shell' of the hydrophilic blocks (Figure 1.5) (Allen *et al.*, 1999a). The process of micellization, or self-assembly, for amphiphilic block copolymers is similar to low molecular weight surfactants and is entropically driven (Alexandridis *et al.*, 1994b). In an aqueous solution at low concentrations, single copolymer molecules exist separately and tend to reside at the air/water interface to remove the hydrophobic block from the aqueous phase in order to minimize free energy (ΔG) (Florence and Attwood, 1988;

Alexandridis *et al.*, 1994b). As the concentration of copolymer is increased, the hydrophilic block interacts with the aqueous solvent through intermolecular interactions, and to stabilize the hydrophobic block, water forms a structured/ordered arrangement around the block resulting in a decrease in the entropy of the water phase (Florence and Attwood, 1988; Alexandridis *et al.*, 1994b). Further increases in the concentration of the copolymer results in random interactions of the hydrophobic blocks between molecules and the displacement of the ordered water structuring surrounding the hydrophobic block (Florence and Attwood, 1988; Alexandridis *et al.*, 1994b). This loss of structured water increases the entropy of the water phase making the association of the hydrophobic blocks a favorable thermodynamic process. The concentration at which self-association occurs is called the critical micelle concentration (CMC). Balancing these association forces are the repulsive forces from the hydrophilic block due to steric and electrostatic interactions at the core-water interface. The balancing of these forces is a factor in determining the number of unimers forming the micelle (aggregation number), the CMC, and the size of the micelle (Allen *et al.*, 1999a).

Typically the CMC values for amphiphilic block copolymers are lower than that of low molecular weight surfactants and depending on the copolymer block architecture, CMC's for block copolymers can range from 10^{-6} – 10^{-7} M compared to low molecular weight surfactants which are in the range of 10^{-3} – 10^{-4} M (Adams *et al.*, 2003). The lower CMC value suggests that micelles formed from amphiphilic block copolymers are more thermodynamically and kinetically stable than low molecular weight surfactants owing to greater intermolecular interactions between the hydrophobic blocks (Yokoyama, 1992; Allen *et al.*, 1999a; Torchilin, 2001; Adams *et al.*, 2003). Block copolymers with low CMC values may resist disassociation when diluted to concentrations below the CMC or require extended

Table 1.2: Some examples of amphiphilic block copolymers

Diblock Copolymer	Reference
poly(ethylene glycol)-*b*-poly(D,L-lactide) 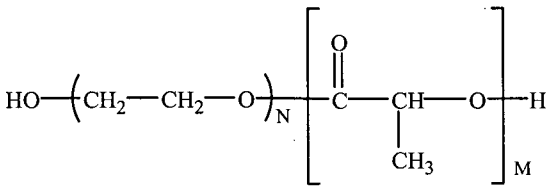	(Burt *et al.*, 1999) (Liggins and Burt, 2002) (Zhang *et al.*, 1996b) (Lee *et al.*, 2004) (Kim *et al.*, 2001)
poly(ethylene oxide)-*b*-poly(β-benzyl L-aspartate) 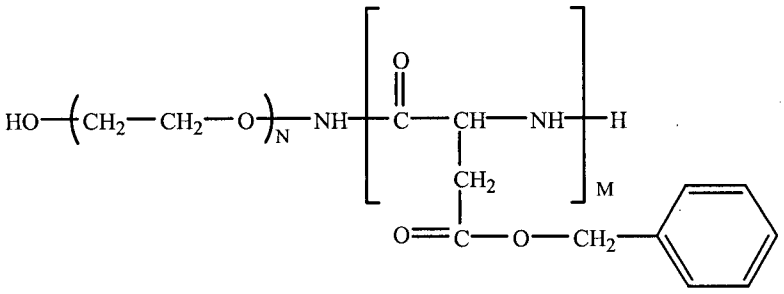	(Kwon *et al.*, 1997) (Kwon *et al.*, 1994) (Kataoka *et al.*, 2000) (Kwon *et al.*, 1994) (Yokoyama *et al.*, 1998b)
poly(ethylene glycol)-*b*-poly(caprolactone) 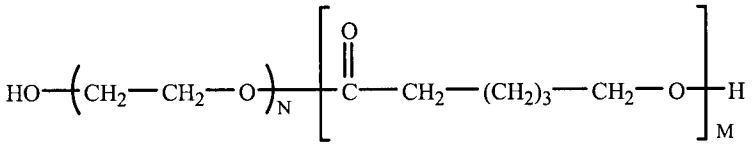	(Allen *et al.*, 1998) (Allen *et al.*, 2000) (Shin *et al.*, 1998) (Zhou *et al.*, 2003) (Soo *et al.*, 2002)
Triblock Copolymer	
poly(ethylene oxide)-*b*-poly(propylene oxide)-*b*-poly(ethylene oxide) (also called Pluronic® or poloxamer) 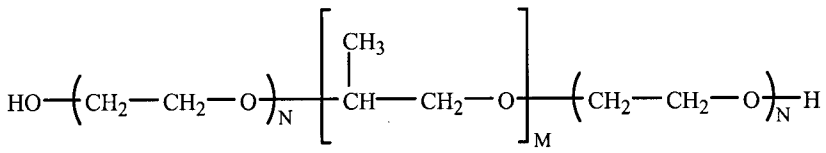	(Kabanov *et al.*, 1989) (Kabanov *et al.*, 1992) (Kabanov *et al.*, 1995) (Kabanov *et al.*, 2002a)

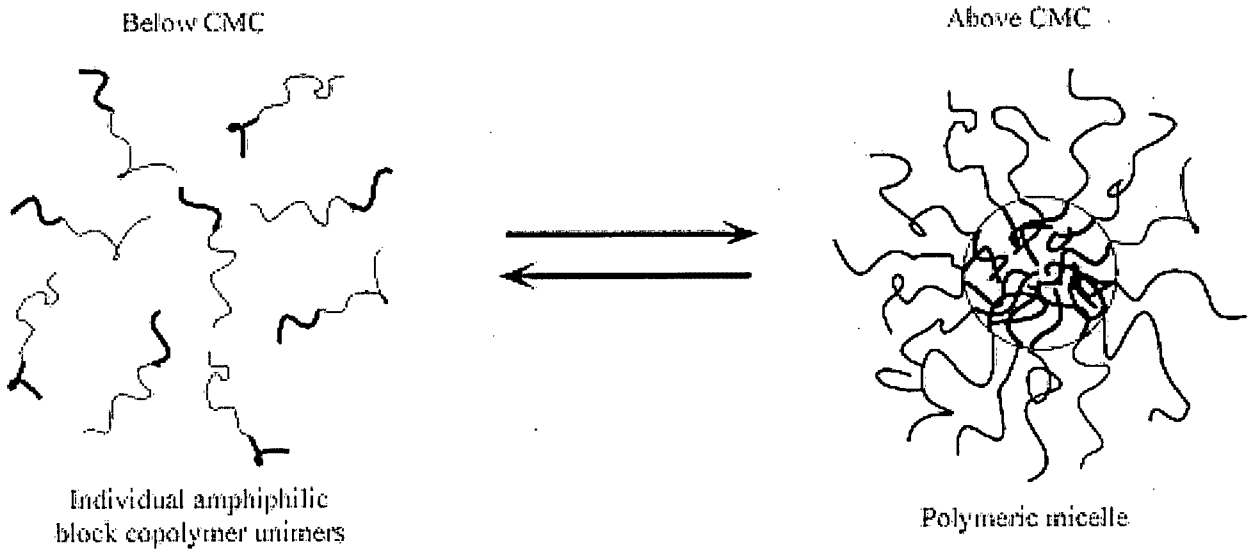

Figure 1.5: A schematic of amphiphilic block copolymer micellization. Below the critical micelle concentration (CMC) the amphiphilic block copolymer exists as unimers in solution. Above the CMC the copolymer are present in equilibrium as micelles. Figure adapted from (Lavasanifar *et al.*, 2002).

periods of time to disassemble compared to low molecular weight surfactants (Allen *et al.*, 1999a).

1.4.2. Application in drug delivery

The use of amphiphilic block copolymer micelles as drug delivery systems has received increasing attention due to their versatility and advantages over other colloidal drug delivery systems. Copolymers with varying structural features and block lengths can be synthesized, allowing for a controlled manipulation of their physical and chemical properties for applications with specific drugs (Liu *et al.*, 2004). One of the primary uses of polymeric micelles is for the solubilization of hydrophobic drugs that have poor aqueous solubility (Kwon *et al.*, 1994; Zhang *et al.*, 1996b; Zhang *et al.*, 1996b; Yokoyama *et al.*, 1998b). Drugs can be either incorporated into polymeric micelles by physical or chemical entrapment techniques. Physical entrapment involves the mixing of drug and copolymer followed by micellization, which allows the drug to partition into the hydrophobic core. Using physical entrapment techniques with methoxypoly(ethylene glycol)-*b*-poly(D,L-lactide) diblock copolymer, Zhang *et al.* demonstrated that the solubility of the hydrophobic drug paclitaxel could be increased by 20-40 fold depending on the length of either the hydrophilic or hydrophobic blocks (Zhang *et al.*, 1996b). Alternatively, chemical conjugation of the drug to the hydrophobic block via degradable linkers has been evaluated as a means to control the extent of drug entrapment (Kwon *et al.*, 1994; Kwon *et al.*, 1995; Yokoyama *et al.*, 1998a; Li and Kwon, 2000; Yoo and Park, 2001). Another growing area of block copolymer research is the use of block ionomer micelles for drug delivery of polyanionic molecules such as oligonucleotides (Katayose and Kataoka, 1998; Kakizawa and Kataoka, 2002). Block ionomers are similar to amphiphilic block copolymers except that the hydrophobic block is

replaced with a polycationic block such as poly(lysine). Stoichiometric complexation with a polyanionic molecule results in charge neutralization that decreases the aqueous solubility of the complex, forming an amphiphilic species that can self-associate above the CMC. Complexation and sequestration of the polyanionic molecule within the core of the micelle has been shown to protect the polynucleotide from nuclease degradation and enhance cellular uptake (Kakizawa and Kataoka, 2002)

An important aspect of block copolymers and polymeric micelles is their potential as a long circulating drug delivery system *in vivo*. The utilization of poly(ethylene glycol) as the hydrophilic block surrounding the micelle can reduce protein adherence (opsonization) and minimize uptake by the phagocytic cells of the reticuloendothelial system, allowing the drug entrapped within the micelles to have a prolonged circulation (Kwon *et al.*, 1994). Additionally, polymeric micelles typically range from 10-100 nm in diameter which may allow for extravasation to tissue sites for passive targeting of drugs (Jones and Leroux, 1999; Torchilin, 2001). Antibody mediated targeting of polymeric micelles can also be achieved by the synthesis of functional groups on the end of the PEG chain which is then used to link immunoglobulins that can target specific antigens on various cellular targets (Yokoyama, 1992).

1.4.3. Application in modulating P-gp activity

Similar to low molecular weight surfactants described in section 1.3.5, amphiphilic block copolymers have demonstrated a modulating effect on drug efflux transporters. To date only Pluronic® triblock copolymers have been evaluated as modulators of drug efflux transporters (Kabanov *et al.*, 2002b; Kabanov *et al.*, 2003). Pluronic® triblock copolymers, also called poloxamers, are composed of hydrophilic polyethylene oxide (PEO) and

hydrophobic polypropylene oxide in an ABA arrangement: $PEO_{n/2}$-PPO_m-$PEO_{n/2}$ (Table 1.2). In an aqueous solvent, Pluronic® copolymers can form micelles capable of solubilizing hydrophobic drugs and by varying the lengths of each blocks, Pluronic® copolymers with different CMC's, HLB's, and solubilization capabilities can be attained (Alexandridis *et al.*, 1994a; Alexandridis *et al.*, 1994b; Kabanov *et al.*, 1995; Nagarajan and Ganesh, 1996; Kozlov *et al.*, 2000).

The use of Pluronic® to overcome MDR was first reported by Paradis *et al.*, where Pluronic P85® micelles loaded with daunorubicin were shown to increase cellular accumulation and lower IC_{50} of daunorubicin in an MDR ovarian carcinoma cell line (SKVLB) compared to free daunorubicin (Paradis *et al.*, 1994). In the sensitive/parental line (SKOV-3) daunorubicin loaded Pluronic P85® micelles had little or no effect on cellular accumulation or toxicity compared to free daunorubicin (Paradis *et al.*, 1994). Similar results were obtained with other MDR drugs such as doxorubicin, epirubicin, vinblastine and mitomycin C in the same MDR ovarian carcinoma cell line (SKVLB) (Alakhov *et al.*, 1996). Pluronic® copolymers have been shown to increase the cellular accumulation and permeability of P-gp substrates across cell line models for intestinal epithelia (Caco-2) and the blood brain barrier capillary endothelial (bovine brain microvessel endothelial cells: BBMEC) (Miller *et al.*, 1997; Batrakova *et al.*, 1998a; Batrakova *et al.*, 1999). Similar to the action of low molecular weight surfactants, Pluronic® was also reported to inhibit MRP activity in a human pancreatic adenocarcinoma cell line (Panc-1) (Miller *et al.*, 1999).

The concentrations of Pluronic® copolymers shown to inhibit efflux pump activity were similar to those of other surfactants in which activity was maximal at or below the CMC of the Pluronic® copolymer (Miller *et al.*, 1997; Batrakova *et al.*, 1998a; Batrakova *et*

al., 1998b). Higher concentrations of Pluronic® above the CMC resulted in a decrease in the modulating activity and was attributed to sequestration of the substrate as well as possible endocytosis and internalization of loaded micelles that underwent recirculation back out into the extracellular milieu (Miller *et al.*, 1997; Batrakova *et al.*, 1998a; Batrakova *et al.*, 1998b). Structure activity relationships comparing different Pluronic® copolymers with varying lengths of the hydrophilic and hydrophobic blocks demonstrated that Pluronic® copolymers with intermediate hydrophobicity were greater at enhancing the cellular accumulation of P-gp substrates (Batrakova *et al.*, 1999).

Previous work with other surfactants suggests that membrane fluidity changes may result in a reduction in P-gp ATPase activity (see section 1.3.5). Studies using Pluronic® copolymers have shown that additional factors likely contribute to the mechanism of P-gp modulation by amphiphilic block copolymers. Kabanov *et al.* have observed that Pluronic® copolymers capable of reducing P-gp activity can elicit a marked ATP depletion within the cell (Batrakova *et al.*, 2001; Batrakova *et al.*, 2001; Kabanov *et al.*, 2001). Since the action of drug efflux transporters, such as P-gp, depend on ATP hydrolysis for pump activity, it is likely that ATP depletion, in combination with membrane lipid interaction effects causing reduced ATPase activity, may contribute to the ability of Pluronic® copolymers to inhibit efflux activity (Batrakova *et al.*, 2001). Understanding how Pluronic® copolymers reduce ATP levels in the cell is still currently under investigation and may involve interactions of Pluronic® with mitochondrial membranes with subsequent disruption of electron transport (Rapoport *et al.*, 2000). This would imply that Pluronic® unimers must be able to enter the cell and interact with mitochondrial membranes. To determine whether Pluronic® can enter cells, Batrakova *et al.* labeled Pluronic P85® with the fluorescent probe, fluorescein, and

showed a strong intracellular fluorescence of BBMEC cells attributed to fluorescein-Pluronic®, suggesting that Pluronic® can pass through the cell membrane and enter the cytoplasm (Batrakova *et al.*, 2001).

1.5. THESIS RATIONALE AND RESEARCH OBJECTIVES

1.5.1. Rationale

There are a large number of drugs that are subject to efflux transport by P-gp and possess poor or variable oral absorption and bioavailability. Inter- and intra-patient variability in intestinal P-gp expression, possible drug-drug interactions involving co-administered P-gp substrates, inhibitors and inducers, and the dose-dependent absorption due to saturation of P-gp can lead to dangerous and unpredictable variability in the disposition of P-gp substrates (Troutman and Thakker, 2003a). Thus, the inhibition of efflux transport proteins in the gastrointestinal epithelium has become a very important issue in improving oral drug delivery. A common means to enhance drug bioavailability is to use surfactants to enhance the permeability of the drug across the intestinal epithelium. Recently, nonionic polyethoxylated surfactants and amphiphilic block copolymers have both been shown to enhance intracellular accumulation of hydrophobic probes and drugs, via inhibition of P-gp mediated drug efflux. It has been suggested that these surfactants integrate within the cell membrane and inhibit P-gp ATPase activity by modulating the properties of the lipid bilayer. It is clear that not only is this mechanism poorly understood, but also the effects of surfactants on enhancing the passive transmembrane diffusion of P-gp substrates have not been addressed. Since lipophilicity of P-gp substrates appears to be a strong determinant of the effectiveness of P-gp mediated efflux as well as an important parameter for passive transmembrane diffusion, the effect of surfactants on overcoming P-gp mediated efflux may be further dependent on

the degree of P-gp substrate hydrophobicity. Therefore, we postulate that the enhancement in cellular permeability of P-gp substrates by surfactants, and in particular amphiphilic diblock copolymers, is strongly influenced by the nature of both the substrate and the surfactant. The goal of this work is to enhance our understanding of the complex relationship between the lipid-membrane environment, P-gp substrate lipophilicity, and the ability of surfactants to modulate P-gp mediated efflux.

1.5.2. Research objectives

1. To synthesize and characterize a novel series of low molecular weight amphiphilic diblock copolymers based on methoxypoly(ethylene glycol) and poly(caprolactone) denoted as MePEG-*b*-PCL.
2. To investigate the effect of MePEG-*b*-PCL block composition on the cellular accumulation of P-gp substrates.
3. To examine the effects of MePEG-*b*-PCL block copolymers on cellular accumulation and transepithelial flux of P-gp substrates differing in lipophilicity.
4. To determine the cellular uptake pathways contributing to enhanced accumulation of P-gp substrates by MePEG-*b*-PCL block copolymers.

Chapter 2

SYNTHESIS AND CHARACTERIZATION OF METHOXYPOLY(ETHYLENE GLYCOL)-*BLOCK*-POLY(CAPROLACTONE) DIBLOCK COPOLYMERS

2.1. INTRODUCTION

The hydrophilic block of a diblock copolymer is generally composed of poly(ethylene glycol), but recently, hydrophilic blocks composed of poly(2-ethyl-2-oxazoline) (Kim *et al.*, 2000; Lee *et al.*, 2003), poly(N-vinyl-2-pyrrolidone) (Benahmed *et al.*, 2001), and poly(N-iso-propylacrylamide) (Leroux *et al.*, 2001) have also been used. The greatest diversification in amphiphilic copolymers arises from the many different hydrophobic blocks which have been synthesized for pharmaceutical applications, such as poly(glycolic acid) (Kim *et al.*, 1999), poly(D,L-lactide) (Burt *et al.*, 1999), poly(caprolactone) (Shin *et al.*, 1998), poly(propylene oxide) (Nagarajan and Ganesh, 1996). Copolymers of the above polymers have also been synthesized as hydrophobic blocks, for example, poly(D,L-lactide-co-caprolactone) (Burt *et al.*, 1999).

The synthesis of amphiphilic block copolymers typically involves a process devoid of termination reactions called "living polymerization". Since there are no termination reactions, the degree of polymerization (DPN) of a block is dependent on the monomer:initiator ratio (M/I), producing blocks of specific lengths and a high degree of monodispersity. The synthesis of linear amphiphilic block copolymers can be done using several different methods. Firstly, sequential anionic polymerization involves initiation by an anionic initiator such as diphenylmethylsodium or potassium with an alkene or cyclic monomer, followed by the propagation of the monomer. After allowing monomer A to polymerize to completion, monomer B is added, propagating from the "living" end of the

polymer chain formed from monomer A. This method has been used to make copolymers such as poly(styrene)-poly(ethylene oxide)-poly(caprolactone) by first synthesizing poly(styrene) via anionic polymerization and then continuing the synthesis by adding ethylene oxide and finally caprolactone (Arnal *et al.*, 2001). This sequential synthesis is very convenient since no re-initiation is required for the propagation of another block and large molecular weight blocks can be formed since there is no termination reaction, allowing the reaction to proceed until no more monomer exists. A second way of making block copolymers is by interchain coupling of preformed oligomers that have terminal reactive groups. This method can produce predetermined sizes of the blocks since varying oligomer sizes can be utilized, but this method has the disadvantage of requiring a purification step to remove unreacted oligomer contaminates. The most common way of making block copolymers is to grow the second block from a preformed oligomer of the first block. The use of mono or difunctional reactive sites on the oligomer produces AB or ABA type block copolymers, respectively. For example, diblock (AB) and triblock (ABA) copolymers of poly(ethylene glycol) and poly(caprolactone) have been synthesized by using either the monofunctional methoxypoly(ethylene glycol) (MePEG) or the difunctional poly(ethylene glycol) as initiators (Bogdanov *et al.*, 1998).

Above the critical micelle concentration, amphiphilic diblock copolymers self-associate in the presence of a solvent that selectively dissolves one of the blocks. In an aqueous environment, the hydrophobic blocks will associate to exclude them from water and form a core, which is stabilized by the hydrophilic blocks of the copolymer forming a shell around it. Polymeric micelles have been used to enhance the solubility of hydrophobic drugs and for delivery of numerous drugs such as paclitaxel, indomethacin, amphotericin B,

adriamycin, and dihydrotestosterone (Zhang *et al.*, 1996b; Yu *et al.*, 1998; Shin *et al.*, 1998; Yokoyama *et al.*, 1998a; Allen *et al.*, 2000). Diblock copolymers composed of poly(ethylene glycol) of MW 2000 with various lengths of poly(caprolactone) (PCL) ranging from a DPN of 14 – 150 have been synthesized and characterized for solubilization and delivery of dihydrotestosterone or neurotrophic agents (Allen *et al.*, 1998; Yu and Eisenberg, 1998; Allen *et al.*, 2000). Indomethacin and paclitaxel have been loaded into diblock copolymers composed of MePEG of 5000 MW and PCL length ranging from 22-110 repeat units (Kim *et al.*, 1998; Shin *et al.*, 1998; Kim and Lee, 2001; Kim *et al.*, 2001). Other groups have synthesized and characterized PEG-*b*-PCL diblock copolymers with molecular weights of 17000 – 25000 (Bogdanov *et al.*, 1998; Gan *et al.*, 1999). Overall, the diblock copolymers produced by these groups were relatively hydrophobic due to the large size of the PCL block and required specialized methods to solubilize the diblock for the formation of micelles. Diblock copolymers were first dissolved in a water miscible solvent such as dimethylformamide or tetrahydrofuran and water was introduced slowly to induce aggregation of the diblock copolymers into micelles and the solution was then dialyzed against water to remove the solvent (Allen *et al.*, 1999a).

Initially, the effect of diblock copolymers on modulating P-gp mediated efflux was screened using several diblock compositions, such as MePEG-*b*-poly(D,L-lactide), MePEG-*b*-poly(glycolide), and MePEG-*b*-poly(caprolactone) (MePEG-*b*-PCL). Results with MePEG-*b*-PCL were promising and this diblock was selected for further study. In order to evaluate structure activity relationships and the effect of diblock physicochemical properties on modulation of P-gp efflux, a series of low molecular weight MePEG-*b*-PCL diblock copolymers were produced. The objective of this chapter was to synthesize and characterize a

novel series of low molecular weight amphiphilic diblock copolymers based on methoxypoly(ethylene glycol) and poly(caprolactone).

2.2. EXPERIMENTAL

2.2.1. Materials

Caprolactone (CL) monomer and MePEG with molecular weights of 550, 750, and 2000 were purchased from Fluka (Oakville, ON). Stannous 2-ethylhexanoate ($Sn(Oct)_2$) and 1,6-diphenyl-1,3,5-hexatriene (DPH) were from Sigma-Aldrich (Oakville, ON). HPLC grade chloroform ($CHCl_3$) was obtained from Fisher Scientific (Nepean, ON). Deuterated $CHCl_3$ ($CDCl_3$) was obtained from Cambridge Isotope Laboratories Inc. (Andover, MA). Poly(ethylene glycol) (PEG) molecular weight standards ranging from 106 to 6450 g/mol were from Polymer Laboratories (Amherst, MA). Hanks balanced salt solution (HBSS) without phenol red and *N*-(2-hydroxyethyl)piperazine-*N'*-2-ethanesulfonate (hepes) was obtained from Invitrogen (Grand Island, NY).

2.2.2. Synthesis of methoxypoly(ethylene glycol)-*block*-poly(caprolactone)

Various weight ratios of MePEG with molecular weight (MW) of 550, 750, or 2000 and CL were added into a 100 mL round bottom flask to a total weight of 50g. A teflon coated magnetic stir bar was introduced and the flask was submersed in a 140^0C heavy mineral oil bath. The reactants were allowed to mix and melt (for MePEG 2000) with gentle stirring for 15 min after which 0.15 mL of $Sn(Oct)_2$ was added. The flask was then sealed using a glass stopper and the reactants were allowed to react for 24h at 140^0C.

2.2.3. Gel permeation chromatography (GPC)

Gel permeation chromatography (GPC) was used to determine the MW and MW distribution of MePEG-*b*-PCL diblock copolymers. The GPC configuration was a Waters

(Mississauga, ON) 717*plus* autosampler, 515 HPLC pump, and 2410 refractive index detector. Two GPC columns connected in series were utilized, one a Styragel HR3 and another a HR0.5 (Waters, Mississauga, ON), with $CHCl_3$ as mobile phase at a flow rate of 1.0 mL/min and helium sparge. Millennium[32] v3.2 GPC software was used for instrument control and data analysis. The number average molecular weight (Mn) and weight average molecular weight (Mw) were determined by preparing a calibration curve based on PEG molecular weight standards and quantitated according to peak retention time. All calibration curves used were generated using Millennium[32] v3.2 GPC software and were prepared before each sample set. A representative calibration curve is shown in Figure 2.1

2.2.4. Nuclear magnetic resonance spectrometry (NMR)

Polymerization products were assessed for PCL degree of polymerization and molar ratio of MePEG:PCL using ^{1}H-NMR. A 10% w/v sample was prepared in $CDCl_3$ and analyzed at 300 mHz using a Bruker AV300 spectrometer. The spectral data were analyzed in terms of peak position and integrated area using MestRe-C 2.3a software.

2.2.5. Critical micelle concentration (CMC)

The CMC for each MePEG-*b*-PCL diblock copolymer was determined by fluorescence spectroscopy using the hydrophobic probe DPH. Serial dilutions of each diblock copolymer in HBSS + 10mM hepes pH = 7.4 were incubated at 37^{0}C protected from light with 10 μM DPH for 24 h. Aliquots of 200 μL of each sample were then placed into a 96 well flat bottom plate and the fluorescence intensity measured using a CytoFluor 400 microplate reader (PerSeptive Biosystems, Framingham, MA) with λ_{EX} = 360 and λ_{EM} = 460. The CMC inflexion point was not well defined, thus linear regression from various points of the upper and lower asymptotes of the curve was performed. This provided a range

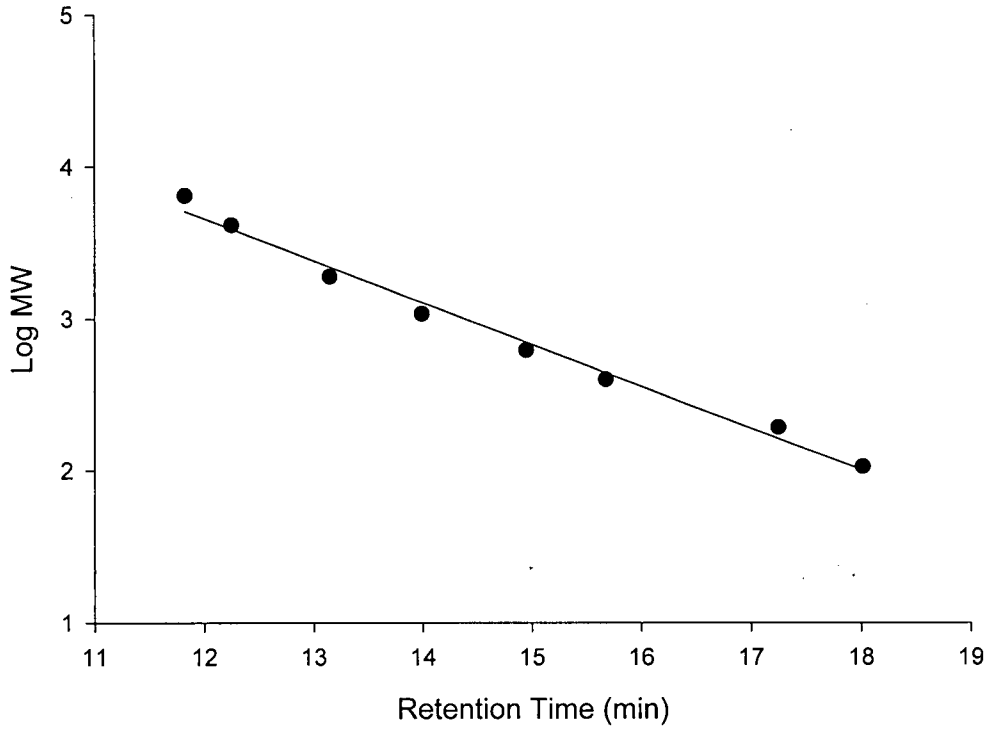

Figure 2.1. Representative GPC calibration curve prepared with PEG molecular weight standards. Mobile phase was $CHCl_3$ at a flow rate of 1 mL/min through two Styragel columns (HR3 and HR0.5) connected in series. Refractive index was used for peak detection.

Regression analysis: $y = -0.275x + 6.96$ $R^2 = 0.988$

of CMC values for each curve, which was then averaged and reported as mean +/- standard deviation.

2.2.6. Micelle size

Light scattering measurements were carried out on a Malvern 3000HS Zetasizer (San Bernardino, CA) with a He-Ne laser (λ = 532nm) and 90^0 collecting optics. Diblock copolymer samples were prepared with HBSS + 10mM hepes pH=7.4 and filtered using a 0.22 μm syringe filter (Millipore, Bedford, MA) prior to measurement. All measurements were done at 37^0C and samples were allowed to equilibrate for 15 min prior to measurement. Data were analyzed using CONTIN algorithms provided by Malvern Zetasizer software and reported as the Z-average as an approximation for the hydrodynamic diameter of the micelles.

2.2.7. Hydrophilic-Lipophilic Balance (HLB)

The HLB was calculated for each diblock copolymer based on the Griffin equation for a series of polyethoxylated amphiphilic compounds (Shin *et al.*, 1998).

$$HLB = 20\left[\frac{M_H}{M_L + M_H}\right] \qquad \text{Equation 2.1}$$

Where, M_H = MW of the hydrophilic block (MePEG) and M_L = MW of the lipophilic block (PCL).

2.3. RESULTS

2.3.1. Synthesis of MePEG-*b*-PCL diblock copolymers

A series of amphiphilic diblock copolymers based on MePEG with MW of 550, 750, and 2000 were synthesized by ring opening polymerization initiated by the free hydroxyl on MePEG. The basic structure of the synthesized diblock copolymers and the synthesis scheme is shown in Scheme 2.1. Table 2.1 summarizes the series of diblock copolymers

synthesized. The theoretical monomer:initiator ratio describes the predicted DPN of PCL after the polymerization has gone to completion. A series of diblock copolymers with increasing PCL length were prepared for MePEG 750, and for the MePEG 550 and 2000 series, diblock copolymers with a fixed length of approximately 5 PCL repeat units were prepared. This design allowed for comparisons of block length by fixing the length of the MePEG chain and varying PCL length, or vice versa.

Time course experiments for the MePEG-*b*-PCL synthesis reaction were performed to determine the degree of caprolactone conversion. Samples with a 60:40 (MePEG 750:CL) feed ratio were prepared and allowed to polymerize for various times ranging from 0 to 24 h. Gel permeation chromotography (GPC) was used to assess the change in MW and the amount of unreacted caprolactone. Figure 2.2 shows chromatographs of these samples. Time zero shows the chromatographs for the monomers before polymerization for MePEG 750 at a retention time of 13.8 min and caprolactone at 17.4 min. By 8 hours, the caprolactone peak was undetectable while the MePEG peak shifted to an earlier retention time indicative of a MW increase as the polymerization proceeds.

A calibration curve for caprolactone was prepared for quantitation of the amount of unreacted caprolactone at various reaction times. A plot of diblock MW and percent unreacted caprolactone as a function of reaction time is shown in Figure 2.3. The MW of the diblock and the percentage of unreacted caprolactone began to plateau after a reaction time of 8 hours. Therefore, a reaction time of 8 hours or more was sufficient to ensure complete conversion of caprolactone.

GPC results demonstrated a single peak for each diblock copolymer synthesized, which shifted to a shorter retention time than the corresponding MePEG oligomer suggesting

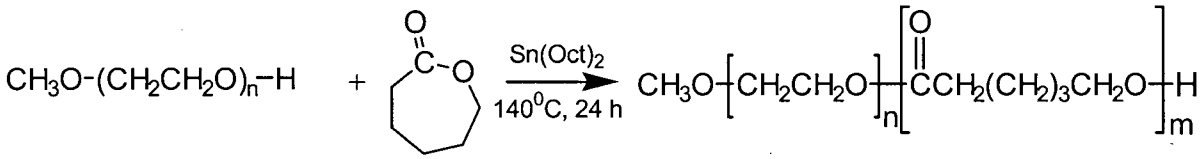

Methoxypoly(ethylene glycol) **Caprolactone** **MePEG-*b*-PCL**

Where, n = degree of polymerization for MePEG = MW / 44

Thus for MePEG 550 n = 12
750 n = 17
2000 n = 45

m = Degree of polymerization of PCL - determined by ^{1}H NMR

Scheme 2.1. Polymerization scheme and structure of MePEG-*b*-PCL diblock copolymers

Table 2.1. Synthesis and characterization data for methoxypoly(ethylene glycol)-*block*-poly(caprolactone) diblock copolymers

Series	Feed Ratio[a]	M/I		Structure / DPN[d]	MW		PDI[g]	HLB	CMC[h] (μM)	Micelle Size[i] (nm)
		Calc.[b]	Expt.[c]		Calc.[e]	Expt.[f]				
MePEG 550	50:50	4.81	4.35	$MePEG_{12}$-*b*-PCL_4	1100	1195	1.12	9.2	66.9 +/- 8.36	N/D
MePEG 750	80:20	1.64	1.75	$MePEG_{17}$-*b*-PCL_2	937	1018	1.09	16.6	2970 +/- 95	12.2 +/- 0.7
	60:40	4.38	4.65	$MePEG_{17}$-*b*-PCL_5	1250	1277	1.10	12.2	243 +/- 70.5	14.6 +/- 0.1
	40:60	9.86	10.1	$MePEG_{17}$-*b*-PCL_{10}	1875	1893	1.10	8.4	5.28 +/- 1.58	19.1 +/- 1.0
MePEG 2000	80:20	4.38	4.53	$MePEG_{45}$-*b*-PCL_5	2500	2467	1.11	18.3	267 +/- 24.3	95.1 +/- 4.1

a) Feed weight ratio of MePEG:caprolactone
b) Calculated monomer:initiator (M/I) based on feed weight ratio.
Where M = mols of caprolactone and I = mols of MePEG
c) Monomer:initiator ratio determined by ^{1}H-NMR. Calculated by comparing the relative peak areas of caprolactone at 1.6 + 1.3 ppm (equivalent to 6 protons) to the MePEG peak at 3.3 ppm (equivalent to 3 protons).
d) Degree of polymerization (DPN) of MePEG = MW_{Mepeg} /44
DPN of PCL = rounded off M/I determined by NMR
e) Calculated molecular weight based on the feed weight ratio.
Eg: MePEG 750 at a feed ratio of 80:20 will have 80% of the final MW = 750 g/mol
Therefore, 100/80=X/750 X = 937 g/mol
f) Average number molecular weight (Mn) determined by GPC
g) Polydispersity index, determined from GPC. PDI = Mw/Mn
h) Calculated using Mn from GPC
i) Mean Z-Average diameter

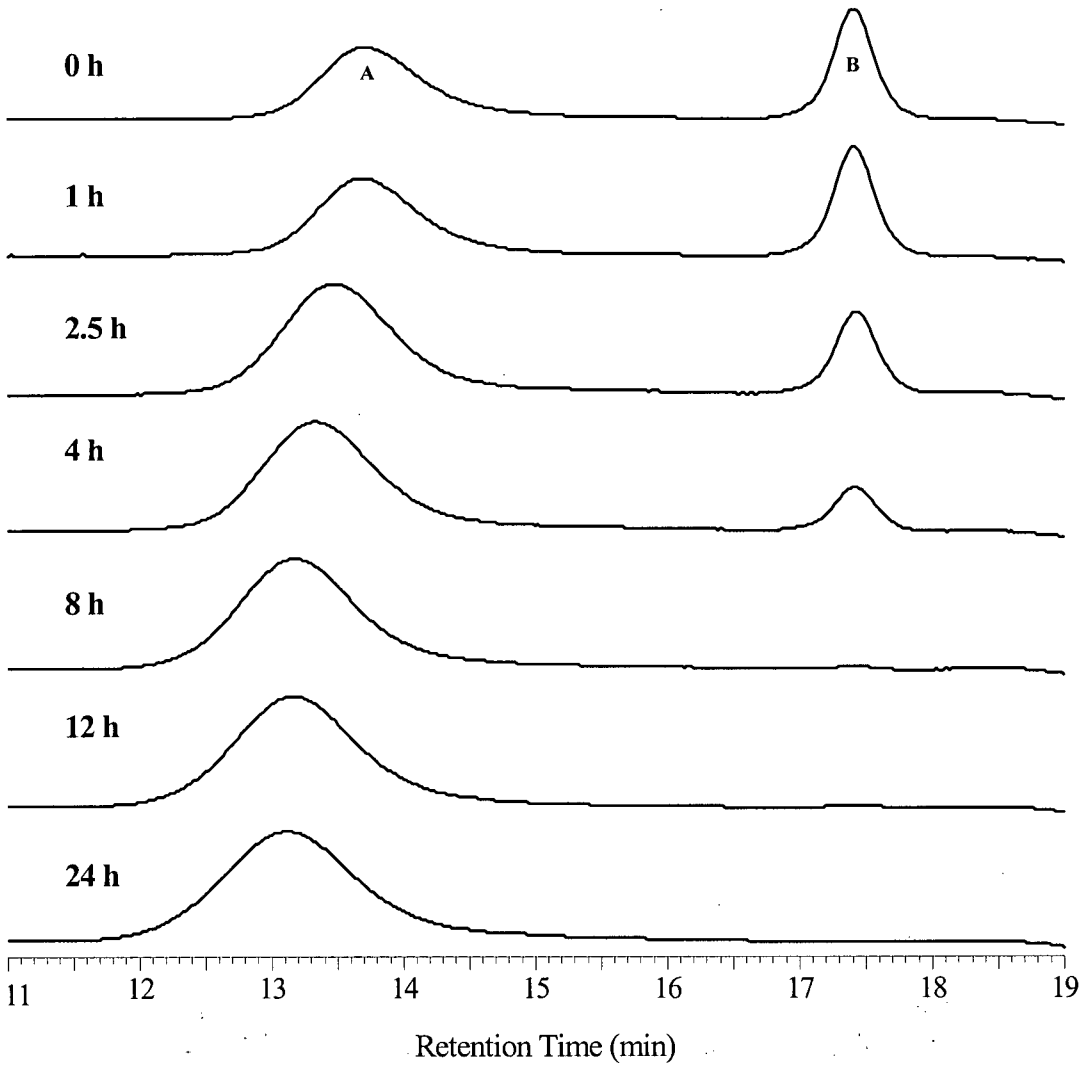

Figure 2.2. GPC chromatographs of MePEG-*b*-PCL polymerization (60:40 MePEG 750:CL feed ratio) after indicated reaction times. Peak A represents MePEG 750 and Peak B is unreacted caprolactone.

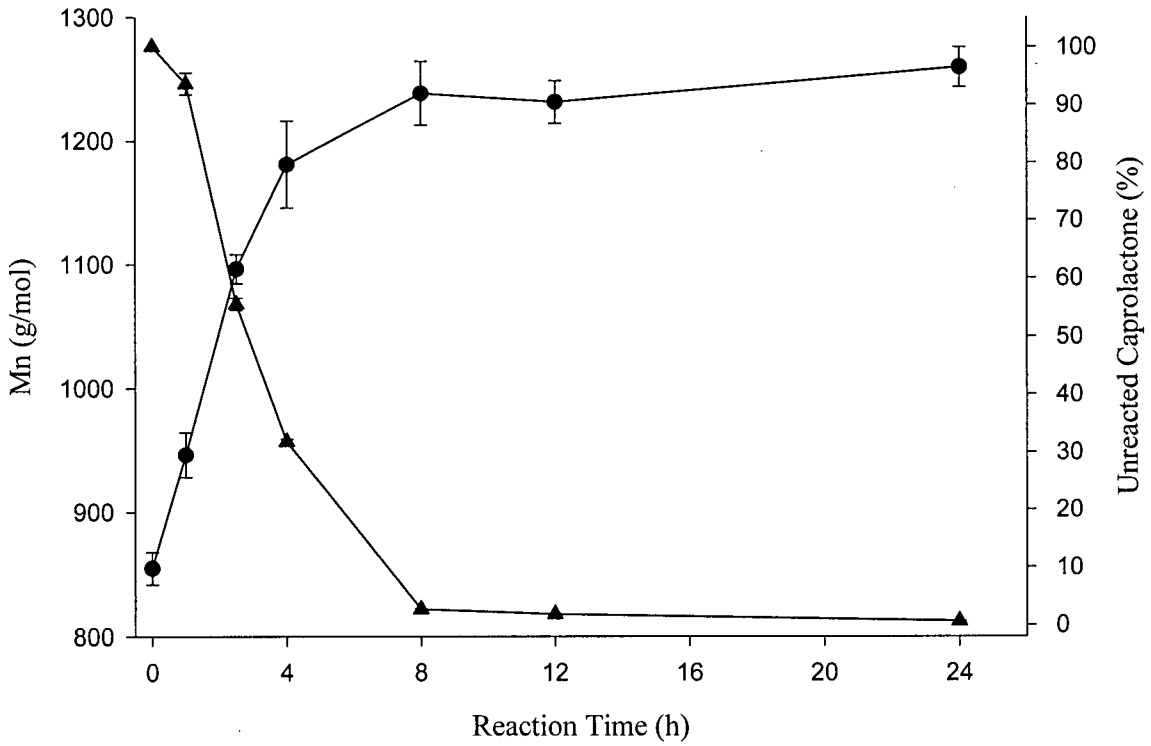

Figure 2.3. The effect of reaction time on the MW of MePEG-*b*-PCL (●) and the percentage of unreacted caprolactone (▲).

an increase in molecular weight (Figure 2.4). No peaks were seen for caprolactone monomer or homopolymer. The molecular weight determined by GPC was very close to the calculated theoretical molecular weight as summarized in Table 2.1. The polydispersity index (PDI) was close to 1 for all diblock copolymers, signifying a narrow molecular weight distribution. The HLB of the diblock copolymers decreased with increasing PCL length and increased from 9.2 to 12 to 18 with increasing length of MePEG with a similar PCL length (Table 2.1). Higher HLB values indicate more hydrophilic amphiphiles and lower HLB values indicate more lipophilic amphiphiles.

^{1}H-NMR spectra of the reactants, MePEG and caprolactone, and a representative spectrum for MePEG-*b*-PCL with the proton assignments are shown in Figure 2.5, 2.6, and 2.7, respectively. Two single peaks can be seen for the unreacted and reacted MePEG oligomer, one at 3.6 ppm from the methylene protons of the oxyethylene repeat unit, and one at 3.3 ppm for the terminal methoxy group (Figure 2.5 and 2.7). A shift upstream in the cyclic caprolactone monomer peaks α (2.5 ppm) and β + β* (1.7 ppm) to positions ε (2.2 ppm), ϕ (1.6 ppm), and γ (1.3 ppm) was observed by comparing the NMR of the caprolactone monomer to the reacted MePEG-*b*-PCL diblock copolymer (Figure 2.6 and 2.7). The appearance of the δ peak at 4.1 ppm for the methylene protons in the last repeat unit of MePEG, demonstrated that poly(caprolactone) polymerized onto MePEG.

The degree of polymerization for PCL was obtained by comparing the integrated peak area of the MePEG block to PCL. The peaks used to establish the degree of polymerization for the PCL block are the combined peak area at 1.6 and 1.3 ppm (ϕ + γ) from the methylene protons of the caprolactone repeat unit to the single resonance peak at 3.3 ppm (α) for the methylene protons of the terminal methoxy group of MePEG (Figure 2.7). The copolymer

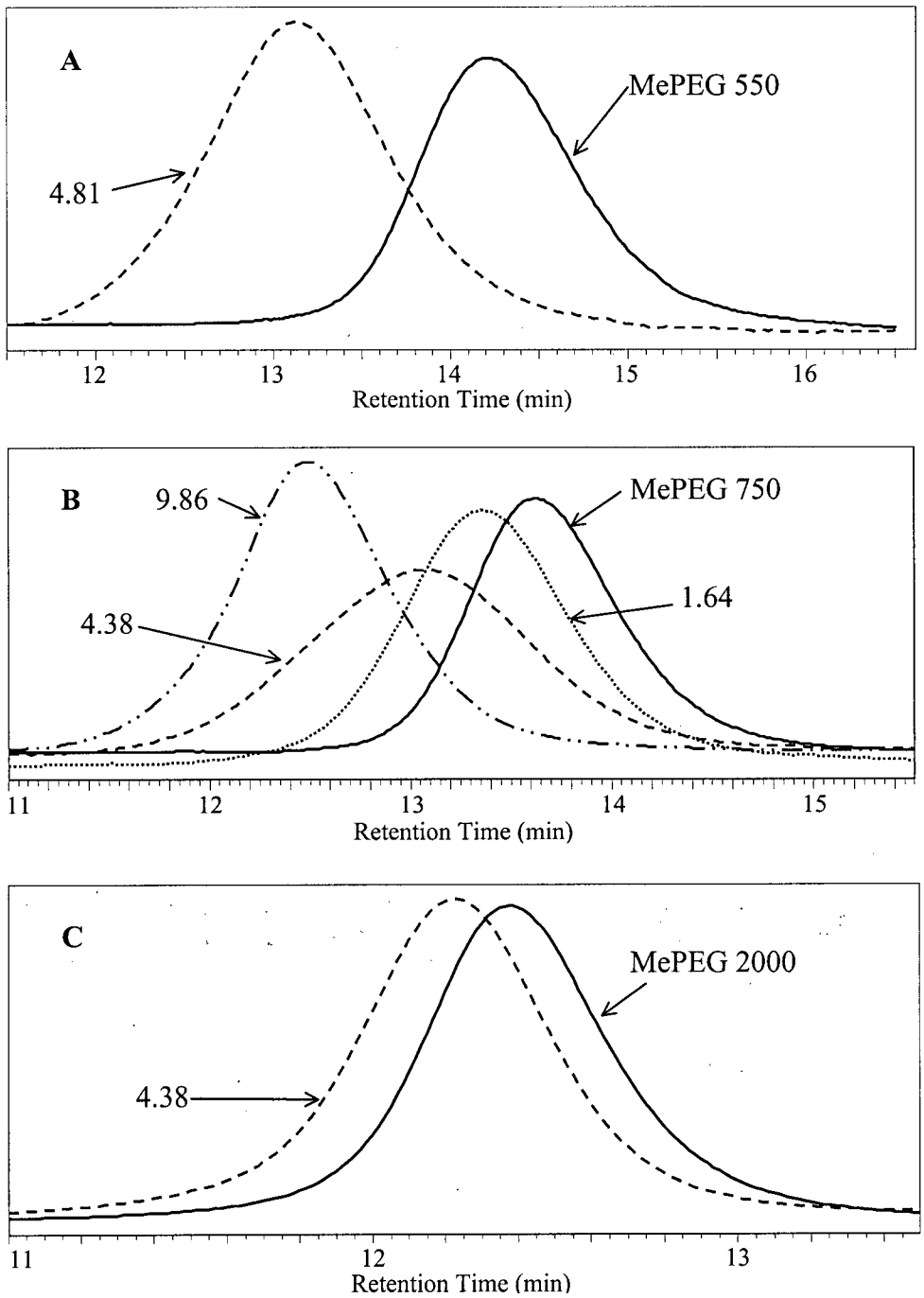

Figure 2.4. GPC chromatographs of MePEG-*b*-PCL diblock copolymers. (A) MePEG 550 series, (B) MePEG 750 series, and (C) MePEG 2000 series. Labeled on the chromatographs is MePEG oligomer before polymerization and the corresponding theoretical M/I ratios for each diblock in the series according to Table 2.1.

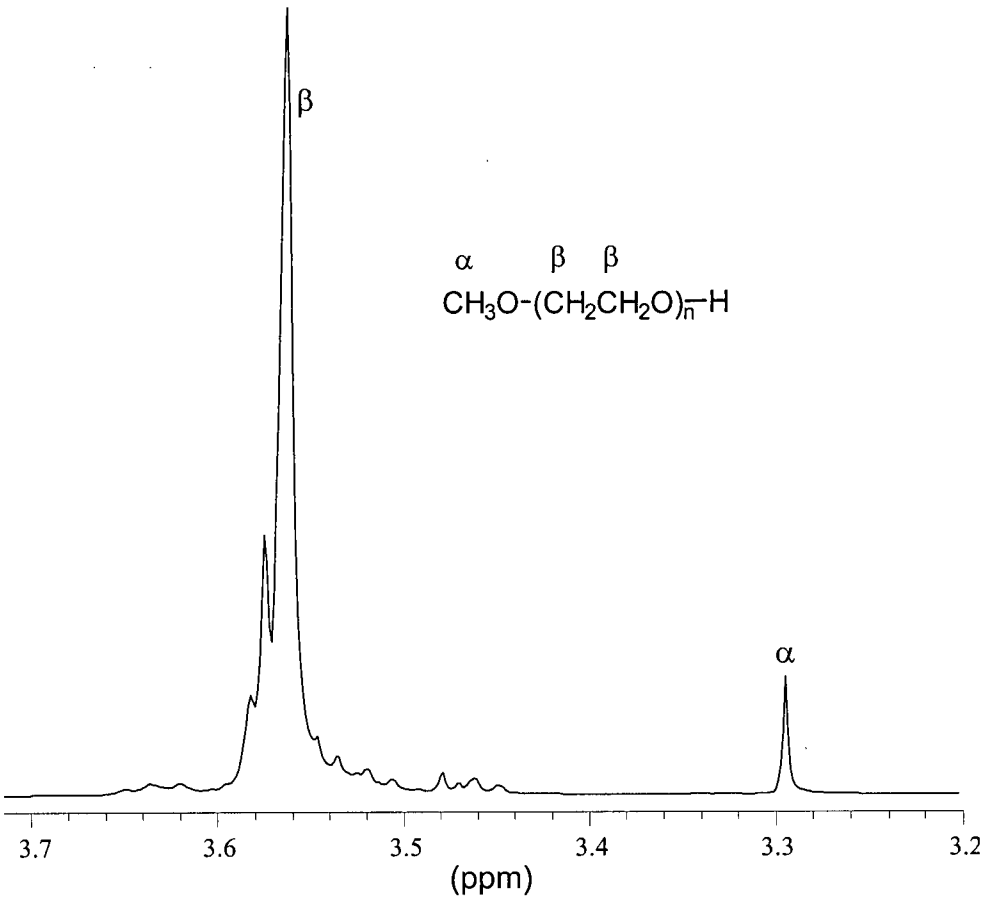

Figure 2.5. ^{1}H-NMR spectrum of methoxy(polyethylene glycol) recorded using a Bruker AV300 spectrometer at 300mHz.

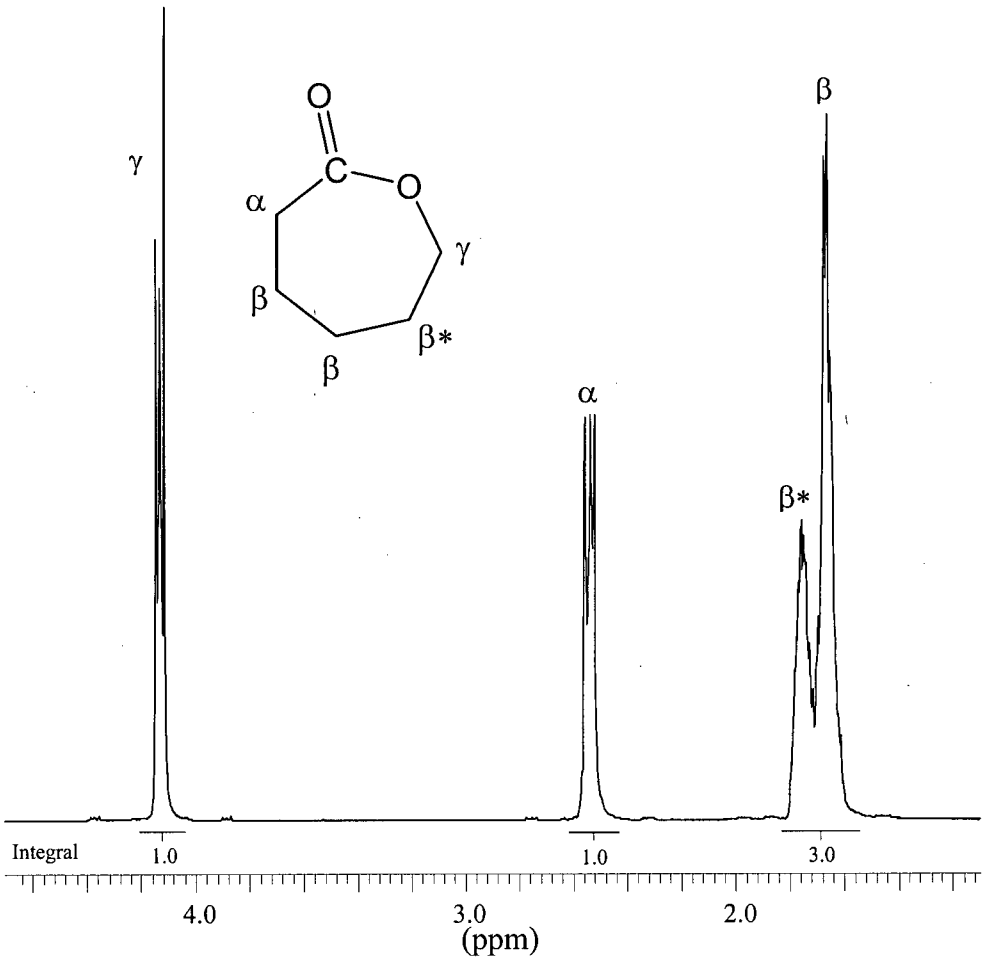

Figure 2.6. ^{1}H-NMR spectrum of caprolactone monomer recorded using a Bruker AV300 spectrometer at 300mHz.

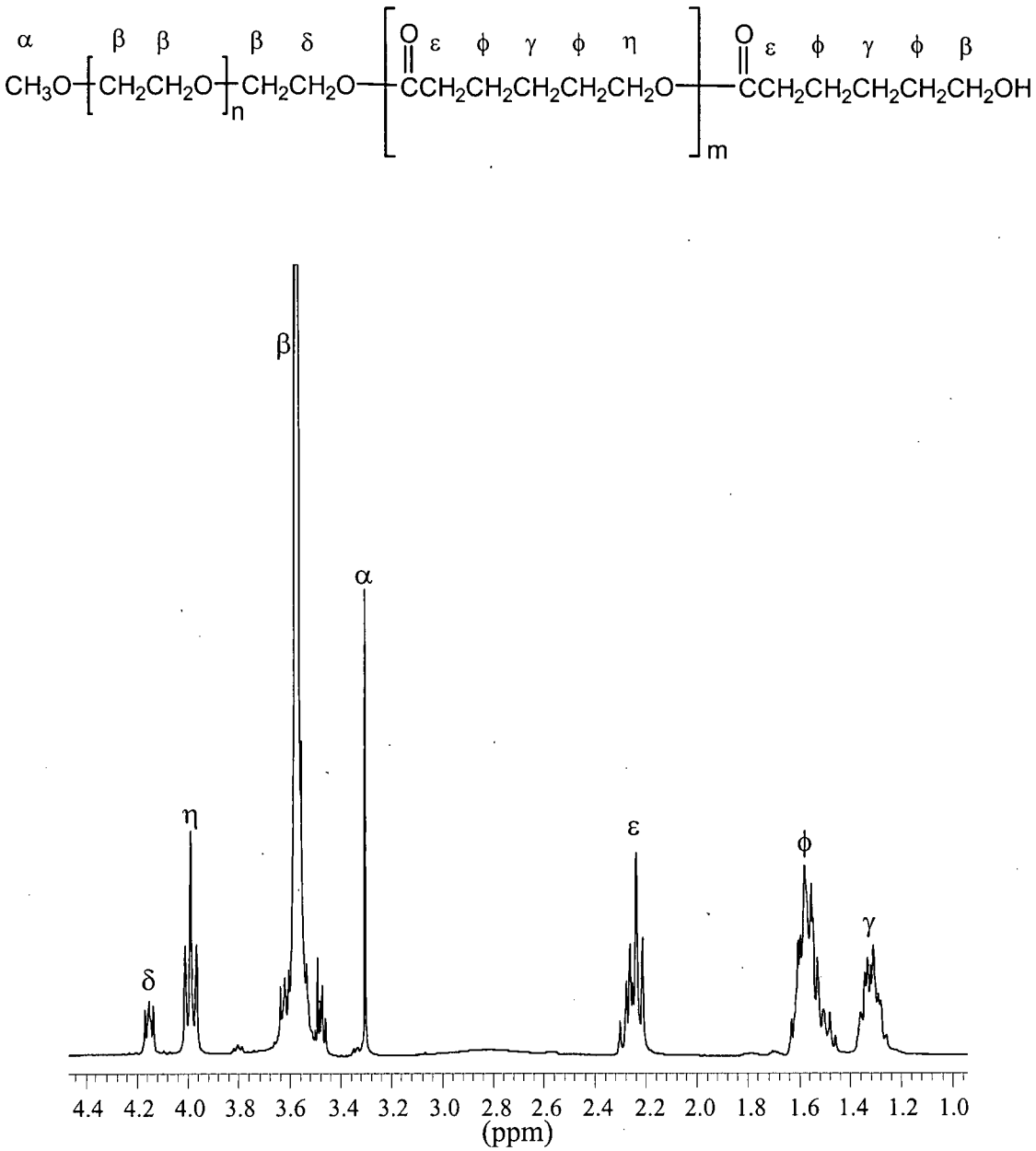

Figure 2.7. A representative ^{1}H-NMR spectrum of MePEG-*b*-PCL diblock copolymer recorded using a Bruker AV300 spectrometer at 300mHz.

nomenclature used describes the degree of polymerization in subscript behind each block, where $MePEG_{17}$-*b*-PCL_5 has 17 repeat units of ethylene glycol and 5 units of caprolactone. Altering feed weight ratios of MePEG to caprolactone monomer produced diblock copolymers with varying PCL lengths with the monomer to initiator ratio determined by NMR agreeing closely with the theoretical M/I (Table 2.1).

2.3.2. Characterization of MePEG-*b*-PCL diblock copolymer self association

The CMC's were determined by fluorescence intensity using DPH as a probe. The fluorescence intensity of DPH rapidly increased once the CMC was achieved (Figure 2.8). The CMC decreased from 2.97 mM to 243 μM to 5.28 μM with increasing PCL length of 2, 5, and 10, respectively for MePEG 750. With a similar PCL length, increasing MePEG from 12 to 17 repeat units increased the CMC from 66.9 μM to 243 μM, but only a small increase to 267 μM was seen with 45 repeat units of MePEG (Table 2.1).

The average hydrodynamic diameter of the micelles and the size distribution was determined by photon correlation spectroscopy (PCS). The diameter increased from 12.2 to 14.6 to 19.1 nm as the PCL block length increased from 2 to 5 to 10, respectively for the MePEG 750 series and increased to 95 nm for MePEG 2000 (Table 2.1). All MePEG-*b*-PCL diblock copolymers measured had a monodisperse distribution as shown in Figure 2.9.

2.4. DISCUSSION

Numerous methods of polymerization have been employed for the synthesis of block copolymers composed of poly(ethylene glycol) and poly(caprolactone). Using PEG diacids and PCL diols of defined molecular weight, Petrova *et al.* utilized step growth polymerization to form poly(ethylene glycol)-poly(caprolactone) multiblock copolymers (Petrova *et al.*, 1998). Consistent with the condensation polymerization method, a low

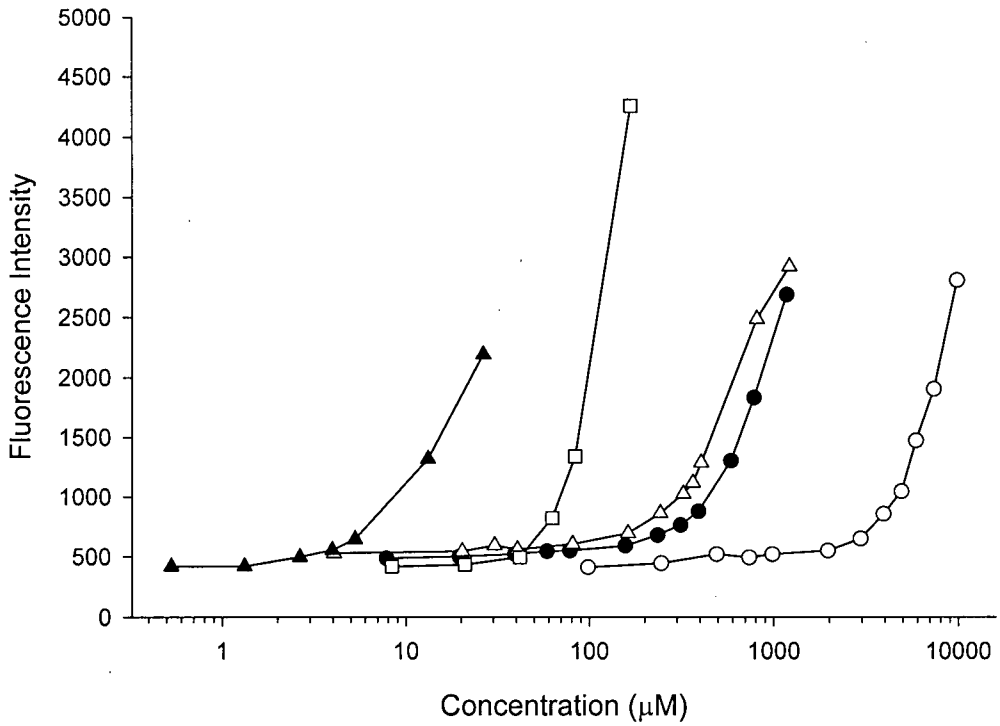

Figure 2.8. Determination of critical micelle concentration (CMC) by fluorescence intensity at 37^0C after incubating with DPH for 24 h. $MePEG_{17}$-*b*-PCL_2 (○), $MePEG_{17}$-*b*-PCL_5 (△), $MePEG_{17}$-*b*-PCL_{10} (▲), $MePEG_{12}$-*b*-PCL_4 (□) and $MePEG_{45}$-*b*-PCL_5 (●).

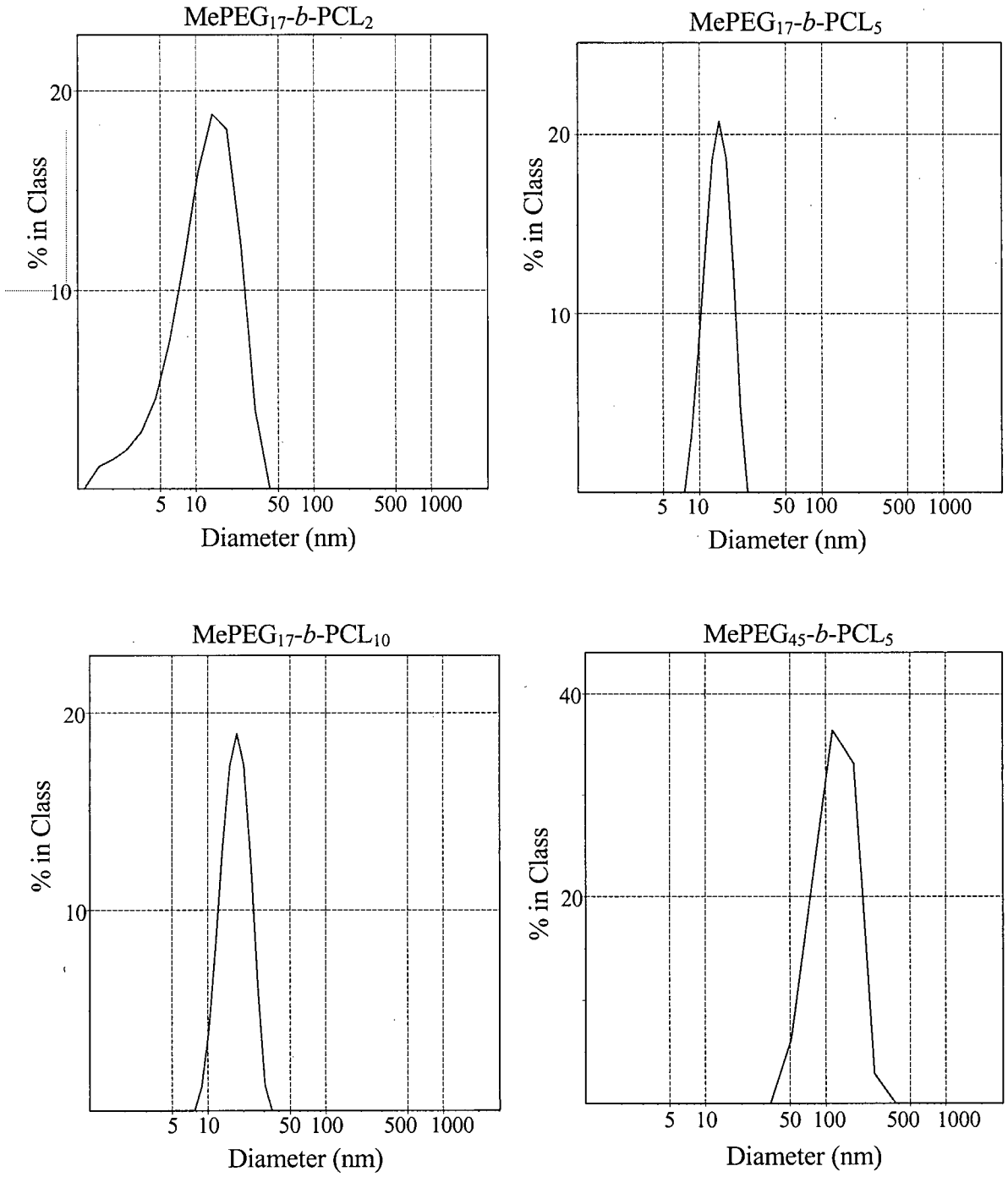

Figure 2.9. Micelle size distribution of MePEG-*b*-PCL diblock copolymers determined by laser light scattering. All measurements were done at 37^0C.

degree of polymerization and large polydispersity index was noted for these multiblock copolymers (Petrova *et al.*, 1998). Non-catalyzed bulk polymerization of caprolactone with the difunctional poly(ethylene glycol) was performed at high temperatures (185^0C) for extended reaction times of upwards of 80h to form PCL-PEG-PCL triblock copolymers (Cerrai *et al.*, 1989). Using monofunctional methoxypoly(ethylene glycol), Shin *et al.* synthesized MePEG-PCL diblock copolymers using a similar non-catalyzed reaction scheme, but found that at higher monomer/initiator ratios the resulting molecular weight was substantially lower than the theoretical molecular weight (Shin *et al.*, 1998). PCL-PEG-PCL triblock copolymers were formed by anionic polymerization using an alkali metal alkoxide derivative of poly(ethylene glycol) (Zhu *et al.*, 1997). Poly(ethylene glycol) was first converted to the potassium alcoholate by refluxing with potassium particles. The resulting potassium poly(ethylene glycol)ate macroinitiator formed a high molecular weight copolymer with high caprolactone conversion over short reaction times (5 min) and low reaction temperatures (30^0C) but a broad molecular weight distribution was found as a result of cyclic and linear oligomer formation from intra and intermolecular transesterification (Zhu *et al.*, 1997). Ring-opening polymerization of caprolactone using aluminum alkoxides to form a poly(ethylene oxide)-diethyl aluminum macroinitiator was used to produce high molecular weight PEG-PCL diblock copolymers with very narrow polydispersity index (Yu and Eisenberg, 1998).

In this work, MePEG-*b*-PCL diblock copolymers were synthesized using stannous octoate ($Sn(Oct)_2$) as a catalyst following similar reaction protocols as previously reported (Bogdanov *et al.*, 1998; Yuan *et al.*, 2000; Zhou *et al.*, 2003). The mechanism for $Sn(Oct)_2$ catalyzed polymerization of lactones is a complex series of reactions involving a

coordination-insertion mechanism similar to metal alkoxides (Dubois *et al.*, 1996) . Initially $Sn(Oct)_2$ reacts with any free hydroxyl group to form a stannous alkoxide initiator followed by coordination and the ring opening insertion of the lactone species into the stannous alkoxide bond (Kricheldorf *et al.*, 2000; Kowalski *et al.*, 2000; Storey and Sherman, 2002). The presence of water in the reaction mixture may act as a hydroxyl source to form stannous alkoxide initiator species, which can result in the formation of PCL homopolymer. Work by Storey *et al.* demonstrated that contaminate water acts more as a catalyst deactivator by forming a stable stannous alcohol derivative that is less efficient as an initiator (Storey and Sherman, 2002). The reduction in the concentration of instantaneously active chain ends did not affect the molecular weight of the diblock copolymers through the formation of homopolymer, but rather affected the kinetics of the reaction (Storey and Sherman, 2002). Although no purification steps were done on the reactants to remove residual water in this work, no evidence of homopolymer was observed in the GPC chromatographs (Figure 2.4).

To our knowledge, there are no reports of the synthesis of MePEG-*b*-PCL diblock copolymers of low molecular weight MePEG of 550 or 750 together with a low DPN of PCL. In comparison to high molecular weight PEG-*b*-PCL diblock copolymers (Allen *et al.*, 1999a), the diblock copolymers synthesized in this work could be dissolved in water using direct dissolution in aqueous media. Samples of the diblock copolymers were melted at 60^0C for 10-15 min and then the desired volume of water/buffer at 37^0C was added. Visual observations of the diblock solutions over 6 hours demonstrated that the hydrophilic copolymers $MePEG_{17}$-*b*-PCL_2, $MePEG_{17}$-*b*-PCL_5, and $MePEG_{45}$-*b*-PCL_5, with HLB values above 10, could be dissolved up to 3 % w/v at 37^0C. The more hydrophobic diblock copolymers $MePEG_{17}$-*b*-PCL_{10} and $MePEG_{12}$-*b*-PCL_4, with HLB values less than 10, could

not be solubilized greater than 1% w/v. Additionally, the $MePEG_{12}$-*b*-PCL_4 diblock appeared to cloud after several minutes in solution over a wide concentration range suggesting that at 37^0C the solution is above the cloud point temperature.

The CMC for the diblock copolymers were determined using fluorescence intensity measurements of DPH. The self-association of the MePEG-*b*-PCL chains into micelles resulted in a hydrophobic core into which DPH partitioned. Since the fluorescence of DPH is sensitive to changes in its environment, partitioning into the hydrophobic PCL core of the micelles will result in an increase in DPH fluorescence at the CMC and will continue to increase as the diblock concentration is further increased (Kabanov *et al.*, 1995; Zhang *et al.*, 1996a). Extrapolation from the point of inflection when the fluorescence intensity increases to the concentration of diblock provides the CMC of the amphiphile. Figure 2.8 shows an increase in the fluorescence intensity of DPH with increasing concentrations of diblock. The inflection point was not well defined for the diblock copolymers and average values were reported in Table 2.1. For each diblock, the molecular weight is an average of a distribution consisting of smaller and larger block lengths. The extent of the molecular weight distribution is measured by the polydispersity index (PDI) where a low PDI indicates a more uniform molecular weight distribution of the diblock. Gao and Eisenberg demonstrated that the CMC of a block copolymer is dependent on the polydispersity index, with a higher PDI resulting in lower CMC values (Gao and Eisenberg, 1993). Although the polydispersity index of the synthesized MePEG-*b*-PCL diblock copolymers was relatively low (~1.1), broadness in the inflexion point was observed due to the polydisperse nature of the system. It has been shown that the CMC of block copolymers is dependent on the nature and length of the hydrophobic and hydrophilic block (Allen *et al.*, 1999a). For short hydrophobic block

lengths (6-30), an increase in hydrophobic block length produced a very rapid decrease in the CMC, while increases in the hydrophilic block length had less dramatic effects on the CMC (Astafieva *et al.*, 1993). This trend was consistent with the MePEG 750 series in this work, where an increase in PCL block length from 2 to 5 units lowered the CMC approximately 10 fold from 2970 μM to 243 μM with a further decrease to 5.3 μM with 10 repeat units of PCL. Increasing MePEG length from 12 to 17 to 45 with a fixed PCL length, increased the CMC from 67 μM to 242 μM to 267 μM, respectively (Table 2.1).

The size of block copolymer micelles has been related to the length of the hydrophobic and hydrophilic blocks and interaction parameters of the blocks with the solvent (Halperin, 1987; Nagarajan and Ganesh, 1989). The hydrodynamic diameters of the MePEG 750 series increased with increasing length of the PCL block from 12 to19 nm (Table 2.1). Micelle size of $MePEG_{12}$-*b*-PCL_4 was not determined as solutions were cloudy over a wide range of concentrations and it was uncertain if this was due to a cloud point phenomenon, non-spherical shape, or secondary aggregation of micelles. Overall, the micelle sizes of the MePEG 750 series were considerably smaller than micelles of similar chemical composition owing to their small block lengths. Shin *et al.* reported diblock copolymers with MePEG 5000 and PCL lengths of 20-80 repeat units with micelle sizes ranging from 50-130 nm (Shin *et al.*, 1998). Allen *et al.* found that micelles composed of PEO_{44}-*b*-PCL_{14} or PEO_{44}-*b*-PCL_{20} had hydrodynamic diameters of 55 and 62 nm, respectively (Allen *et al.*, 1998). Table 2.1 shows that $MePEG_{45}$-*b*-PCL_5 had a size of 95 nm which was larger than the micelles produced in Allen *et al.*'s work (Allen *et al.*, 1998). This difference may be due to the method of micelle preparation, as direct dissolution may have permitted more water to be

entrapped in the core, which resulted in a less condensed core and larger overall hydrodynamic diameter, compared to the solvent precipitation method used by Allen *et al.*

2.5. CONCLUSION

A novel series of short block length amphiphilic diblock copolymers based on MePEG and PCL was synthesized by ring-opening polymerization using $Sn(Oct)_2$ as a catalyst. Altering the feed weight ratio of MePEG:CL produced diblock copolymers with varying lengths of PCL and the M/I ratio determined by NMR agreed closely with the theoretical M/I ratio. GPC results showed an increase in molecular weight of the MePEG oligomer peak after polymerization and NMR spectroscopy confirmed the formation of MePEG-*b*-PCL. The diblock copolymers formed micelles above the CMC values and hydrophobicity, solubility, CMC, and micelle size, were dependent on the block lengths of the diblock copolymers.

Chapter 3

COMPARATIVE CACO-2 CELLULAR ACCUMULATION OF TWO HOMOLOGOUS P-GLYCOPROTEIN SUBSTRATES: EFFECTS OF METHOXYPOLY(ETHYLENE GLYCOL)-*BLOCK*-POLY(CAPROLACTONE) DIBLOCK COPOLYMERS

3.1. INTRODUCTION

The action of the efflux transport protein, P-glycoprotein (P-gp), expressed on the apical surface of the intestinal epithelia can serve as an absorption barrier to limit the oral availability of hydrophobic drugs from the gastrointestinal tract (Hunter *et al.*, 1993a; Van Asperen *et al.*, 1997; Sparreboom *et al.*, 1997; Meerum Terwogt *et al.*, 1998; Van Asperen *et al.*, 1998). Susceptible drugs have reduced membrane permeability as a result of P-gp removing drug from the enterocyte as it enters, thus limiting the amount that crosses into the general circulation. It has been suggested that the function of P-gp may involve substrate transport from the lipid bilayers of the plasma membrane to the external medium ('vacuum cleaner' hypothesis) (Romsicki and Sharom, 1999). Within this hypothesis, P-gp could function as a 'flippase', catalyzing the translocation of hydrophobic substrates present in the cell membrane from the inner to the outer leaflet (Higgins and Gottesman, 1992). P-gp substrates are molecules that typically possess a degree of hydrophobicity and it has been proposed that substrate partitioning into the membrane is a rate-limiting step for the interaction with the P-gp binding domain within the lipid membrane (Seelig and Landwojtowicz, 2000). Eytan *et al.* evaluated a series of P-gp substrates, rhodamine dyes, for P-gp mediated exclusion from rodent and human tumor MDR lines, their ability to stimulate ATPase activity, and transmembrane movement rate across P-gp reconstituted liposomes (Eytan *et al.*, 1997). The transmembrane or transbilayer movement rate was the

major factor determining the efficiency of P-gp in excluding rhodamine dyes from MDR cells (Eytan *et al.*, 1997). The transbilayer movement rates across multilamellar lipid vesicles or liposomes for numerous P-gp substrates and P-gp modulators demonstrated that substrates have a tendency to reside longer in the membrane allowing efficient P-gp efflux, while modulators can enter and move across the lipid bilayer at a faster rate and overcome the outward efflux (Eytan *et al.*, 1996). Thus, the ability of the substrate to enter the membrane and the rate at which it can diffuse through, or the length of time it resides within the membrane, appear to be important parameters dictating the effectiveness of P-gp efflux of drugs.

There are numerous studies demonstrating that P-gp mediated efflux of drugs may be inhibited by the use of non-ionic surfactants. Co-administration of compounds susceptible to P-gp mediated efflux, with amphiphilic agents such as polysorbates, vitamin E TPGS, Solutol, and Cremophor EL® has shown enhanced cellular accumulation and improved transepithelial flux of P-gp substrates (Woodcock *et al.*, 1990; Woodcock *et al.*, 1992; Buckingham *et al.*, 1996; Nerurkar *et al.*, 1996; Lo *et al.*, 1998; Dintaman and Silverman, 1999; Bogman *et al.*, 2003). Recently, A-B-A type amphiphilic block copolymers of poly(ethylene oxide)-*b*-poly(propylene oxide)-*b*-poly(ethylene oxide) also known as poloxamer or Pluronic® block copolymers, have been shown to enhance cellular accumulation, membrane permeability, and to modulate multidrug resistance of numerous P-gp substrates (Paradis *et al.*, 1994; Alakhov *et al.*, 1996; Miller *et al.*, 1997; Batrakova *et al.*, 1998a; Batrakova *et al.*, 1998b; Batrakova *et al.*, 1999; Batrakova *et al.*, 1999). Batrakova *et al.* found that Pluronic® block copolymers could enhance caco-2 cell accumulation of a P-gp substrate at concentrations below the CMC of the Pluronic® copolymers (Batrakova *et al.*,

1998a). The activity of Pluronic® copolymers was also shown to be dependent on the hydrophilic-lipophilic balance (HLB), with the most potent Pluronic® copolymers being those with intermediate hydrophobicity (Batrakova *et al.*, 1999).

The mechanism for surfactants inhibiting P-gp mediated efflux appears to involve interactions with the lipid bilayer. Sinicrope *et al.* showed that alterations in membrane lipid fluidity of canalicular membrane vesicles influenced the P-gp modulated accumulation of MDR drugs (Sinicrope *et al.*, 1992). Dudeja *et al.* found that surfactants that improved intracellular accumulation of a P-gp substrate in overexpressing cells, also reduced membrane lipid fluidity (Dudeja *et al.*, 1995). Moreover, no fluidity change was observed with surfactants that did not enhance accumulation in an overexpressing cell line (Dudeja *et al.*, 1995). Membrane fluidization by various agents, including surfactants, was shown to modulate drug efflux from MDR cells and substantially reduce P-gp ATPase activity (Regev *et al.*, 1999). It has been suggested that amphiphilic Pluronic® triblock copolymers inhibited P-gp via a dual mechanism involving a reduction in membrane microviscosity and cellular depletion of ATP levels (Batrakova *et al.*, 2001).

Chapter 2 described the synthesis and characterization of a novel series of low molecular weight amphiphilic diblock copolymers composed of methoxypoly(ethylene glycol) and poly(caprolactone) (MePEG-*b*-PCL). Diblock copolymers with varying lengths of either MePEG or PCL provided a range of diblock copolymers with different CMC, HLB and micelle size (Table 2.1). To our knowledge, no studies have been carried out to determine whether amphiphilic diblock copolymers, such as MePEG-*b*-PCL, possess an ability to modulate P-gp mediated efflux of drugs. Studies for this chapter were designed to test the hypothesis that diblock structure and physiochemical properties of MePEG-*b*-PCL

copolymers, including block lengths, hydrophobicity (HLB), and CMC will influence caco-2 cellular accumulation of a P-gp substrate. Two structurally homologous P-gp substrates, rhodamine 123 (R-123) and rhodamine 6G (R-6G), were selected as model probes (Figure 3.1). Both of these xanthene dye derivatives have been utilized extensively as P-gp substrates to measure the extent of chemosensitization by inhibitors (Neyfakh, 1988; Lampidis *et al.*, 1989; Sarver *et al.*, 2002). The fluorescent rhodamine dyes are hydrophobic cations differing in their relative hydrophobicity. The addition of methyl and ethyl groups on R-6G makes this dye more lipophilic with a partition coefficient (Kpart) of 115.6 compared to R-123 with a Kpart of 3.4 (Figure 3.1) (Lampidis *et al.*, 1989). The effects of the diblock copolymers on P-gp mediated efflux of two chemotherapeutic drugs and well established P-gp substrates, paclitaxel and doxorubicin, were also studied.

The P-gp expressing cells utilized for these studies were the human colon adenocarcinoma cells, caco-2. Caco-2 has become the "gold standard" model for the *in vitro* evaluation of absorption and transepithelial transport (Bailey *et al.*, 1996; Artursson *et al.*, 2001). Caco-2 cells undergo spontaneous enterocytic differentiation and polarization once they reach confluency in culture (Pinto *et al.*, 1983). Completely differentiated monolayers of caco-2 cells display microvilli and brush border hydrolases on the apical surface, and express endogenous transport systems that are similar to human intestinal epithelium (Pinto *et al.*, 1983; Hidalgo *et al.*, 1989; Hidalgo and Jibin, 1996). Because of this structural and functional homology with intestinal epithelium, the primary utility of caco-2 cells has been for accumulation and transepithelial transport experiments to evaluate transcellular or paracellular absorption, and either passive or carrier mediated uptake of drugs (Anderberg *et al.*, 1992; Anderberg and Artursson, 1993; Artursson *et al.*, 2001). Furthermore, the

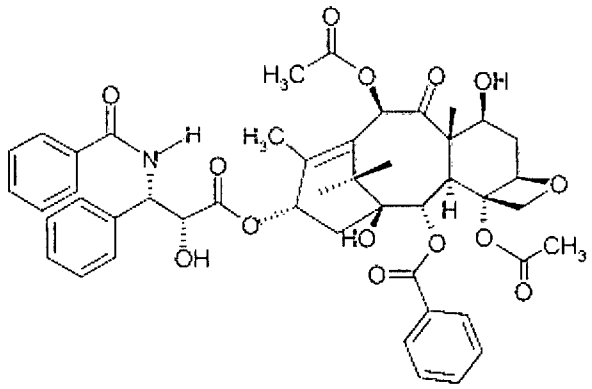

Paclitaxel
(PTX)

Molecular weight = 854
Kpart = 99 (Song *et al.*, 1997)

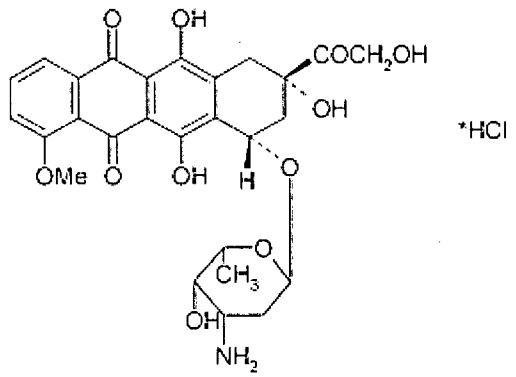

Doxorubicin
(DOX)

Molecular weight = 543.5
Kpart = 0.52 (Song *et al.*, 1997)

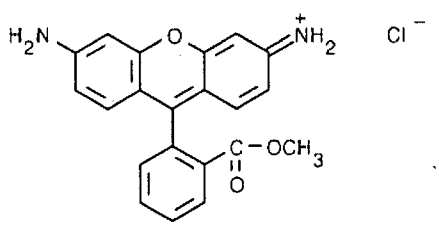

Rhodamine 123
(R-123)

Molecular weight = 380.8
Kpart = 3.4 (Lampidis *et al.*, 1989)
Kpart = 6.9 (Eytan *et al.*, 1996)
R_f = 0.2 (Eytan *et al.*, 1997)

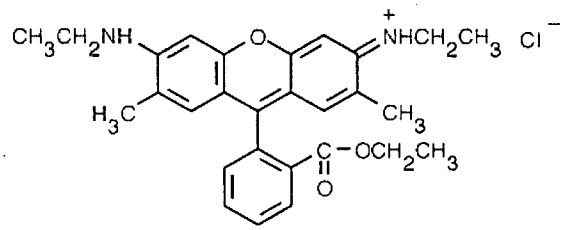

Rhodamine 6G
(R-6G)

Molecular weight = 479.02
Kpart = 115.6 (Lampidis *et al.*, 1989)
R_f = 0.53 (Eytan *et al.*, 1997)

Figure 3.1. Structure and physiochemical properties of paclitaxel, doxorubicin, rhodamine 123 and rhodamine 6G. Kpart = octanol/water partition coefficient. R_f denotes the retention factor of the compound when chromatographed on silica-gel with a chloroform/methanol/water mixture (190:30:1).

expression of endogenous transporters such as oligopeptide, monocarboxylic acid, and the efflux transporters P-gp and multidrug resistance related protein (MRP), has allowed for the characterization of these transporters at the cellular and molecular level and evaluation of their role in drug transport and efflux (Hunter *et al.*, 1993b; Hidalgo *et al.*, 1995; Tsuji and Tamai, 1996; Hidalgo and Jibin, 1996; Dantzig, 1997; Gutmann *et al.*, 1999). The objectives of these studies were: (1) to investigate the effect of MePEG-*b*-PCL block composition on the cellular accumulation of P-gp substrates, and (2) examine the effects of MePEG-*b*-PCL block copolymers on cellular accumulation of P-gp substrates differing in lipophilicity.

3.2. EXPERIMENTAL

3.2.1. Materials

MePEG with molecular weight of 750 was purchased from Fluka (Oakville, ON). Verapamil, cyclosporine A (CSA), rhodamine 123 (R-123), rhodamine 6G (R-6G), Triton X-100, and probenecid were obtained from Sigma-Aldrich (Oakville, ON). Paclitaxel (PTX) was supplied by Hauser (Boulder, CO). Doxorubicin (DOX) was purchased from Hande Tech (Houston, TX). ^{3}H-Paclitaxel and ^{14}C-doxorubicin were obtained from Amersham Biosciences (Piscataway, NJ) with a specific activity of 66.6 GBq/mmol and 2.15 GBq/mmol, respectively. Diblock copolymer consisting of MePEG of molecular weight = 2000 and 9 repeat units of D,L-lactide, designated $MePEG_{44}$-*b*-$PDLLA_9$ was generously supplied by Angiotech Pharmaceuticals (Vancouver, BC).

Cell culture media and supplements, which include Dulbecco's modified eagle's medium (DMEM), non-essential amino acids, L-glutamine, penicillin/streptomycin, and fetal bovine serum (FBS), were from Invitrogen (Grand Island, NY). Hanks balanced salt solution without phenol red (HBSS), phosphate buffered saline (PBS), trypan blue, and *N*-(2-

hydroxyethyl)piperazine-*N'*-2-ethanesulfonate (hepes) were also from Invitrogen (Grand Island, NY).

3.2.2. General Equipment

The list below describes the laboratory equipment utilized during the course of this work.

CO_2 water-jacketed incubator (Forma Scienific, Marjetta, OH)

Labgard laminar flow biological safety cabinet (Nuaire Inc. Plymouth, MN)

Isotemp 220 water bath (Fisher Scientific, Nepean, ON)

Allegra 6 Centrifuge (Beckman Coulter, Mississauga, ON)

Maxi Mix II vortex (Thermolyne, Dubuque, IO)

Axiovert 25 inverted microscope (Carl Zeiss, Don Mills, ON)

Eppendorf 5415D centrifuge (Brinkmann, Mississauga, ON)

Model 8000 pH meter (VWR Scientific, Mississauga, ON)

Bright line hemacytometer (Sigma-Aldrich, Oakville, ON)

Model 370 magnetic stirrer/heater (VWR Scientific, Mississauga, ON)

Micromaster compound microscope (Fisher Scientific, Nepean, ON)

PB153 and PB302 balances (Mettler Toledo, Greifensee, Switzerland)

Eppendorf series 2100 adjustable volume pipettes (Brinkmann, Mississauga, ON)

3.2.3. Cell Culture

3.2.3.1. Maintenance

The human colon adenocarcinoma cell line, caco-2, was obtained from ATCC (Rockville, MD) as passage 17. Caco-2 cells were grown in a humidified atmosphere of 5% CO_2 at 37^0C and maintained in DMEM supplemented with 10 %v/v heat inactivated fetal

bovine serum (HI-FBS), 1.0 %v/v NEAA, 1.0 %v/v L-glutamine, and 100 UI/mL penicillin and 100 μg/mL streptomycin. Supplements such as non-essential amino acids, L-glutamine and penicillin/streptomycin were supplied from the manufacturer as concentrated solutions and used as supplied. Fetal bovine serum was sourced from USA and heat inactivated by incubating at 55^0C for 30 min. Stock cultures were grown in filtered T-175 cm^2 flasks (BD-Falcon, BD Biosciences, Bedford, MA) at an initial seed density of 5000 cells/cm^2. Growth media was changed in flasks and plates every second day. Cells were routinely monitored for mycoplasma contamination using an ELISA Mycoplasma Detection Kit (Roche Diagnostics Corporation, Indianapolis, IN)

3.2.3.2. Subculturing

Upon reaching 80-90 % confluency in the T-175 flasks, caco-2 cells were subcultured or split. Spent media was removed from the flasks and the adherent cells were washed with PBS. Wash solutions were then removed and cells were dissociated using 0.25% trypsin + 1.0 mM EDTA in Ca^{++} and Mg^{++} free HBSS (Invitrogen, Grand Island, NY) for 5-10 min at 37^0C. The resulting cell suspension was collected and centrifuged at 125xg for 5 min. The supernatant was then decanted and an appropriate volume (5-15 mL) of growth media was added to resuspend the cells. An aliquot (~150 μL) of the resuspended caco-2 cells was removed to determine cell density and cell viability using trypan blue exclusion. Trypan blue is an impermeable dye to viable cells but upon death, the cells become permeable and stain a blue color that can be readily distinguished from viable cells. The trypan blue exclusion assay involved a 1:1 dilution of the cell suspension with 0.4 %w/v trypan blue in PBS. The number of viable cells and dead cells were counted using a hemacytometer and then related to the overall viability and cell density (cells/mL) of the suspended cells. Cells were then

seeded into T-175 flasks at 5000 cells/cm^2, as well as 48 and 96 well flat bottom plates (Corning Costar, Cambridge, MA) at a density of 40 000 cells/cm^2 and labeled with the next consecutive passage number. Only passages 25-45 were used throughout this work.

To ensure a constant supply of low passage numbers, a seed bank of caco-2 cells was established. Cells were resuspended in cryoprotectant medium composed of growth media described in section 3.2.3.1, supplemented with 5 %v/v dimethyl sulfoxide (DMSO, Sigma-Aldrich, Oakville, ON) at a density of 2x10^6 cells/mL. Cells aliquoted into 2 mL cryovials (VWR Scientific, Mississauga, ON) were then placed in a Nalgene Cryo 1^{0}C Freezing Container (Nalge Nunc International, Rochester, NY) and set into a –70^{0}C freezer for 12 h. This provides a controlled freezing rate of the cells at –1^{0}C/min. Once frozen, the cryovials are then stored long term in a liquid nitrogen dewer.

3.2.4. Reverse transcription coupled polymerize chain reaction (RT-PCR)

RT-PCR was used to qualitatively determine the presence of the MDR-1 gene in the caco-2 cell line. Total cellular RNA was isolated from caco-2 cells of passage no. 27 after culturing in a 48 well plate for 16 days. Trizol reagent (Invitrogen, Grand Island, NY) was used for RNA isolation, using the protocol supplied by the manufacturer. All water used throughout the RT-PCR work was diethylpyrocarbonate (DEPC) treated (Invitrogen, Grand Island, NY). The RNA purity was determined by the OD_{260}/OD_{280} ratio and the integrity was evaluated by electrophoresis on a 0.66 M formaldehyde/1.5% agarose gel with ethidium bromide detection. Two μg of RNA was reverse transcribed using Superscript II (Invitrogen, Grand Island, NY) with oligo $(dt)_{12-18}$ primer and dNTP mix (Invitrogen, Grand Island, NY) following manufacturer protocols. The resulting cDNA (2.5 μL) was amplified using T*aq* DNA polymerase (Invitrogen, Grand Island, NY) following manufacturer protocols with

forward primer 5'-GTC ATT GTG GAG AAA GGA AAT CAT G-3' and reverse primer 5'-ATT CCA AGG GCT AGA AAC AAT AGT G-3', producing a 478 bp amplicon (Schmiedlin-Ren *et al.*, 1997). The sample underwent 50 cycles of 60 sec 95^0C denaturation and 75 sec combined annealing and extension at 65^0C followed by a 10 min 65^0C final extension cycle using a Minicycler (MJ Research Inc. Watertown, MA). The final PCR product was separated by electrophoresis using a 1.5% agarose gel and visualized with ethidium bromide. Positive control was mRNA from the P-gp overexpressing cell line, MCF7/ADR, generously supplied by Dr. Tom Chang from the University of British Columbia, Faculty of Pharmaceutical sciences

3.2.5. Immunodetection of P-glycoprotein

Caco-2 cells were harvested and lysed using the Mem-PER eukaryotic membrane protein extraction kit (Pierce, Rockford, IL) according to manufacturer's protocol. Thirty μg of membrane protein was electrophoresed on a 10% SDS-Page gel and then electroblotted onto a 0.45 μm PVDF membrane (Biorad, Mississauga, ON) at 80V for 2 h and 50V for 2 h. The membrane was incubated overnight at 4°C in blocking buffer (1% nonfat dried milk + 0.1% Tween-20 in PBS). The membrane was incubated for 2 h with a 1:300 dilution of C219 primary monoclonal antibody (Signet, Dedham MA). After rinsing 3 times with blocking buffer, the membrane was incubated for 1 h with a 1:2000 dilution of rabbit IgG anti-mouse HRP-conjugated antibody (Sigma, Oakville, ON). The membrane was then rinsed with 0.1% Tween-20 in PBS and P-gp was visualized using chemiluminescence (Western Lightning Chemiluminescence Reagent, Perkin Elmer, Woodbridge, ON) as per manufacturer's protocol.

3.2.6. Caco-2 cellular accumulation studies

For all accumulation experiments, caco-2 cells were grown in 48 well plates for a minimum of 14 days before being used for experimentation between days 14 and 21. All treatment solutions (diblock copolymers, substrates, and inhibitors) were prepared with HBSS + 10 mM hepes pH=7.4 unless otherwise stated and are generally referred to as "assay buffer" throughout this work. For comparison purposes, standard P-gp inhibitors verapamil and CSA were used as positive controls and are referred to as "P-gp inhibitor(s)".

3.2.6.1. Cellular accumulation of rhodamine dyes

Caco-2 cellular accumulation of the P-gp substrates R-123 and R-6G was determined with or without P-gp inhibitors and various concentrations of MePEG-*b*-PCL diblock copolymers described in Table 2.1 and with $MePEG_{44}$-*b*-$PDLLA_9$. Probenecid was also used to evaluate substrate specificity of R-123 and R-6G for MRP. Solutions of 5 μM R-123 or 0.25 μM R-6G in assay buffer with diblock or P-gp inhibitors were equilibrated at 37^{0}C for a minimum of 60 min before use. Caco-2 cells grown on 48 well plates were washed with assay buffer several times to remove all traces of media, then allowed to equilibrate with 500 μL of assay buffer in each well for 15 min at 37^{0}C. The assay buffer was then removed and 500 μL of each treatment group were added to three wells, with one set of 3 wells used for negative control (assay buffer only). Cells were incubated for 90 min at 37^{0}C, after which the samples were removed and the plate placed on ice. Each well was washed twice with 500 μL of ice cold PBS to remove all traces of extracellular dye. To each well, 125 μL of 1% triton X-100 was added to solubilize the cells for approximately 10 min. This extract was collected into a 1.5 mL microcentrifuge tube and an additional 125 μL of 1% triton X-100 was added to the wells for rinsing, then collected into the well's corresponding

microcentrifuge tube (total volume was 250 μL). Tubes were vortexed briefly, centrifuged at 14 000 rpm for 5 min to pellet cellular debris and the supernatant removed. Into a 96 well flat bottom plate, three 50 μL aliquots of the supernatant from each well were placed for fluorescence measurement. The cellular fluorescence intensity was measured using a CytoFluor 4000 fluorescence microplate reader (PerSeptive Biosystems, Framingham, MA) with λ_{EX}=485 nm and λ_{EM}=530 nm (with filter bandwidths of 20 and 25 nm respectively) for R-123 and λ_{EX}=508 and λ_{EM}=560 (both with filter bandwidths of 20 nm) for R-6G. Calibration curves of each rhodamine in 1% triton X-100 were used for quantitation. Cellular accumulation was normalized with respect to total protein content in each well. Three 10 μL aliquots of supernatant from each well were used to determine total protein using the micro BCA protein assay kit (Pierce, Rockford, IL) following the method specified by the manufacturer.

3.2.6.2. Cellular accumulation of paclitaxel and doxorubicin

The accumulation of paclitaxel and doxorubicin by caco-2 cells was determined with $MePEG_{17}$-*b*-PCL_5 diblock copolymer and P-gp inhibitors following similar methodology as outlined in section 3.2.6.1. Cells were exposed to either 0.5 μM paclitaxel or 10 μM doxorubicin with approximately $1.5x10^5$ dpm/mL prepared by mixing an aliquot of "hot" (^{3}H-PTX, ^{14}C-DOX labeled) and "cold" (unlabeled) paclitaxel or doxorubicin. No change in paclitaxel specific activity was found over the time course of the experiment since the concentration of paclitaxel used was below the solubility limit of 1 μM (Liggins *et al.*, 1997). The entire well contents were collected into scintillation vials and cocktail was added (CytoScint, ICN, Costa Mesa, CA). Samples were counted using a LS6000TA scintillation counter (Beckman Instruments Inc., Fullerton, CA). A set of 6 wells per experimental plate

were collected individually for total protein content as described in section 3.2.6.1 and used for normalization of data.

3.2.6.3. Intracellular distribution of rhodamine dyes

Caco-2 cells were grown on 8 well Lab-tek chamber glass slides (Nalge Nunc International, Naperville, IL) for a minimum of 14 days under the same culture conditions as described in section 3.2.3. Cells were then washed with assay buffer and exposed to 5 μM R-123 or 0.25 μM R-6G in assay buffer, with or without $MePEG_{17}$-*b*-PCL_5 diblock copolymer for 90 min at 37^0C. After incubation the cells were washed with ice cold PBS and immediately viewed using an Axiophat confocal microscope using a standard rhodamine filter set and 40x objective (Carl Zeiss, Don Mills, ON).

3.2.7. Lactate dehydrogenase release

Lactate dehydrogenase (LDH) release was measured using an LDH assay kit (CytoTox 96, Promega, Madison, WI). Briefly, caco-2 cells grown in flat bottom 96 well plates were washed with assay buffer and pre-incubated with assay buffer for 15 min at 37^0C. Serially diluted concentrations of MePEG-*b*-PCL diblock copolymers in assay buffer were added to wells, with assay buffer only used for control and maximum release groups. Plates were incubated at 37^0C for 90 min. Triton X-100 was added to provide maximum LDH release. The plate was spun at 1500 rpm at 4^0C and an aliquot of supernatant taken to analyze for LDH using reagents and methods provided by the kit manufacturer.

3.2.8. Binding of rhodamine dyes within MePEG-*b*-PCL micelles

In a micellar solution, a solute can partition into the hydrophobic core of the micelle and equilibrate between the micelle core and the aqueous milieu. The total amount of solute (St) in the system is therefore given by:

$$St = Sf + Sm \qquad \text{Equation 3.1}$$

where Sf is the amount free or unbound and Sm is the amount micellized or bound. The micellized fraction of solute (Fb) is given by:

$$Fb = \frac{Sm}{Sm + Sf} \qquad \text{Equation 3.2}$$

Equilibrium dialysis was performed to evaluate the fraction of R-123 and R-6G bound within MePEG-*b*-PCL micelles. A 5 mL equilibrium dialysis cell from Bel-Art Products (Pequannock, NJ) was used with a Spectra/Por membrane with molecular weight cut off of 1000 obtained from Spectrum Laboratories (Rancho Dominguez, CA). Initial experimentation evaluated the time to equilibrium using 5 μM R-123 and 0.25 μM R-6G in assay buffer placed in the donor compartment with an equal volume of assay buffer placed in the receiver side. The dialysis cell was placed at 37^0C in an Innova 4000 incubator shaker (New Brunswick Scientific, Edison, NJ) set at 100 rpm. Aliquots were taken from both the donor and receiver side at various time points. The fluorescent intensity of R-123 and R-6G were measured as described in section 3.2.6.1 and quantified using a standard curve. Once the time to equilibrium was determined for R-123 and R-6G alone, all sampling for MePEG-*b*-PCL with R-123 or R-6G was done after this point to ensure equilibrium had been attained. All experimental procedures used 5 μM R-123 and 0.25 μM R-6G with MePEG-*b*-PCL diblock copolymer solutions and were carried out as described above. Each diblock solution was allowed to equilibrate for approximately 1 h prior to placing 5 mL in the donor chamber of the diffusion cell, with 5 mL of assay buffer in the receiver chamber.

3.2.9. Data reporting and statistical comparisons

The experimental design for each study provided 3 or more independent samples per treatment group. This was considered to be one sample set (N = 1) composed of 3

independent samples, for example, a cellular accumulation study done in a 48 well plate was considered to be one sample set with each well corresponding to N=1 number of samples per treatment group. The reproducibility of the sample means between each sample set was used for analysis and was reported as the mean +/- standard error of the mean (SEM) with the N value representing the number of sample sets used in the analysis. However, results reported as mean +/- standard deviation (SD) implies analysis of the independent samples within a sample set with the N value representing the number of samples. Statistical analysis was performed using Sigmastat v2.0 software (SPSS Inc, Chicago, IL) with a significance value of $P<0.05$. Two tailed two-sample t-test and analysis of variance (ANOVA) was used for comparisons between groups with a significance level of 5% ($p<0.5$) considered to be statistically significant. Student Newman Keuls post hoc test was chosen for pairwise comparisons following ANOVA.

3.3. RESULTS

3.3.1. Caco-2 model assessment and assay development

Assay development studies demonstrated no significant difference in R-123 accumulation between caco-2 cells grown for either 2 or 3 weeks post seeding into 48 well plates (Figure 3.2). There was a significant increase in R-123 and R-6G accumulation when cells were treated with either 50 and 100 μM verapamil compared to R-123 and R-6G alone (Figure 3.2 and 3.3). No change in accumulation was observed between 100 μM and 50 μM verapamil with R-123 and R-6G (Figure 3.2 and 3.3). Cyclosporine A (CSA) significantly enhanced ($p<0.05$) R-123 accumulation when caco-2 cells were treated with 1, 4 or 8 μM CSA (Figure 3.4). Based on these studies, optimal CSA and verapamil concentrations of 4 μM and 50 μM, respectively, were selected. The evidence also showed that cellular

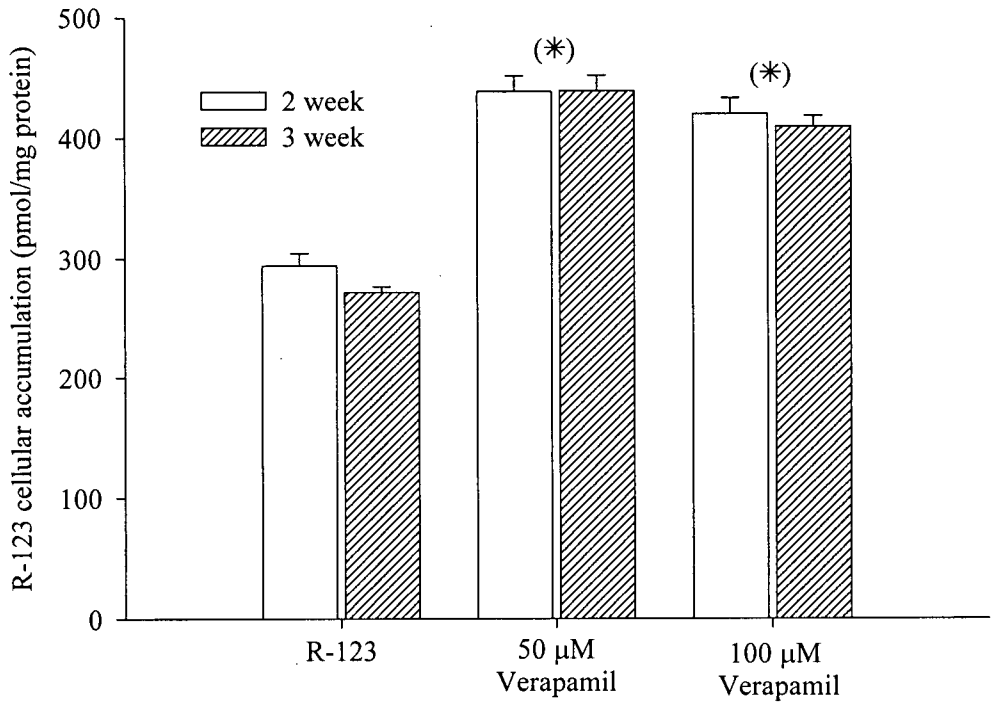

Figure 3.2. The effect of caco-2 culture time and verapamil concentration on accumulation of 5 μM R-123 at 37^0C for 90 min. Data expressed as mean +/- SEM (N=3). One-way ANOVA with pairwise comparisons using Student Newman Keuls test was performed with $p<0.05$, (*) Statistically significant compared to R-123.

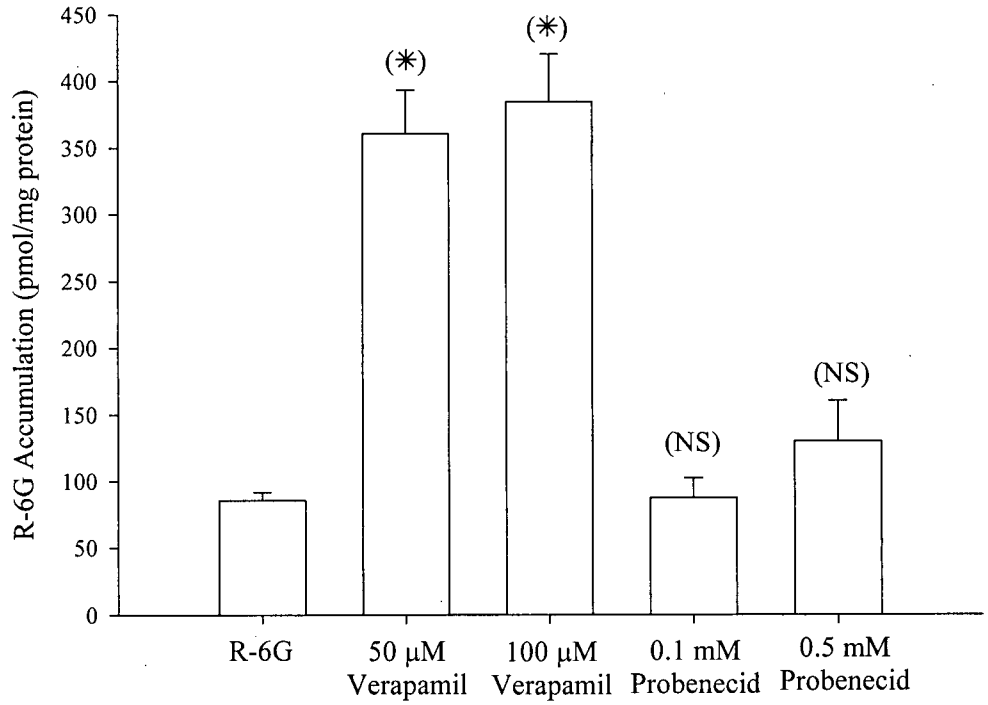

Figure 3.3. Evaluation of verapamil and probenecid concentration on accumulation of 0.25 µM R-6G at 37^0C for 90 min. Data expressed as mean +/- SEM (N=3). One-way ANOVA with pairwise comparisons using Student Newman Keuls test was performed with $p<0.05$, (*) Statistically significant compared to R-6G.

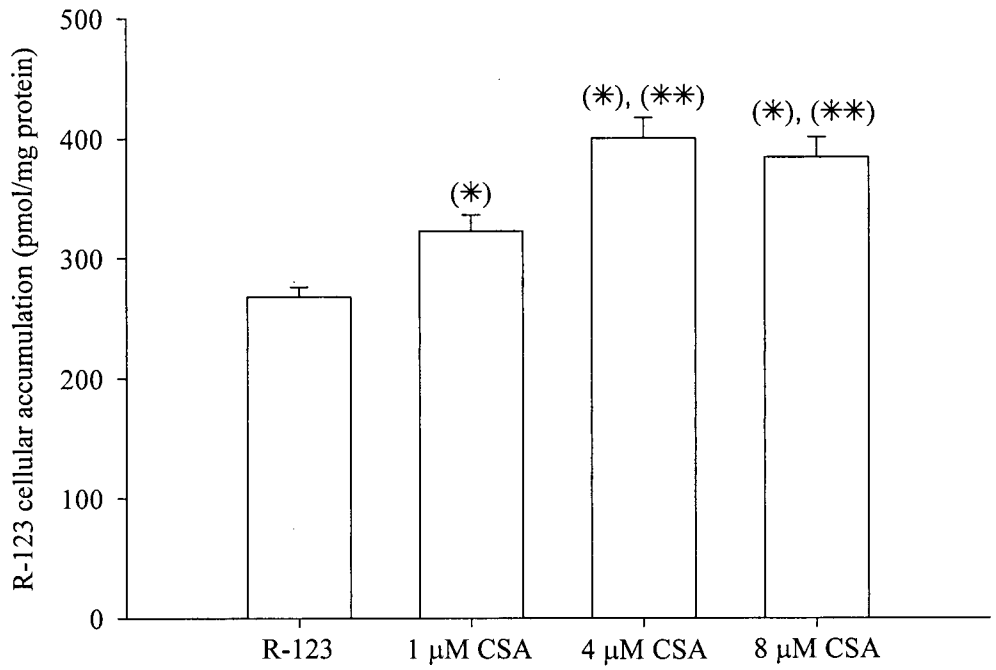

Figure 3.4. Evaluation of cyclosporine A (CSA) concentration on accumulation of 5 μM R-123 at 37^0C for 90 min. Data expressed as mean +/- SD (N=6). One-way ANOVA with pairwise comparisons using Student Newman Keuls test was performed with $p<0.05$, (*) Statistically significant compared to R-123, (**) Statistically significant compared to 1 μM CSA.

accumulation experimentation could be conducted between 2-3 weeks post seeding. To determine the specificity of R-123 and R-6G for the efflux transporter MRP, accumulation experiments were performed with the MRP inhibitor, probenecid. At 0.1 and 0.5 mM probenecid, there was no significant increase in R-123 or R-6G accumulation, suggesting that MRP does not appear to be responsible for reduced R-123 and R-6G accumulation in this model system (Figure 3.3 and 3.5).

The expression of P-gp by caco-2 cells was determined by assaying for MDR-1 mRNA using RT-PCR and by immunodetection of P-gp protein using Western blot analysis. Figure 3.6A demonstrates the presence of a 478 bp amplicon of the MDR-1 gene mRNA in the lane with the P-gp overexpressing human breast carcinoma cell line, MCF7/ADR, and in caco-2 cells. The water lane was a negative control to ensure the observed bands were not from contaminating DNA (Figure 3.6A). Western blot analysis on caco-2 cell membrane extracts was performed using the C219 (MDR) antibody that recognizes an internal, highly conserved amino acid sequence found in both MDR1 and MDR3 isoforms of P-glycoprotein. Although the MW markers were not observed on the x-ray film, the band labeled as P-gp in Figure 3.6B corresponded to approximately 170 kDa, which is the MW of the transmembrane glycoprotein, P-gp.

3.3.2. Caco-2 cellular accumulation of P-glycoprotein substrates in the presence of MePEG-*b*-PCL diblock copolymers

3.3.2.1. R-123 accumulation

The "A" series in Figures 3.7 to 3.11 show the cellular accumulation profiles for 5 μM R-123 by caco-2 cells when combined with standard P-gp inhibitors or various concentrations of the different MePEG-*b*-PCL diblock copolymers. In general, for all five

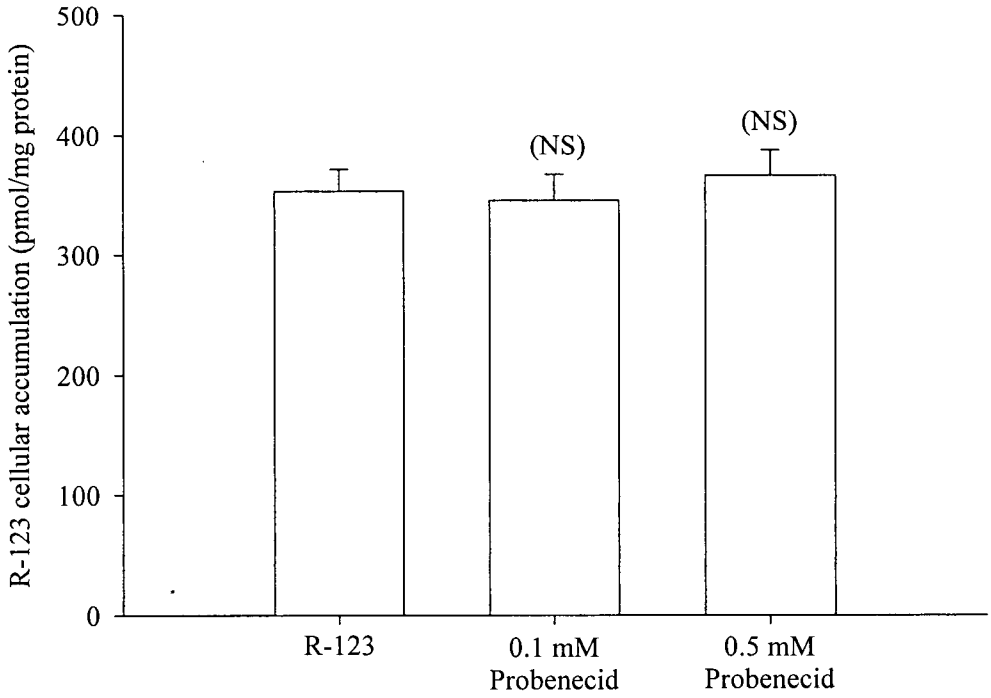

Figure 3.5. Effect of the MRP inhibitor, probenecid, on accumulation of 5 μM R-123 at 37^0C for 90 min. Data expressed as mean +/- SEM (N=3). One-way ANOVA with pairwise comparisons using Student Newman Keuls test was performed with $p<0.05$, (NS) Not statistically significant compared to R-123 alone.

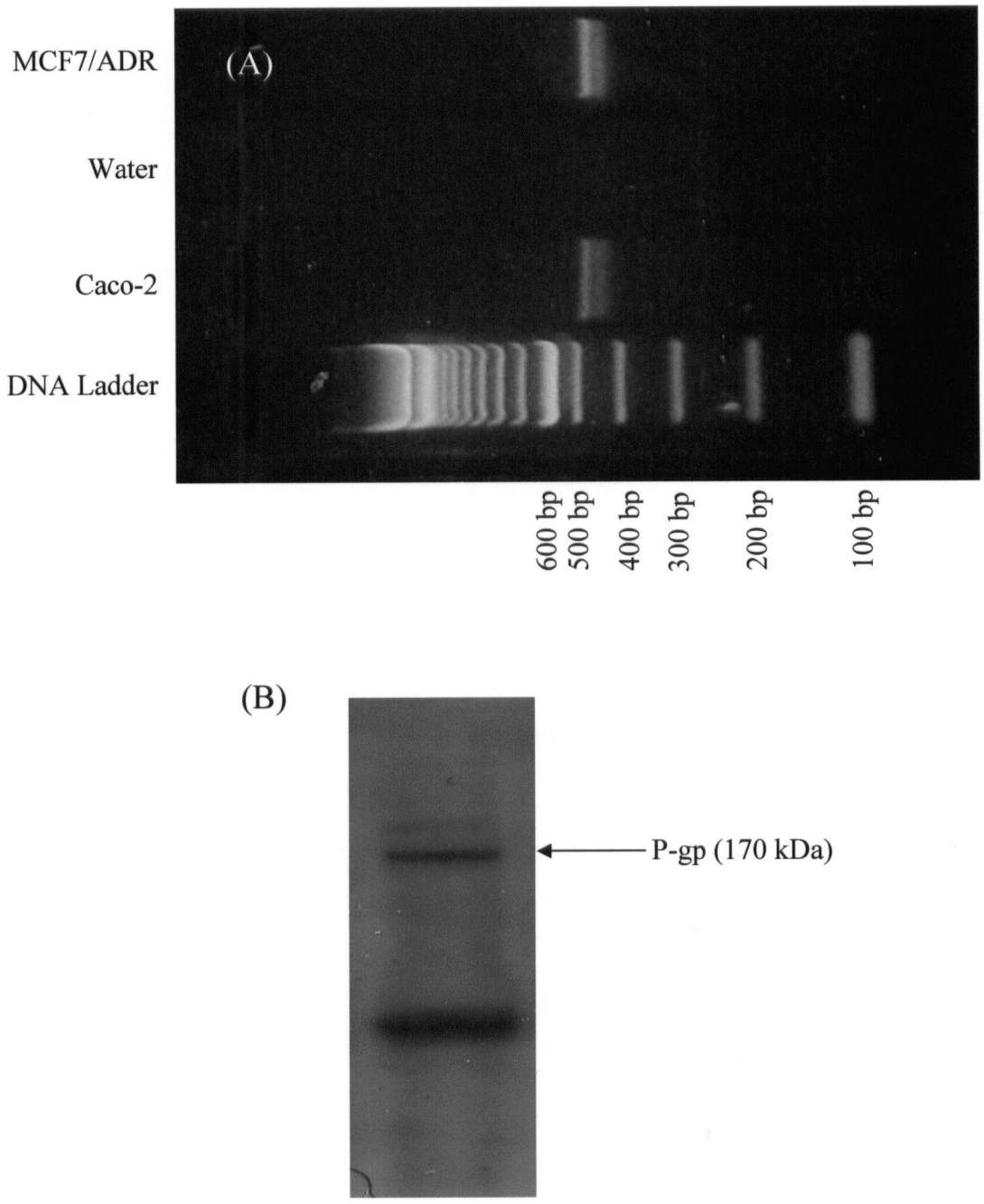

Figure 3.6. Detection of MDR-1 gene expression in caco-2 cells using (A) RT-PCR producing a 478 bp amplican and (B) immunodetection of P-gp by Western blot analysis.

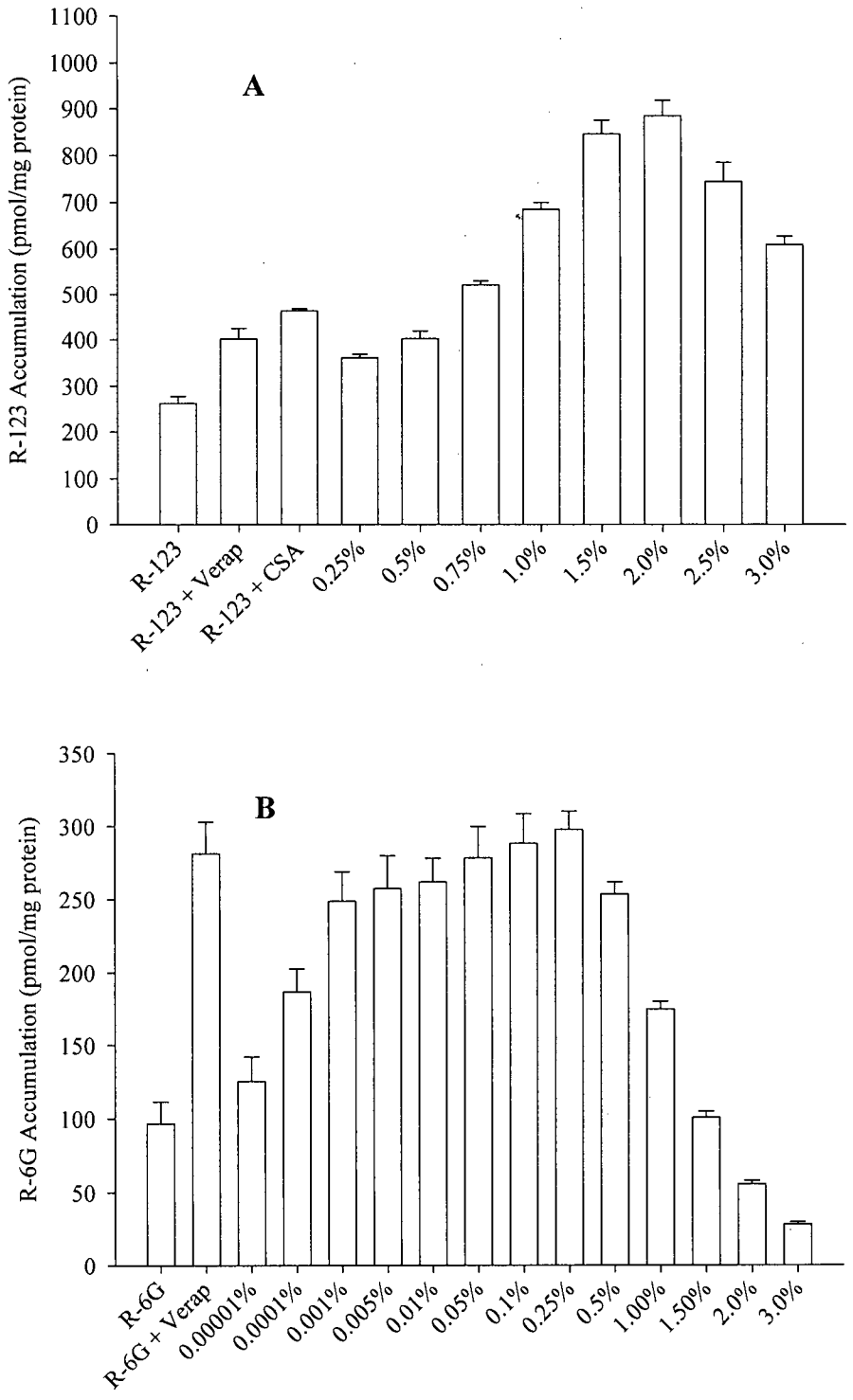

Figure 3.7. Effect of $MePEG_{17}$-*b*-PCL_2 concentration ranging from 0.00001% to 3% on cellular accumulation of (A) 5 μM R-123 and (B) 0.25 μM R-6G by caco-2 cells at 37^0C for 90 min. Data expressed as mean +/- SEM (N=3).

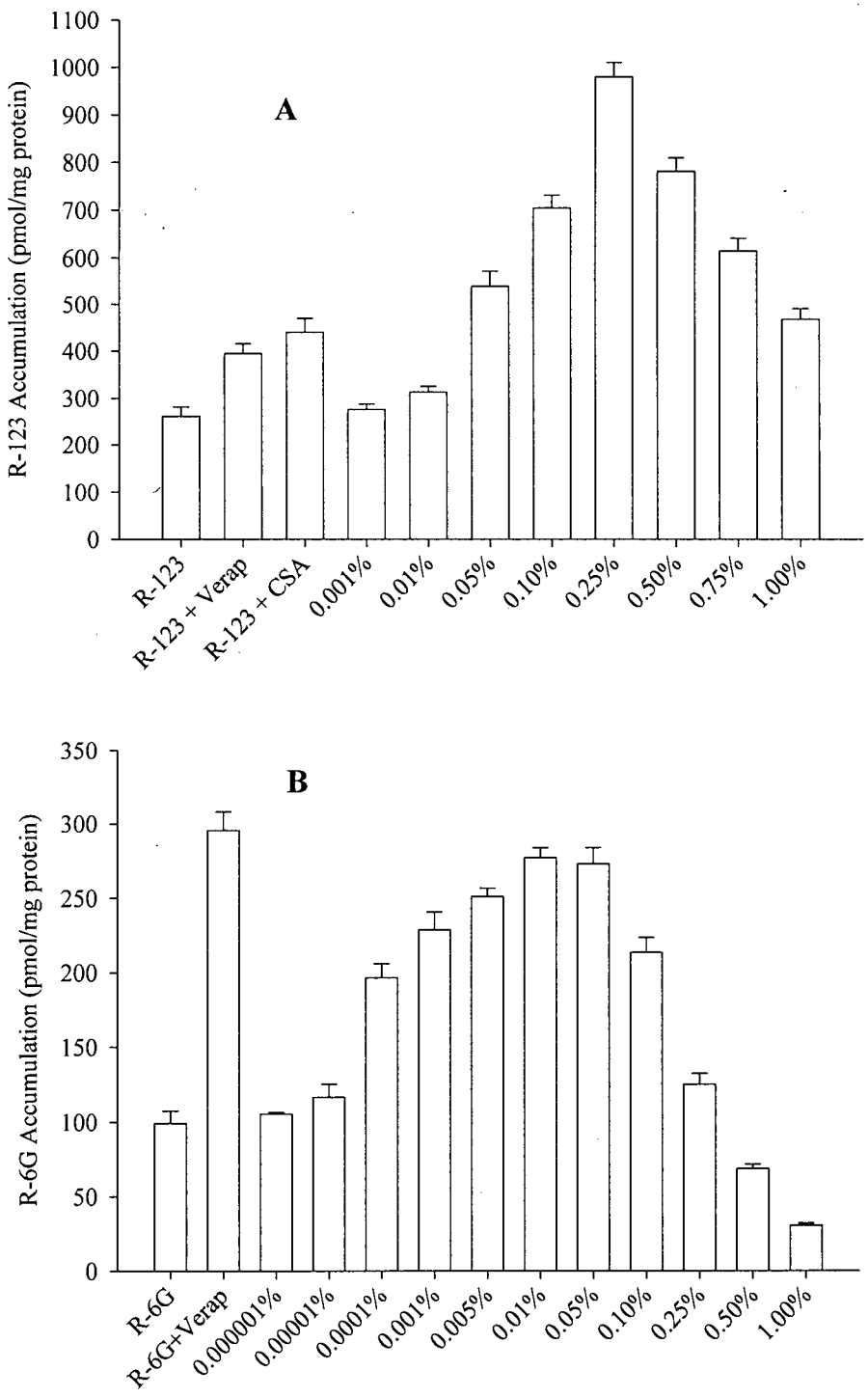

Figure 3.8. Effect of $MePEG_{17}$-*b*-PCL_5 concentration ranging from 0.000001% to 1% on cellular accumulation of (A) 5 μM R-123 and (B) 0.25 μM R-6G by caco-2 cells at 37^0C for 90 min. Data expressed as mean +/- SEM (N=3).

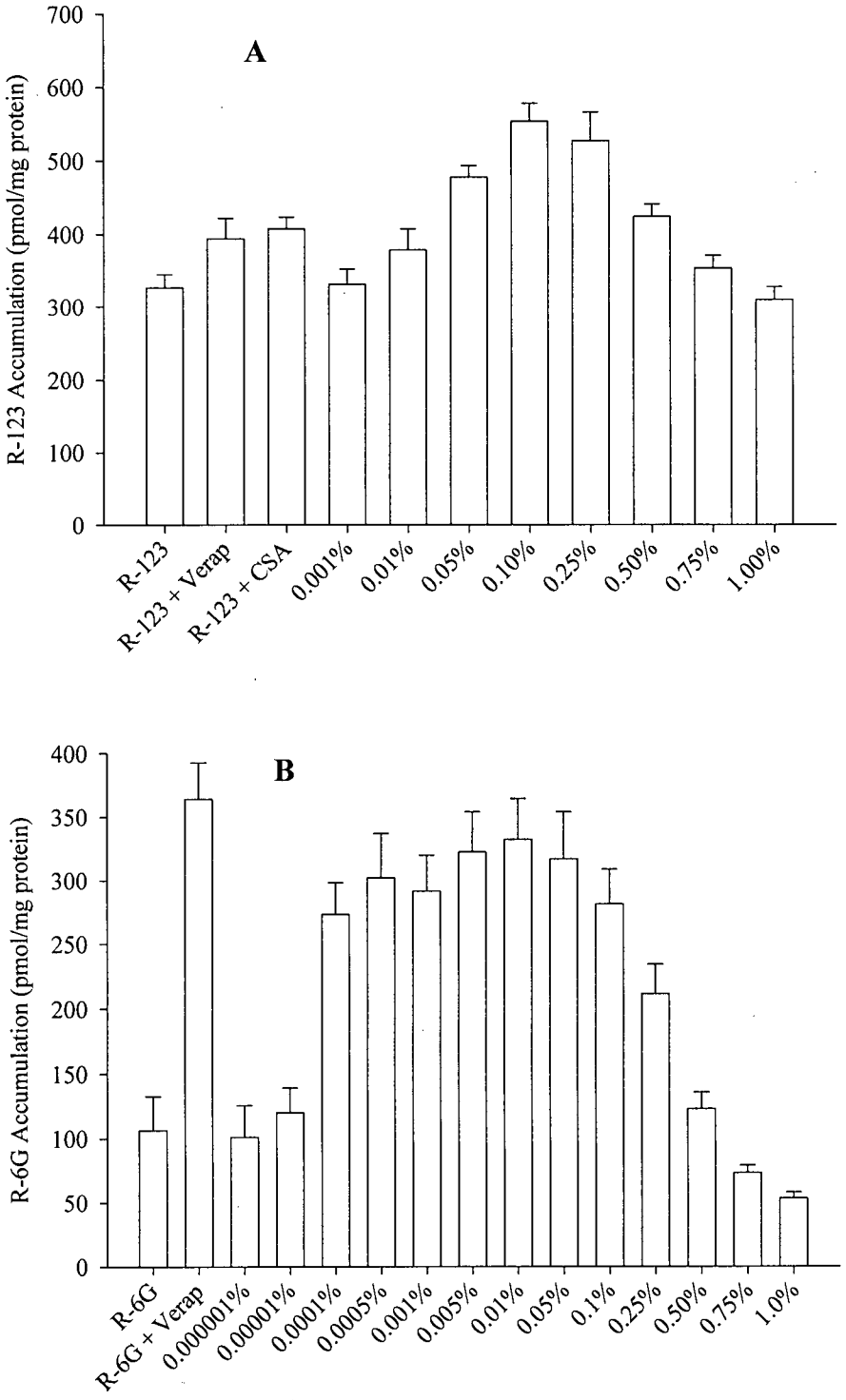

Figure 3.9. Effect of $MePEG_{17}$-*b*-PCL_{10} concentration ranging from 0.000001% to 1% on cellular accumulation of (A) 5 μM R-123 and (B) 0.25 μM R-6G by caco-2 cells at 37^0C for 90 min. Data expressed as mean +/- SEM (N=3).

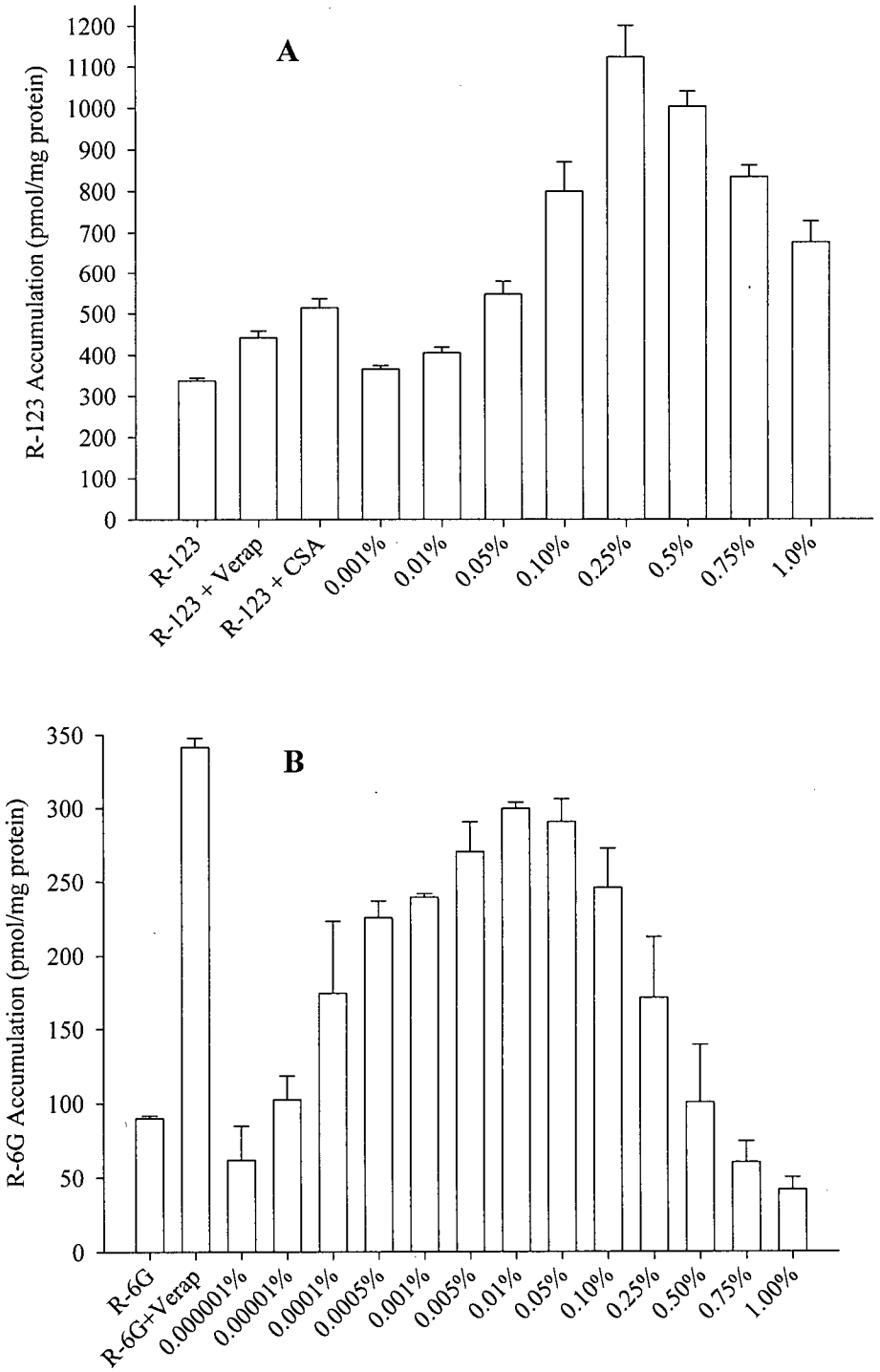

Figure 3.10. Effect of $MePEG_{12}$-*b*-PCL_4 concentration ranging from 0.000001% to 1% on cellular accumulation of (A) 5 μM R-123 and (B) 0.25 μM R-6G by caco-2 cells at 37^0C for 90 min. Data expressed as mean +/- SEM (N=3).

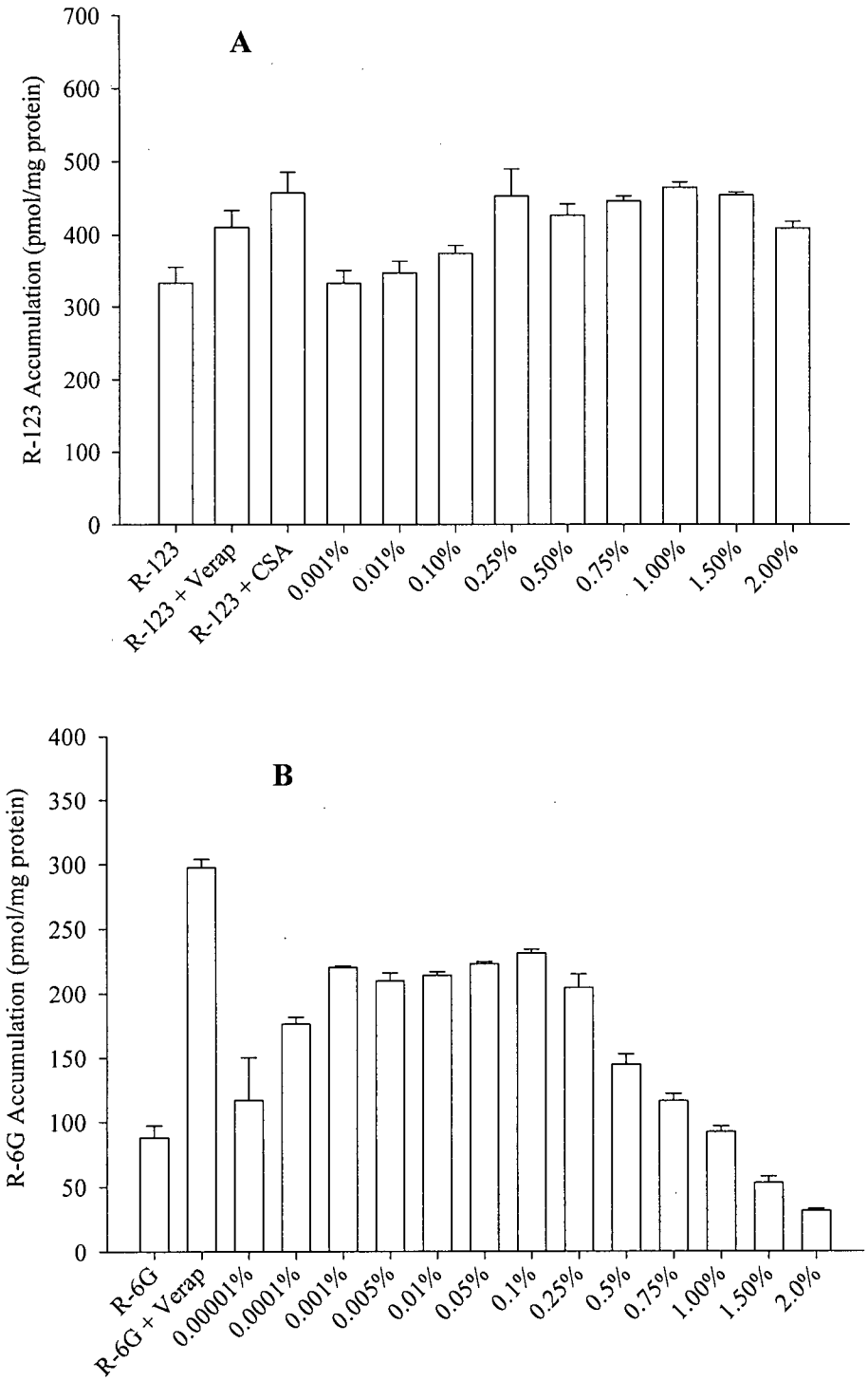

Figure 3.11. Effect of $MePEG_{45}$-*b*-PCL_5 concentration ranging from 0.00001% to 2% on cellular accumulation of (A) 5 μM R-123 and (B) 0.25 μM R-6G by caco-2 cells at 37^0C for 90 min. Data expressed as mean +/- SEM (N=3).

diblock copolymers evaluated, as the concentration of MePEG-*b*-PCL increased the accumulation of R-123 increased up to a critical concentration of diblock, after which R-123 accumulation began to decrease. This pattern of increasing R-123 accumulation with increasing diblock concentration was not as pronounced for $MePEG_{45}$-*b*-PCL_5, as the overall enhancement was lower compared to the other four MePEG-*b*-PCL diblock copolymers (Figure 3.11A). The accumulation of R-123 over a range of MePEG-*b*-PCL diblock concentrations was greater than or equal to the level of accumulation observed with the P-gp inhibitors verapamil (50 μM) and CSA (4 μM). The concentrations required for maximal increase in R-123 accumulation for all five MePEG-*b*-PCL diblock copolymers were in the order of 6 to 100 fold higher than their respective CMC values, with little or no enhancement observed below the CMC (Table 3.1 and Figures 3.7 to 3.11 "A" series). To compare the effect of diblock composition and the magnitude of R-123 accumulation enhancement, Table 3.1 provides the Accumulation Enhancement Factor (AEF) for all treatment groups. The AEF describes the relative fold increase in R-123 accumulation and was determined from the ratio of R-123 accumulation with P-gp inhibitors or MePEG-*b*-PCL at the peak effect to the accumulation of R-123 alone. AEF values for verapamil and CSA were 1.5 and 1.7, respectively, compared to MePEG-*b*-PCL diblock copolymers, which ranged from 1.7 to 3.8. For the MePEG 750 series, an increase in the PCL chain length from 2 to 5 repeat units had no effect on the AEF (Table 3.1). However, a further increase in the PCL block length from 5 to 10 markedly reduced the AEF from 3.8 to 1.9. Increasing the molecular weight of MePEG from 550 to 750 with a PCL length of 5 resulted in similar AEF values of 3.4 and 3.8, respectively, but the AEF was decreased to 1.7 with MePEG 2000. The concentration of $MePEG_{17}$-*b*-PCL_2 diblock copolymer required to enhance R-123 accumulation was higher

Table 3.1: The concentration of MePEG-*b*-PCL diblock copolymers producing maximum enhanced accumulation of 5 μM R-123 and 0.25 μM R-6G by caco-2 cells and the Accumulation Enhancement Factor (AEF).

Diblock Copolymer Series	Treatment Group	HLB	CMC[a] (%w/v)	Peak Effect Conc. (%w/v)		AEF[b]	
				R-123	R-6G	R-123	R-6G
	50 μM Verapamil	N/A	N/A	N/A	N/A	1.5[c]	3.3[c]
	4 μM CSA	N/A	N/A	N/A	N/A	1.7[c]	N/D
MePEG 550	$MePEG_{12}$-*b*-PCL_4	9.2	0.008	0.25	0.01	3.4	3.3
MePEG 750	$MePEG_{17}$-*b*-PCL_2	16.6	0.303	2.00	0.25	3.4	3.1
	$MePEG_{17}$-*b*-PCL_5	12.2	0.031	0.25	0.01	3.8	2.8
	$MePEG_{17}$-*b*-PCL_{10}	8.4	0.001	0.10	0.01	1.9	3.1
MePEG 2000	$MePEG_{45}$-*b*-PCL_5	18.3	0.066	1.00	0.10	1.7	2.6

a) Critical micelle concentration (CMC) reported in %w/v from Table 2.1
b) AEF determined as the ratio of R-123 or R-6G accumulation with MePEG-*b*-PCL diblock copolymers or P-gp inhibitors to accumulation of R-123 or R-6G alone
c) AEF value represents an average of all experimental groups from the series of studies

relative to the other diblock copolymers tested. It was possible that given the low degree of polymerization of PCL, that a large MePEG 750 oligomer fraction was in solution. To evaluate whether MePEG 750 oligomers were partially responsible for the enhanced R-123 accumulation, studies were carried out using MePEG 750 at concentrations ranging from 0.1% to 3% w/v. Figure 3.12 shows that MePEG 750 as high as 3% w/v had no effect on R-123 accumulation.

3.3.2.2. R-6G accumulation

Using varying concentrations of the different MePEG-*b*-PCL diblock copolymers, the accumulation of R-6G (0.25 μM) was evaluated in caco-2 cells and the results are displayed in the "B" series of Figures 3.7 to 3.11. Similar to previous results with R-123 (Figures 3.7 to 3.11 "A" series), the accumulation profiles for R-6G followed the trend of increasing accumulation with increasing diblock concentration, followed by a decline at higher diblock concentrations. The concentration range of diblock over which accumulation of R-6G increased occurred over a broad range, with concentrations as low as 0.0001% w/v diblock resulting in enhanced R-6G accumulation. The enhancement of R-6G accumulation increased as the MePEG-*b*-PCL concentration increased, reaching a maximum at or near the copolymer's respective CMC (Figures 3.7 to 3.11 "B" series and Table 3.1). However, the concentration of $MePEG_{17}$-*b*-PCL_{10} that produced maximum R-6G accumulation was 10 fold higher than the CMC (Table 3.1). Overall, an AEF of approximately 3 was demonstrated for R-6G accumulation enhancement with the P-gp inhibitor verapamil and for all MePEG-*b*-PCL diblock copolymers (Table 3.1).

3.3.2.3. Comparison of R-123 to R-6G accumulation

Although similarities between R-123 and R-6G accumulation profiles with the

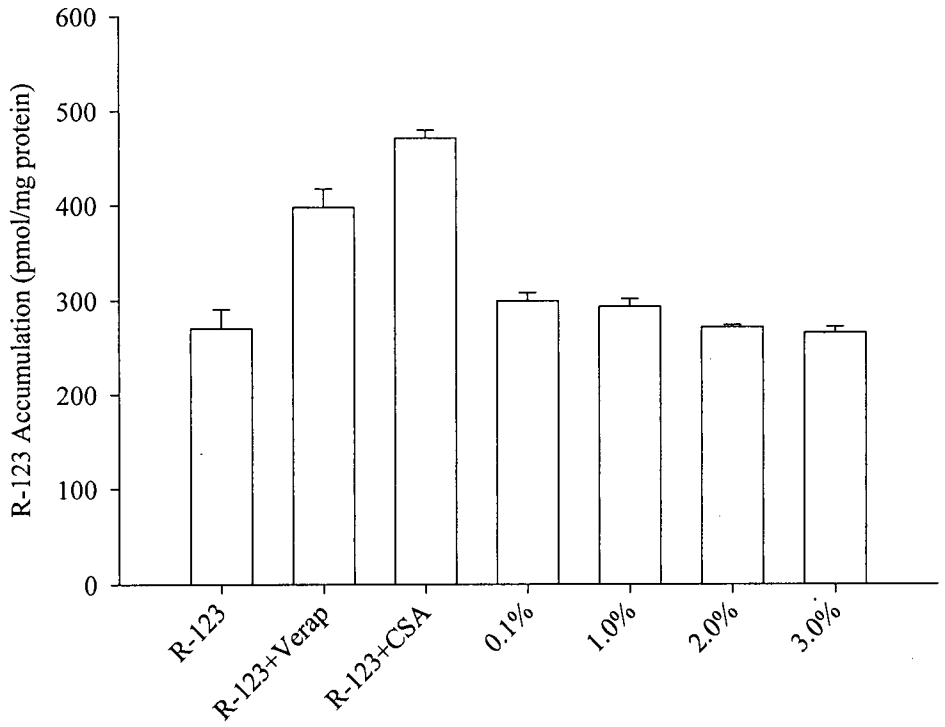

Figure 3.12. Caco-2 cellular accumulation of 5 μM R-123 at 37^0C for 90 min with verapamil, CSA and various concentrations of MePEG 750 oligomers. Data expressed as mean +/- SEM (N=3).

different MePEG-*b*-PCL diblock copolymers were noted, there were pronounced differences. The standard P-gp inhibitors, verapamil and CSA, demonstrated a 1.5 and 1.7 fold increase in R-123 accumulation compared to R-6G accumulation where verapamil produced a 3.3 fold increase (Table 3.1). AEF values for R-6G accumulation in the presence of verapamil and all diblock copolymers were similar, whereas AEF values for R-123 accumulation appeared to be dependent on block composition, with diblock HLB's ranging from 9-17 producing high AEF's (Figure 3.13). Two diblock copolymers, $MePEG_{17}$-*b*-PCL_{10} and $MePEG_{45}$-*b*-PCL_5, produced a marginal increase in R-123 accumulation (AEF of 1.9 to 1.7 respectively), which was no greater than verapamil or CSA. However, both $MePEG_{17}$-*b*-PCL_{10} and $MePEG_{45}$-*b*-PCL_5 were capable of enhancing R-6G accumulation 3.1 and 2.6 fold respectively (Table 3.1). Maximal enhancement of R-6G accumulation was achievable with 8-25 fold lower diblock concentrations compared to R-123 (Table 3.1). The concentration range over which enhanced R-123 accumulation was observed, was greater than or equal to the CMC of the diblock copolymers, while enhanced R-6G accumulation was found at concentrations less than or equal to the CMC of the diblock copolymers (Figures 3.7 to 3.11 A and B).

3.3.2.4. Cellular accumulation of R-123 and R-6G with $MePEG_{44}$-*b*-$PDLLA_9$

Figure 3.14A and B show the cellular accumulation of R-123 and R-6G in the presence of the $MePEG_{44}$-*b*-$PDLLA_9$ diblock copolymer, respectively. No enhancement in R-123 accumulation was found over a wide range of $MePEG_{44}$-*b*-$PDLLA_9$ concentrations (Figure 3.14A). However, there was an enhanced R-6G accumulation with an AEF of 2.6 at a $MePEG_{44}$-*b*-$PDLLA_9$ concentration of 0.001% w/v (Figure 3.14B).

3.3.2.5. Intracellular distribution of R-123 and R-6G

The intracellular localization of R-123 and R-6G was examined using confocal

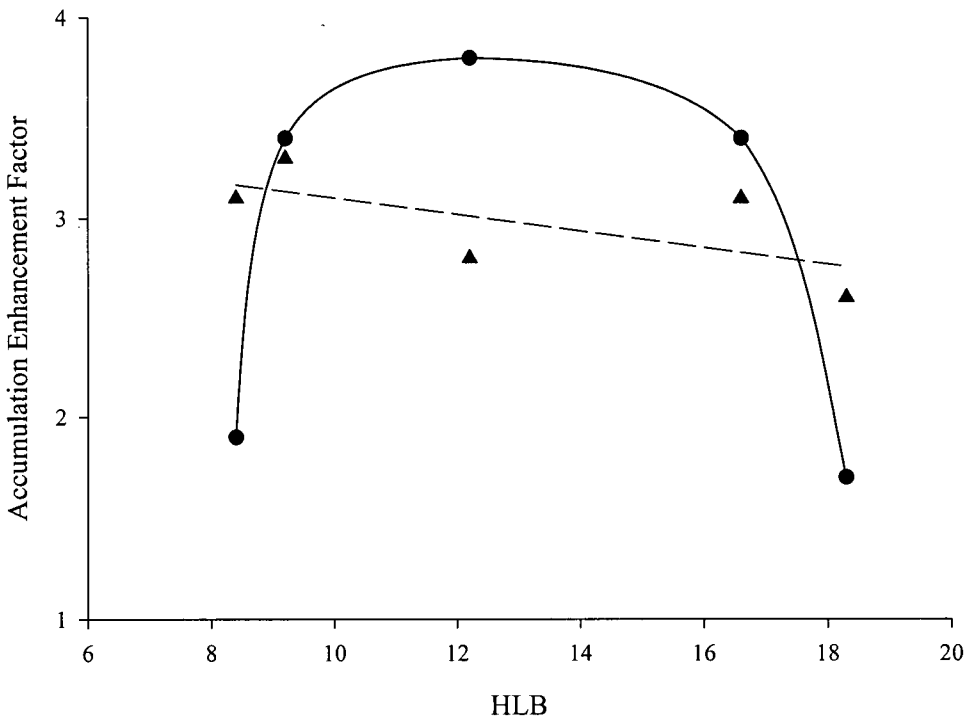

Figure 3.13. Relationship MePEG-*b*-PCL diblock copolymer HLB with (●) R-123 and (▲) R-6G Accumulation Enhancement Factor

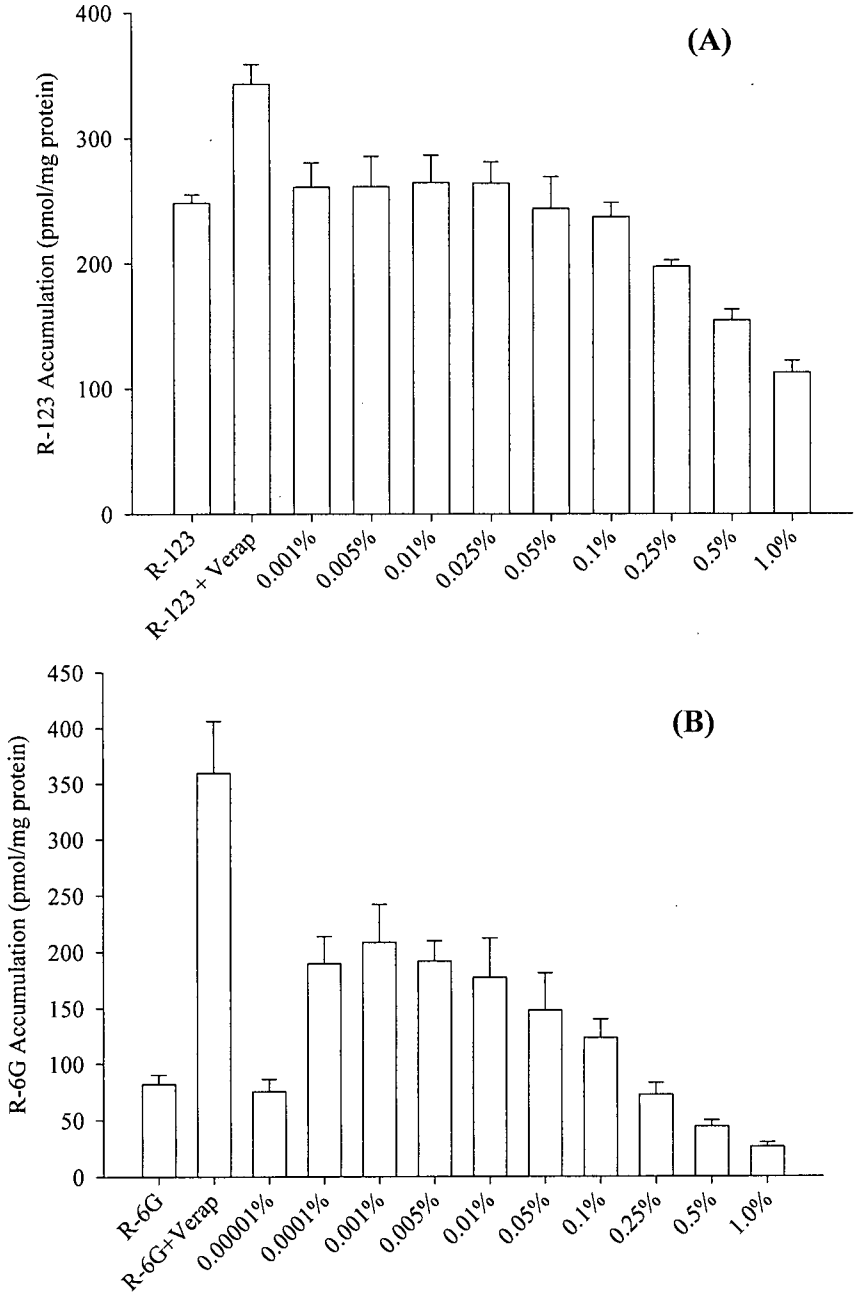

Figure 3.14. Effect of $MePEG_{44}$-*b*-$PDLLA_9$ concentration on cellular accumulation of (A) 5 μM R-123 and (B) 0.25 μM R-6G by caco-2 cells at 37^0C for 90 min. Data expressed as mean +/- SEM (N=3).

fluorescence microscopy. Intracellular distribution patterns of the probes in assay buffer, and the probes in the presence of a concentration of $MePEG_{17}$-*b*-PCL_5 that resulted in maximum accumulation enhancement, were compared. Figures 3.15A and 3.16A display a punctated pattern of fluorescence localized within the cells after exposure to 5 μM R-123 and 0.25 μM R-6G in assay buffer, respectively. In the presence of 0.25% $MePEG_{17}$-*b*-PCL_5, R-123 fluorescence was distributed in a diffuse manner throughout the cytosol (Figure 3.15B). A similar pattern of fluorescence was observed for R-6G with 0.01% $MePEG_{17}$-*b*-PCL_5 (Figure 3.16B).

3.3.2.6. Comparison of paclitaxel and doxorubicin caco-2 cellular accumulation

Additional caco-2 accumulation studies involved two P-gp substrates, paclitaxel (PTX) and doxorubicin (DOX), with assay buffer, verapamil or various concentrations of $MePEG_{17}$-*b*-PCL_5. Similar to R-6G, PTX is hydrophobic and similar to R-123, DOX is charged and more hydrophilic. As observed for the rhodamine dyes, PTX and DOX showed an increase in the accumulation with increasing diblock concentration up to a critical concentration, followed by a decline in accumulation (Figure 3.17 and 3.18). PTX accumulation reached a maximum in the presence of 0.01% $MePEG_{17}$-*b*-PCL_5 with an AEF of 2.2 (Figure 3.17). The AEF for PTX accumulation with 50 μM verapamil was 2.9. In contrast, there was no increased DOX accumulation in the presence of verapamil up to 200 μM (Figure 3.18). Furthermore, a high concentration of 1.0% $MePEG_{17}$-*b*-PCL_5 was required to maximally increase DOX accumulation with an AEF of 1.8 (Figure 3.18).

3.3.3. Cytotoxicity of MePEG-*b*-PCL diblock copolymers

The release of cytoplasmic LDH induced by MePEG-*b*-PCL diblock copolymers from caco-2 cells is shown in Figure 3.19. MePEG-*b*-PCL diblock copolymers caused LDH

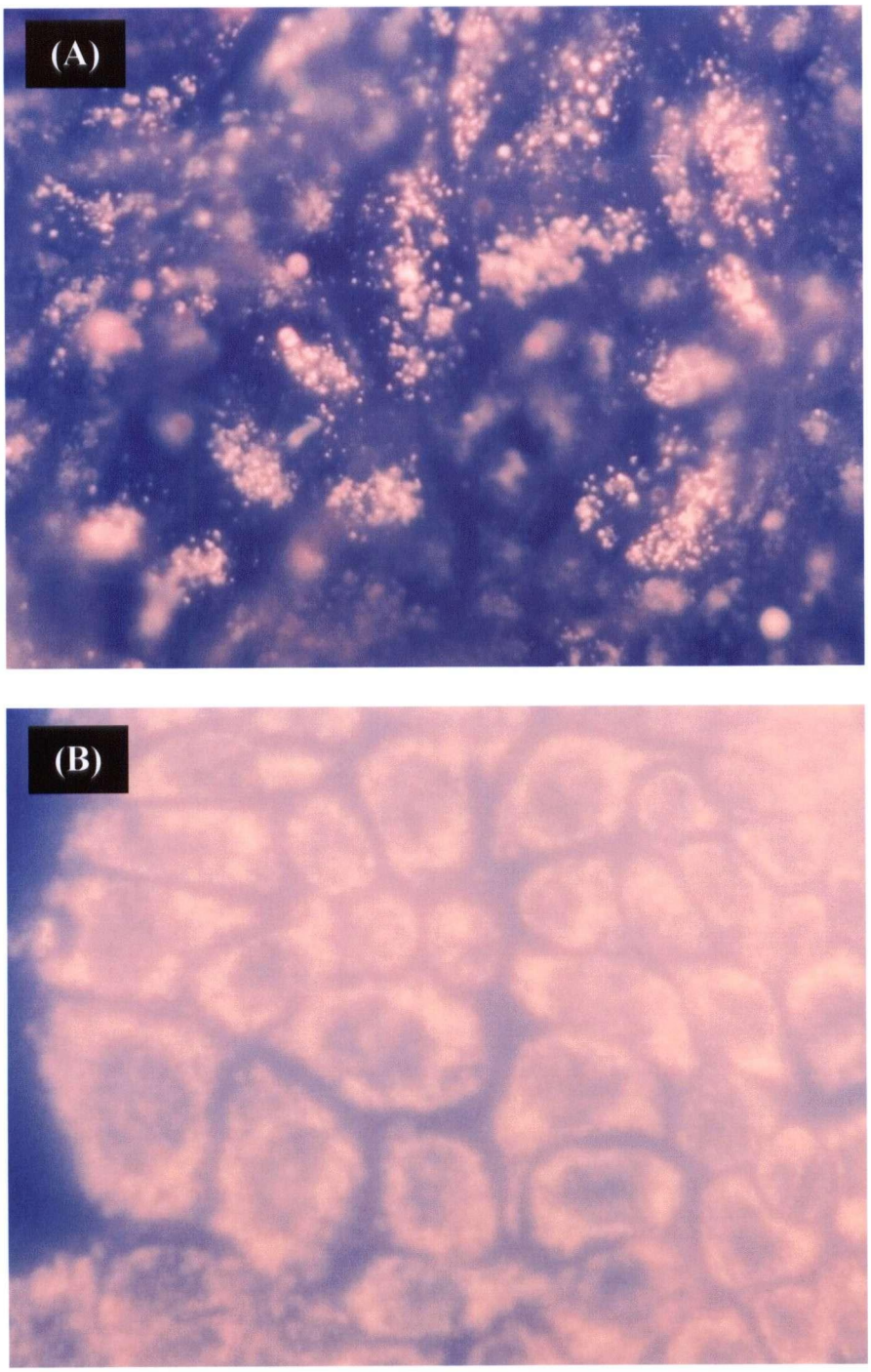

Figure 3.15. Confocal fluorescence microscopy photographs of R-123 accumulation by caco-2 cells after exposure to either (A) 5.0 μM R-123 in assay buffer or (B) 5.0 μM R-123 with 0.25% $MePEG_{17}$-*b*-PCL_5 for 90 min at 37^0C. Photographs were taken using a 40x objective.

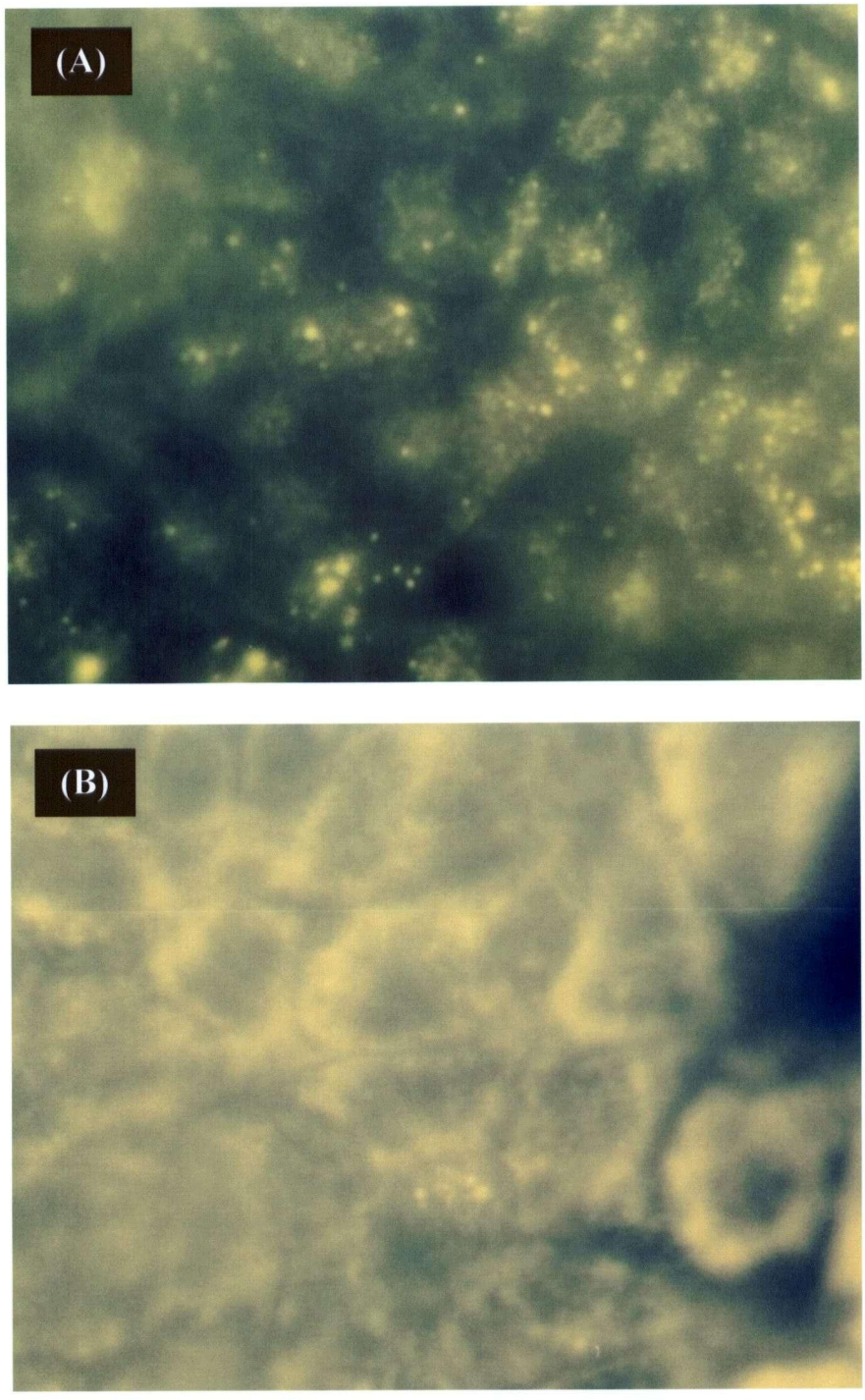

Figure 3.16. Confocal fluorescence microscopy photographs of R-6G accumulation by caco-2 cells after exposure to either (A) 0.25 μM R-6G in assay buffer or (B) 0.25 μM R-6G with 0.01% $MePEG_{17}$-*b*-PCL_5 for 90 min at 37^0C. Photographs were taken using a 40x objective.

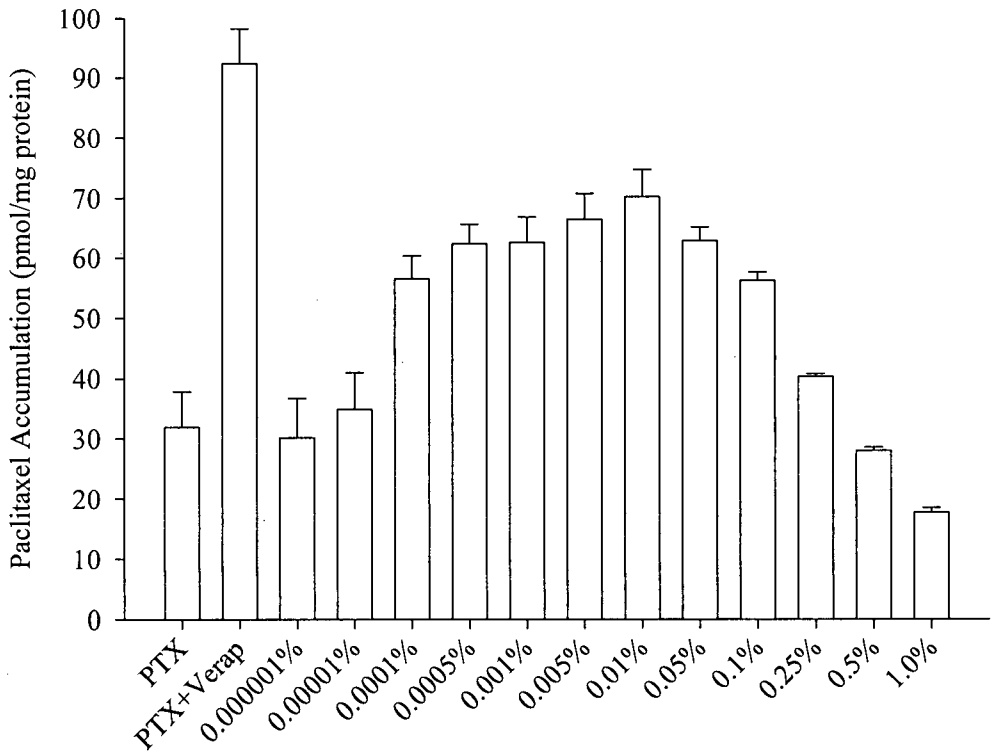

Figure 3.17. Caco-2 cellular accumulation of 0.5 μM paclitaxel at 37^0C for 90 min with various concentrations of $MePEG_{17}$-*b*-PCL_5. Data expressed as mean +/- SEM (N=3).

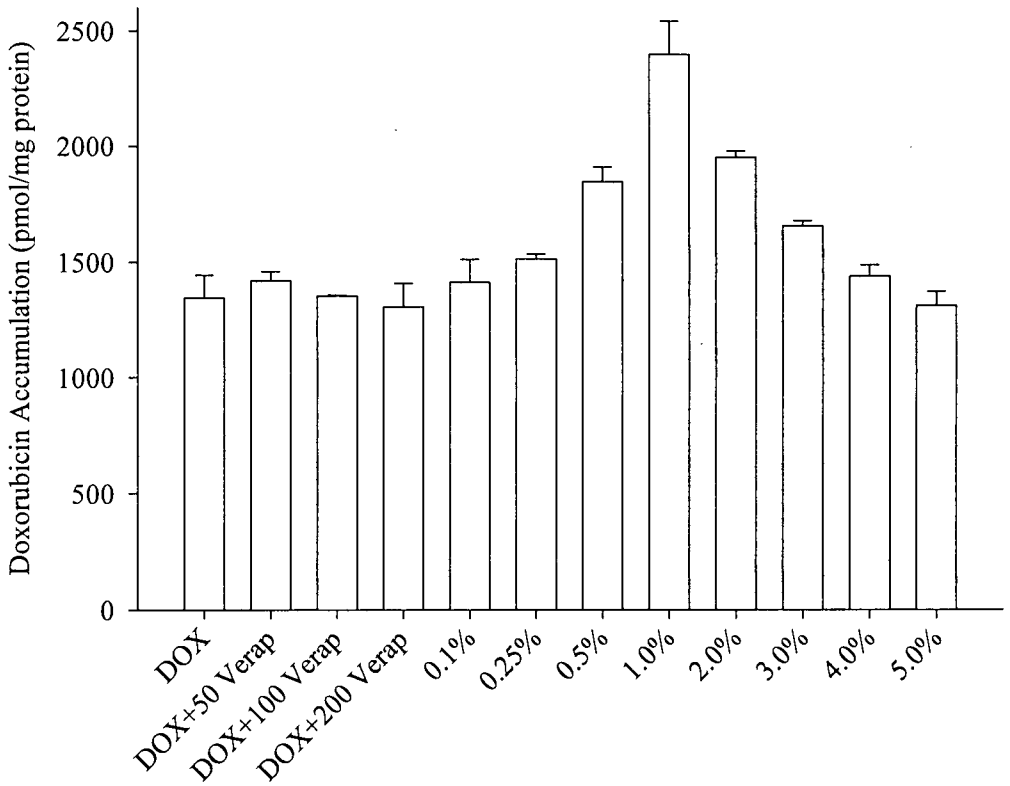

Figure 3.18. Caco-2 cellular accumulation of 10 μM doxorubicin at 37^{0}C for 90 min with various concentrations of MePEG$_{17}$-*b*-PCL$_5$ and verapamil. Data expressed as mean +/- SEM (N=2).

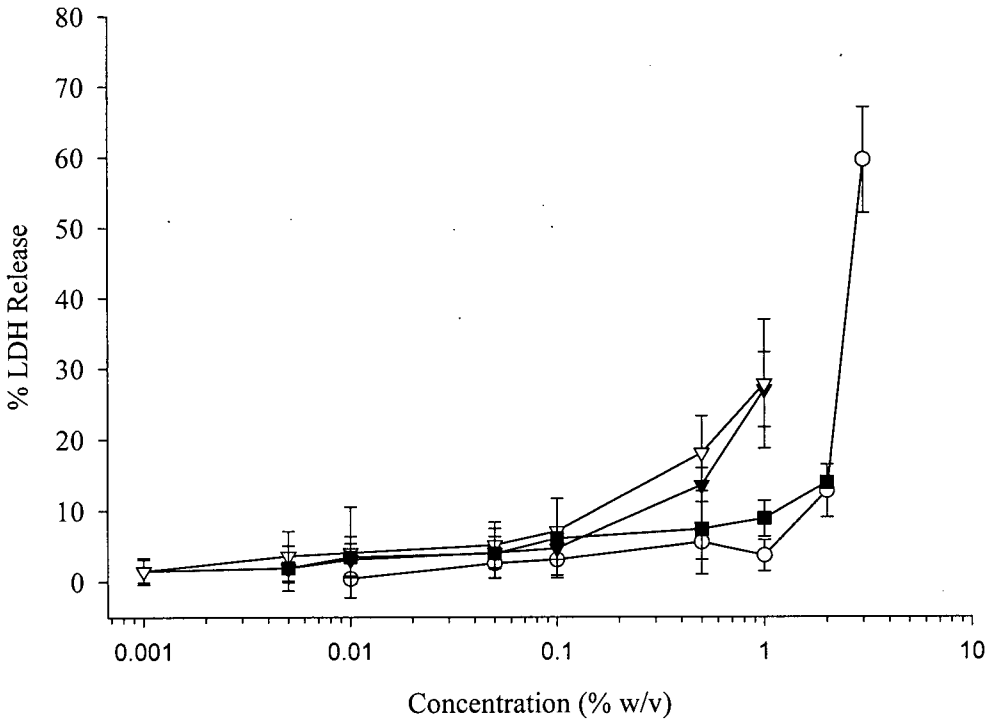

Figure 3.19. LDH release from caco-2 cells induced by varying concentrations of $MePEG_{17}$-*b*-PCL_2 (○), $MePEG_{17}$-*b*-PCL_5 (▼), $MePEG_{17}$-*b*-PCL_{10} (▽), and $MePEG_{45}$-*b*-PCL_4 (■). Incubation was for 1.5 h at 37^0C. Data expressed as the mean +/- SEM (N=3).

release at concentrations above 0.5% w/v for $MePEG_{17}$-*b*-PCL_5 and $MePEG_{17}$-*b*-PCL_{10}. However, $MePEG_{45}$-*b*-PCL_4 did not induce LDH release up to 2.0%w/v and $MePEG_{17}$-*b*-PCL_2 resulted in less than 10% release at 2.0% w/v, but caused 60% release at 3.0% w/v.

3.3.4. Time dependent accumulation of R-123 and R-6G

The rate of R-123 and R-6G accumulation was assessed over 2-3 h with verapamil and MePEG-*b*-PCL diblock copolymers at concentrations which previously demonstrated maximum accumulation enhancement (Figure 3.20 and 3.21). For R-123, 0.25% $MePEG_{17}$-*b*-PCL_5 and 2.0% $MePEG_{17}$-*b*-PCL_2 diblock copolymer produced a rapid increase in R-123 accumulation compared to R-123 alone or R-123 with verapamil over the first 15 min (Figure 3.20). However, there was no rapid increase in R-6G accumulation for 0.01% $MePEG_{17}$-*b*-PCL_5 and 0.25% $MePEG_{17}$-*b*-PCL_2 diblock copolymers at early time points (Figure 3.21). The accumulation versus time curves were fit to a first order exponential rise equation using Sigmaplot version 5 software (SPSS Inc., Chicago, IL) and the accumulation rate constants determined. Table 3.2 shows that both R-123 with assay buffer and verapamil had similar rate constants of 0.013 and 0.01 min^{-1}, respectively. The rate constants for $MePEG_{17}$-*b*-PCL_5 and $MePEG_{17}$-*b*-PCL_2 diblock copolymer were higher than verapamil or R-123 alone at 0.032 min^{-1} and 0.043 min^{-1}, respectively, while the rate constants for $MePEG_{17}$-*b*-PCL_{10} (0.015 min^{-1}) and $MePEG_{45}$-*b*-PCL_5 (0.02 min^{-1}) were similar to R-123 alone. For R-6G accumulation, the rate constants for $MePEG_{17}$-*b*-PCL_5 and $MePEG_{17}$-*b*-PCL_2 diblock copolymer were similar to R-6G with buffer and verapamil (Table 3.2).

3.3.5. Solubilization of R-123 and R-6G within MePEG-*b*-PCL micelles

The extent of R-123 and R-6G solubilization within MePEG-*b*-PCL diblock copolymer micelles was determined using equilibrium dialysis. By convention in this work,

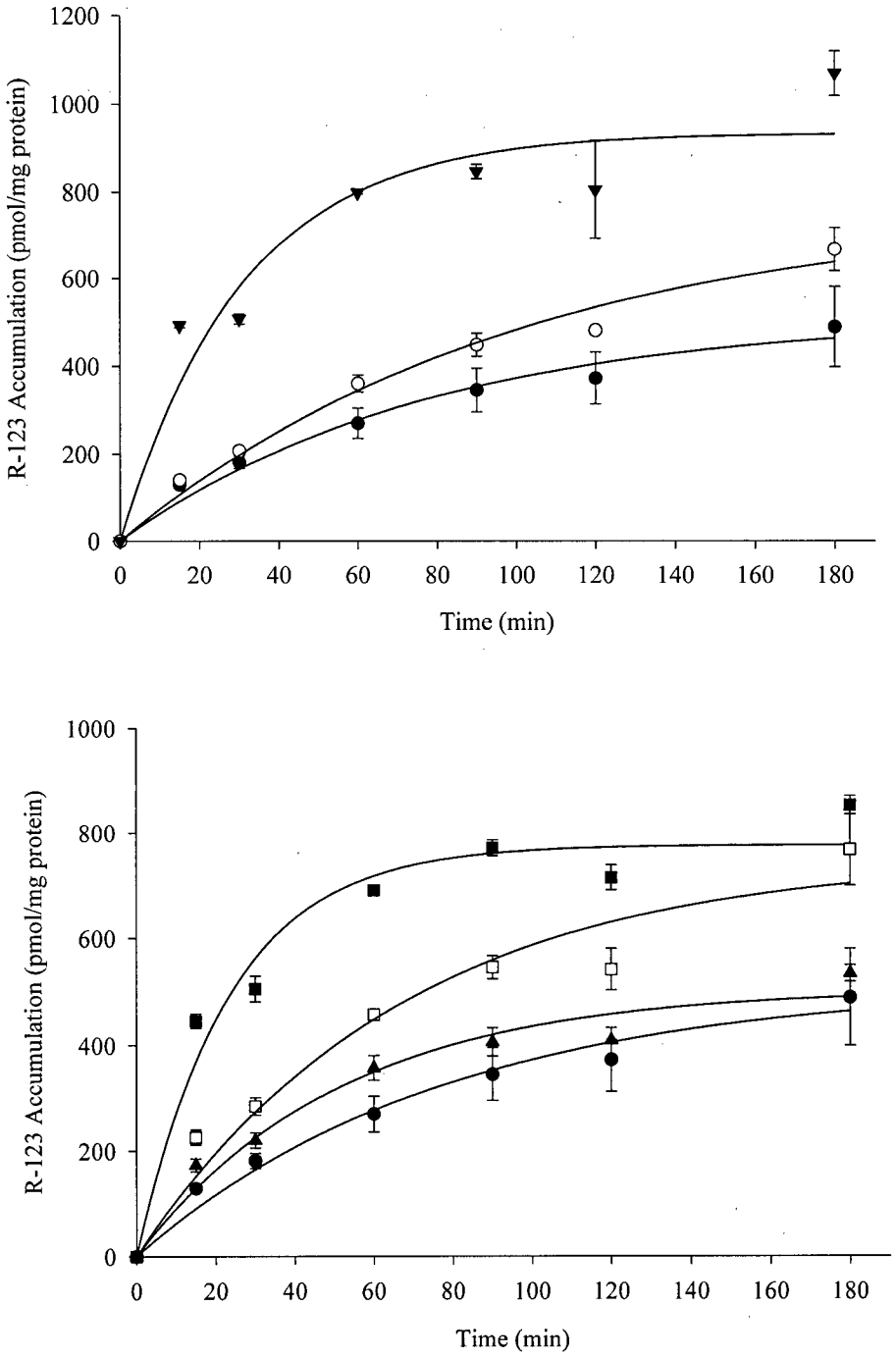

Figure 3.20. The rate of R-123 accumulation by caco-2 cells. Caco-2 cells were incubated at 37^0C with 5 μM R-123 in (●) assay buffer, (○) 50 μM verapamil, (▼) 0.25% $MePEG_{17}$-*b*-PCL_5, (■) 2.0% $MePEG_{17}$-*b*-PCL_2, (□) 0.1% $MePEG_{17}$-*b*-PCL_{10}, (▲) 1.0% $MePEG_{45}$-*b*-PCL_5. Data expressed as the mean +/- SEM (N=3).

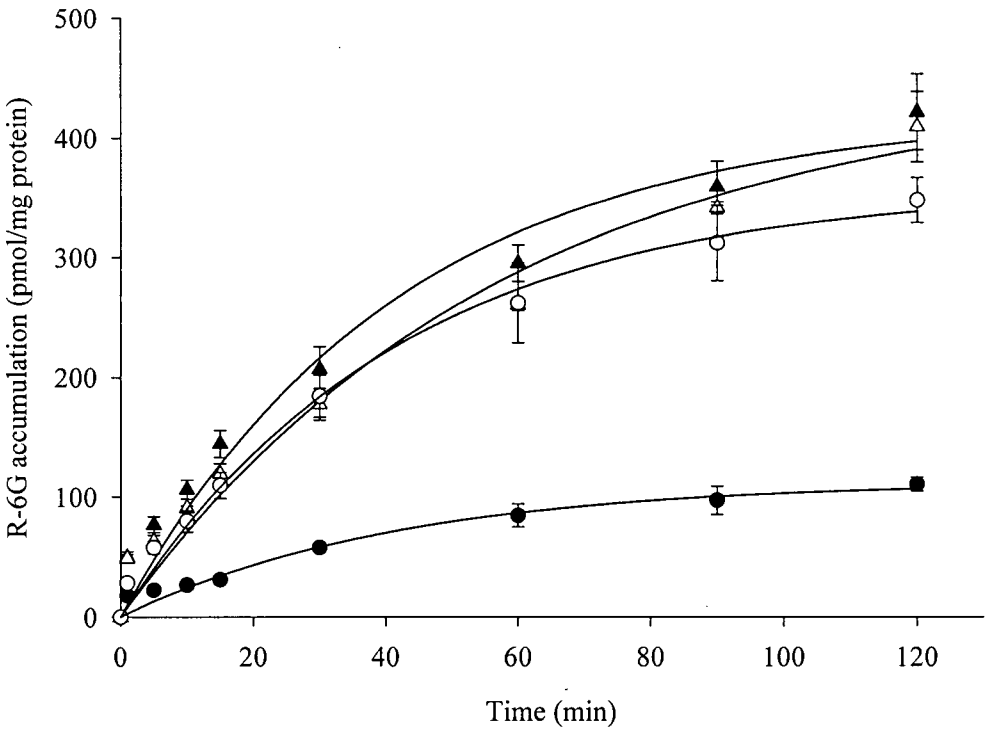

Figure 3.21. The rate of R-6G accumulation by caco-2 cells. Caco-2 cells were incubated at 37^0C with 0.25 μM R-6G in (●) assay buffer, (○) 50 μM verapamil, (▲) 0.25% $MePEG_{17}$-*b*-PCL_2 and (▽) 0.01% $MePEG_{17}$-*b*-PCL_5. Data expressed as the mean +/- SEM (N=4).

Table 3.2: Rate constants (k) and coefficient of variation for curve fitting (R^2) for R-123 and R-6G accumulation over time with verapamil or MePEG-*b*-PCL diblock copolymers at the peak accumulation enhancement concentrations.

Diblock Copolymer Series	Treatment group[a]	R-123		R-6G	
		k (min^{-1})	R^2	k (min^{-1})	R^2
	Buffer	0.013	0.978	0.024	0.971
	50 μM Verapamil	0.010	0.984	0.024	0.993
MePEG 750	$MePEG_{17}$-*b*-PCL_2	0.043	0.962	0.024	0.973
	$MePEG_{17}$-*b*-PCL_5	0.032	0.924	0.017	0.973
	$MePEG_{17}$-*b*-PCL_{10}	0.015	0.954	N/D	N/D
MePEG 2000	$MePEG_{45}$-*b*-PCL_5	0.020	0.966	N/D	N/D

(a) Concentrations of diblock used with R-123 and R-6G are the peak accumulation enhancement concentrations reported in Table 3.1.

the terms "bound" and "binding" describe the incorporation or solubilization of probe within the micellar core and do not refer to any intermolecular interactions. The bound/solubilized fraction (Fb) of R-123 and R-6G with increasing concentrations of MePEG-*b*-PCL diblock copolymers is shown in Figures 3.22 to 3.25 'A' series and 'B' series, respectively. An increase in the Fb for R-123 and R-6G was observed with increasing MePEG-*b*-PCL diblock concentrations for all four diblock copolymers evaluated. The Fb for R-123 and R-6G using $MePEG_{12}$-*b*-PCL_4 diblock was not determined since cloudiness in the micellar solution was observed over the desired concentration range, possibly due to the cloud point phenomenon at 37^0C that may affect solubilization of R-123 and R-6G. The Fb for R-6G was consistently higher than for R-123 at corresponding concentrations for each MePEG-*b*-PCL diblock (Figure 3.22 to 3.25 'A' and 'B' series). For R-123 binding, approximately 10 to 30% of the R-123 in solution was bound within micelles at diblock concentrations of 2.0, 0.25, 0.1% and 1.0% for $MePEG_{17}$-*b*-PCL_2, $MePEG_{17}$-*b*-PCL_5, $MePEG_{17}$-*b*-PCL_{10}, $MePEG_{45}$-*b*-PCL_5, respectively, which corresponded to the peak accumulation concentration for R-123 (Table 3.1). Below the peak R-123 accumulation concentrations for these diblock copolymers, the binding of R-123 was less than 20%. Further increases in the bound fraction were observed as the diblock concentration was increased beyond the peak R-123 accumulation concentration. This corresponded to the decrease in R-123 accumulation observed at high diblock concentrations (Figure 3.7 to 3.9 and 3.11 'A' series).

Since the concentrations of the diblock copolymers that produced maximum R-6G accumulation were in the vicinity of their respective CMC values, less than 10% R-6G binding was observed at the peak accumulation concentrations for R-6G (Table 3.1). However, the one exception was for $MePEG_{17}$-*b*-PCL_{10}, where the peak accumulation

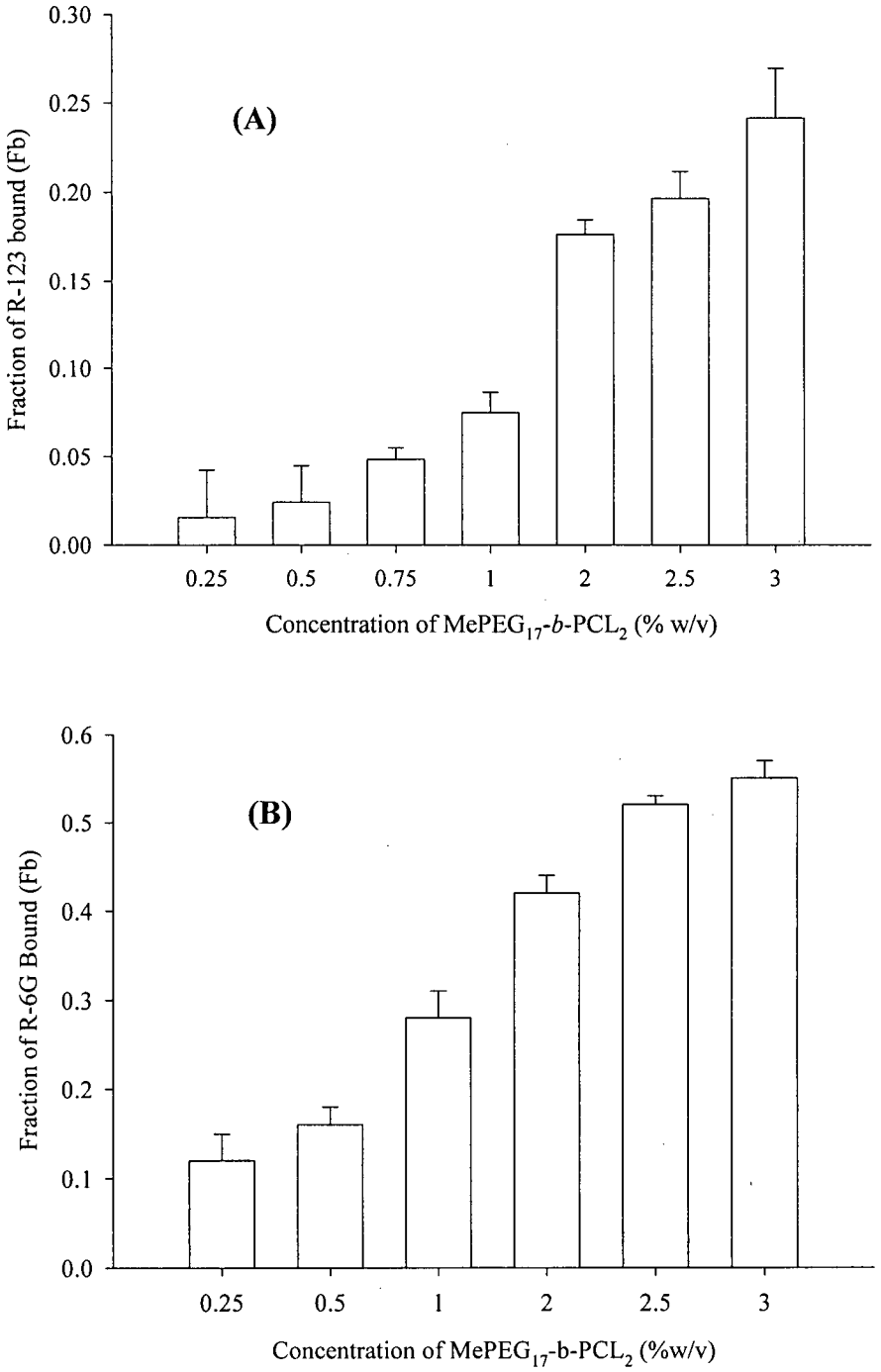

Figure 3.22. Fraction of (A) R-123 and (B) R-6G bound within varying concentrations of $MePEG_{17}$-*b*-PCL_2 micelles. Data expressed as the mean +/- SD (N=3).

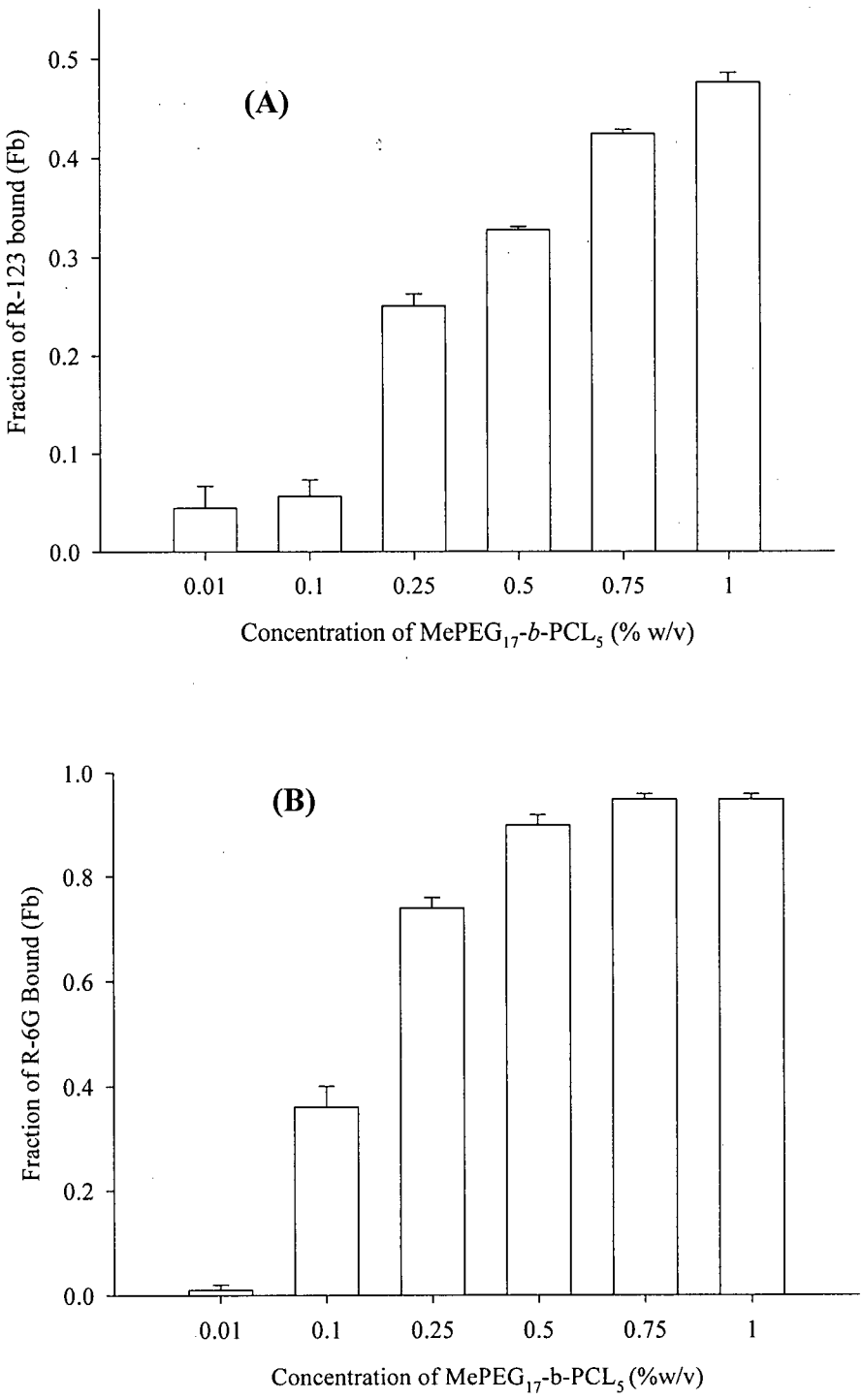

Figure 3.23. Fraction of (A) R-123 and (B) R-6G bound within varying concentrations of $MePEG_{17}$-*b*-PCL_5 micelles. Data expressed as the mean +/- SD (N=3).

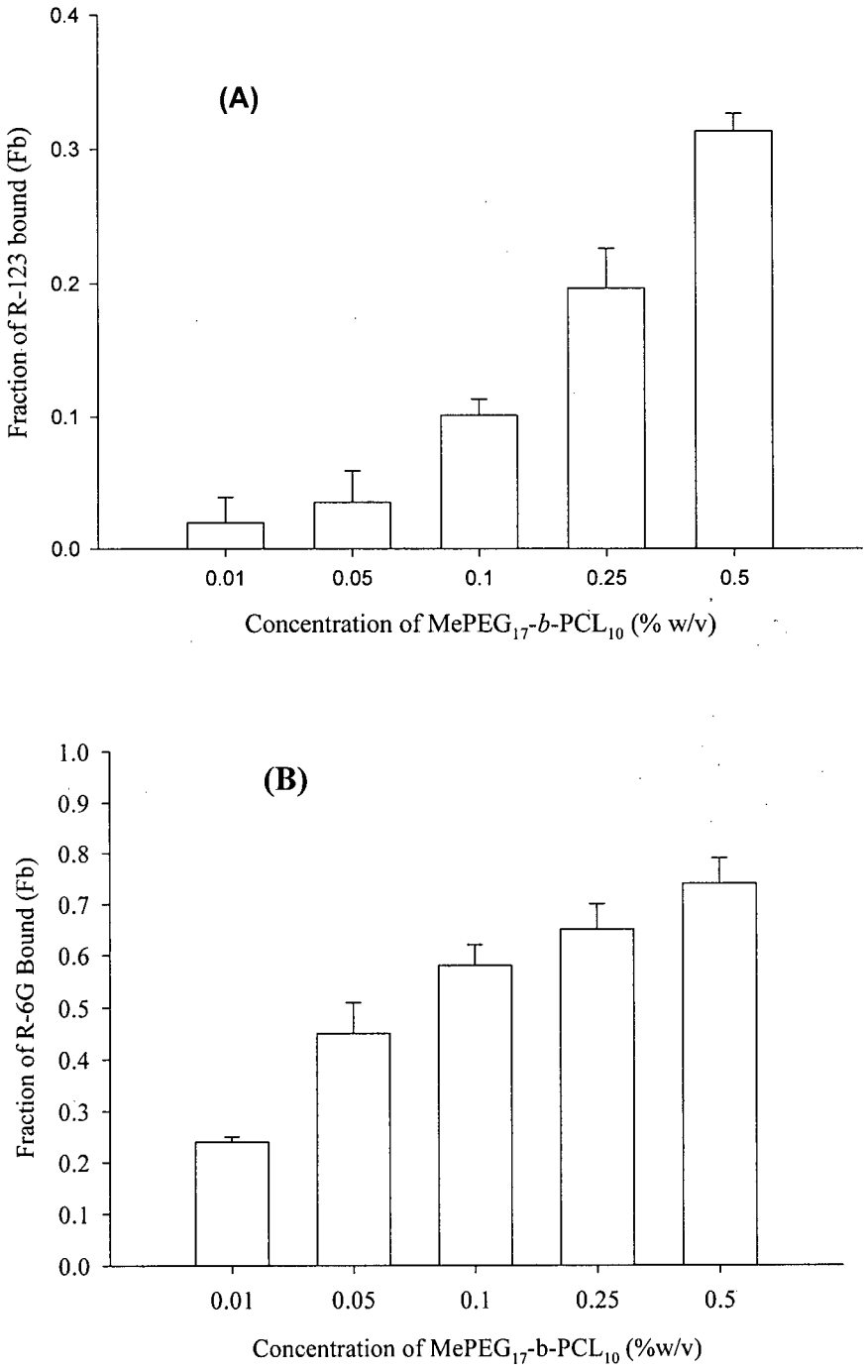

Figure 3.24. Fraction of (A) R-123 and (B) R-6G bound within varying concentrations of $MePEG_{17}$-*b*-PCL_{10} micelles. Data expressed as the mean +/- SD (N=3).

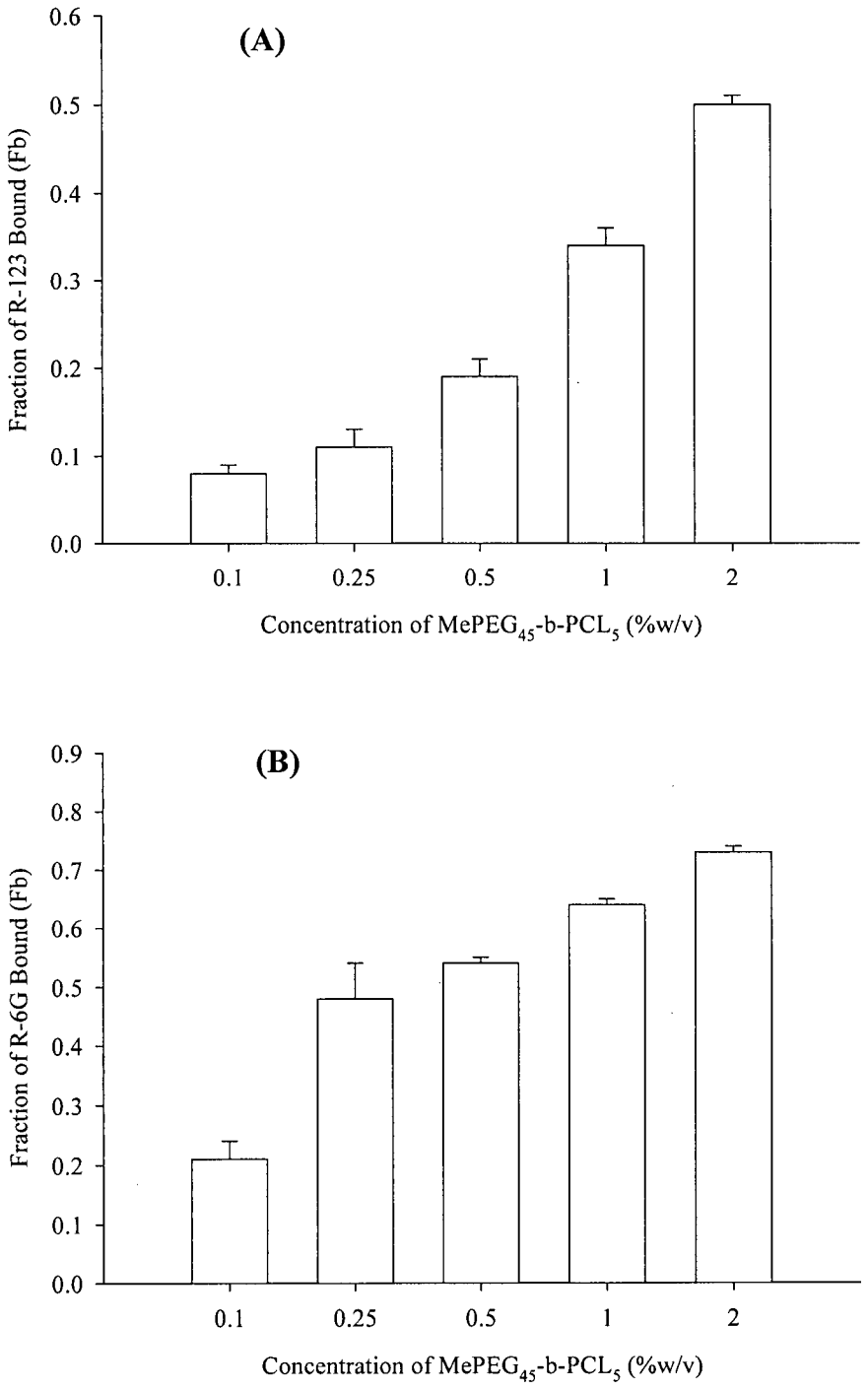

Figure 3.25. Fraction of (A) R-123 and (B) R-6G bound within varying concentrations of $MePEG_{45}$-*b*-PCL_5 micelles. Data expressed as the mean +/- SD (N=3).

concentration for R-6G was 10 fold higher than the CMC and R-6G association was approximately 25%. Concentrations greater than the peak accumulation concentration for R-6G demonstrated increasing R-6G binding with increasing diblock concentration that corresponded with the decrease in R-6G accumulation observed at high diblock concentrations (Figure 3.7 to 3.9 and 3.11 'B' series).

To explore the relationship of R-123 and R-6G binding with the structure of the MePEG-*b*-PCL diblock copolymers and to compare differences in the binding between R-123 and R-6G, the following equations were derived from the binding studies. Above the CMC of a surfactant, there is an equilibrium between free and micelle solubilized solute:

$$\text{Free Solute (Sf)} + \text{Micelles (Saa)} \underset{\longleftarrow}{\xrightarrow{\text{Ka}}} \text{Solute bound in micelles (Sm)}$$

$$\text{Ka} = \frac{\text{Sm}}{\text{Sf}(\text{Saa})} \qquad \text{Equation 3.3}$$

The equilibrium binding coefficient is Ka and Saa is the concentration of surface-active agent in micelle form (mol/L) and is the total surfactant concentration (Saa_t) minus the CMC (mol/L):

$$(\text{Saa}) = (\text{Saa}_t) - \text{CMC} \qquad \text{Equation 3.4}$$

Recall equation 3.2 from section 3.2.8:

$$\text{Fb} = \frac{\text{Sm}}{\text{Sm} + \text{Sf}} \qquad \text{Equation 3.2}$$

Combining equations 3.2 and 3.3 gives:

$$\text{Fb} = \frac{\text{Ka(Saa)}}{1 + \text{Ka(Saa)}} \qquad \text{Equation 3.5}$$

Transforming equation 3.5 to a Scatchard rearrangement gives:

$$\frac{Fb}{Saa} = Ka - FbKa \qquad \text{Equation 3.6}$$

Therefore a plot of Fb/Saa versus Fb should give a straight line with a slope of -Ka.

For each MePEG-*b*-PCL diblock evaluated for R-123 and R-6G binding, a Scatchard plot was constructed and the binding coefficient (Ka) determined and shown in Table 3.3. For R-123, an increase in the PCL block for the MePEG 750 series from 2 to 5 units increased the binding coefficient approximately 16 fold. However, a further increase in the PCL block length from 5 to 10 units had a smaller increase in the binding coefficient (1.7 fold). Increasing the MePEG block to a MW of 2000 with a PCL block of 5 produced a similar Ka of 207 M^{-1} compared to 169 M^{-1} for the MePEG 750 series diblock with 5 PCL units. Plotting the Ka for R-123 as a function of the number of PCL units produced an increase followed by a plateau for R-123 binding, where an increase in the core block length did not increase the binding appreciably (Figure 3.26A).

The binding coefficients for R-6G were substantially larger than R-123 for corresponding MePEG-*b*-PCL diblock copolymers (Table 3.3). A similar trend of increasing Ka for R-6G with increasing PCL block length of the MePEG 750 series was observed and was a linear relationship over the range of block lengths evaluated (Figure 3.26B).

3.3.6. Corrected values for R-123 and R-6G accumulation with $MePEG_{17}$-*b*-PCL_5

At higher MePEG-*b*-PCL concentrations a decrease in R-123 and R-6G accumulation was observed for all diblock copolymers (Figure 3.7 to 3.11 A and B). Figures 3.22 to 3.25 A and B demonstrated that the bound fractions of R-123 and R-6G increased with increasing concentration of MePEG-*b*-PCL diblock copolymers. Since the R-123 and R-6G concentrations used in these accumulation studies was fixed at 5 μM and 0.25 μM, respectively, and if it is assumed that only the free concentration was able to enter the cells,

Table 3.3: Binding coefficients and regression analysis obtained from Scatchard plots for 5 μM R-123 and 0.25 μM R-6G binding studies with MePEG-*b*-PCL micelles.

Series	Diblock Copolymer	R-123[a]		R-6G[a]	
		Ka (M^{-1})	R^2	Ka (M^{-1})	R^2
MePEG 550	$MePEG_{12}$-*b*-PCL_4	N/D	N/D	N/D	N/D
MePEG 750	$MePEG_{17}$-*b*-PCL_2	10.25	0.771	139.1	0.860
	$MePEG_{17}$-*b*-PCL_5	169.6	0.657	874.4	0.958
	$MePEG_{17}$-*b*-PCL_{10}	295.7	0.943	9273	0.916
MePEG 2000	$MePEG_{45}$-*b*-PCL_5	207.1	0.909	1994	0.833

a) The binding coefficient (Ka) is obtained from the slope of the line from linear regression analysis with a coefficient of variation (R^2)

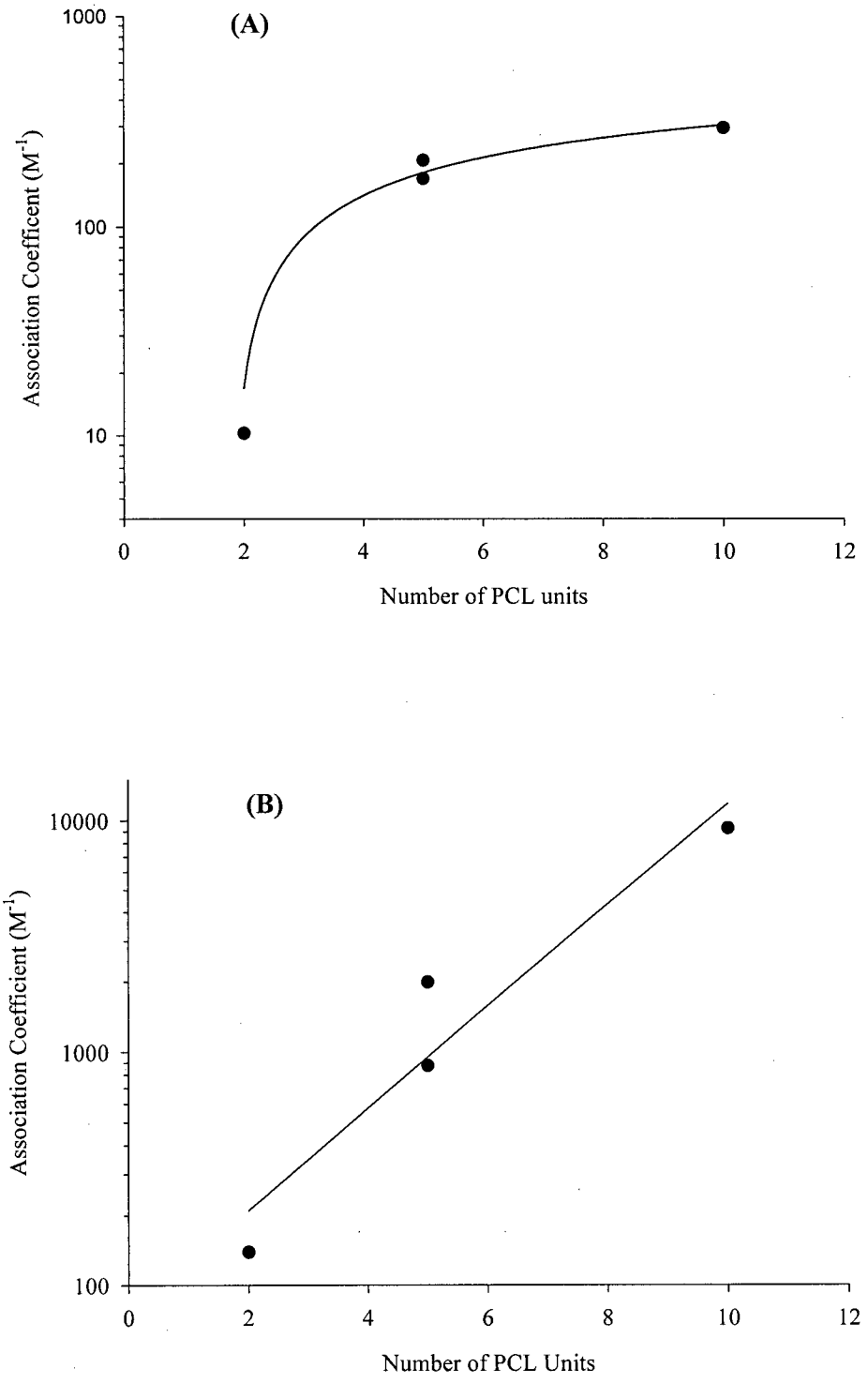

Figure 3.26. Relationship of binding coefficient (Ka) for (A) R-123 and (B) R-6G with hydrophobic block (PCL) length of MePEG-*b*-PCL diblock copolymers.

then at higher concentrations of MePEG-*b*-PCL diblock copolymers the actual concentration available for accumulation into cells should be proportional to the free fraction. Therefore, the R-123 and R-6G accumulation profiles for MePEG-*b*-PCL diblock copolymers can be corrected based on the free fraction of R-123 or R-6G at each MePEG-*b*-PCL concentration. The free fraction (Ff) of R-123 is given by:

$$Ff = \frac{Sf}{Sm + Sf} \qquad \text{Equation 3.7}$$

Combining equations 3.3 and 3.7 gives:

$$Ff = \frac{1}{1 + Ka(Saa)} \qquad \text{Equation 3.8}$$

Since Ka is known, at a given concentration of MePEG-*b*-PCL, the amounts of R-123 or R-6G in the cells can be divided by the free faction (Equation 3.8) to give a so-called "corrected" accumulation level. Using the calculated free fraction values, the R-123 and R-6G accumulation profiles for $MePEG_{17}$-*b*-PCL_5 were corrected and are shown in Figure 3.27 A and B, respectively. For R-123, the extent of "corrected" cellular accumulation at $MePEG_{17}$-*b*-PCL_5 concentrations between 0.25% and 1.0% appeared to be similar and at a higher level than the uncorrected value (Figure 3.27 A). Similarly, R-6G "corrected" accumulation was consistantly higher at concentrations ranging from 0.05% to 0.5% $MePEG_{17}$-*b*-PCL_5 (Figure 3.27 B).

3.4. Discussion

Amphiphilic block copolymers have primarily been utilized as solubilizing vehicles for hydrophobic drugs owing to their self-assembly properties (Zhang *et al.*, 1996b; Allen *et al.*, 1998; Allen *et al.*, 2000; Soo *et al.*, 2002). *In vivo*, some amphiphilic block copolymers have demonstrated long plasma circulation times and passive targeting properties

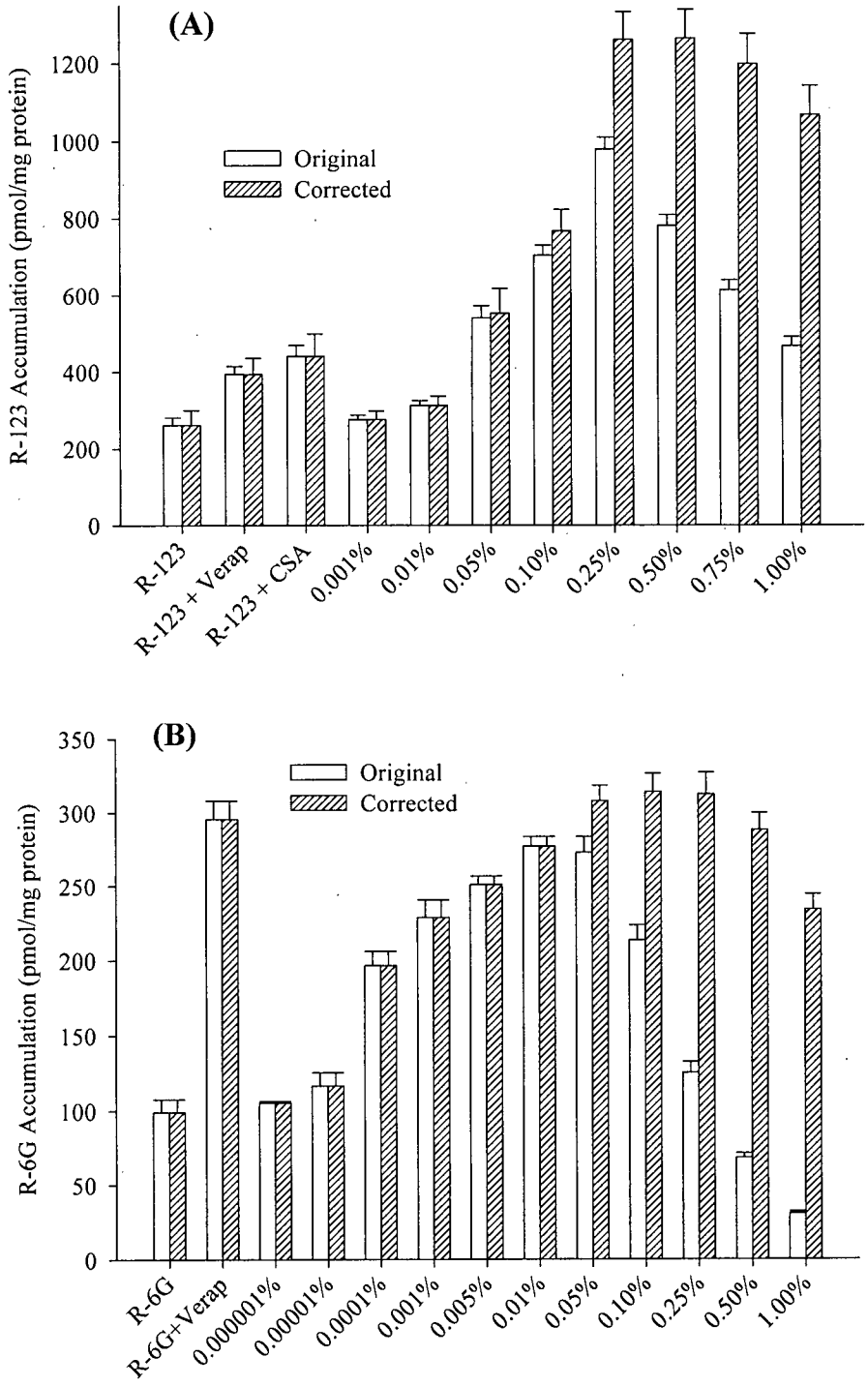

Figure 3.27. Comparison of (A) 5 μM R-123 and (B) 0.25 μM R-6G accumulation by caco-2 cells with $MePEG_{17}$-*b*-PCL_5 diblock copolymer (original) with accumulation concentrations corrected for free fraction. Data expressed as mean +/- SEM (N=3).

(Kwon *et al.*, 1994; Kim *et al.*, 2001; Nishiyama *et al.*, 2003). To date, only Pluronic® triblock copolymers have shown biological response modifying activity beyond their primary use as solubilizing and sterically stabilizing excipients (Paradis *et al.*, 1994; Batrakova *et al.*, 1998a). In this work, a novel series of low molecular weight MePEG-*b*-PCL diblock copolymers has been synthesized with varying compositions and evaluated for their biological response modifying activity in terms of enhancing accumulation of P-gp substrates in caco-2 cells.

The model system chosen to determine the effect of MePEG-*b*-PCL on cellular accumulation of P-gp substrates was the human colon adenocarcinoma cell line, caco-2. Upon confluency in culture, caco-2 spontaneously differentiates into a phenotype similar to small intestinal enterocytes providing an appropriate model to evaluate intestinal permeation of drugs (Pinto *et al.*, 1983). Model assessment studies prior to evaluation of the diblock copolymers were performed to ensure that under the culture conditions employed, that P-gp was expressed and functional. Previous work by Hosoya *et al.* has demonstrated that P-gp is continuously expressed throughout the culturing of caco-2, but may not be fully functional at early time points after confluency (Hosoya *et al.*, 1996). Furthermore, expression of intestinal transporters, including P-gp, in caco-2 cells appears to diminish at higher passage numbers (>70) (Hidalgo and Jibin, 1996; Yu *et al.*, 1997). The detection of MDR-1 gene expression was performed using RT-PCR and Western blot immunodetection. Both assays demonstrated the presence of MDR-1 gene expression in terms of MDR-1 mRNA (478 bp amplicon) and P-gp protein in our caco-2 cells (Figure 3.6). Figures 3.2 and 3.3 showed that R-123 and R-6G accumulation was increased in the presence of the P-gp inhibitor verapamil at a concentration of 50 μM. However, the magnitude of accumulation enhancement by

verapamil was much greater for R-6G (approximately 4.3 fold) than for R-123 (approximately 1.5 fold) (Figure 3.2 and 3.3). To ensure that verapamil was functioning as a P-gp inhibitor for R-123, the accumulation of R-123 with varying concentrations of cyclosporin A (CSA) was studied. Figure 3.4 shows that R-123 accumulation by caco-2 was maximally enhanced by approximately 1.5 fold using 4 μM CSA, similar to the enhancement by verapamil. Thus, R-123 and R-6G accumulation can be enhanced using established P-gp inhibitors in our model system, suggesting that both R-123 and R-6G are suitable P-gp substrates for these studies.

Figure 3.2 also shows that no significant difference in R-123 accumulation was found between 2 to 3 week old caco-2 monolayers, suggesting that under these culture conditions, caco-2 cells were exhibiting P-gp activity, with full functionality occurring at approximately 2 weeks, consistent with the findings of Hosoya *et al.* (Hosoya *et al.*, 1996). Therefore, experiments were conducted after a minimum of 14 days post seeding into flat bottom plates and limited to passage numbers between 25-45.

In addition to the expression of P-gp, caco-2 has been shown to express other efflux transporters such as the multidrug resistance-associated protein (MRP) (Gutmann *et al.*, 1999; Hirohashi *et al.*, 2000; Taipalensuu *et al.*, 2001). Furthermore, several studies have suggested that R-123 may be a substrate for MRP as well as P-gp (Twentyman *et al.*, 1994; van der Sandt *et al.*, 2000; Saengkhae *et al.*, 2003). To establish that MRP mediated efflux of R-123 and R-6G was not a significant factor in the caco-2 model, the accumulation of R-123 and R-6G by caco-2 cells with the MRP inhibitor, probenecid, was determined and the results shown in Figure 3.3 and 3.5 (Gollapudi *et al.*, 1997). For both R-123 and R-6G, probenecid up to 0.5 mM did not significantly increase the accumulation compared to R-123

and R-6G alone, suggesting that the efflux of R-123 and R-6G in the caco-2 model is primarily associated with P-gp (Figure 3.3 and 3.5).

The effects of MePEG-*b*-PCL diblock copolymer composition on the accumulation of two homologous P-gp substrates differing in relative hydrophobicity, R-123 (hydrophilic) and R-6G (hydrophobic), are shown in Figures 3.7 to 3.11 A and B, respectively, and summarized in Table 3.1. For both substrates, as the concentration of MePEG-*b*-PCL diblock copolymers was increased the accumulation increased reaching a maximum at a critical diblock concentration, after which the accumulation decreased. At the maximum accumulation concentration for $MePEG_{17}$-*b*-PCL_5 diblock copolymer, fluorescence microscopy studies demonstrated that the enhanced cellular accumulation was the result of an increase in the cytosolic deposition of the substrates (Figure 3.15 and 3.16). The variations in MePEG and PCL block length are represented in Table 3.1 along with the calculated hydrophilic and lipophilic balance (HLB) values from Chapter 2. Recently, several investigations have described optimal amphiphile structures for reversal of MDR. Utilizing an extensive series of Pluronic® triblock copolymers varying in hydrophobic and hydrophilic block lengths, Batrakova *et al.* investigated the relationship between block copolymer composition and modification of P-gp mediated efflux (Batrakova *et al.*, 1999; Batrakova *et al.*, 2003). Using R-123 as a model P-gp substrate, they determined that block copolymers possessing intermediate hydrophobic block lengths, short hydrophilic blocks and with HLB's less than 20, were most effective at inhibiting P-gp mediated efflux in bovine brain microvessel endothelial cells (BBMEC) and in the MDR overexpressing cancer cell line, KBv (Batrakova *et al.*, 1999; Batrakova *et al.*, 2003). Lo studied the effect on epirubicin flux across caco-2 cells of a series of non-ionic surfactants with increasing HLB values and

showed that optimal P-gp modulation activity occurred with surfactants with intermediate HLB values ranging from 10 to 17 (Lo, 2003). Similar to other reported studies, it was found that intermediate to high HLB MePEG-*b*-PCL diblock copolymers (HLB 9-17) were more effective at enhancing accumulation of the hydrophilic R-123, and accumulation of the hydrophobic R-6G was in a similar range over the evaluated HLB range.

Recently, Hugger *et al.* demonstrated that a commonly used pharmaceutical excipient, poly(ethylene glycol) (PEG), reduced efflux transporter activity in caco-2 cells (Hugger *et al.*, 2002a). Using paclitaxel and doxorubicin as substrates, PEG with molecular weight of 300 reduced the basolateral to apical transport in a concentration dependent manner, and 20% PEG-300 completely reversed the efflux (Hugger *et al.*, 2002a). R-123 accumulation was maximally enhanced using 2.0% w/v $MePEG_{17}$-*b*-PCL_2 (Table 3.1). Since the degree of polymerization of the PCL block was very low, the polydisperse nature of these copolymers could result in a proportion of the diblock containing free MePEG oligomer. To ensure the enhanced R-123 accumulation observed with $MePEG_{17}$-*b*-PCL_2 was not due in part to MePEG 750 oligomers, the accumulation of R-123 was measured in the presence of MePEG 750. Figure 3.12 showed that up to 3.0% MePEG 750, there was no enhancement of R-123 accumulation suggesting the enhanced accumulation was due to the diblock copolymer and not free MePEG oligomer.

As seen in Figures 3.7 to 3.11 'A' series, for all MePEG-*b*-PCL diblock copolymers, R-123 accumulation enhancement began at concentrations of diblock close to the CMC, increasing to a maximum with a diblock concentration in the order of 6 to 100 fold higher than their respective CMC values (Table 3.1). However, for the hydrophobic R-6G, enhanced accumulation occurred at concentrations well below the diblock CMC and reached

a maximum near the vicinity of the CMC values of the MePEG-*b*-PCL diblock copolymers (Figures 3.7 to 3.11 'B' series and Table 3.1). In contrast, R-123 accumulation in caco-2 cells in the presence of Pluronic® triblock copolymers reached maximum accumulation levels in the proximity of the CMC and higher Pluronic® concentrations resulted in a drop in accumulation (Miller *et al.*, 1997; Batrakova *et al.*, 1998a; Batrakova *et al.*, 1999). Similarly, work by Nerurkar *et al.* demonstrated that the apical to basolateral (AP→BL) transport of a model peptide susceptible to P-gp efflux could be enhanced using polysorbate 80 or Cremophor EL® (Nerurkar *et al.*, 1996; Nerurkar *et al.*, 1997). The AP→BL transport increased at concentrations of polysorbate 80 or Cremophor EL® below the CMC and reached a maximum in the vicinity of the CMC, after which AP→BL transport decreased with further increases in concentration (Nerurkar *et al.*, 1996; Nerurkar *et al.*, 1997). Nerurkar *et al.* concluded that since the transport increased up to and reached a maximum at the CMC, that the free surfactant unimers were responsible for inhibiting P-gp efflux transport (Nerurkar *et al.*, 1997).

If free amphiphile unimers are responsible for attenuating P-gp drug efflux, how they accomplish this is not clearly understood. Recent work has shown that membrane fluidization by nonionic surfactants and other fluidizers can reduce P-gp ATPase activity by altering the lipid order around P-gp (Romsicki and Sharom, 1999; Regev *et al.*, 1999). Amphiphiles have also been shown to fluidize membranes which was found to correlate with the increase in membrane permeability of P-gp substrates (Drori *et al.*, 1995; Regev *et al.*, 1999; Batrakova *et al.*, 2001). This suggests that amphiphiles may act on P-gp in a non-specific manner and not by classical competitive interactions. Therefore, we speculate that the ability of free unimers to partition into the cell membrane and achieve a threshold

concentration of unimers in the membrane will be important parameters governing the modulation of P-gp activity. It is possible that below the CMC, MePEG-*b*-PCL diblock unimers may not have partitioned into the membrane at sufficient concentrations to inhibit P-gp activity and enhance R-123 accumulation. Recent work by Xia and Onyuksel demonstrated that for uptake into, and permeabilization of cell membranes, a surfactant must exhibit a surface pressure greater than 25 dyne/cm and surfactants with surface pressures lower than this threshold may not accumulate into the membrane at sufficient concentrations (Xia and Onyuksel, 2000). Surfactants were shown to achieve this threshold value below the CMC suggesting that micelles were not required to permeate or solubilize membranes (Xia and Onyuksel, 2000). Xia and Onyuksel concluded that penetration enhancement resulted from partitioning of the free surfactant unimers into membranes and that micelles were acting as a "depot" for free unimer and maintaining the micelle/unimer equilibrium, as unimer was partitioned into the cell membrane (Xia and Onyuksel, 2000). This suggests that the high concentration above the CMC required for MePEG-*b*-PCL to enhance R-123 accumulation may be due to micelle being a "depot" for free unimer to reach the threshold concentration of unimer within the membrane, resulting in reduced P-gp activity and enhanced R-123 accumulation. However, this does not explain the very different R-6G accumulation profile observed with increasing MePEG-*b*-PCL concentration. Accumulation of R-6G was maximally enhanced with 8-25 fold lower MePEG-*b*-PCL concentrations compared to R-123 (Table 3.1) and concentrations of diblock as low as 0.0001% were sufficient to enhance cellular accumulation (Figures 3.7 to 3.11 'B' series). Therefore, the threshold concentration for modulation of P-gp activity was attained at much lower concentrations of diblock copolymer. This difference in the concentration of diblock required for enhanced R-123 and

R-6G accumulation further suggests that additional pathways besides P-gp efflux inhibition may be involved in the accumulation enhancement by MePEG-*b*-PCL diblock copolymers for P-gp substrates with different relative hydrophobicities.

The accumulation of doxorubicin and paclitaxel in the presence of $MePEG_{17}$-*b*-PCL_5 diblock copolymer was carried out to substantiate our results with R-123 and R-6G showing that the diblock concentration required to enhance the cellular accumulation varied with the relative hydrophobicity of the P-gp substrate. Both drugs are well established P-gp substrates with octanol/water partition coefficients reported to be 99 and 0.52 for paclitaxel and doxorubicin, respectively (Song *et al.*, 1997). The accumulation profile for paclitaxel was similar (Figure 3.17) to the accumulation profile of R-6G with $MePEG_{17}$-*b*-PCL_5 diblock copolymer (Figure 3.8B). Maximum accumulation occurred at the same $MePEG_{17}$-*b*-PCL_5 concentration of 0.01%, with concentrations as low as 0.0001% enhancing paclitaxel accumulation (Figure 3.17). Accumulation enhancement with doxorubicin required a high concentration of 1.0%, well above the CMC of $MePEG_{17}$-*b*-PCL_5, analogous to the peak accumulation concentration of 0.25% for R-123 (Figure 3.18). These results further support our hypothesis that additional pathways may be involved in MePEG-*b*-PCL accumulation enhancement of P-gp substrates depending upon their degree of hydrophobicity.

Surfactants are commonly used as permeation enhancers to improve membrane permeability of a drug, by altering membrane integrity and facilitating increased drug transmembrane diffusion (Swenson and Curatolo, 1992; Anderberg and Artursson, 1993; Erukova *et al.*, 2000). Therefore, the effect of surfactants on P-gp activity may be a secondary consequence of the membrane disorder facilitated by the amphiphiles and not the only mechanism responsible for enhanced permeability of a P-gp substrate. Figures 3.20 and

3.21 show the rate and extent of R-123 and R-6G accumulation into caco-2 cells, respectively, in the presence of MePEG-*b*-PCL diblock copolymers. The rate constant for R-123 accumulation in the presence of verapamil was similar to R-123 in buffer, suggesting that even though verapamil inhibited P-gp activity and allowed more R-123 to accumulate intracellularly, the transmembrane movement rate of R-123 was not altered (Table 3.2). Similarly, R-123 accumulation in the presence of $MePEG_{17}$-*b*-PCL_{10} and $MePEG_{45}$-*b*-PCL_5, showed similar rate constants to R-123 with or without verapamil. However, there was a rapid increase in R-123 accumulation in the presence of $MePEG_{17}$-*b*-PCL_2 and $MePEG_{17}$-*b*-PCL_5 diblock copolymers, with rate constants approximately 3-4 fold higher than R-123 with or without verapamil (Table 3.2). This increase in the accumulation rate with $MePEG_{17}$-*b*-PCL_2 and $MePEG_{17}$-*b*-PCL_5 may be due to membrane permeabilization resulting in a faster transmembrane movement rate for R-123. The rate constants for R-6G accumulation were similar for R-6G in buffer, verapamil and for $MePEG_{17}$-*b*-PCL_2 and $MePEG_{17}$-*b*-PCL_5 (Table 3.2). This suggests that R-6G accumulation enhancement by $MePEG_{17}$-*b*-PCL_2 and $MePEG_{17}$-*b*-PCL_5 may not be associated with a membrane permeabilization effect, but rather may involve primarily only inhibition of P-gp activity.

Substrates with higher partition coefficients (Kpart) would be predicted, within the solubility-diffusion model of passive diffusion, to be able to enter and move across the membrane more readily and to a greater extent than substrates with a low Kpart. Thus, the hydrophilic R-123 with its low Kpart (Figure 3.1) should have a slow transmembrane movement rate, and the relative amount of R-123 reaching the P-gp binding domain within the membrane and ultimately inside the cell, will be less than that of the hydrophobic R-6G. The higher Kpart for R-6G would allow for R-6G to penetrate and move rapidly through the

membrane, reaching a high concentration at the P-gp binding domain and intracellular localization. This suggests that efflux activity of P-gp should reduce R-6G accumulation to a greater extent than R-123. Eytan *et al.* compared the accumulation of R-6G and R-123 into MDR overexpressing cells relative to the sensitive parental cell line, and demonstrated that P-gp efflux activity reduced the cellular accumulation of R-6G to a greater extent than R-123 (Eytan *et al.*, 1997). In this work, a direct comparison between the extent of R-123 and R-6G accumulation cannot be made since equimolar concentrations of R-123 and R-6G were not used. However, in the presence of the P-gp inhibitors verapamil and CSA, lower AEF values for R-123 were obtained compared to R-6G, which was likely due to the differences in Kpart values for the two substrates (Table 3.1). A larger AEF value for R-123 was found with $MePEG_{12}$-*b*-PCL_4, $MePEG_{17}$-*b*-PCL_2, and $MePEG_{17}$-*b*-PCL_5 compared to verapamil or CSA, and may be due to these diblock copolymers acting as more effective inhibitors of P-gp. Alternatively, the diblock copolymers may have enhanced the membrane permeability of R-123, promoting a greater transmembrane diffusion of R-123 into the cell in addition to modulation of P-gp activity. The R-123 AEF values in the presence of $MePEG_{17}$-*b*-PCL_{10} and $MePEG_{45}$-*b*-PCL_5 were similar to verapamil and CSA suggesting that enhanced accumulation may be the result of modulating P-gp activity and not by enhanced transmembrane diffusion. Table 3.1 shows that for R-6G, all MePEG-*b*-PCL diblock copolymers produced similar AEF values to verapamil and hence, enhanced accumulation with R-6G may be confined primarily to inhibition of P-gp activity.

The differences observed in accumulation enhancement caused by diblock copolymers and P-gp inhibitors in the presence of substrates differing in their relative hydrophobicity is further illustrated by the data in Figure 3.14A and B, which shows the

accumulation of R-123 and R-6G with $MePEG_{45}$-*b*-$PDLLA_9$ respectively. $MePEG_{45}$-*b*-$PDLLA_9$ is a diblock copolymer with similar MePEG composition to $MePEG_{45}$-*b*-PCL_5, but it possesses poly(D,L-lactide) as the hydrophobic block instead of poly(caprolactone). Accumulation of R-123 was not enhanced over a wide range of $MePEG_{45}$-*b*-$PDLLA_9$ concentrations (Figure 3.14A). However, $MePEG_{45}$-*b*-$PDLLA_9$ was able to increase the accumulation of R-6G with an AEF of approximately 2.6 (Figure 3.14B), which was lower than that of verapamil, suggesting that $MePEG_{45}$-*b*-$PDLLA_9$ is capable of inhibiting P-gp activity but was not as effective as verapamil.

Consistent with other amphiphiles, the accumulation of R-123 and R-6G decreased at high concentrations of MePEG-*b*-PCL diblock copolymer (Figures 3.7 to 3.11 A and B). Figures 3.22 to 3.25 A and B showed that the R-123 and R-6G bound fraction increased as the concentration of MePEG-*b*-PCL diblock copolymer was increased. This increase in micelle-binding was observed at concentrations of MePEG-*b*-PCL at or just above concentrations of diblock required for peak cellular accumulation activity (Figures 3.7 to 3.11 and 3.22 to 3.25 A and B). With further increases in MePEG-*b*-PCL concentration the bound fraction increased which coincided with the drop in accumulation for both R-123 and R-6G as the diblock concentration was increased beyond the peak activity concentration (Figures 3.7 to 3.11 and 3.12 to 3.25 A and B). This indicates that a reduction in the free R-123 and R-6G concentration available for cellular uptake may be a significant factor in the decrease in cellular accumulation observed at high MePEG-*b*-PCL diblock concentrations. A similar decrease in accumulation observed with polysorbate 80 and Cremophor EL® was thought to be due to a decreasing free fraction of drug or substrate, resulting from bound drug being solubilized within micelles as the concentration of surfactant increased above the

CMC. Hence the amount of available drug for cellular uptake decreased, resulting in a decrease in the cellular accumulation (Nerurkar *et al.*, 1997).

At high concentrations of Pluronic® triblock copolymer above the CMC, a transient increase in R-123 accumulation was observed which decreased over time and was sensitive to ATP depletion (Miller *et al.*, 1997). The investigators proposed that R-123 bound within the Pluronic® micelles entered the cell via endocytosis at earlier time points and over time were recirculated back out resulting in a decreased accumulation (Miller *et al.*, 1997; Batrakova *et al.*, 1998a; Batrakova *et al.*, 1998b). Since maximum accumulation of R-123 was with MePEG-*b*-PCL concentrations above the CMC, the affect of vesicular uptake and recirculation of micellized R-123 cannot be ruled out.

The use of high surfactant concentrations can result in lysis or solubilization of membranes with loss of membrane organization and cell death (Helenius and Simons, 1975; Sakai *et al.*, 1998). Hence, it was necessary to ensure the viability of the caco-2 cells after exposure to MePEG-*b*-PCL diblock copolymers and lactate dehydrogenase (LDH) release from the cytoplasm was monitored as an indicator of cell toxicity. Over the range of MePEG-*b*-PCL diblock concentrations that enhanced R-123 and R-6G accumulation, no toxic effects of the surfactants on caco-2 cells were observed using LDH as a marker for cytotoxicity (Figure 3.19). Although no LDH release was noted over a broad range of concentrations, other toxicity assays need to be employed to determine non-membrane dependent effects of MePEG-b-PCL diblock copolymers on cytotoxicity. However, high concentrations beyond the maximum accumulation concentrations for MePEG-*b*-PCL diblock copolymers induced varying degrees of LDH release depending on block composition of the diblock (Figure 3.19). This suggests that cytotoxicity effects and some

cell lysis may further compound the decrease in R-123 or R-6G accumulation observed at higher diblock concentrations.

Table 3.3 shows that for each MePEG-*b*-PCL diblock evaluated, the binding coefficient for R-6G was several orders of magnitude higher than R-123. This finding is consistent with the relative hydrophobicity of R-6G being more favorable for partitioning into the hydrophobic core of the diblock compared to the hydrophilic R-123. Figure 3.26 shows a plot of the PCL block length dependence on the binding coefficient of R-123 and R-6G. For R-123 the binding coefficient reached a plateau with an increase in the PCL block length, suggesting that as the hydrophobicity of the core increased, the binding of the hydrophilic R-123 in micelles was not as favorable. For R-6G a linear increase in binding coefficient was observed with increasing PCL block length.

The binding coefficients calculated for each diblock and substrate combination provided a means of determining the concentration of substrate bound within micelles or free in solution at a given micelle concentration and substrate concentration. Sequestration of the substrate within micelles decreased the concentration of substrate available for diffusion and was likely responsible for the decrease in accumulation and permeability at high surfactant concentrations (Nerurkar *et al.*, 1997). Nerurker *et al.* found that correcting the permeability coefficient for free fraction of solute at high surfactant resulted in a constant permeability coefficient at higher surfactant concentrations (Nerurkar *et al.*, 1997). Furthermore, the permeability coefficient of amprenavir was found to be constant at high surfactant concentrations when corrected for free fraction (Yu *et al.*, 1999). It was assumed that at high concentrations of MePEG-*b*-PCL, the decrease in R-123 and R-6G accumulation was the result of a decrease in the free fraction available for cellular uptake as described above and

that micelle uptake was negligible. Accordingly, accumulation was corrected based on the free fraction of R-123 and R-6G at high diblock concentrations. Figure 3.27 shows the "corrected" accumulation profile for R-123 and R-6G compared to the original uncorrected accumulation profile with $MePEG_{17}$-*b*-PCL_5. For R-123, at concentrations of 0.25% and higher, an increase in the accumulation was observed for corrected values of R-123 free fraction compared to uncorrected values (Figure 3.27A). Accumulation was also higher and constant beyond 0.05% $MePEG_{17}$-*b*-PCL_5 for R-6G (Figure 3.27B). However, for both P-gp substrates a decrease in the corrected accumulation at 1.0% $MePEG_{17}$-*b*-PCL_5 was observed which might be attributed to cellular toxicity since LDH release studies (Figure 3.19) demonstrated approximately 25% LDH release at this concentration.

3.5. CONCLUSION

This work presents the first evidence demonstrating the use of MePEG-*b*-PCL amphiphilic diblock copolymers to increase the cellular accumulation of P-gp substrates into caco-2 cells. A substantially different rate of substrate accumulation and MePEG-*b*-PCL concentration profile for enhanced accumulation was observed depending upon the hydrophobicity of the P-gp substrate selected. Cellular accumulation of the relatively hydrophilic P-gp substrate, R-123, was enhanced at high concentrations of MePEG-*b*-PCL diblock copolymers above their CMC with little activity below the CMC. Cellular accumulation with a relatively hydrophobic substrate, R-6G, was maximally enhanced over a wide range of diblock concentrations lower or close to the CMC and which also corresponded to an 8-25 fold reduction in diblock concentration compared to R-123. Similar accumulation enhancement profiles with MePEG-*b*-PCL were observed with two additional P-gp substrates, doxorubicin and paclitaxel, which have large differences in their relative

hydrophobicities. At high diblock copolymer concentrations, R-123 and R-6G accumulation decreased and was likely due to substantial partitioning of R-123 and R-6G into micelles, reducing the free fraction available for cellular uptake. Cytotoxicity probably further reduced R-123 and R-6G accumulation at high diblock copolymer concentrations. The difference in MePEG-*b*-PCL diblock composition and concentrations required to enhance the accumulation of P-gp substrates with different relative hydrophobicities suggests that additional pathways may be involved besides a reduction of P-gp mediated efflux. From these studies and analysis of the current literature, several pathways are proposed which could contribute to the enhanced accumulation of R-123 and R-6G. MePEG-*b*-PCL unimers partition into the membrane and may either reduce P-gp efflux and/or increase membrane permeability of R-123 or R-6G via enhanced transmembrane diffusion. Micelles may be acting as a 'depot' for free unimer partitioning into the membrane, such that a threshold concentration is reached in the membrane for modulation of P-gp efflux and enhancement of R-123 accumulation. The high concentration of diblock above the CMC suggests that micelle-associated R-123 may enter via endocytosis.

Chapter 4

PROPOSED PATHWAYS OF ENHANCED CACO-2 CELL PERMEABILITY OF P-GLYCOPROTEIN SUBSTRATES BY METHOXYPOLY(ETHYLENE GLYCOL)-*BLOCK*-POLY(CAPROLACTONE) DIBLOCK COPOLYMERS

4.1. INTRODUCTION

Low molecular weight MePEG-*b*-PCL amphiphilic diblock copolymers were shown to enhance the caco-2 cellular accumulation of compounds susceptible to P-gp mediated efflux (Chapter 3). P-gp substrates with different relative hydrophobicities, hydrophilic rhodamine 123 (R-123) and hydrophobic rhodamine 6G (R-6G), demonstrated different accumulation profiles with MePEG-*b*-PCL. Both R-123 and R-6G cellular accumulation increased with increasing concentration of MePEG-*b*-PCL copolymers up to a maximum, after which accumulation decreased. The MePEG-*b*-PCL copolymers maximally enhanced R-123 accumulation at concentrations above the critical micelle concentration (CMC) with little or no activity below the CMC, whereas R-6G accumulation was maximally enhanced at concentrations below and up to the diblock CMC. The differences in the accumulation enhancement profile shown by the P-gp substrates suggest that MePEG-*b*-PCL diblock copolymers may enhance the cellular accumulation through a combination of different pathways, depending upon the physicochemical properties of the substrates.

It is well established in the literature that surfactant molecules possess the ability to partition into membranes and alter membrane integrity (Swenson and Curatolo, 1992; Jones, 1999; Aungst, 2000). This disruption in the membrane barrier properties by surfactants has been utilized to enhance the permeability of drugs across cell membranes (Anderberg *et al.*, 1992; Swenson *et al.*, 1994a; Swenson *et al.*, 1994b; Werner *et al.*, 1996). Depending on the concentration, surfactants can induce pores or channels within the membrane, a process

involving extraction of phospholipids or proteins (Swenson and Curatolo, 1992; Jones, 1999). Several surfactants, which have been evaluated as permeation enhancers for poorly permeable drugs, have also been shown to enhance the permeability of P-gp substrates. The non-ionic surfactant polysorbate 80 increased the permeability of transport markers in caco-2 cells (Anderberg *et al.*, 1992) and improved the permeability of proteins susceptible to P-gp mediated efflux (Nerurkar *et al.*, 1996; Nerurkar *et al.*, 1997). Yamazaki *et al.* showed that polysorbate 80 enhanced cellular accumulation of an epipodophyllotoxin derivative susceptible to P-gp mediated efflux, which was attributed to an enhanced influx of drug and not a reduction in P-gp mediated efflux (Yamazaki *et al.*, 2000). A Pluronic® triblock copolymer has also been shown to enhance the transmembrane movement rate of compounds such as doxorubicin across model lipid bilayers (Erukova *et al.*, 2000). Thus, it is possible that the interactions of surfactants with all membranes may result in increased membrane permeability and an increase in the transmembrane diffusion rate of a P-gp substrate such that it overcomes the outward efflux of P-gp. P-gp substrates (such as R-123 and R-6G) differing in their structure, hydrophobicity and other physicochemical properties, will possess different membrane permeability characteristics and may be influenced differently by MePEG-*b*-PCL diblock copolymer induced permeability changes in the lipid bilayer.

Alterations in membrane lipid fluidity by membrane fluidizers such as surfactants, have been suggested to reduce P-gp ATPase activity or drug efflux activity, resulting in a reduced efflux of the substrate (Sinicrope *et al.*, 1992; Drori *et al.*, 1995; Regev *et al.*, 1999). Batrakova *et al.* proposed that membrane perturbations induced by Pluronic® could decrease the affinity of ATP for its binding site and interfere with the ATPase activity (Batrakova *et al.*, 2001). Poly(ethylene glycol) (PEG 300) inhibited P-gp in caco-2 cells enhancing the

permeability of paclitaxel and doxorubicin (Hugger *et al.*, 2002a). This study found that the fluidity of the polar head group regions of caco-2 cell membranes was decreased, but that there was no effect on the fluidity of the nonpolar core regions of the membrane in the presence of PEG 300. Rege *et al.* suggested that the Pgp inhibitory effects of polysorbate 80, Cremophor EL® and Vitamin E TPGS were related to the modulation of caco-2 cell membrane fluidity, where polysorbate 80 and Cremophor EL® fluidized bilayers, while Vitamin E TPGS rigidized lipid bilayers (Rege *et al.*, 2002). Therefore, surfactant interactions with the membrane may reduce P-gp mediated efflux activity through non-specific interactions with P-gp and result in a net influx of substrate.

Given the concentrations of MePEG-*b*-PCL diblock above the CMC required to enhance the accumulation of the relatively hydrophilic P-gp substrates, R-123 and doxorubicin, it was thought possible that endocytosis of micelle-incorporated substrate may be involved. Endocytosis of micellized compounds has been previously demonstrated for diblock copolymers composed of poly(ethylene glycol)-*block*-poly(caprolactone) (PEO-*b*-PCL) in PC12 and P19 cell lines (Allen *et al.*, 1999b; Luo *et al.*, 2002) Decreases in R-123 accumulation in cells treated with Pluronic® copolymers was suggested to be due to the recirculation of micelle-incorporated R-123 via vesicular transport mechanisms (Miller *et al.*, 1997; Batrakova *et al.*, 1998b).

Based on the results from Chapter 3 and the current literature, the role of three possible pathways has been proposed in the caco-2 cellular accumulation enhancement of P-gp substrates in the presence of MePEG-*b*-PCL copolymers: Increase in substrate membrane permeability, inhibition of P-gp mediated efflux, and/or vesicular transport of micellized substrate. The overall objective of these studies was to determine the cellular uptake

pathways contributing to enhanced caco-2 cellular accumulation of P-gp substrates by MePEG-*b*-PCL block copolymers. For this work, $MePEG_{17}$-*b*-PCL_5 diblock copolymer was selected since it demonstrated optimal solubility characteristics and R-123/R-6G accumulation enhancement activity. The objectives were to investigate the effects of endocytosis inhibitors, ATP depletion condition, and non-P-gp expressing cells on cellular accumulation of P-gp substrates and to compare the directional transepithelial fluxes in the presence of MePEG-*b*-PCL copolymer. Additionally, the effect of MePEG-*b*-PCL on membrane permeabilization and P-gp ATPase activity was investigated.

4.2. EXPERIMENTAL

4.2.1. Materials

Sucrose, sodium phosphate dibasic heptahydrate ($Na_2HPO_4 \bullet 7H_2O$), calcium chloride dihydrate ($CaCl_2 \bullet 2H_2O$), magnesium sulfate ($MgSO_4 \bullet 7H_2O$), potassium dihydrogen phosphate (KH_2PO_4), sodium chloride (NaCl), and ammonium chloride (NH_4Cl) were from Fisher Scientific (Nepean, ON). Potassium cyanide (KCN), lucifer yellow (LY), potassium chloride (KCl), sodium bicarbonate ($NaHCO_3$), N-(2-hydroxyethyl)piperazine-N'-2-ethanesulfonate (hepes), verapamil, cyclosporine A (CSA), rhodamine 123 (R-123), rhodamine 6G (R-6G), brefeldin A (Br-A), and 2-deoxy-D-glucose (DOG) were obtained from Sigma-Aldrich (St. Louis, MO). All tissue culture reagents were from Invitrogen/Life Technologies (Grand Island, NY).

Chemicals for the P-gp ATPase assay included sodium dodecyl sulfate (SDS) from Fluka (Oakville, ON). Ammonium molybdate was obtained from Caledon Laboratories Ltd (Georgetown, ON) and zinc acetate from Fisher Scientific (Nepean, ON). Ascorbic acid, sodium azide, sodium orthovanadate (NaOV), 2(N-morpholino)ethane sulfonic acid (MES),

potassium chloride (KCl), antifoam A concentrate, tris(hydroxymethyl)aminomethane (Tris base), dithiothreitol (DTT), ethylene glycol-bis(β-aminoethyl ether)-N,N,N',N'-tetraacetic acid (EGTA), potassium phosphate dibasic (K_2HPO_4), and the magnesium salt of adenosine 5'-triphosphate (MgATP) were all purchased from Sigma (Oakville, ON).

4.2.2. Buffer composition

Buffer composition for Hank's balanced salt solution (HBSS) without glucose contains the same formula for HBSS as described by the manufacturer (Invitrogen, Grand Island, NY) without the addition of glucose:

Hank's balanced salt solution (HBSS) without glucose + 10 mM hepes pH = 7.4	
$CaCl_2 \cdot 2H_2O$ 0.185 g/L	KH_2PO_4 0.06 g/L
NaCl 8.0 g/L	$MgSO_4 \cdot 7H_2O$ 0.2 g/L
KCl 0.4 g/L	$NaHCO_3$ 0.35 g/L
$Na_2HPO_4 \cdot 7H_2O$ 0.9 g/L	hepes 2.38 g/L

Buffer used for the P-gp ATPase assay will be denoted as Tris-Mes buffer and has the following composition:

Tris-Mes buffer pH = 6.8	
MES 9.78 g/L	DTT 0.318 g/L
EGTA 0.76 g/L	Sodium azide 0.326 g/L
KCl 3.72 g/L	
Add Tris base until pH = 6.8	

4.2.3. Cell culture

The human colon adenocarcinoma cell lines caco-2, HT-29, and SW-620 were obtained from ATCC. Cells were grown in a humidified atmosphere of 5% CO_2 at 37^0C. Caco-2 was maintained in culture as described in Section 3.2.3.1. McCoys 5A media with 10% HI-FBS, 1.0% L-glutamine, and 100 UI/mL penicillin and 100 μg/mL streptomycin was used for HT-29. SW-620 had the same composition as for HT-29 except RPMI 1640 media

was used. Stock cultures were grown in T-175 cm^2 flasks (BD-Falcon, BD Biosciences, Bedford, MA) at a seed density of 5000 cells/cm^2. Upon 80-90 % confluency, cells were split using 0.25% trypsin + 1.0 mM EDTA (Invitrogen, Grand Island, NY). Cells were counted using a hemocytometer and viability performed using the trypan blue exclusion assay as described in section 3.2.3.2. Cells were seeded into 48 well flat bottom plates (Corning Costar, Cambridge, MA) at a density of 40 000 cells/cm^2 and grown in plates for a minimum of 14 days for caco-2 and 7 days for HT-29 and SW-620 before being used for experimentation. Media were changed in plates and T-175 flasks every second day.

For directional flux experiments, caco-2 cells were seeded at a density of 60 000 cells/cm^2 onto collagen coated PTFE (polytetrafluoroethylene) membrane (Transwell-COL, Corning Costar, Cambridge, MA) with a pore size of 0.4 μm and insert diameter of 12 mm. Media were changed every second day, with 0.5 mL placed on the apical (AP) side and 1.5 mL in the basolateral (BL) side. Cell monolayers were used for experiments between 21 to 28 days post seeding to allow for differentiation and tight junction formation. Transepithelial electrical resistance (TEER) was monitored routinely using a Millicell-ERS (Millipore, Bedford, MA).

4.2.4. Cellular accumulation studies

Cellular accumulation of R-123 by caco-2, HT-29, and SW-620 was carried out as previously described in Section 3.2.6.1. Briefly, cells grown in 48 well plates were exposed to 5 μM R-123 or 0.25 μM R-6G in either assay buffer (HBSS + 10mM hepes, pH=7.4) alone or in solutions of MePEG-*b*-PCL diblock copolymers. The standard P-glycoprotein (P-gp) inhibitors, verapamil (50 μM) or CSA (4 μM) were used as positive controls. Cells were incubated for 90 min at 37^0C. The cellular fluorescence intensity was measured using a

CytoFluor 4000 fluorescence microplate reader (PerSeptive Biosystems, Framingham, MA) with λ_{EX}=485 nm and λ_{EM}=530 nm (with filter bandwidths of 20 and 25 nm respectively) for R-123 and λ_{EX}=508 and λ_{EM}=560 (both with filter bandwidths of 20 nm) for R-6G. Cellular accumulation was normalized with respect to total protein content in each well using the BCA protein assay method (Pierce, Rockford, IL).

4.2.5. ATP depletion

Caco-2 cells grown in 48 well plates were washed 2 times with glucose free HBSS + 10 mM hepes (glucose free assay buffer) and pre-incubated in glucose free assay buffer at 37^{0}C for 15 min. The buffer was removed and the cells pretreated with 1.5 mM potassium cyanide (KCN) + 25 mM deoxyglucose (DOG) in glucose free assay buffer for 30 min at 37^{0}C. The pretreatment solution was removed and 0.5 mL of 5 μM R-123 containing 1.5 mM KCN + 25 mM DOG in glucose free assay buffer, with or without various concentrations of $MePEG_{17}$-*b*-PCL_5 diblock copolymer, were then added to each well. Cells were incubated at 37^{0}C for 90 min, after which the solutions were removed and the plate placed on ice. Cells in each well were collected and R-123 concentrations determined as described in Section 3.2.6.1.

4.2.6. Endocytosis inhibition

Caco-2 cells grown in 48 well plates were washed 2 times with assay buffer and pre-incubated in assay buffer at 37^{0}C for 15 min. The buffer was removed and the cells pretreated with either 75 mM NH_4Cl or 20 μM brefeldin A in assay buffer for 60 min or 0.45 M sucrose for 30 min at 37^{0}C. The pretreatment solution was removed and 0.5 mL of 5 μM R-123 containing the corresponding endocytosis inhibitor in assay buffer, with or without various concentrations of $MePEG_{17}$-*b*-PCL_5 diblock copolymer, were added to each well.

Cells were incubated at 37^{0}C for 90 min, after which the solutions were removed and the plate placed on ice. Cells in each well were collected and R-123 concentrations determined as described in Section 3.2.6.1.

As a control for endocytosis inhibition, cellular accumulation with the fluid phase endocytosis marker, lucifer yellow (LY), was performed. Cells were treated with inhibitors as described above and LY was used at a concentration of 0.5 mM. LY fluorescence was determined using a fluorescence microplate reader (CytoFluor 4000) with λ_{EX}=450 and λ_{EM}=530 (with filter bandwidths of 50 and 25 nm, respectively) and normalized to total cellular protein.

4.2.7. R-123 and R-6G directional flux

The flux of R-123 and R-6G across caco-2 monolayers was determined in the apical to basolateral (AP→BL) and the BL→AP directions. Caco-2 cells grown on Transwell inserts as described in Section 4.2.3 were washed with assay buffer and allowed to equilibrate with assay buffer at 37^{0}C for 15 min. For AP→BL flux, 0.5 mL of either 5 μM R-123 or 0.25 μM R-6G with assay buffer, 50 μM verapamil, 0.01% w/v MePEG$_{17}$-*b*-PCL$_5$, or 0.25% w/v MePEG$_{17}$-*b*-PCL$_5$ were placed on the AP side and 1.5 mL of assay buffer placed on the BL side. The plate was placed on an orbital shaker (Microshaker, Bellco Biotechnology, Vineland, NJ) set to 50-75 rpm at 37^{0}C. At specified time points, the transwell inserts were lifted out and placed in a new well containing 1.5 mL of assay buffer. The amount of R-123 or R-6G in the basolateral solution was determined using a fluorescence microplate reader (CytoFluor 4000, PerSeptive Biosystems, Framingham, MA) with λ_{EX}=485 nm and λ_{EM}=530 nm (with filter bandwidths of 20 and 25 nm, respectively) for R-123 and λ_{EX}=508 and λ_{EM}=560 (both with filter bandwidths of 20 nm) for R-6G.

For BL→AP flux, 1.5 mL of 5 μM R-123 or 0.25 μM R-6G in assay buffer were placed on the BL side and 0.5 mL of assay buffer, 50 μM verapamil, 0.01% w/v $MePEG_{17}$-*b*-PCL_5, or 0.25% w/v $MePEG_{17}$-*b*-PCL_5 were placed on the AP side. Aliquots of 50 μL were taken from the AP side at each time point for R-123 and R-6G quantitation and 50 μL of fresh solution were replaced.

As a control for caco-2 cell monolayer integrity, TEER was monitored before and after experimentation. Lucifer yellow flux (1 mM) was also measured in the presence of assay buffer and with 0.25% w/v $MePEG_{17}$-*b*-PCL_5.

The apparent permeability coefficient (P_{app}) was calculated using the following equation:

$$Papp = \frac{\Delta Q}{\Delta t \cdot A \cdot Co} \qquad \text{Equation 4.1}$$

Where ΔQ is the amount of R-123/R-6G transported during the time interval Δt, Co is the concentration of R-123/R-6G applied to the donor side and A is the monolayer surface area.

The amounts of R-123 and R-6G accumulated by caco-2 cells at the conclusion of the directional transport experiments were measured. Cell monolayers were rinsed with ice cold PBS after which the membrane support was excised using a scalpel. The membrane was then placed in 1% triton X-100 to solubilize the cells. The cellular debris and membrane were pelleted by centifugation and aliquots of the supernatant measured for R-123 and R-6G fluorescence and protein content as described in Section 3.2.6.1.

4.2.8. Erythrocyte hemolysis

Fresh blood was collected from healthy volunteers by venipuncture into heparin containing vacutainer tubes (VWR Scientific, Mississauga, ON). Erythrocytes were isolated by centrifugation for 5 min at 1500 rpm using an Allegra 6 centrifuge (Beckman Coulter,

Mississauga, ON). The plasma was removed and the packed erythrocytes were washed three times with phosphate buffered saline pH 7.4 (PBS). The cells were then resuspended in PBS and counted using a hemocytometer. A concentration of 2 x 10^8 cells/mL in PBS was prepared and stored on ice until use within 2 hours. Diblock copolymers were prepared in PBS at 37^0C at twice the desired concentration and 0.5 mL of each solution was pipetted into a 1.5 mL microcentrifuge tube. The erythrocyte suspension was warmed to 37^0C and 0.5 mL added to each polymer solution. This provided a 1:1 dilution of diblock copolymer and erythrocytes to a final concentration of $1x10^8$ cells/mL. Spontaneous hemolysis control group was determined by incubating erythrocytes at $1x10^8$ cells/mL in PBS alone. 100% hemolysis was induced by adding 0.5 mL of 2% Triton-X 100 to 0.5 mL of the erythrocyte suspension. The microcentrifuge tubes were capped and incubated in a 37^0C water bath and gently inverted at 15 min intervals to prevent sedimentation. At appropriate times, the tubes were centrifuged at 14 000 rpm for 15 sec to sediment the erythrocytes and the supernatant was collected. Hemoglobin release was detected by absorbance spectroscopy at 540 nm (8452A diode array spectrophotometer, Hewlett Packard, Kirkland, PQ). Each time point had three replicate tubes for each diblock concentration and control group (spontaneous and 100% hemolysis). The percent hemolysis at each time point was determined using the following equation:

$$\%\ \text{Hemolysis} = \frac{\text{abs}_{\text{sample}} - \text{abs}_{\text{spontaneous}}}{\text{abs}_{100\%\ \text{hemolysis}}} x100 \qquad \text{Equation 4.2}$$

4.2.9. P-gp ATPase assay

An isolated human P-gp membrane suspension from Gentest (Woburn, MO) and methods described by the manufacturer were used. This assay involved monitoring the changes in the liberation of phosphate from the cleavage of ATP catalyzed by P-gp ATPase.

A 60 μL reaction mixture contained 40 μg of P-gp containing membranes, various concentrations of MePEG-*b*-PCL and/or substrate, and 3-5 mM MgATP all in Tris-Mes buffer and was incubated at 37^{0}C for 20 min. An identical reaction mixture containing 100 μM sodium orthovanadate (NaOV) was assayed in parallel. Orthovanadate inhibited P-gp by trapping MgADP in the nucleotide binding site. Thus, ATPase activity measured in the presence of orthovanadate represented non-P-gp ATPase activity and was subtracted from the activity generated without orthovanadate to yield vanadate-sensitive ATPase activity. The reaction was stopped by the addition of 30 μL of 10 % SDS + antifoam A. Two additional reaction mixtures (+ and - orthovanadate) but without MgATP, were prepared and incubated with the others, and then supplemented with SDS and MgATP, to represent time = 0 min of reaction. The incubations were followed with addition of 200 μL of 35 mM ammonium molybdate in 15 mM zinc acetate:10 % ascorbic acid (1:4) and incubated for an additional 20 min at 37^{0}C. The liberation of inorganic phosphate was detected by its absorbance at 650 nm and quantitated by comparing the absorbance to a phosphate standard curve.

4.3. RESULTS

4.3.1. Role of endocytosis in enhanced R-123 accumulation by $MePEG_{17}$-*b*-PCL_5

Caco-2 cells were treated with endocytosis inhibitors such as hyperosmotic sucrose (0.45 M), 75 mM ammonium chloride, or 20 μM brefeldin A. Control studies using the fluid phase marker lucifer yellow (LY) demonstrated a 40-50% reduction in LY cellular uptake when treated with the endocytosis inhibitors (Figure 4.1). Using varying concentrations of $MePEG_{17}$-*b*-PCL_5, accumulation of 5 μM R-123 was determined in the presence of these endocytosis inhibitors. Figure 4.2 shows that the levels of R-123 accumulation were similar

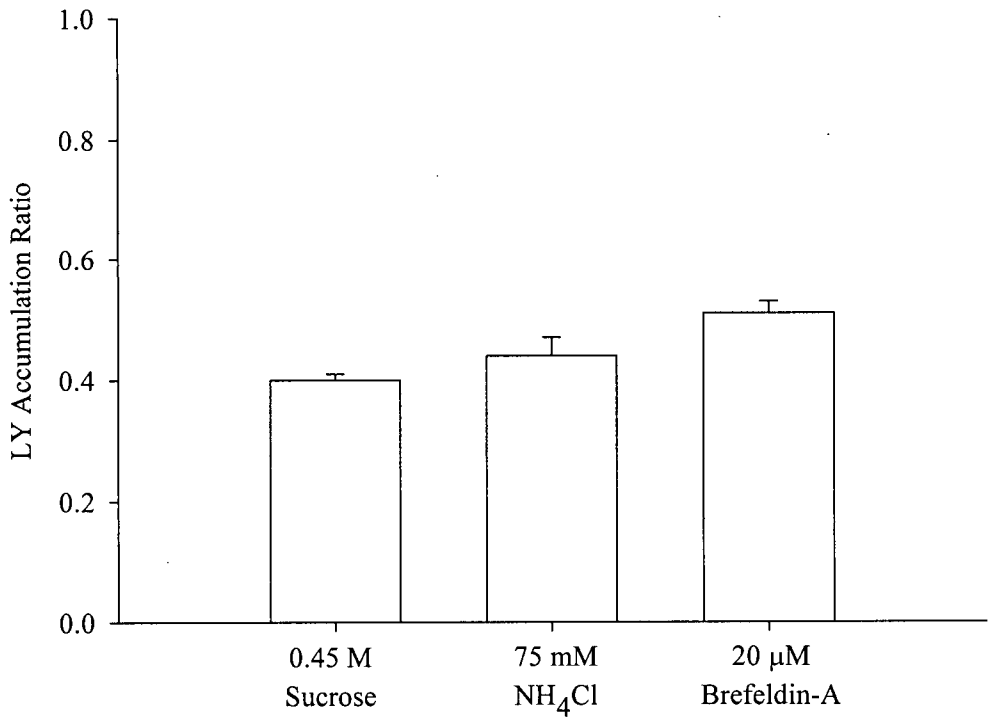

Figure 4.1: Lucifer yellow (LY) accumulation ratio with endocytosis inhibitors. LY accumulation by caco-2 with or without endocytosis inhibitors was measured at 37^0C for 90 min. Accumulation ratio is the amount of LY accumulated in the presence of inhibitors to the amount of LY accumulated without inhibitors. Data expressed as mean +/- SD with N=3.

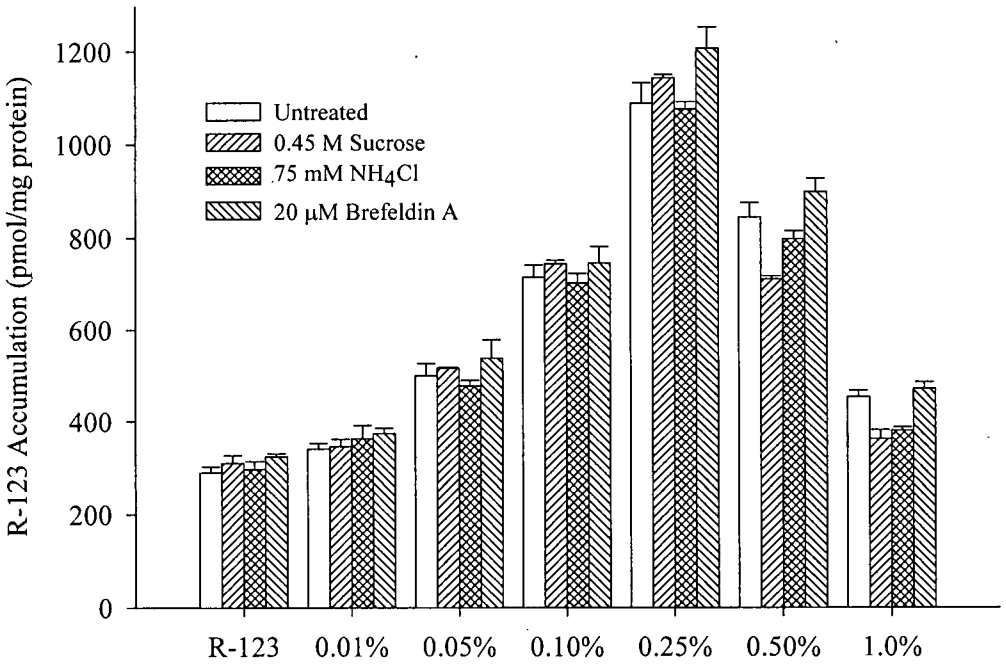

Figure 4.2: R-123 accumulation by caco-2 cells comparing untreated to treatment with endocytosis inhibitors in the presence of increasing concentrations of $MePEG_{17}$-*b*-PCL_5. Cells were treated with 5 μM R-123 containing either 0.45 M sucrose, 75 mM NH_4Cl, or 20 μM brefeldin A with varying concentrations of $MePEG_{17}$-*b*-PCL_5 (0.01% to 1.0% w/v) for 90 min at 37^0C. R-123 with inhibitors but without diblock was used as control. Data expressed as mean +/- SEM with N=3.

when treated with endocytosis inhibitors compared to untreated control group (no inhibitors). Figure 4.2 also demonstrates that R-123 accumulation increased up to a critical concentration of 0.25% $MePEG_{17}$-*b*-PCL_5 and then decreased both with and without the inclusion of endocytosis inhibitors, consistent with the results obtained in the previous chapter (Figure 3.7A).

4.3.2. Directional flux across caco-2 monolayers

Monolayer integrity was assessed by monitoring the change in transepithelial electrical resistance (TEER) and flux of lucifer yellow (LY) at various time points post seeding into Transwell membrane inserts. Figure 4.3 shows a decline in LY flux after 14 days in culture and an increasing TEER value, which appears to level off after 16 days. This suggested that tight junction formation of the monolayer was complete within 14 days. Therefore, monolayers were maintained in culture for a minimum of 3 weeks to ensure complete differentiation and monolayer integrity before directional flux experimentation was performed. Prior to the flux experiments with R-123 and R-6G, any loss of monolayer integrity due to the inclusion of $MePEG_{17}$-*b*-PCL_5 during the course of the experiment was assessed by monitoring the flux of LY over 2 h in the presence or absence of 0.25% $MePEG_{17}$-*b*-PCL_5 and by monitoring the TEER before and after the LY flux experiment. No significant difference in the TEER and LY transport with $MePEG_{17}$-*b*-PCL_5 diblock was observed compared to assay buffer group, suggesting that the integrity of the tight junctions was maintained during treatment (Table 4.1).

4.3.2.1. R-123 directional flux

The AP→BL absorptive flux of R-123 was determined by exposing the monolayers to either R-123 with assay buffer, or to R-123 in combination with 50 μM verapamil or

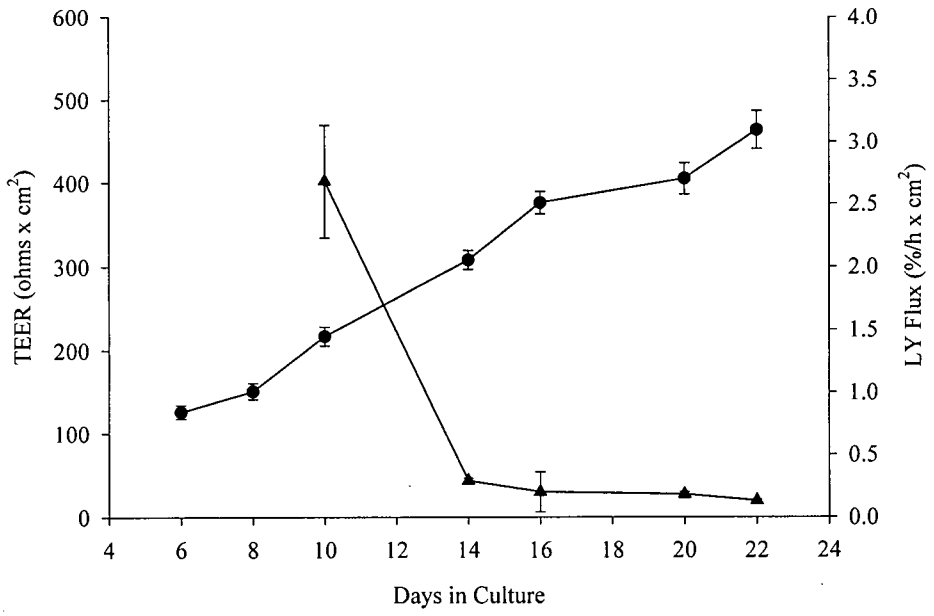

Figure 4.3: Evaluation of caco-2 monolayer integrity in Transwell inserts. TEER (●), and LY flux (▲) assessed over 3 weeks. Data represented as the mean +/- SD.

Table 4.1: TEER ratio and amount of LY transported in assay buffer and in the presence of diblock copolymer for caco-2 monolayers grown on Transwell membrane inserts. TEER measurements conducted before and after directional flux experimentation and LY transport represents the cumulative amount of LY transported in the AP→BL direction over 120 min at 37^0C.

Treatment Group	TEER ratio[a]	% LY transport[b]
Assay Buffer	1.06 +/- 0.01	0.42 +/- 0.06
0.25% $MePEG_{17}$-*b*-PCL_5	1.07 +/- 0.03 (ns)	0.37 +/- 0.03 (ns)

Two-tailed two sample t-test used to compare treatment group to assay buffer group. (ns) = not statistically significant $p>0.05$.

a) TEER ratio = $TEER_{after\ expt}$ / $TEER_{before\ expt}$
b) % LY transport = (Amt LY transported / Amt LY applied)x100

$MePEG_{17}$-*b*-PCL_5 at concentrations above (0.25%) or below (0.01%) the CMC on the apical surface and monitoring the amount of R-123 entering the basolateral side. Figure 4.4A demonstrates that compared to R-123 alone, verapamil or 0.01% $MePEG_{17}$-*b*-PCL_5 did not increase the amount transported across caco-2 cells. However, 0.25% diblock showed a small, but not statistically significant increase in the R-123 flux. Apparent permeability coefficients for AP→BL ($Papp_{AP\rightarrow BL}$) compared in Table 4.2 showed no significant differences between verapamil and diblock treatment compared to R-123 alone.

The BL→AP secretory flux of R-123 was measured by placing R-123 on the basolateral side and either assay buffer, 50 μM verapamil or 0.01% and 0.25% $MePEG_{17}$-*b*-PCL_5 on the apical surface and monitoring the amount of R-123 entering the apical side. Verapamil and 0.25% diblock lowered the BL→AP flux of R-123 to the same extent and 0.01% diblock also lowered the flux but not down to the same level (Figure 4.4B). The corresponding $Papp_{BL\rightarrow AP}$ values for R-123 flux were significantly reduced with exposure to verapamil or 0.25% diblock (Table 4.2).

4.3.2.2. R-123 cellular accumulation after directional flux experiment

R-123 accumulation by caco-2 monolayers at the conclusion of the directional flux studies is shown in Figure 4.5. For AP→BL, 0.25% diblock increased the accumulation approximately 5 fold compared to verapamil which increased cellular accumulation approximately 2 fold (Figure 4.5A). The amount of R-123 accumulated by caco-2 cells in the BL→AP direction was similar for verapamil and 0.25% diblock, with both demonstrating approximately a 2 fold increase (Figure 4.5B). In either direction, 0.01% diblock showed little or no increase in R-123 accumulation compared to R-123 with assay buffer (Figure 4.5 A and B). The overall extent of R-123 cellular accumulation for all treatment groups in the

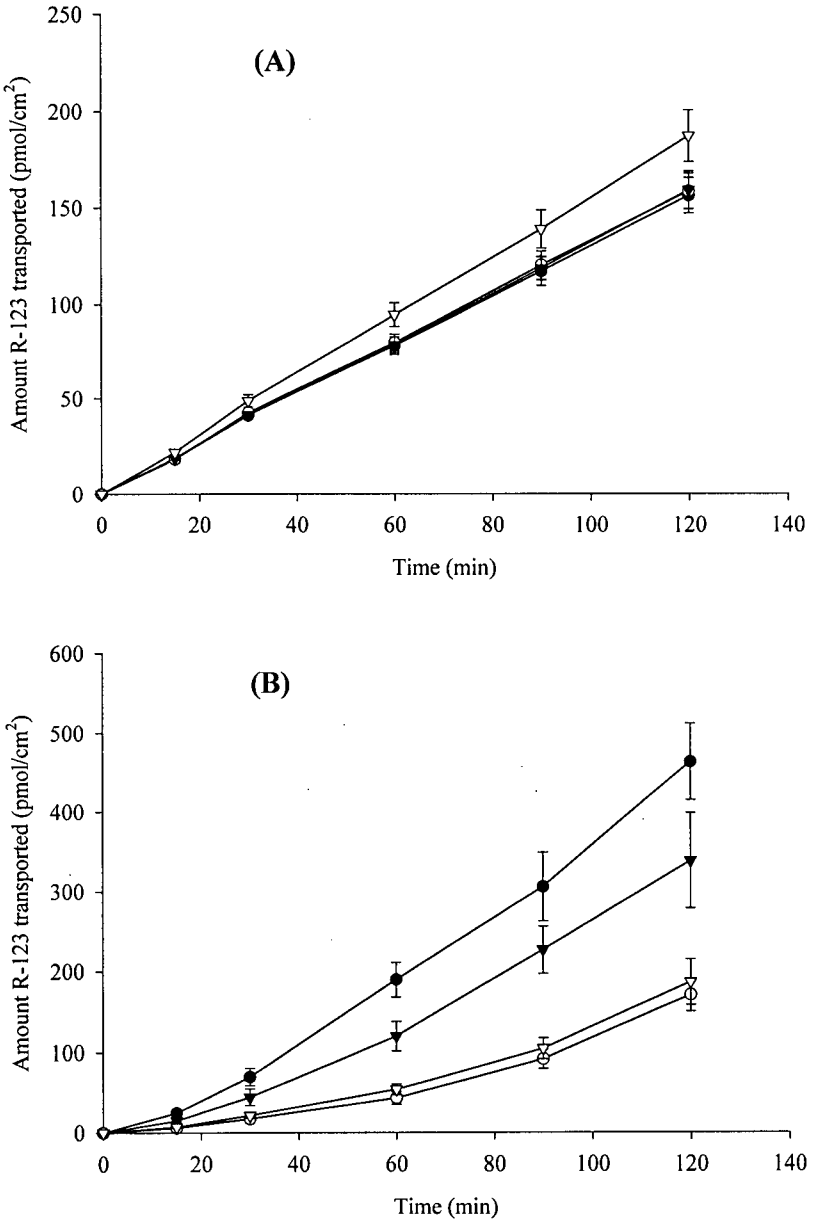

Figure 4.4: Directional flux of 5 μM R-123 across caco-2 monolayers over 120 min at 37^0C. R-123 AP→BL flux (A) measured the amount of R-123 in the BL solution when R-123 was placed on the AP side in the presence of (●) HBSS+10mM hepes, (○) 50 μM verapamil, (▼) 0.01% $MePEG_{17}$-*b*-PCL_5, or (▽) 0.25% $MePEG_{17}$-*b*-PCL_5. BL→AP flux of R-123 (B) was determined by placing R-123 on the BL side and monitoring the amount that entered the AP side which was exposed to (●) HBSS+10mM hepes, (○) 50 μM verapamil, (▼) 0.01% $MePEG_{17}$-*b*-PCL_5, or (▽) 0.25% $MePEG_{17}$-*b*-PCL_5. Data expressed as the cumulative amount of R-123 transported across a unit area of caco-2 monolayers and represented as the mean +/- SEM with N=3.

Table 4.2: Apparent permeability coefficients (Papp) for R-123 flux across caco-2 monolayers in the AP→BL and BL→AP direction. Data expressed as mean +/- SEM with N=3.

Treatment Group	AP→BL P_{app} x 10^{-6} (cm/s)	BL→AP P_{app} x 10^{-6} (cm/s)	Efflux Ratio[a]
Assay Buffer	4.31 +/- 0.26	13.8 +/- 1.62	3.20
50 μM Verapamil	4.40 +/- 0.27 (ns)	5.05 +/- 0.61 (✶)	1.15
0.01% $MePEG_{17}$-*b*-PCL_5	4.40 +/- 0.28 (ns)	10.3 +/- 1.68 (ns)	2.34
0.25% $MePEG_{17}$-*b*-PCL_5	5.17 +/- 0.38 (ns)	5.52 +/- 0.82 (✶)	1.06

AP→BL: One-way ANOVA with pairwise comparisons using Student Newman Keuls test used for statistical analysis. (ns) = not statistical significant ($p>0.05$).
BL→AP: One-way ANOVA with pairwise comparisons using Student Newman Keuls test used for statistical analysis. (ns) = not statistical significant to assay buffer ($p>0.05$). (✶) = Statistically significant compared to assay buffer and 0.01% diblock ($p<0.05$).
a) Efflux Ratio = $Papp_{BL\rightarrow AP}$ / $Papp_{AP\rightarrow BL}$

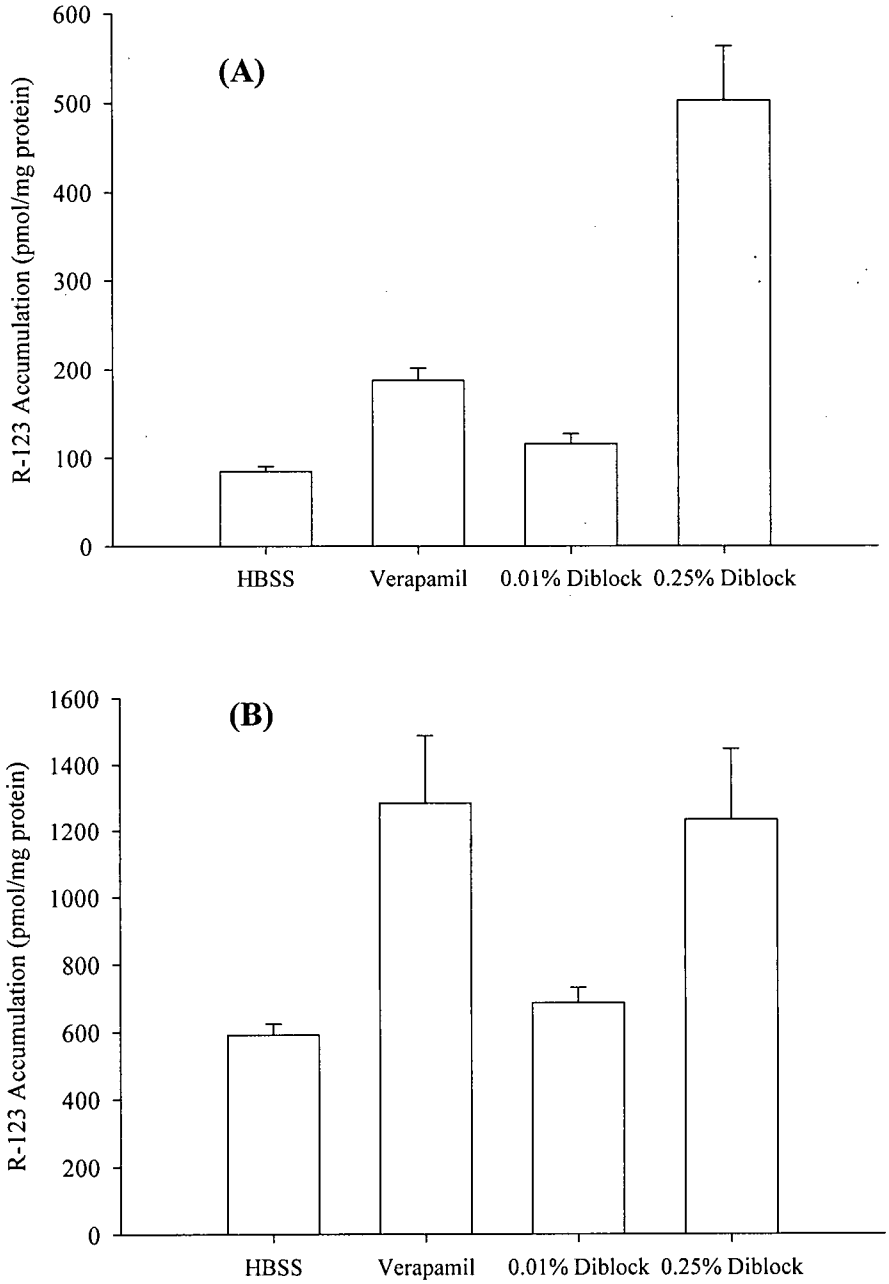

Figure 4.5: R-123 accumulation by caco-2 monolayers at the conclusion of the directional flux studies. Transwell membranes were excised and cells lysed to quantitate the cellular fluorescence. (A) Cellular accumulation in the AP→BL direction and (B) BL→AP direction. Data expressed as mean +/- SEM with N=3.

BL→AP direction was substantially higher then the extent of R-123 cellular accumulation in the AP→BL direction (Figure 4.5 A and B). For example, 0.25% diblock produced R-123 accumulation values of approximately 500 pmol/mg protein and 1200 pmol/mg protein for AP→BL and BL→AP directions, respectively.

4.3.2.3. R-6G directional flux

Figure 4.6A displays the AP→BL flux of R-6G across caco-2 monolayers over 120 min with 50 μM verapamil or $MePEG_{17}$-*b*-PCL_5 diblock copolymer at concentrations below the CMC (0.01%) and above the CMC (0.25%). Compared to R-6G in assay buffer, both verapamil and 0.25% $MePEG_{17}$-*b*-PCL_5 displayed greater AP→BL flux over the time studied with $Papp_{AP\rightarrow BL}$ significantly different to that of R-6G in assay buffer (Table 4.3). Furthermore, 0.25% $MePEG_{17}$-*b*-PCL_5 significantly enhanced the flux of R-6G greater than verapamil with a $Papp_{AP\rightarrow BL}$ of $9.58x10^{-6}$ cm/s compared to $6.35x10^{-6}$ cm/s for verapamil (Table 4.3). However, 0.01% $MePEG_{17}$-*b*-PCL_5 did not demonstrate an increase the AP→BL flux compared to R-6G in assay buffer (Table 4.3).

A high BL→AP flux of R-6G in assay buffer was observed with a $Papp_{BL\rightarrow AP}$ of $36.8x10^{-6}$ cm/s, which was significantly reduced with verapamil and both concentrations of $MePEG_{17}$-*b*-PCL_5 (Figure 4.6B and Table 4.3). Additionally, both verapamil and 0.25% $MePEG_{17}$-*b*-PCL_5 reduced the BL→AP flux of R-6G to a similar $Papp_{BL\rightarrow AP}$, 14.8 and 16 $x10^{-6}$ cm/s, respectively, which was significantly lower than 0.01% $MePEG_{17}$-*b*-PCL_5.

4.3.2.4. R-6G cellular accumulation after directional flux experiment

At the conclusion of the directional flux studies, the cell monolayer was excised to determine the extent of R-6G accumulation. Figure 4.7A shows the accumulation after the AP→BL flux studies. Verapamil, 0.01% and 0.25% $MePEG_{17}$-*b*-PCL_5 all enhanced the

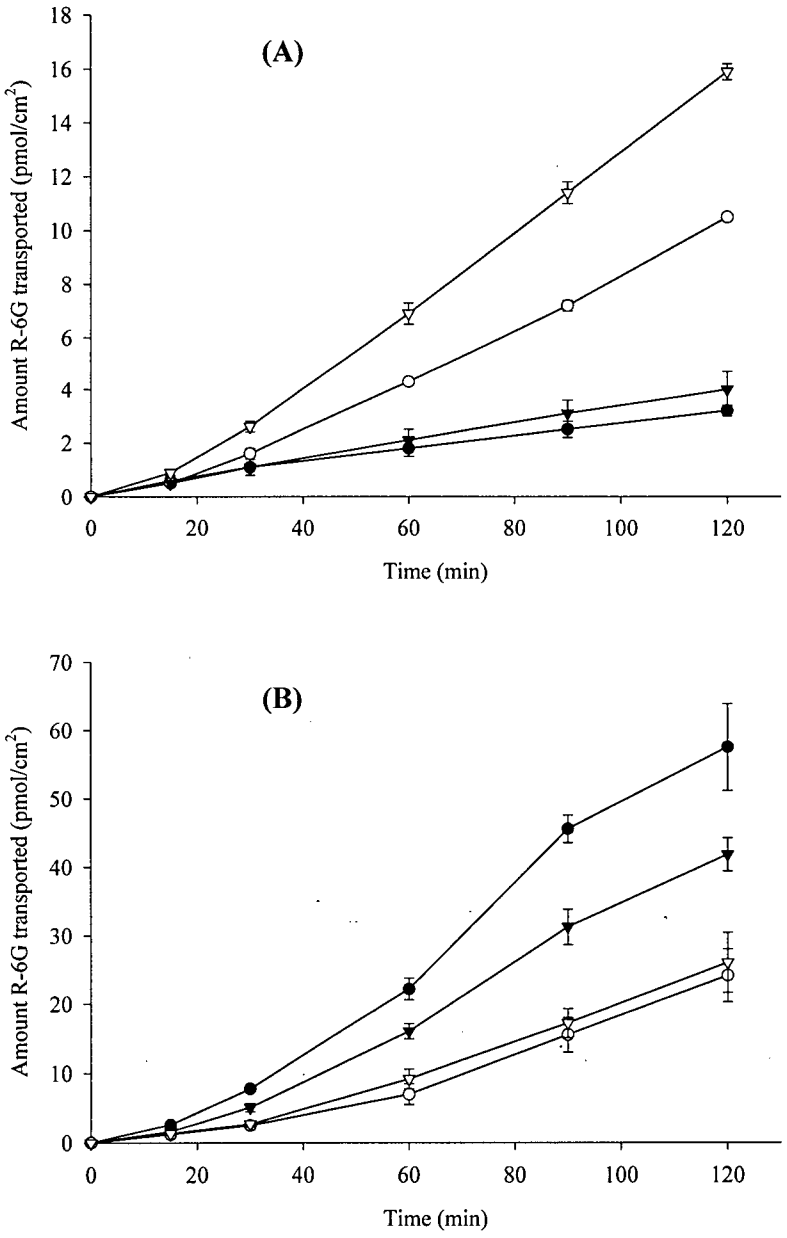

Figure 4.6: Directional flux of 0.25 μM R-6G across caco-2 monolayers over 120 min at 37^{0}C. R-6G AP→BL flux (A) measured the amount of R-6G in the BL solution when R-6G was placed on the AP side in the presence of (●) HBSS+10mM hepes, (○) 50 μM verapamil, (▼) 0.01% MePEG$_{17}$-*b*-PCL$_5$, or (▽) 0.25% MePEG$_{17}$-*b*-PCL$_5$. BL→AP flux of R-6G (B) was determined by placing R-6G on the BL side and monitoring the amount that entered the AP side which was exposed to (●) HBSS+10mM hepes, (○) 50 μM verapamil, (▼) 0.01% MePEG$_{17}$-*b*-PCL$_5$, or (▽) 0.25% MePEG$_{17}$-*b*-PCL$_5$. Data expressed as the cumulative amount of R-6G transported across a unit area of caco-2 monolayers and represented as the mean +/- SD with N=6.

Table 4.3: Apparent permeability coefficients (Papp) for R-6G flux across caco-2 monolayers in the AP→BL and BL→AP direction. Data expressed as mean +/- SD with N=6 for AP→BL and N=4 for BL→AP.

Treatment Group	AP→BL P_{app} x 10^{-6} (cm/s)	BL→AP P_{app} x 10^{-6} (cm/s)	Efflux Ratio[a]
Assay Buffer	1.61 +/- 0.09	36.8 +/- 3.60	22.8
50 μM Verapamil	6.35 +/- 0.14 (*)	14.8 +/- 2.25 (**)	2.33
0.01% $MePEG_{17}$-*b*-PCL_5	2.25 +/- 0.39 (ns)	26.6 +/- 1.55 (*)	11.8
0.25% $MePEG_{17}$-*b*-PCL_5	9.58 +/- 0.21 (**)	16.0 +/- 2.50 (**)	1.67

AP→BL: One-way ANOVA with pairwise comparisons using Student Newman Keuls test used for statistical analysis. (ns) = not statistical significant to assay buffer ($p>0.05$). (*) = Statistically significant compared to assay buffer and 0.01% diblock ($p<0.05$). (**) = Statistically significant comparison to assay buffer, verapamil and 0.01% diblock ($p<0.05$).
BL→AP: One-way ANOVA with pairwise comparisons using Student Newman Keuls test used for statistical analysis. (*) = Statistically significant compared to assay buffer ($p<0.05$). (**) = Statistically significant compared to assay buffer and 0.01% ($p<0.05$).
a) Efflux Ratio = $Papp_{BL\rightarrow AP}$ / $Papp_{AP\rightarrow BL}$

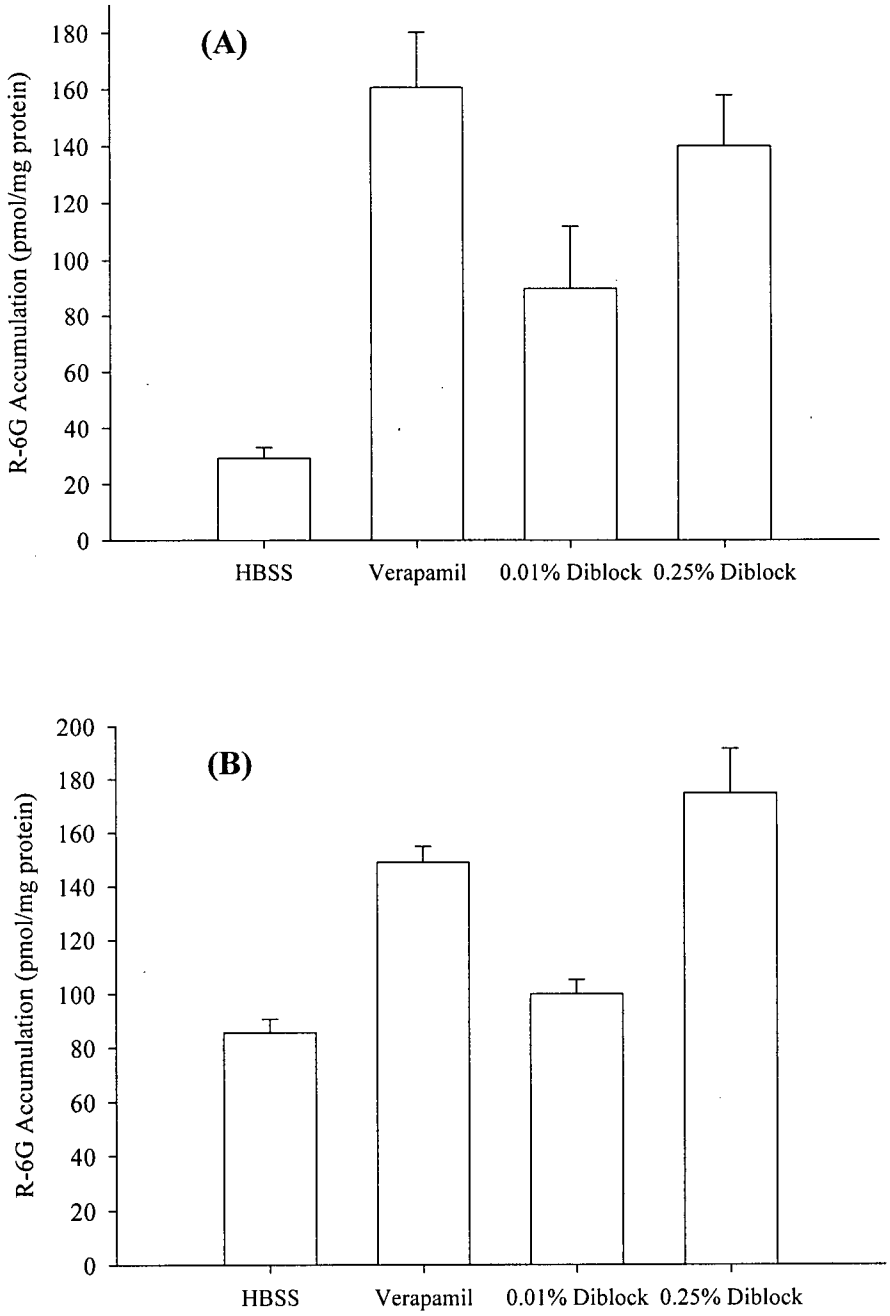

Figure 4.7: R-6G accumulation by caco-2 monolayers at the conclusion of the directional flux studies. Transwell membranes were excised and cells lysed to quantitate the cellular fluorescence. (A) Cellular accumulation in the AP→BL direction and (B) BL→AP direction. Data expressed as mean +/- SD with N=6.

cellular accumulation of R-6G greater than assay buffer alone. Both verapamil and 0.25% $MePEG_{17}$-*b*-PCL_5 enhanced the accumulation approximately 5 fold with 0.01% $MePEG_{17}$-*b*-PCL_5 producing a lower enhancement of approximately 3 fold. In the BL→AP direction, the accumulation was similar to the AP→BL direction, with both verapamil and 0.25% $MePEG_{17}$-*b*-PCL_5 giving similar levels of R-6G accumulation that were approximately 2 fold greater than assay buffer (Figure 4.7B). 0.01% $MePEG_{17}$-*b*-PCL_5 produced a similar level of R-6G cellular accumulation compared to assay buffer (Figure 4.7B).

4.3.3. R-123 accumulation under ATP depletion conditions

Caco-2 cells were pretreated for 30 min with an inhibitor of oxidative phosphorylation, KCN, and an inhibitor of glycolysis, DOG. All R-123 samples contained 1.5 mM KCN and 25 mM DOG during the accumulation time period. Figure 4.8 shows the R-123 accumulation by ATP depleted caco-2 cells with various concentrations of $MePEG_{17}$-*b*-PCL_5 diblock copolymer. Accumulation of R-123 under ATP depletion conditions was significantly increased approximately 3 fold compared to R-123 accumulation by untreated cells. R-123 accumulation was significantly increased with the addition of 0.05, 0.1, or 0.25% $MePEG_{17}$-*b*-PCL_5 compared to the R-123 accumulation without diblock under ATP depleted conditions.

4.3.4. Hemolysis of erythrocytes by MePEG-*b*-PCL diblock copolymers

The $MePEG_{17}$-*b*-PCL_2 diblock copolymer caused a rapid induction of hemolysis at concentrations as low at 0.25% w/v as shown in Figure 4.9A. The hemolytic effect was concentration dependent with ~60% hemolysis occurring within 1 hour with 2% w/v diblock. The time course of hemolysis induced by $MePEG_{17}$-*b*-PCL_5 was similar to that of $MePEG_{17}$-*b*-PCL_2 in that the diblock induced a rapid lysis during the first 1 to 2 hours followed by a

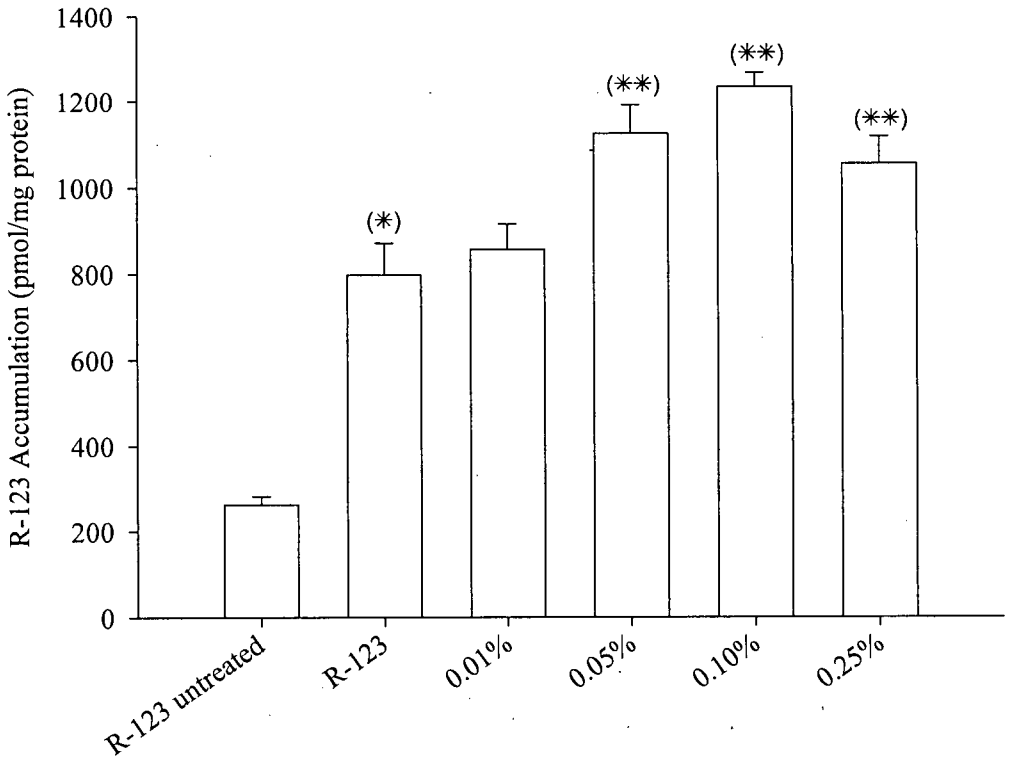

Figure 4.8: R-123 accumulation by caco-2 cells under ATP depleted conditions. Caco-2 cells were exposed to 5 μM R-123 in glucose free assay buffer containing 1.5 mM KCN + 25 mM DOG and varying concentrations of $MePEG_{17}$-*b*-PCL_5 for 90 min at 37^0C. 5 μM R-123 accumulation by ATP depleted and untreated cells without diblock copolymer was used as control. Data expressed as mean +/- SEM with N=3. Two-tailed two sample T-test with $p<0.05$ was used to compare R-123 accumulation groups. (*) Statistically significant comparison of R-123 accumulation of untreated cells to ATP depleted cells. (**) Statistically significant comparison of R-123 accumulation with diblock copolymer compared to R-123 alone under ATP depletion.

slower increase in lysis over the following 2 hours (Figure 4.10A). The concentration range for the induction of hemolysis for $MePEG_{17}$-*b*-PCL_5 was between 0.05 and 0.25%, approximately one tenth the concentrations of the $MePEG_{17}$-*b*-PCL_2 copolymer causing similar rates and levels of hemolysis. Up to 2h, the $MePEG_{17}$-*b*-PCL_{10} diblock copolymer caused only minor hemolytic effects at all concentrations studied as shown in Figure 4.11A. Only after 2 hours incubation did the higher concentrations (0.05 and 0.1%) induce any hemolysis, however levels remained below 20%. $MePEG_{12}$-*b*-PCL_4 induced almost no hemolysis at one hour, however by 4 hours this diblock had induced significant levels of hemolysis as seen in Figure 4.12A. The $MePEG_{45}$-*b*-PCL_4 diblock copolymer failed to induce significant hemolysis at concentrations as high as 1.0% (Figure 4.13).

The 'B' series in Figures 4.9 to 4.12 shows the correlation between R-123 accumulation by caco-2 cells with $MePEG_{17}$-*b*-PCL_2, $MePEG_{17}$-*b*-PCL_5, $MePEG_{17}$-*b*-PCL_{10}, or $MePEG_{12}$-*b*-PCL_4 with the percent hemolysis at the 4 hour time point. For all four diblock copolymers, there was a strong correlation (R= 0.945 for $MePEG_{17}$-*b*-PCL_2, R = 0.985 for $MePEG_{17}$-*b*-PCL_5, R = 0.999 for $MePEG_{17}$-*b*-PCL_{10}, and R = 0.986 for $MePEG_{12}$-*b*-PCL_4) between the degree of hemolysis and R-123 accumulation at the corresponding concentrations of diblock. However, no correlation was found for $MePEG_{45}$-*b*-PCL_4 since only low levels of R-123 accumulation and hemolysis were observed (Figure 3.11A and Figure 4.13). Additionally, the hemolysis of RBC's was measured with various concentrations of $MePEG_{45}$-*b*-$PDLLA_9$ diblock copolymer. No hemolysis was found with $MePEG_{45}$-*b*-$PDLLA_9$ at concentrations ranging from 0.5 to 2.0% w/v over 4 hours (data not shown).

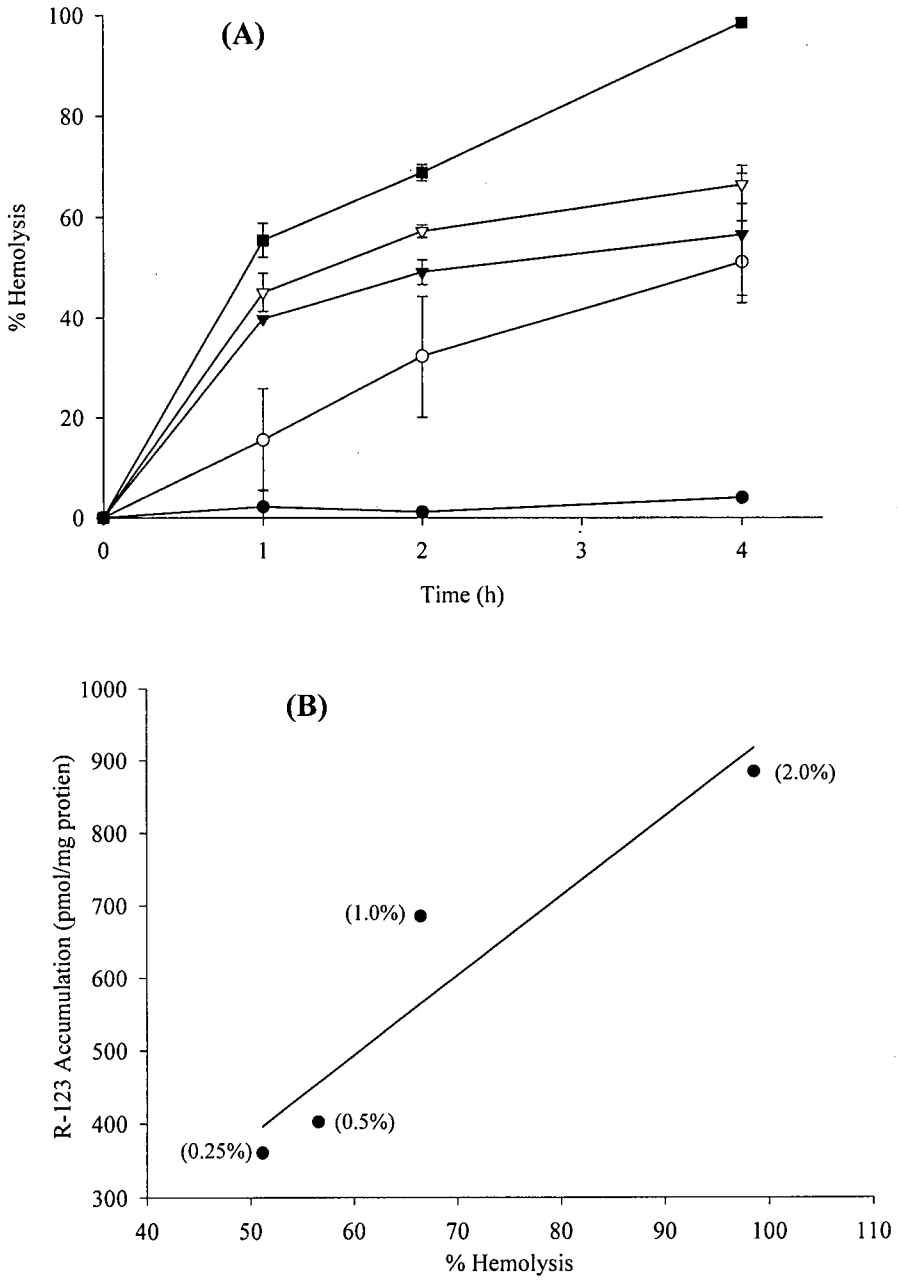

Figure 4.9: (A) Time course of RBC hemolysis induced by $MePEG_{17}$-*b*-PCL_2 at 37^0C with concentrations of (●) 0.1% w/v, (○) 0.25% w/v, (▼) 0.5% w/v, (▽) 1.0% w/v, and (■) 2.0% w/v. Data represents mean +/- SD (N=3). (B) Correlation of R-123 accumulation in caco-2 cells with $MePEG_{17}$-*b*-PCL_2 (Figure 3.6A) with % hemolysis at 4 h. The concentration of $MePEG_{17}$-*b*-PCL_2 for each data point is represented in brackets.

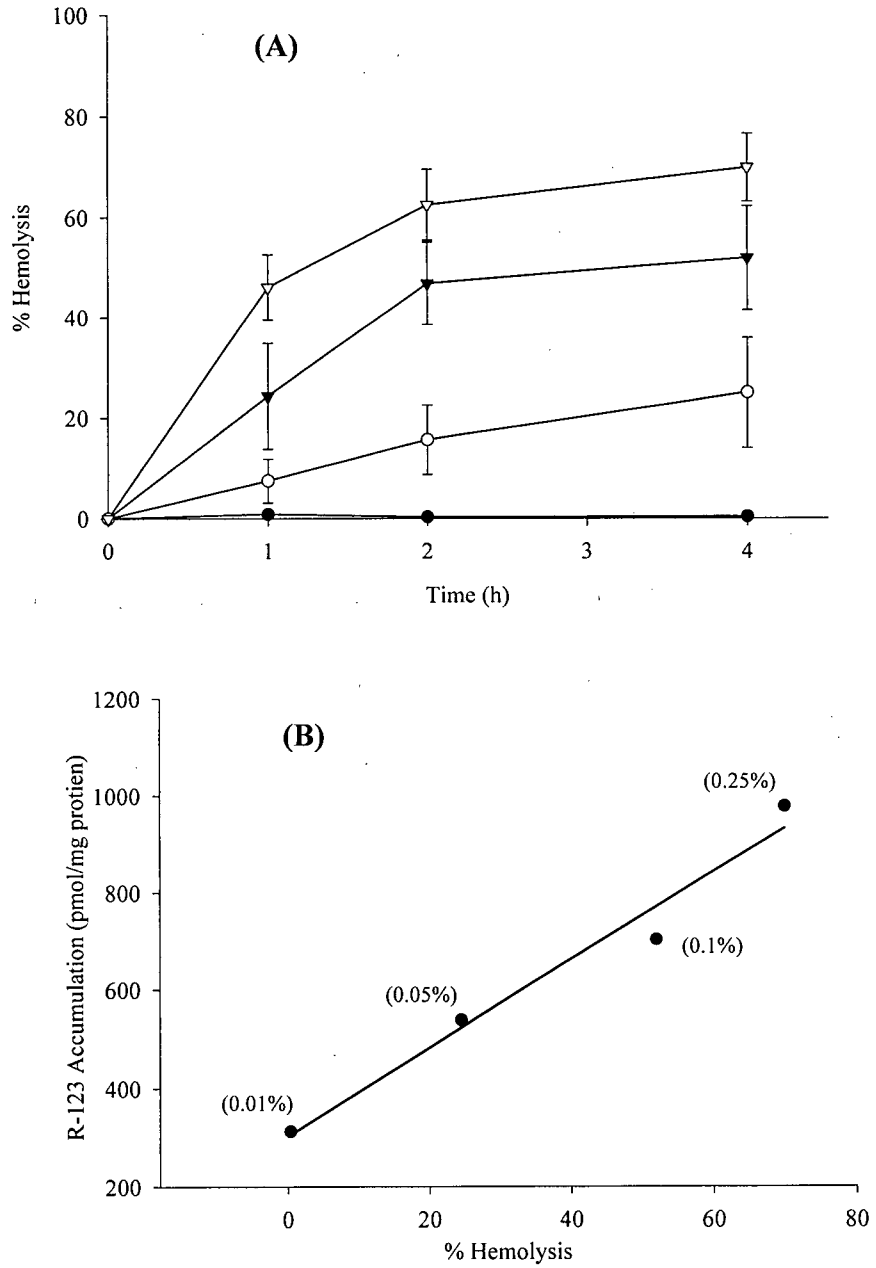

Figure 4.10: (A) Time course of RBC hemolysis induced by $MePEG_{17}$-*b*-PCL_5 at 37^0C with concentrations of (●) 0.01% w/v, (○) 0.05% w/v, (▼) 0.1% w/v, and (▽) 0.25% w/v. Data represents mean +/- SD (N=3). (B) Correlation of R-123 accumulation in caco-2 cells with $MePEG_{17}$-*b*-PCL_5 (Figure 3.7A) with % hemolysis at 4 h. The concentration of $MePEG_{17}$-*b*-PCL_5 for each data point is represented in brackets.

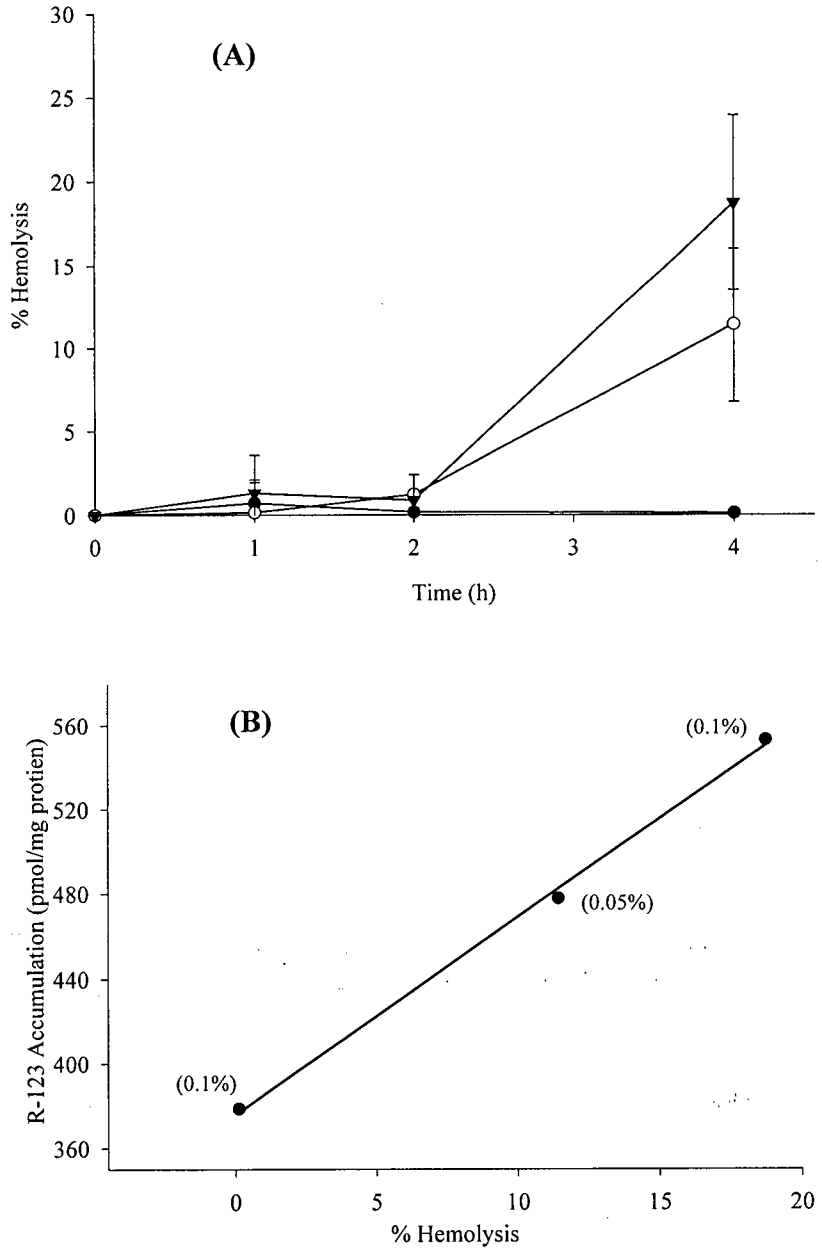

Figure 4.11: (A) Time course of RBC hemolysis induced by $MePEG_{17}$-*b*-PCL_{10} at 37^0C with concentrations of (●) 0.01% w/v, (○) 0.05% w/v, and (▼) 0.1% w/v. Data represents mean +/- SD (N=3). (B) Correlation of R-123 accumulation in caco-2 cells with $MePEG_{17}$-*b*-PCL_{10} (Figure 3.8A) with % hemolysis at 4 h. The concentration of $MePEG_{17}$-*b*-PCL_{10} for each data point is represented in brackets.

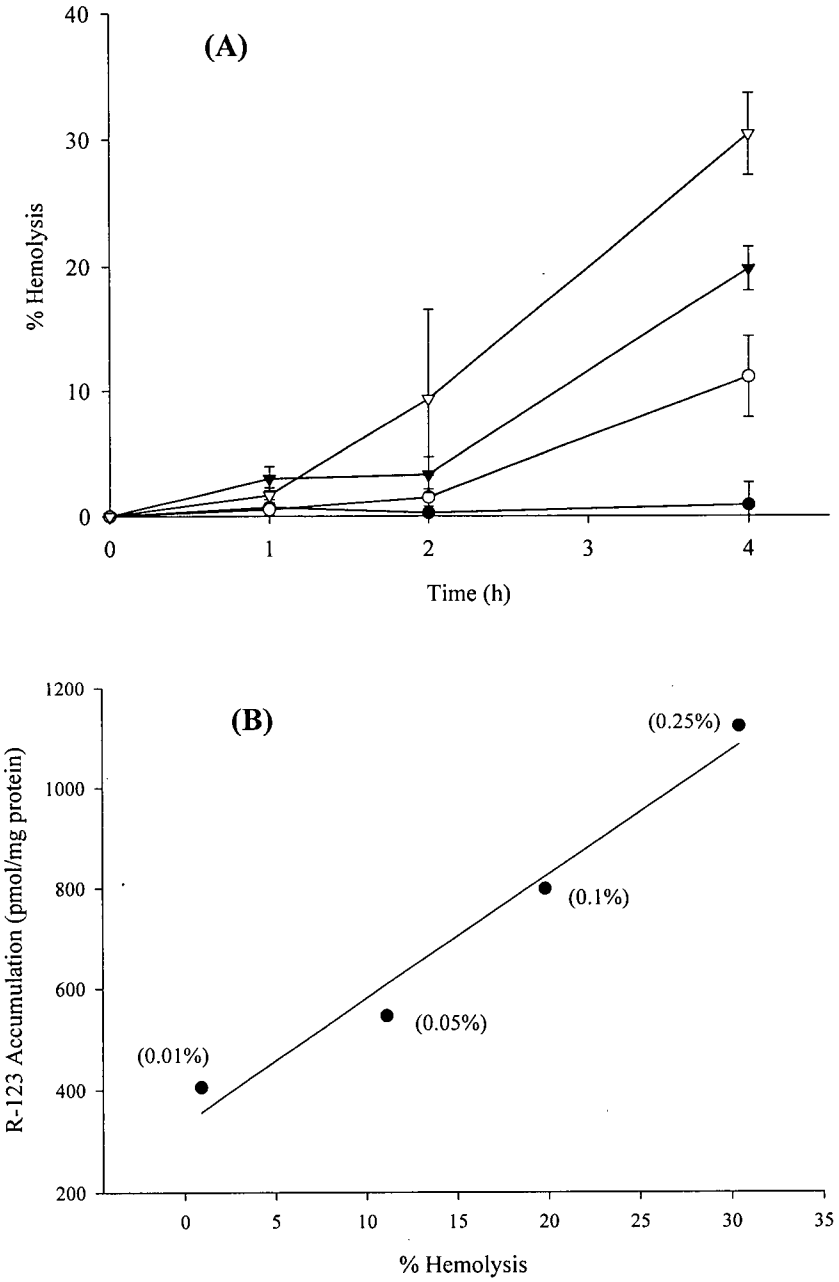

Figure 4.12: (A) Time course of RBC hemolysis induced by $MePEG_{12}$-*b*-PCL_4 at 37^0C with concentrations of (●) 0.01% w/v, (○) 0.05% w/v, (▼) 0.1% w/v, and (▽) 0.25% w/v. Data represents mean +/- SD (N=3). (B) Correlation of R-123 accumulation in caco-2 cells with $MePEG_{12}$-*b*-PCL_4 (Figure 3.9A) with % hemolysis at 4 h. The concentration of $MePEG_{12}$-*b*-PCL_4 for each data point is represented in brackets.

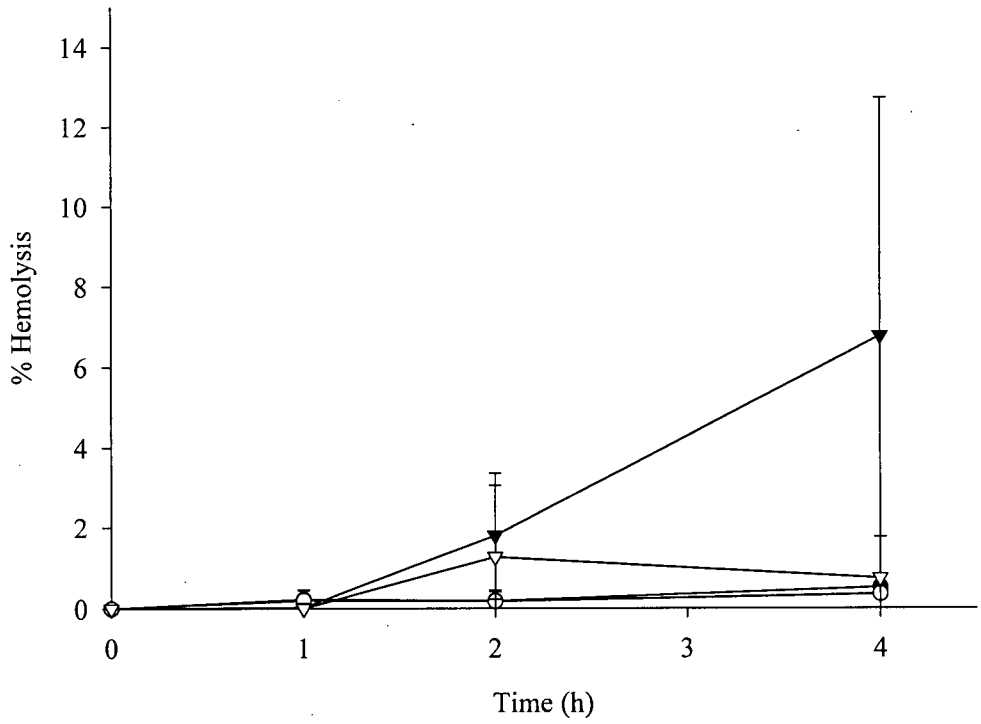

Figure 4.13: Time course of RBC hemolysis induced by $MePEG_{45}$-*b*-PCL_4 at 37^{0}C at concentrations of (●) 0.01% w/v, (○) 0.1% w/v, (▼) 0.5% w/v, and (▽) 1.0% w/v. Data represent mean +/- SD (N=3).

4.3.5. R-123 accumulation by non-P-gp expressing cell lines

Figure 4.14A and B shows the cellular accumulation of R-123 with either HT-29 or SW-620 human colon adenocarcinoma cell lines, respectively. For both cell lines, R-123 accumulation with verapamil was similar to the level of R-123 alone and increasing concentrations of $MePEG_{17}$-*b*-PCL_5 produced no enhancement of R-123 accumulation with either cell line (Figure 4.14A and B).

4.3.6. Effect of $MePEG_{17}$-*b*-PCL_5 on P-gp ATPase activity

The effect of $MePEG_{17}$-*b*-PCL_5 diblock copolymer on P-gp ATPase activity is shown in Figure 4.15. Isolated membranes containing human P-gp were exposed to a range of diblock concentrations (0.0001% to 0.25% w/v) that spanned the concentrations that demonstrating maximum accumulation enhancement for R-123 or R-6G (Figure 3.8 A and B). The buffer group represented basal ATPase activity of P-gp, which was stimulated by the addition of 50 μM verapamil (Figure 4.15). $MePEG_{17}$-*b*-PCL_5 stimulated P-gp ATPase activity in a concentration dependent manner with 0.001% to 0.25% w/v diblock concentrations showing a significant increase in ATPase activity compared to buffer alone.

To evaluate whether substrate binding with P-gp could alter the effect of $MePEG_{17}$-*b*-PCL_5 on P-gp ATPase activity, both R-123 and R-6G were added to various concentrations of $MePEG_{17}$-*b*-PCL_5. Figure 4.16A shows that 5 μM R-123 alone did not produce any change in P-gp ATPase activity, while $MePEG_{17}$-*b*-PCL_5 in combination with R-123 still demonstrated a significant concentration dependent stimulation of P-gp ATPase activity similar to results in Figure 4.15. In contrast, 0.25 μM R-6G produced a significant increase in P-gp ATPase activity compared to buffer alone (Figure 4.16B). When $MePEG_{17}$-*b*-PCL_5 was combined with 0.25 μM R-6G, all diblock concentrations produced a significant increase

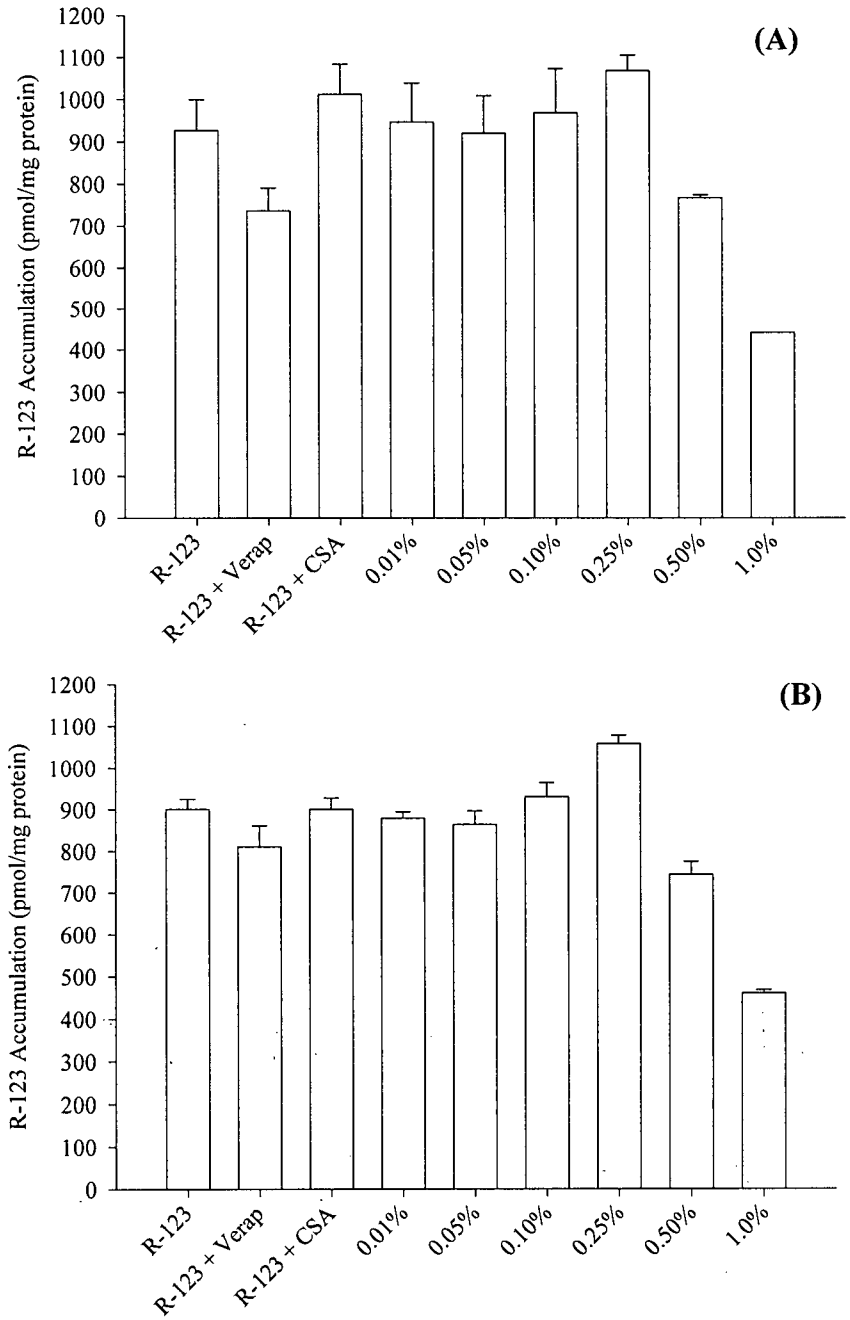

Figure 4.14: Accumulation of R-123 with (A) HT-29 and (B) SW-620 cells. Cells were treated with 5 μM R-123 containing varying concentrations of $MePEG_{17}$-*b*-PCL_5 for 90 min at 37^0C. R-123 alone and with P-gp inhibitors were used as controls. Data expressed as mean +/- SD with N=6.

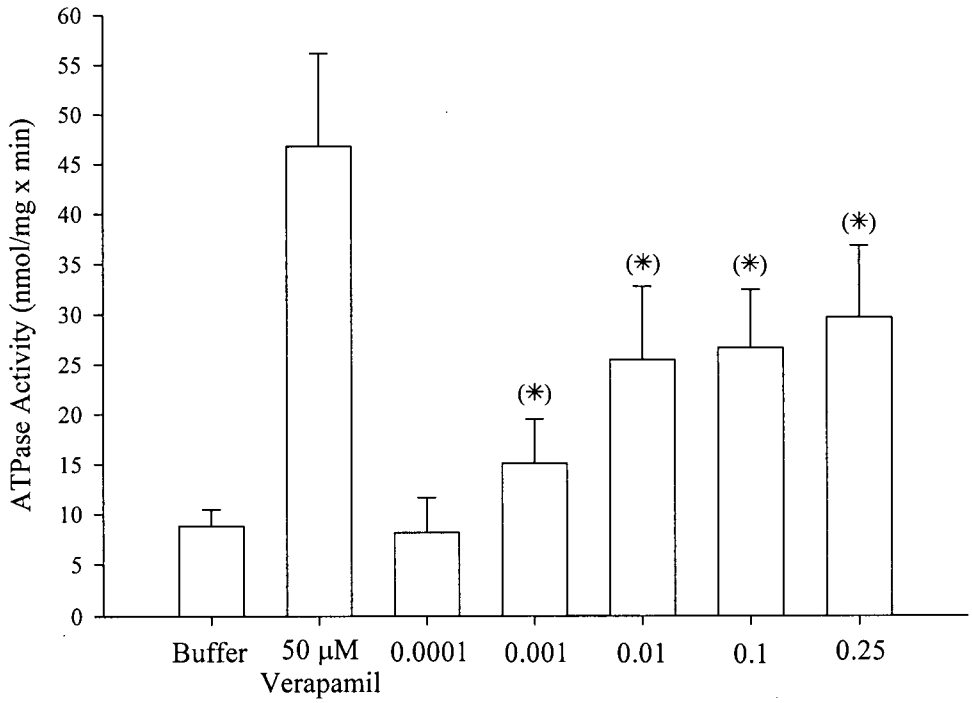

Figure 4.15: Effect of $MePEG_{17}$-*b*-PCL_5 diblock copolymer concentration (% w/v) on P-gp ATPase activity in isolated human P-gp containing membranes. Data represent the mean +/- SD (N=4). Two-tailed two sample t-test with $p<0.05$ was used to compare buffer group with treatment groups. (*) Statistically significant comparison.

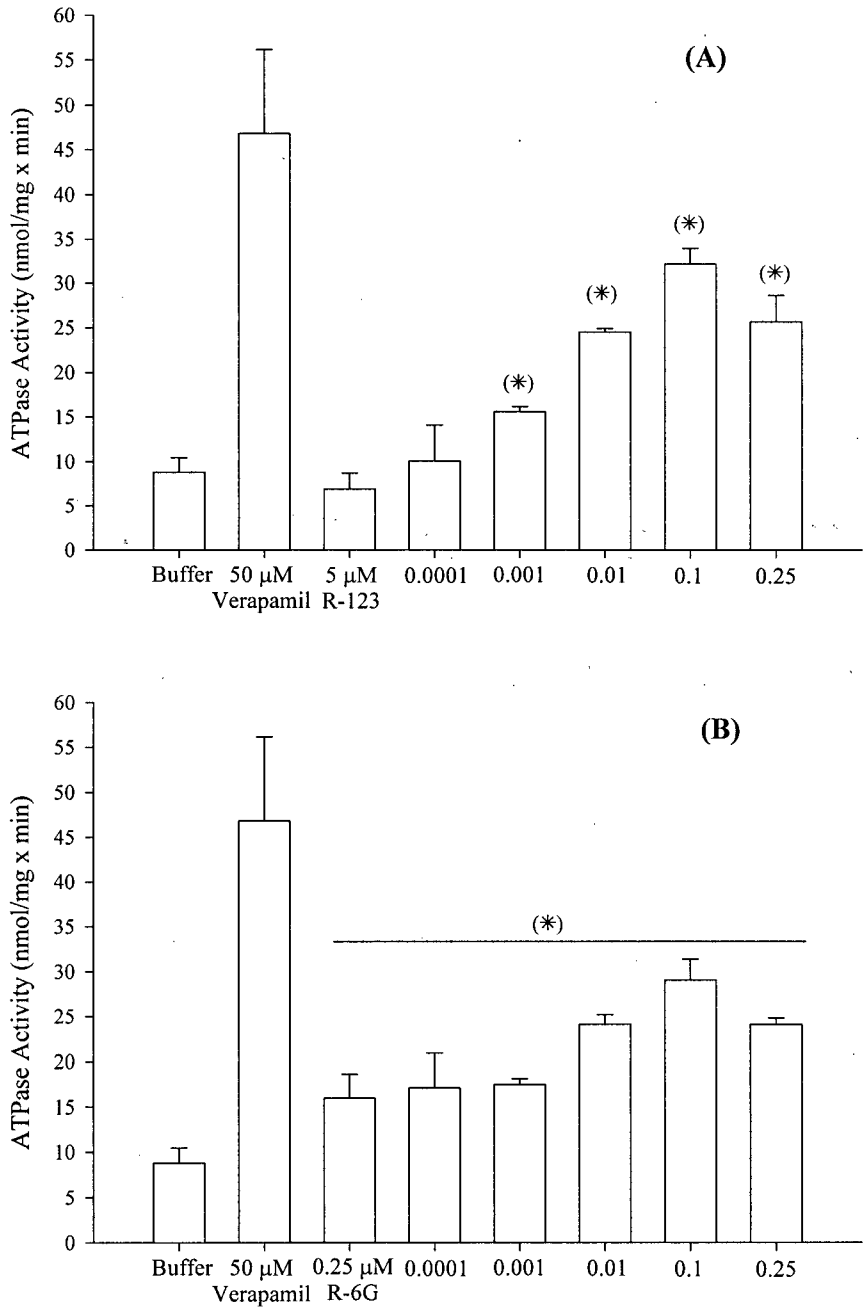

Figure 4.16: Effect of (A) 5 µM R-123 and (B) 0.25 µM R-6G with various concentrations (% w/v) of $MePEG_{17}$-*b*-PCL_5 diblock copolymer on P-gp ATPase activity in isolated human P-gp containing membranes. Data represent the mean +/- SD (N=3). Two-tailed two sample t-test with $p<0.05$ was used to compare buffer group with treatment groups. (*) Statistically significant comparison.

in P-gp ATPase activity (Figure 4.16B).

4.4. DISCUSSION

In Chapter 3, a series of MePEG-*b*-PCL amphiphilic diblock copolymers varying in MePEG and PCL length were shown to enhance the accumulation of the relatively hydrophilic R-123 and the hydrophobic R-6G P-gp substrates within caco-2 cells. The diblock copolymer with the greatest ability to enhance accumulation was found to be composed of MePEG with 17 repeat units (MePEG of molecular weight 750) and with 5 repeat units of PCL, denoted as $MePEG_{17}$-*b*-PCL_5. R-123 accumulation was increased 3.8 fold in the presence of 0.25% of $MePEG_{17}$-*b*-PCL_5 and R-6G accumulation was increased 2.8 fold with 0.01% $MePEG_{17}$-*b*-PCL_5 (Table 3.1). Thus, $MePEG_{17}$-*b*-PCL_5 was chosen for further studies attempting to elucidate the pathways involved in enhancement of cellular accumulation of R-123 and R-6G.

The concentration of $MePEG_{17}$-*b*-PCL_5 producing maximum R-123 accumulation was approximately 10 fold higher than the critical micelle concentration (CMC = 0.03% w/v) with minimal enhancement of accumulation found at concentrations below the CMC (Figure 3.8A). This is in contrast to the concentration of $MePEG_{17}$-*b*-PCL_5 required to enhance R-6G accumulation, where maximum enhancement occurred at or below the CMC (Figure 3.8B). However for both R-123 and R-6G, high concentrations of $MePEG_{17}$-*b*-PCL_5 resulted in a substantial decrease in accumulation (Figure 3.8A and B). These results for R-123 differ from the findings of other investigators who showed that some surfactants, including the triblock copolymers in the Pluronic® series, enhanced cell accumulation or flux of P-gp substrates at concentrations well below the CMC (Nerurkar *et al.*, 1997; Batrakova *et al.*, 1998a). Substrate accumulation or flux was maximal close to the CMC of the amphiphiles

and free surfactant unimers were suggested to be the species primarily responsible for the inhibition of P-gp (Nerurkar *et al.*, 1997; Batrakova *et al.*, 1998a; Batrakova *et al.*, 1998b). The decrease in accumulation at concentrations above the CMC for these surfactants was suggested to be due to substantial micellization of the P-gp substrate which reduced the free concentration of substrate available for entry into the cell (Nerurkar *et al.*, 1997).

The binding of R-123 with $MePEG_{17}$-*b*-PCL_5 micelles showed that approximately 25% of a 5 μM R-123 solution was bound within micelles at 0.25% $MePEG_{17}$-*b*-PCL_5 diblock, which increased to 50% binding at 1.0% $MePEG_{17}$-*b*-PCL_5 (Figure 3.23A). Although the extent of R-123 bound within $MePEG_{17}$-*b*-PCL_5 micelles was relatively low at the maximal accumulation enhancement concentration of 0.25% $MePEG_{17}$-*b*-PCL_5, it was possible that enhanced accumulation of R-123 with $MePEG_{17}$-*b*-PCL_5 may have occurred, at least in part, by an endocytotic pathway involving uptake of micelle-bound R-123. Endocytosis of micellized compounds has been previously shown for chemically similar diblock copolymers composed of poly(ethylene glycol)-*block*-poly(caprolactone) in PC12 and P19 cell lines (Allen *et al.*, 1999b; Luo *et al.*, 2002). Therefore, to determine whether R-123 loaded $MePEG_{17}$-*b*-PCL_5 micelles contributed to enhanced R-123 accumulation via an endocytotic pathway, R-123 accumulation was evaluated in the presence of endocytosis inhibitors.

Preliminary studies evaluated common endocytosis inhibitors such as monensin and cytochalasin B. However, it was shown that these compounds increased R-123 accumulation and that this may have been due to P-gp modulation by the endocytosis inhibitors (data not shown). The endocytosis inhibitors selected have been reported to affect various stages of the endocytotic process without modulating the activity of P-gp. Hyperosmotic sucrose

inhibits fluid phase and receptor mediated endocytosis, ammonium chloride is used to increase the pH of the endosomes and thus prevent the acidification of the endocytotic pathway, and the macrocyclic antibiotic, brefeldin A (Br-A), can cause morphological changes in the endosomes and inhibit recycling between the endoplasmic reticulum and the cis-golgi complex (Giocondi *et al.*, 1995; Mellman, 1996; Zelphati and Szoka, 1996).

In control experiments with the fluid phase marker lucifer yellow (LY), all three inhibitors reduced cellular LY accumulation to approximately 40-50% in the caco-2 model, demonstrating that the endocytotic pathway was inhibited under the experimental conditions (Figure 4.1). Using varying concentrations of $MePEG_{17}$-*b*-PCL_5, accumulation of 5 μM R-123 was determined in the presence of these endocytosis inhibitors. Figure 4.2 shows that R-123 accumulation with $MePEG_{17}$-*b*-PCL_5 at concentrations above the CMC, in the presence of endocytosis inhibitors, was similar to the untreated control group. The absence of any reduction in R-123 accumulation with endocytosis inhibitors over a range of concentrations, tested suggested that endocytosis of micellized R-123 was not a pathway contributing to the R-123 accumulation enhancement.

It was speculated that $MePEG_{17}$-*b*-PCL_5 micelles could be functioning as a 'depot' for free unimers that partitioned into the membrane and either reached a threshold concentration for P-gp inhibition, or promoted substrate influx through enhanced R-123 membrane permeability. Therefore, studies evaluating the effect of $MePEG_{17}$-*b*-PCL_5 diblock on the directional flux of R-123 and R-6G across caco-2 monolayers were carried out to assess inhibitory effects on P-gp mediated efflux activity. Concentrations of $MePEG_{17}$-*b*-PCL_5 employed in these studies were either below the CMC (0.01%) or above the CMC (0.25%). Since P-gp transports substrate in the BL→AP direction, inhibition of P-gp activity

should reduce the BL→AP directional flux and increase the AP→BL flux. Therefore, efflux ratios ($Papp_{BL\rightarrow AP}$ / $Papp_{AP\rightarrow BL}$) were determined to assess the possible role of P-gp modulation by $MePEG_{17}$-*b*-PCL_5 diblock. In general, it has been established that efflux ratios of greater than 2.0 are indicative of the involvement of an efflux mechanism and in the presence of an inhibitor, efflux ratios are typically reduced to approximately 1.0 (Polli *et al.*, 2001).

During the flux experiments the TEER was monitored before and after the experiment and the flux of LY was monitored in the presence or absence of 0.25% $MePEG_{17}$-*b*-PCL_5 to determine any change in tight junction integrity over the course of the experiment. A large increase in LY flux or a decrease in the TEER would be indicative of a decrease in monolayer integrity and also might indicate that the diblock could enhance R-123 or R-6G flux via effects on the paracellular transport pathway. No significant difference in the TEER and LY transport with $MePEG_{17}$-*b*-PCL_5 diblock was observed compared to assay buffer group suggesting that the integrity of the tight junctions was maintained during treatment (Table 4.1).

The efflux ratio of R-123 and R-6G with assay buffer was 3.2 and 22.8 respectively, confirming their polarized efflux by P-gp (Table 4.2 and 4.3). The R-6G efflux ratio was substantially higher than R-123. The more hydrophobic R-6G may be able to penetrate into the nonpolar core of the membrane more effectively, and more extensively, giving greater access to the P-gp binding site, promoting increased efflux. In comparison, the hydrophilic R-123 may penetrate the nonpolar membrane core relatively poorly and interact less effectively with the P-gp binding site. In the presence of verapamil and 0.25% $MePEG_{17}$-*b*-

PCL_5, efflux ratios of R-123 were reduced to 1.15 and 1.06, respectively, indicative of inhibitory effects on P-gp mediated efflux of R-123 (Table 4.2).

Interestingly, the $Papp_{AP\rightarrow BL}$ values for verapamil and both concentrations of $MePEG_{17}$-*b*-PCL_5 were not statistically different from the $Papp_{AP\rightarrow BL}$ for R-123 in assay buffer (Table 4.2). The $Papp_{BL\rightarrow AP}$ was significantly reduced with verapamil and 0.25% $MePEG_{17}$-*b*-PCL_5 compared to R-123 with assay buffer (Table 4.2). This indicates that verapamil and $MePEG_{17}$-*b*-PCL_5 were able to inhibit the secretory R-123 efflux through caco-2 monolayers but did not enhance the absorptive AP→BL influx. Hence, although R-123 cellular accumulation studies with $MePEG_{17}$-*b*-PCL_5 consistently showed an approximately 4 fold increase in R-123 accumulation compared to R-123 alone (Figure 3.8A), no increase in the AP→BL flux was observed. Similar results have been described by Altenberg *et al.* who showed that verapamil did not enhance R-123 influx despite abolishing R-123 efflux in P-gp overexpressing Chinese hamster lung fibroblasts (Altenberg *et al.*, 1994).

Recent work by Troutman and Thakker demonstrated a similar lack of R-123 flux enhancement in the AP→BL direction when caco-2 cells were treated with a P-gp inhibitor (Troutman and Thakker, 2003b). The inability of P-gp inhibitors to increase AP→BL flux of R-123 was thought to be the result of poor membrane penetration of R-123 owing to its cationic charge and low octanol/water partition coefficient (Lampidis *et al.*, 1989; Eytan *et al.*, 1996; Eytan *et al.*, 1997; Troutman and Thakker, 2003b). Furthermore, a large BL→AP flux of R-123 was shown which was significantly decreased using a P-gp inhibitor, similar to our observations (Figure 4.4B) (Troutman and Thakker, 2003b). Since R-123 cannot penetrate the lipid membrane effectively, kinetic evidence suggested that the large BL→AP

flux of R-123 was the result of an unknown influx transporter in the BL membrane that actively transported R-123 into the cell and was then transported by P-gp out of the cell (Troutman and Thakker, 2003b). Apically applied P-gp inhibitors would then be able to effectively decrease the BL→AP flux through modulation of P-gp. This asymmetry in the flux for R-123 was further found for doxorubicin, another hydrophilic compound with poor membrane permeability (Troutman and Thakker, 2003b).

At the conclusion of the AP→BL and BL→AP directional flux studies the caco-2 monolayers were excised to determine the extent of R-123 accumulation occurring through either the AP membrane or the BL membrane. Assessment of R-123 accumulation after the AP→BL flux study was considered to be analogous to R-123 accumulation studies previously determined in flat bottom plates and should describe effects of verapamil and $MePEG_{17}$-*b*-PCL_5 on the influx of R-123 across the AP membrane. Approximately 5 fold and 2 fold increases in R-123 cellular accumulation were observed after the AP→BL flux experiment with 0.25% $MePEG_{17}$-*b*-PCL_5 and verapamil, respectively, suggesting that $MePEG_{17}$-*b*-PCL_5 might have inhibited P-gp to a greater extent than verapamil (Figure 4.5A). On the other hand, Table 4.2 and Figure 4.5B show that the $Papp_{BL\rightarrow AP}$ and the extent of R-123 accumulation was similar for verapamil and 0.25% $MePEG_{17}$-*b*-PCL_5, demonstrating that they are equally effective at reducing the apical efflux of R-123. Hence, it seems unlikely that the differences observed in R-123 accumulation after AP→BL flux studies for verapamil and diblock can be explained solely by inhibition of P-gp efflux. We suggest that there may be a combination of mechanisms including both P-gp efflux inhibition and changes in R-123 membrane permeability caused by diblock interactions with the AP membrane. Furthermore, the significantly larger R-123 cell accumulation following

BL→AP flux experiments compared to AP→BL flux experiments, in the presence of either verapamil or 0.25% $MePEG_{17}$-*b*-PCL_5 diblock, indicates that R-123 crossed the BL membrane relatively easily and produced higher intracellular concentrations (Figure 4.5 A and B). This observation may provide indirect support for the concept proposed by Troutman and Thakker that the BL membrane of caco-2 cells may possess an active transporter pumping R-123 into the cell (Troutman and Thakker, 2003b). Hence, the apparent high BL membrane permeability may in fact be due to this proposed active transport pump and not a result of intrinsic membrane permeability of R-123.

If the diblock caused an increase in R-123 membrane permeability leading to an increase in R-123 influx through the AP membrane, why this did not translate to an increase in the $Papp_{AP\rightarrow BL}$ is not clear. For AP→BL flux to occur for R-123, once inside the cell R-123 must cross the BL membrane. Since the intracellular localization of R-123 primarily resides within the mitochondria, this deposition may act as an intracellular sink reducing the concentration gradient across the BL membrane and effectively reducing the AP→BL flux. In Chapter 3, confocal fluorescence microscopy studies were carried out for the R-123 fluorescence localization within caco-2 cells when exposed to either R-123 in assay buffer or with 0.25% $MePEG_{17}$-*b*-PCL_5 (Figure 3.15A and B). A lower level of R-123 fluorescence and a punctated pattern was observed throughout the cells with assay buffer (Figure 3.15A). This pattern is indicative of the localization of R-123 within the mitochondria (Eytan *et al.*, 1997). With 0.25% $MePEG_{17}$-*b*-PCL_5 an intense and diffuse fluorescence was observed throughout the cytosol with no discernable punctation due to the fluorescence intensity (Figure 3.15B). From the micrograph in Figure 3.15B, it appears that there was extensive cytosolic deposition of R-123, which should be available for diffusion across the BL

membrane. The low partition coefficient and charged nature of R-123 may have limited the BL membrane permeability of R-123 once inside the cell and reduced AP→BL flux. Although a greater influx through the AP membrane occurred with $MePEG_{17}$-*b*-PCL_5, this did not significantly increase the overall $Papp_{AP\rightarrow BL}$ for R-123, possibly due to the lack of $MePEG_{17}$-*b*-PCL_5 effects on the BL membrane since exposure was on the apical surface.

In contrast to R-123, the $Papp_{AP\rightarrow BL}$ for R-6G was significantly increased with verapamil and 0.25% $MePEG_{17}$-*b*-PCL_5 (Table 4.3). The R-6G efflux ratio was reduced from 22.8 with buffer to 2.33 and 1.67 with verapamil and 0.25% $MePEG_{17}$-*b*-PCL_5, respectively, indicative of a reduction in P-gp efflux activity (Table 4.3). Although, 0.01% $MePEG_{17}$-*b*-PCL_5 produced the maximal R-6G accumulation enhancement in cellular accumulation studies (see previous chapter, Figure 3.8B), there was no significant increase in the $Papp_{AP\rightarrow BL}$ and the efflux ratio was only reduced to 11.8, from a value of 22.8 for R-6G with buffer (Table 4.3). Additionally, Table 4.3 shows that the $Papp_{BL\rightarrow AP}$ for 0.25% $MePEG_{17}$-*b*-PCL_5 was lower than 0.01% $MePEG_{17}$-*b*-PCL_5, suggesting that a concentration of 0.25% was more effective at inhibiting P-gp efflux.

Similar to the studies with R-123, at the conclusion of the directional flux experiments, the concentration accumulated into caco-2 cells was determined. Figure 4.7A shows that cellular accumulation of R-6G in the AP→BL direction was higher for 0.25% $MePEG_{17}$-*b*-PCL_5 than 0.01% $MePEG_{17}$-*b*-PCL_5 and was a similar level to verapamil. Similarly in the BL→AP direction, 0.25% $MePEG_{17}$-*b*-PCL_5 produced greater accumulation of R-6G compared to 0.01% $MePEG_{17}$-*b*-PCL_5 (Figure 4.7B). These findings were in contrast to previous cellular accumulation studies with R-6G in Chapter 3, where maximal accumulation enhancement of R-6G was found at 0.01% diblock. At 0.25% diblock, the

accumulation was substantially reduced due to the extensive partitioning or binding of R-6G (75%) within micelles at this concentration (Figure 3.8B and 3.23B). However, the accumulation profile "corrected" for free fraction of R-6G showed that 0.25% $MePEG_{17}$-*b*-PCL_5 produced a high level of accumulation. Thus, the greater accumulation at 0.25% diblock obtained after flux studies may result from altered R-6G binding characteristics as follows. The extent of R-6G accumulation by caco-2 cells in the cellular accumulation studies, where cells were grown on flat bottom plates, depends on the free drug concentration in the apical solution. At equilibrium, free R-6G concentration in solution is in equilibrium with the cellular R-6G concentration. Since the free R-6G concentration with 0.25% $MePEG_{17}$-*b*-PCL_5 is lower due to extensive micelle binding, the equilibrium R-6G concentration inside the cells should be low (as seen in Figure 3.8B). Since the free concentration of R-6G with 0.01 % $MePEG_{17}$-*b*-PCL_5 was close to the total R-6G concentration applied (Figure 3.23B), more R-6G would be available to enter the cell and at equilibrium, the cellular concentration would be higher than for R-6G with 0.25% $MePEG_{17}$-*b*-PCL_5. In the flux experiments, caco-2 cells were in contact with an additional basolateral solution. R-6G is transported across the cell and into the basolateral solution, and additional free R-6G then moves into the cell. To maintain the free R-6G concentration, the equilibrium is shifted and R-6G partitions out of the micelle and into solution. Additionally, the "corrected" accumulation (Figure 3.27B) shows that 0.25% diblock increased accumulation of R-6G greater than 0.01% diblock, suggesting that a greater inhibitory activity on P-gp efflux may also contribute to the greater $Papp_{AP \rightarrow BL}$ found with 0.25% $MePEG_{17}$-*b*-PCL_5 compared to 0.01% $MePEG_{17}$-*b*-PCL_5.

In an attempt to determine the possible contribution of an altered membrane permeability resulting from surfactant interaction with caco-2 membranes, R-123 accumulation studies were performed under ATP depletion conditions. It was hypothesized that if caco-2 cells were depleted of ATP, the ability of P-gp to function as an efflux transporter would be abolished and any observed increase in R-123 accumulation by $MePEG_{17}$-*b*-PCL_5 should be the result of increased transmembrane diffusion caused by R-123 membrane permeability changes. Several groups have demonstrated an increase in P-gp substrate accumulation under ATP depletion (See *et al.*, 1974; Asaumi *et al.*, 1999). Using similar conditions, the accumulation of R-123 in assay buffer was increased by depleting caco-2 cells of ATP (Figure 4.8). There was a statistically significant increase in the R-123 accumulation in the presence of $MePEG_{17}$-*b*-PCL_5 diblock compared to the accumulation of R-123 in assay buffer when caco-2 cells were treated with metabolic inhibitors (Figure 4.8). This increase may indicate that the diblock increased the transmembrane passive diffusion of R-123. However the contributions of diblock inhibition of residual P-gp activity that may not have been abolished from the ATP depletion treatment cannot be ruled out.

These results suggest that $MePEG_{17}$-*b*-PCL_5 diblock copolymer may enhance the passive transmembrane diffusion of the hydrophilic R-123 by membrane permeabilization effects in addition to P-gp efflux inhibition. The insertion of surfactant molecules into a membrane is typically associated with a disruption of membrane order and integrity, which can increase the permeability of drugs (Swenson and Curatolo, 1992; Jones, 1999). Therefore, $MePEG_{17}$-*b*-PCL_5 may have exerted a membrane perturbing effect that promoted enhanced R-123 accumulation. Using erythrocyte hemolysis as a measure for membrane perturbation, the effects of MePEG-*b*-PCL diblock copolymers were investigated.

Measurements of erythrocyte hemolysis have been commonly used to investigate membrane perturbation effects by agents such as surfactants and inflammatory microcrystals (Jackson *et al.*, 1996; Vinardell and Infante, 1999). Insertion into the membrane of a perturbing agent can disrupt the erythrocyte membrane, resulting in colloid osmotic swelling and the release of hemoglobin (Jackson *et al.*, 1996). As seen in Figures 4.9 to 4.13 "A" series, MePEG-*b*-PCL diblock copolymers were capable of inducing erythrocyte hemolysis with increasing concentrations depending on the length of either the MePEG or PCL block. The same diblock concentrations of $MePEG_2$-*b*-PCL_2 (2.0%) and $MePEG_{17}$-*b*-PCL_5 (0.25%) that demonstrated a high AEF for R-123 and an increase in the R-123 accumulation rate constant (Table 3.1 and 3.2), both induced high degree of hemolysis over 4 hours (Figure 4.9A and 4.10A). Good correlations were obtained between extent of hemolysis and R-123 accumulation for $MePEG_2$-*b*-PCL_2 (R=0.945) and $MePEG_{17}$-*b*-PCL_5 (R=0.985) (Figure 4.9B and 4.10B). Diblock copolymers that produced a low R-123 AEF and no change in the R-123 accumulation rate constant (Table 3.1 and 3.2), $MePEG_{17}$-*b*-PCL_{10} and $MePEG_{45}$-*b*-PCL_5, did not cause extensive hemolysis (Figure 4.11A and 4.13A). Similarly, the $MePEG_{45}$-*b*-$PDLLA_9$ diblock copolymer, which did not enhance R-123 accumulation (Figure 3.14A), had no measurable levels of hemolysis over the same concentration range (data not shown). These results indicate that MePEG-*b*-PCL diblock copolymers that enhanced the rate and extent of R-123 accumulation, also perturbed the membranes, while diblock copolymers with little or no enhancement of R-123 accumulation did not alter membrane integrity to the same extent.

To further demonstrate whether $MePEG_{17}$-*b*-PCL_5 diblock copolymer enhanced the membrane permeability of R-123, two colon adenocarcinoma cell lines, HT-29 and SW-620,

which have been shown to be negative for MDR1 mRNA, were evaluated for R-123 accumulation (Tomonaga *et al.*, 1996; Beaumont *et al.*, 1998). It was hypothesized that membrane perturbation by $MePEG_{17}$-*b*-PCL_5 should enhance R-123 accumulation in non-P-gp expressing cells, similar to that observed with caco-2 cells. As shown in Figure 4.14 A and B, R-123 accumulation with buffer was similar for both HT-29 and SW-620 and the presence of verapamil and CSA had no effect on R-123 accumulation. This confirmed that P-gp was either not expressed in these cells, or was non-functional. The fact that increasing concentration of $MePEG_{17}$-*b*-PCL_5 did not increase R-123 levels over controls for both cell lines (Figure 4.14 A and B), would indicate that $MePEG_{17}$-*b*-PCL_5 interactions with membranes did not result in a non-specific membrane permeablization effect. However, the dependence of cell type and membrane composition on surfactant induced membrane permeablization may account for these results. Investigations as far back as 1961 have demonstrated that surfactants can permeabilize or disrupt cell membranes to varying degrees depending on the cell line (Hodes *et al.*, 1961). Furthermore, membrane composition can influence the degree of permeability induced by surfactants. The inclusion of increasing concentrations of ceramide lipid into liposomes has been shown to reduce permeabilization by surfactants(Lopez *et al.*, 1999). Hence, the absence of an effect of diblock on membrane permeability and accumulation enhancement may have been due to the inability of the diblock to perturb the membranes of these particular cell lines, HT-29 and SW-620.

As discussed in Section 1.3.3 of Chapter 1, the membrane environment surrounding P-gp can greatly influence efflux activity. P-gp ATPase activity can be stimulated in a more rigid membrane environment (Rothnie *et al.*, 2001) or inhibited substantially by addition of membrane fluidizers (Regev *et al.*, 1999). The ability of surfactants to inhibit P-gp efflux has

been attributed to reduced P-gp ATPase activity through membrane fluidization effects. Regev *et al.* demonstrated that membrane fluidizers including ether, benzyl alchohol, and the surfactant polysorbate 20 completely abolished P-gp ATPase activity (Regev *et al.*, 1999). The amphiphilic triblock copolymer, Pluronic® P85, reduced basal and verapamil stimulated P-gp ATPase activity at concentrations that inhibited P-gp efflux of R-123 and induced an increase in membrane fluidity (Batrakova *et al.*, 2001). It is evident that the relationships between surfactant induced changes in membrane fluidity and P-gp inhibitory activity are still unclear. Using known membrane fluidizers, Sinicrope *et al.* showed a correlation between increased rat liver canalicular membrane vesicle fluidity with P-gp inhibition (Sinicrope *et al.*, 1992). However, Dudeja *et al.* demonstrated that Solutol HS15, polysorbate 40 and Cremophor EL® were capable of inhibiting P-gp activity in an MDR clone of a human epidermoid carcinoma cell line, KB 8-5-11, and this correlated with a decrease in the membrane fluidity (Dudeja *et al.*, 1995). Rege *et al.* showed differential membrane fluidity effects by three surfactants (Rege *et al.*, 2002). Polysorbate 80 and Cremophor EL® increased the fluidity of caco-2 cell membranes while Vitamin E TPGS rigidized caco-2 cell membranes, all at concentrations that reduced the BL to AP efflux of R-123 across caco-2 cells (Rege *et al.*, 2002). Additionally, Cremophor EL® and Tween 80® were found to inhibit P-gp activity in caco-2 cells but not in the MDR-MDCK cell line (Hugger *et al.*, 2002b). These authors found that differences in P-gp inhibition between the different cell types could not be explained by differences in membrane fluidity, since Cremophor EL® did not change membrane fluidity in either cell line while polysorbate 80 produced an increased membrane fluidity, but at different concentrations between the two cell lines (Hugger *et al.*, 2002b). Therefore, both increases and decrease in membrane

fluidity have been shown to influence P-gp efflux activity, but how they accomplish this remains poorly understood and may involve other mechanisms including P-gp ATPase inhibition. A P-gp ATPase assay was employed to determine whether $MePEG_{17}$-*b*-PCL_5 diblock influenced P-gp activity via P-gp ATPase inhibition. Using human P-gp reconstituted in membrane vesicles, increasing concentrations of $MePEG_{17}$-*b*-PCL_5 (0.001% to 0.25%) significantly stimulated the basal P-gp ATPase activity compared to buffer control group (Figure 4.15). The $MePEG_{17}$-*b*-PCL_5 concentrations of 0.01% and 0.25%, which enhanced R-6G and R-123 accumulation by caco-2 cells, respectively (Table 3.1), both stimulated ATPase activity approximately 3 fold over buffer control (Figure 4.15). Figure 4.16 A and B shows that R-6G and not R-123, significantly stimulated P-gp ATPase activity. For both R-123 and R-6G in the presence of $MePEG_{17}$-*b*-PCL_5 concentrations, a similar increased level of P-gp ATPase activity was found compared to diblock alone (Figures 4.15 and 4.16 A and B). This stimulation of ATPase activity by $MePEG_{17}$-*b*-PCL_5 diblock differs from the reported activity of other surfactants which decreased P-gp ATPase activity (Regev *et al.*, 1999; Batrakova *et al.*, 2001). The nonionic surfactant Triton X-100 has been shown to stimulate P-gp ATPase activity in isolated P-gp at low concentrations (Doige *et al.*, 1993; Sharom, 1997a). In contrast, Regev *et al.* found that Triton X-100 abolished P-gp ATPase activity and there was an associated increase in membrane fluidity (Regev *et al.*, 1999). Both groups used isolated and purified P-gp, but the lipid compositions used to reconstitute P-gp were different and it is possible that effect of membrane composition may be a significant factor contributing to the mechanism of P-gp ATPase inhibition by surfactants. These results indicate that $MePEG_{17}$-*b*-PCL_5 may have altered the assay membrane vesicle environment, increasing or decreasing membrane fluidity, and increased P-gp ATPase activity within the

model membrane system. It should also be noted that $MePEG_{17}$-*b*-PCL_5 might have interacted directly with P-gp, inducing ATPase activity. Hence, these data may not be appropriate to extrapolate to effects in caco-2 cell membranes.

4.5. CONCLUSION

The ability of $MePEG_{17}$-*b*-PCL_5 diblock to enhance the cellular accumulation of the P-gp substrates, R-123 and R-6G, may involve a combination of pathways depending on the hydrophobicity of the P-gp substrate. For the hydrophilic R-123, $MePEG_{17}$-*b*-PCL_5 enhanced the cellular accumulation of R-123 at high concentrations of diblock above the CMC, which did not appear to involve endocytosis of micellized R-123. This suggests that $MePEG_{17}$-*b*-PCL_5 micelles may provide a 'depot' for free unimer to interact with the cell membrane and contribute either to enhanced passive transmembrane diffusion of R-123 through membrane permeability changes, or inhibition of P-gp mediated efflux, or both. $MePEG_{17}$-*b*-PCL_5 greatly enhanced the cellular accumulation of R-123 in the directional flux studies in the absence of an increase in the AP to BL flux. It is proposed that the basolateral membrane permeability of R-123 may limit the AP→BL flux. In contrast, $MePEG_{17}$-*b*-PCL_5 was able to enhance the AP to BL flux of the hydrophobic R-6G. ATP depletion studies demonstrated that $MePEG_{17}$-*b*-PCL_5 increased the accumulation of R-123 possibly through a membrane permeabilization effect. Erythrocyte hemolysis studies also provided evidence that $MePEG_{17}$-*b*-PCL_5 caused membrane perturbation effects. These effects could result in enhanced transmembrane diffusion of R-123.

Chapter 5

SUMMARIZING DISCUSSION

There are a large number of drugs that are subject to efflux transport by P-gp and possess poor or variable oral absorption and bioavailability. Thus, the inhibition of efflux transport proteins in the gastrointestinal epithelium has become a very important issue in improving oral drug delivery. The group of triblock copolymers known as poloxamers or Pluronic® copolymers have been extensively investigated as inhibitors of P-gp mediated drug efflux and clinical studies are underway using Pluronic® micellar formulations of an anticancer drug to inhibit P-gp efflux and treat drug resistant tumors (Alakhov *et al.*, 1999)

Using the caco-2 cell line as an intestinal epithelial cell model and R-123 as a P-gp substrate, we obtained the first evidence demonstrating the ability of amphiphilic MePEG-*b*-PCL diblock copolymers to enhance the uptake of R-123 into caco-2 cells via pathways that involved the inhibition of P-gp mediated efflux transport. In order to explore the relationship between the structure of the MePEG-*b*-PCL diblock copolymers and their activity in terms of increasing cellular accumulation, a novel series of low molecular weight MePEG-*b*-PCL diblock copolymers were synthesized and characterized, as described in Chapter 2. With a MePEG molecular weight of 550, 750 or 2000 and PCL block lengths ranging from 2-10 repeat units, these diblock copolymers were considerably smaller than MePEG-*b*-PCL copolymers synthesized by other groups. As the degree of polymerization of PCL increased, CMC and HLB values decreased and partition coefficients and hydrodynamic diameters increased. Diblock copolymer micelles typically dissociate slowly into unimers when diluted below the CMC and show enhanced thermodynamic and kinetic stability (Allen *et al.*, 1999a). MePEG-*b*-PCL diblock copolymers with intermediate to high HLB values (HLB 9-

17) were found to be more effective at enhancing accumulation of R-123, similar to the findings of Batrakova and coworkers using Pluronic® copolymers. The diblock copolymer with optimal solubility characteristics in water and P-gp substrate accumulation enhancement activity was found to be $MePEG_{17}$-*b*-PCL_5.

The complex and unique relationship of P-gp with its membrane environment has hampered understanding of P-gp efflux activity, substrate specificity and the development of inhibitors. In accordance with the hydrophobic vacuum cleaner model for P-gp activity, the extent of substrate membrane partitioning and substrate transmembrane diffusion have been shown to be important determinants for P-gp efflux activity of a substrate. The use of non-ionic surfactants or amphiphiles as modulators of P-gp mediated efflux also requires consideration of the ability of these agents to perturb cell membranes and act as permeation enhancers for poorly permeable drugs (Swenson and Curatolo, 1992; Imanidis *et al.*, 1995; Aungst, 2000). For example, Yamazaki *et al.* demonstrated that polysorbate 80 enhanced the cellular accumulation of an epipodophyllotoxin derivative susceptible to P-gp mediated efflux, and this was attributed to an increased flux of drug and not to an inhibition of Pgp mediated efflux (Yamazaki *et al.*, 2000). Similarly, Pluronic® copolymers have been shown to enhance the diffusion of doxorubicin across model lipid bilayers (Erukova *et al.*, 2000). These investigations indicate that surfactant interactions with membranes leading to increased membrane permeability may play an important role in enhancing the transmembrane diffusion of a P-gp substrate and cell accumulation, independent of the inhibitory effects of these surfactants on P-gp.

In chapters 3 and 4 of the thesis, the effectiveness of MePEG-*b*-PCL diblock copolymers in modulating P-gp efflux of two substrates differing in hydrophobicity was

evaluated and studies were conducted in an attempt to more clearly understand the mechanism and pathway(s) involved for diblock mediated modulation of P-gp efflux. To evaluate the effects of the diblock copolymers on caco-2 cellular accumulation, two structurally homologous P-gp substrates were selected that differed in their hydrophobicity, the hydrophilic R-123 and the hydrophobic R-6G. MePEG-*b*-PCL diblock copolymers that enhanced R-123 accumulation required a high concentration approximately 6-100 fold higher than the CMC, whereas R-6G was enhanced at concentrations well below and up to the CMC. A similar effect was observed with two anticancer drugs that are well-established P-gp substrates, paclitaxel (hydrophobic) and doxorubicin (hydrophilic), where paclitaxel accumulation was enhanced at diblock concentrations below the CMC and doxorubicin was enhanced at concentrations above the CMC. The dramatic differences observed in the accumulation patterns for the two P-gp substrates in the presence of amphiphilic diblock copolymers were new and exciting findings, not previously reported and emphasized the importance of considering both the nature of the substrate and inhibitor in delineating the complex mechanisms of P-gp absorptive drug transport.

Xia and Onyuksel studied the permeabilization of cell membranes by surfactants and concluded that free surfactant unimers partitioned into membranes and accumulated to achieve a threshold concentration resulting in permeation enhancement (Xia and Onyuksel, 2000). They also suggested that micelles acted as a "depot" for free unimer. Our studies of the rate of accumulation of R-123 into caco-2 cells in the presence of diblock copolymers showed that there was a rapid influx rate of R-123 over 15 min and this was suggested to be due to membrane permeabilization causing increased R-123 transmembrane diffusion. In chapter 4, the directional flux studies permitted the elucidation of permeability coefficients

and examination of the pathways by which diblock copolymers enhanced substrate accumulation. Since P-gp transports substrate in the BL→AP direction, inhibition of P-gp should reduce the BL→AP directional flux and increase the AP→BL flux. For R-123, the diblock $MePEG_{17}$-*b*-PCL_5 and standard P-gp inhibitors were unable to increase the absorptive AP→BL flux, but inhibited secretory BL→AP flux. R-123 accumulation in caco-2 cells was assessed following the directional flux studies and showed a significantly larger R-123 accumulation after BL→AP experiments compared to AP→BL experiments in the presence of either verapamil or $MePEG_{17}$-*b*-PCL_5. It was hypothesized that the large R-123 accumulation following BL→AP flux with diblock on the apical membrane could be caused by rapid passage of R-123 across the BL membrane possibly due to an active transporter pumping R-123 into the cell, as proposed by Troutman and Thakker (Troutman and Thakker, 2003b). Since differences in the R-123 accumulation after AP→BL flux for diblock and verapamil could not be explained solely on the basis of inhibition of P-gp efflux, we proposed that there was a combination of mechanisms including both P-gp efflux inhibition and changes in R-123 membrane permeability caused by diblock interactions with the AP membrane. If the diblock caused an increase in R-123 membrane permeability leading to an increase in R-123 influx through the AP membrane, why this did not translate to an increase in AP→BL permeability coefficient is not clear, but may be related to the poor permeability of R-123 moving from the cell cytoplasm across the BL membrane. We speculated that the ability of diblock copolymers to enhance the cellular accumulation of R-123 at high concentrations well above the CMC of the diblock involved the following mechanism. Diblock copolymer micelles provided a depot of free unimers to partition into the caco-2 cell membrane and achieve a threshold concentration of unimers in the membrane. This resulted

in an enhanced passive transmembrane diffusion of R-123 through membrane permeability changes or inhibition of P-gp mediated efflux or both. At high diblock copolymer concentrations R-123 accumulation decreased and was suggested to be most likely due to substantial partitioning of R-123 into micelles reducing free R-123 concentrations available for cellular uptake. Cytotoxicity may further reduce R-123 accumulation at high diblock copolymer concentrations.

The markedly lower concentrations of diblock required to enhance R-6G accumulation compared to R-123 suggested that the diblock unimers partitioned into the caco-2 membrane and that the threshold concentration for modulation of P-gp activity could be attained at much lower diblock concentrations. Also in contrast to findings with R-123, rates of R-6G accumulation into caco-2 cells were not influenced by diblock or verapamil indicating that R-6G accumulation enhancement by diblock copolymers may not be associated with a membrane permeabilization effect, but rather may involve inhibition of efflux transporters, in particular P-gp. Directional flux studies for R-6G showed that diblock was capable of increasing the absorptive flux and decreasing the secretory flux. R-6G possessed a high partition coefficient and would have rapid transmembrane diffusion rate compared to R-123 and we believe that R-6G should reach a high concentration at the P-gp binding domain allowing for a more efficient P-gp efflux activity for R-6G compared to R-123.

In summary, diblock partitioning into the membrane may cause perturbation of the membrane and these changes in the lipid environment of the membrane lead to both inhibition of P-gp activity and increased membrane permeability due to increased passive transmembrane movement of the substrate. P-gp substrates differing in their structure,

hydrophobicity and amphiphilicity will possess different membrane partitioning and transmembrane diffusion and will therefore differ in the extent to which they are influenced by diblock induced changes in membrane lipid environment. The studies described in this thesis emphasize the importance of considering both the nature of the substrate and inhibitor in delineating the complex mechanisms of P-gp inhibition by surfactants. These results suggest that MePEG-*b*-PCL copolymers exhibit a biological response modifying effect, which could potentially be utilized to enhance the oral bioavailability of drugs subject to efflux transport by P-gp and possibly also to overcome multidrug resistance in cancer chemotherapy. The MePEG-*b*-PCL copolymers may be considered potentially suitable formulation excipients since the hydrophobic core-forming block of PCL is a biocompatible, biodegradable polyester and MePEG is a well-established additive in many drug delivery systems.

To further the development of MePEG-*b*-PCL diblock copolymers as oral bioavailability enhancers, the effect of diblock copolymers *in situ* and *in vivo* using everted rat gut experiments and pharmacokinetic studies will need to be considered. Additionally, to further understand the relationship between the nature of the P-gp substrate and the diblock requires the evaluation of a larger series of P-gp substrates differing in their chemical structure and relative hydrophobicity. To delineate the processes of membrane permeablization and P-gp efflux inhibition by MePEG-b-PCL and the contribution of these pathways with substrates of varying hydrophobicity will require the use of an additional cell line model. Although caco-2 is an acceptable model for P-gp studies and for evaluation of intestinal permeation enhancement, the lack of a non-P-gp expressing clone complicates these studies. Comparisons between different cells lines is difficult to interpret since

surfactant and substrate interactions may vary depending on cell types and membrane compositions. A cell line able to provide a P-gp overexpressing clone and a wild type/parental line would be ideal for delineating membrane permeabilization and P-gp inhibition effects by MePEG-b-PCL. Therefore, the extent and rate of accumulation enhancement of P-gp substrates in the wild type can be compared to the P-gp overexpressing clone to establish effects on membrane permeabilization. Additionally, membrane perturbation studies in these cell lines should be evaluated to determine the effect of MePEG-b-PCL on membrane fluidity (microviscosity).

REFERENCES

Adams, M.L., Lavasanifar, A., and Kwon, G.S. Amphiphilic block copolymers for drug delivery. Journal of Pharmaceutical Sciences. 92 (2003) 1343-1355.

Adibi, S.A. The oligopeptide transporter (Pept-1) in human intestine: biology and function. Gastroenterology. 113 (1997) 332-340.

Alakhov, V.Y., Moskaleva, E.Y., Batrakova, E.V., and Kabanov, A.V. Hypersensitization of multidrug resistant human ovarian carcinoma cells by pluronic P85 block copolymer. Bioconjugate Chemistry. 7 (1996) 209-216.

Alakhov, V., Klinski, E., Li, S., Pietrzynski, G., Venne, A., Batrakova, E., Bronitch, T., and Kabanov, A. Block copolymer-based formulation of doxorubicin. From cell screen to clinical trials. Colloids and Surfaces, B: Biointerfaces. 16 (1999) 113-134.

Alexandridis, P., Athanassiou, V., Fukuda, S., and Hatton, T.A. Surface activity of poly(ethylene oxide)-block-poly(propylene oxide)-block-poly(ethylene oxide) copolymers. Langmuir. 10 (1994a) 2604-2612.

Alexandridis, P., Holzwarth, J.F., and Hatton, T.A. Micellization of poly(ethylene oxide)-poly(propylene oxide)-poly(ethylene oxide) triblock copolymers in aqueous solutions: Thermodynamics of copolymer association. Macromolecules. 27 (1994b) 2414-2425.

Allen, C., Han, J., Yu, Y., Maysinger, D., and Eisenberg, A. Polycaprolactone-b-poly(ethylene oxide) copolymer micelles as a delivery vehicle for dihydrotestosterone. Journal of Controlled Release. 63 (2000) 275-286.

Allen, C., Maysinger, D., and Eisenberg, A. Nano-engineering block copolymer aggregates for drug delivery. Colloids and Surfaces B: Biointerfaces. 16 (1999a) 3-27.

Allen, C., Yu, Y., Eisenberg, A., and Maysinger, D. Cellular internalization of PCL(20)-b-PEO(44) block copolymer micelles. Biochimica et Biophysica Acta. 1421 (1999b) 32-38.

Allen, C., Yu, Y., Maysinger, D., and Eisenberg, A. Polycaprolactone-b-poly(ethylene oxide) block copolymer micelles as a novel drug delivery vehicle for neurotrophic agents FK506 and L-685,818. Bioconjugate Chemistry. 9 (1998) 564-572.

Altenberg, G.A., Vanoye, C.G., Horton, J.K., and Reuss, L. Unidirectional fluxes of rhodamine 123 in multidrug-resistant cells: evidence against direct drug extrusion from the plasma membrane. Proceedings of the National Academy of Sciences of the United States of America. 91 (1994) 4654-4657.

Anderberg, E.K. and Artursson, P. Epithelial transport of drugs in cell culture. VIII: Effects of sodium dodecyl sulfate on cell membrane and tight junction permeability in human intestinal epithelial (Caco-2) cells. Journal of Pharmaceutical Sciences. 82 (1993) 392-398.

Anderberg, E.K., Nyström, C., and Artursson, P. Epithelial transport of drugs in cell culture. VII: Effects of pharmaceutical surfactant excipients and bile acids on transepithelial permeability in monolayers of human intestinal epithelial (Caco-2) cells. Journal of Pharmaceutical Sciences. 81 (1992) 879-887.

Andreoli, T.E., Hoffman, J.F., Fanestil, D.D., Schultz, S.G., and Editors. Membrane Physiology. 2nd ed. Plenum Medical Book Company, (1989) pp. 396 pp.

Arimori, K. and Nakano, M. Drug exsorption from blood into the gastrointestinal tract. Pharmaceutical Research. 15 (1998) 371-376.

Arnal, M.L., Balsamo, V., Lopez-Carrasquero, F., Contreras, J., Carrillo, M., Schmalz, H., Abetz, V., Laredo, E., and Mueller, A.J. Synthesis and characterization of polystyrene-b-poly(ethylene oxide)-b-poly(epsilon-caprolactone) block copolymers. Macromolecules. 34 (2001) 7973-7982.

Artursson, P., Palm, K., and Luthman, K. Caco-2 monolayers in experimental and theoretical predictions of drug transport. Advanced Drug Delivery Reviews. 46 (2001) 27-43.

Asaumi, J., Kawasaki, S., Kuroda, M., Takeda, Y., Kishi, K., and Hiraki, Y. Influence of metabolic inhibitors on the intracellular accumulation and retention of adriamycin. Anticancer Research. 19 (1999) 615-618.

Astafieva, I., Zhong, X.F., and Eisenberg, A. Critical micellization phenomena in block polyelectrolyte solutions. Macromolecules. 26 (1993) 7339-7352.

Aungst, B.J. P-glycoprotein, secretory transport, and other barriers to the oral delivery of anti-HIV drugs. Advanced Drug Delivery Reviews. 39 (1999) 105-116.

Aungst, B.J. Intestinal permeation enhancers. Journal of Pharmaceutical Sciences. 89 (2000) 429-442.

Avdeef, A. Absorption and drug development: Solubility, permeability, and charge state. John Wiley and Sons, New Jersey (2003) pp. 287.

Ayesh, S., Shao, Y.M., and Stein, W.D. Co-operative, competitive and non-competitive interactions between modulators of P-glycoprotein. Biochimica et Biophysica Acta. 1316 (1996) 8-18.

Ayrton, A. and Morgan, P. Role of transport proteins in drug absorption, distribution, and excretion. Xenobiotica. 31 (2001) 469-497.

Bailey, C.A., Bryla, P., and Malick, A.W. The use of the intestinal epithelial cell culture model, Caco-2, in pharmaceutical development. Advanced Drug Delivery Reviews. 22 (1996) 85-103.

Balasubramanian, S.V. and Straubinger, R.M. Taxol-lipid interactions: Taxol-dependent effects on the physical properties of model membranes. Biochemistry. 33 (1994) 8941-

8947.

Bardelmeijer, H.A., Ouwehand, M., Malingre, M.M., Schellens, J.H.M., Beijnen, J.H., and van Tellingen, O. Entrapment by Cremophor EL decreases the absorption of paclitaxel from the gut. Cancer Chemotherapy and Pharmacology. 49 (2002) 119-125.

Barnes, K.M., Dickstein, B., Cutler, G.B.J., Fojo, T., and Bates, S.E. Steroid treatment, accumulation, and antagonism of P-glycoprotein in multidrug-resistant cells. Biochemistry. 35 (1996) 4820-4827.

Barrand, M.A., Bagrij, T., and Neo, S.Y. Multidrug resistance-associated protein: a protein distinct from P-glycoprotein involved in cytotoxic drug expulsion. General Pharmacology. 28 (1997) 639-645.

Batrakova, E., Lee, S., Li, S., Venne, A., Alakhov, V., and Kabanov, A. Fundamental relationships between the composition of pluronic block copolymers and their hypersensitization effect in MDR cancer cells. Pharmaceutical Research. 16 (1999) 1373-1379.

Batrakova, E.V., Han, H.Y., Alakhov, V.Y.u., Miller, D.W., and Kabanov, A.V. Effects of pluronic block copolymers on drug absorption in Caco-2 cell monolayers. Pharmaceutical Research. 15 (1998a) 850-855.

Batrakova, E.V., Han, H.Y., Miller, D.W., and Kabanov, A.V. Effects of pluronic P85 unimers and micelles on drug permeability in polarized BBMEC and Caco-2 cells. Pharmaceutical Research. 15 (1998b) 1525-1532.

Batrakova, E.V., Li, S., Elmquist, W.F., Miller, D.W., Alakhov, V.Y., and Kabanov, A.V. Mechanism of sensitization of MDR cancer cells by Pluronic block copolymers: Selective energy depletion. British Journal of Cancer. 85 (2001) 1987-1997.

Batrakova, E.V., Li, S., Miller, D.W., and Kabanov, A.V. Pluronic P85 increases permeability of a broad spectrum of drugs in polarized BBMEC and Caco-2 cell monolayers. Pharmaceutical Research. 16 (1999) 1366-1372.

Batrakova, E.V., Li, S., Vinogradov, S.V., Alakhov, V.Y., Miller, D.W., and Kabanov, A.V. Mechanism of pluronic effect on P-glycoprotein efflux system in blood-brain barrier: contributions of energy depletion and membrane fluidization. Journal of Pharmacology and Experimental Therapeutics. 299 (2001) 483-493.

Batrakova, E.V., Li, S., Alakhov, V.Y., Miller, D.W., and Kabanov, A.V. Optimal structure requirements for pluronic block copolymers in modifying P-glycoprotein drug efflux transporter activity in bovine brain microvessel endothelial cells. Journal of Pharmacology and Experimental Therapeutics. 304 (2003) 845-854.

Beaumont, P.O., Moore, M.J., Ahmad, K., Payne, M.M., Lee, C., and Riddick, D.S. Role of glutathione S-transferases in the resistance of human colon cancer cell lines to doxorubicin. Cancer Research. 58 (1998) 947-955.

Benahmed, A., Ranger, M., and Leroux, J.C. Novel polymeric micelles based on the amphiphilic diblock copolymer poly(N-vinyl-2-pyrrolidone)-block-poly(D,L-lactide). Pharmaceutical Research. 18 (2001) 323-328.

Benet, L.Z. and Cummins, C.L. The drug efflux-metabolism alliance: Biochemical aspects. Advanced Drug Delivery Reviews. 50 (2001) S3-S11.

Bogdanov, B., Vidts, A., Van Deb Bulke, A., Verbeeck, R., and Schacht, E. Synthesis and thermal properties of poly(ethylene glycol)-poly(epsilon-caprolactone) copolymers. Polymer. 39 (1998) 1631-1636.

Bogman, K., Erne-Brand, F., Alsenz, J., and Drewe, J. The role of surfactants in the reversal of active transport mediated by multidrug resistance proteins. Journal of Pharmaceutical Sciences. 92 (2003) 1250-1261.

Bonina, F., Lanza, M., Montenegro, L., Salerno, L., Smeriglio, P., Trombetta, D., and Saija, A. Transport of alpha-tocopherol and its derivatives through erythrocyte membranes. Pharmaceutical Research. 13 (1996) 1343-1347.

Borst, P., Evers, R., Kool, M., and Wijnholds, J. The multidrug resistance protein family. Biochimica et Biophysica Acta. 1461 (1999) 347-357.

Brodin, B., Nielsen, C.U., Steffansen, B., and Frokjaer, S. Transport of peptidomimetic drugs by the intestinal di/tri-peptide transporter, PepT1. Pharmacology & Toxicology. 90 (2002) 285-296.

Buckingham, L.E., Balasubramanian, M., Safa, A.R., Shah, H., Komarov, P., Emanuele, R.M., and Coon, J.S. Reversal of multi-drug resistance in vitro by fatty acid-PEG-fatty acid diesters. International Journal of Cancer. 65 (1996) 74-79.

Burt, H.M., Zhang, X., Toleikis, P., Embree, L., and Hunter, W.L. Development of copolymers of poly(d,l-lactide) and methoxypolyethylene glycol as micellar carriers of paclitaxel. Colloids and Surfaces B: Biointerfaces. 16 (1999) 161-171.

Camenisch, G., Folkers, G., and van de Waterbeemd, H. Review of theoretical passive drug absorption models: historical background, recent developments and limitations. Pharmaceutica Acta Helvetiae. 71 (1996) 309-327.

Cerrai, P., Tricoli, M., Andruzzi, F., Paci, M., and Paci, M. Polyether-polyester block copolymers by noncatalyzed polymerization of epsilon-caprolactone with polyethylene glycol. Polymer. 30 (1989) 338-343.

Chan, L.M.S., Lowes, S., and Hirst, B.H. The ABCs of drug transport in intestine and liver: efflux proteins limiting drug absorption and bioavailability. European Journal of Pharmaceutical Sciences. 21 (2004) 25-51.

Chiou, W.L. Effect of 'unstirred' water layer in the intestine on the rate and extent of absorption after oral administration. Biopharmaceutics and Drug Disposition. 15 (1994)

709-717.

Chiu, Y., Higaki, K., Neudeck, B.L., Barnett, J.L., Welage, L.S., and Amidon, G.L. Human jejunal permeability of cyclosporin A: influence of surfactants on P-glycoprotein efflux in Caco-2 cells. Pharmaceutical Research. 20 (2003) 749-756.

Cho, M.J., Adson, A., and Kezdy, F.J. Transepithelial transport of aliphatic carboxylic acids studied in Madin Darby canine kidney (MDCK) cell monolayers. Pharmaceutical Research. 7 (1990) 325-331.

Cole, S.P.C., Bhardwaj, G., Gerlach, J.H., Mackie, J.E., Grant, C.E., Almquist, K.C., Stewart, A.J., Kurz, E.U., Duncan, A.M.V., and Deeley, R.G. Overexpression of a transporter gene in a multidrug-resistant human lung cancer cell line. Science. 258 (1992) 1650-1654.

Coon, J.S., Knudson, W., Clodfelter, K., Lu, B., and Weinstein, R.S. Solutol HS 15, nontoxic polyoxyethylene esters of 12-hydroxystearic acid, reverses multidrug resistance. Cancer Research. 51 (1991) 897-902.

Cordon-Cardo, C., OBrien, J.P., Boccia, J., Casals, D., Bertino, J.R., and Melamed, M.R. Expression of the multidrug resistance gene product (P- glycoprotein) in human normal and tumor tissues. Journal of Histochemistry and Cytochemistry. 38 (1990) 1277-1287.

Cordon-Cardo, C., O'Brien, J.P., Casals, D., Rittman-Grauer, L., Biedler, J.L., Melamed, M.R., and Bertino, J.R. Multidrug-resistance gene (P-glycoprotein) is expressed by endothelial cells at blood-brain barrier sites. Proceedings of the National Academy of Sciences of the United States of America. 86 (1989) 695-698.

Cullis, P.R. and Hope, M.J. Physical properties and functional roles of lipids in membranes. New Comprehensive Biochemistry. 20 (1991) 1-41.

Cummins, C.L., Jacobsen, W., and Benet, L.Z. Unmasking the dynamic interplay between intestinal P-glycoprotein and CYP3A4. Journal of Pharmacology and Experimental Therapeutics. 300 (2002) 1036-1045.

Daleke, D.L. Regulation of transbilayer plasma membrane phospholipid asymmetry. Journal of Lipid Research. 44 (2003) 233-242.

Dantzig, A.H. Oral absorption of B-lactams by intestinal peptide transport proteins. Advanced Drug Delivery Reviews. 23 (1997) 63-76.

Daugherty, A.L. and Mrsny, R.J. Regulation of the intestinal epithelial paracellular barrier. Pharmaceutical Science and Technology Today. 2 (1999a) 281-287.

Daugherty, A.L. and Mrsny, R.J. Transcellular uptake mechanisms of the intestinal epithelial barrier Part one. Pharmaceutical Science and Technology Today. 2 (1999b) 144-151.

Dintaman, J.M. and Silverman, J.A. Inhibition of P-glycoprotein by D-alpha-tocopheryl

polyethylene glycol 1000 succinate (TPGS). Pharmaceutical Research. 16 (1999) 1550-1556.

Doige, C.A., Yu, X., and Sharom, F.J. The effects of lipids and detergents on ATPase-active P-glycoprotein. Biochimica et Biophysica Acta. 1146 (1993) 65-72.

Drescher, S., Glaeser, H., Murdter, T., Hitzl, M., Eichelbaum, M., and Fromm, M.F. P-glycoprotein-mediated intestinal and biliary digoxin transport in humans. Clinical Pharmacology and Therapeutics. 73 (2003) 223-231.

Drori, S., Eytan, G.D., and Assaraf, Y.G. Potentiation of anticancer-drug cytotoxicity by multidrug-resistance chemosensitizers involves alterations in membrane fluidity leading to increased membrane permeability. European Journal of Biochemistry. 228 (1995) 1020-1029.

Dubois, Ph., Ropson, N., Jerome, R., and Teyssie, P. Macromolecular engineering of polylactones and polylactides. 19. Kinetics of ring-opening polymerization of epsilon-caprolactone initiated with functional aluminum alkoxides. Macromolecules. 29 (1996) 1965-1975.

Dudeja, P.K., Anderson, K.M., Harris, J.S., Buckingham, L., and Coon, J.S. Reversal of multidrug resistance phenotype by surfactants: relationship to membrane lipid fluidity. Archives of Biochemistry and Biophysics. 319 (1995) 309-315.

Endo, M., Yamamoto, T., and Ijuin, T. Effect of nonionic surfactants on the percutaneous absorption of tenoxicam. Chemical and Pharmaceutical Bulletin. 44 (1996) 865-867.

Erukova, V.Yu., Krylova, O.O., Antonenko, Y.N., and Melik-Nubarov, N.S. Effect of ethylene oxide and propylene oxide block copolymers on the permeability of bilayer lipid membranes to small solutes including doxorubicin. Biochimica et Biophysica Acta. 1468 (2000) 73-86.

Eytan, G.D., Regev, R., Oren, G., and Assaraf, Y.G. The role of passive transbilayer drug movement in multidrug resistance and its modulation. Journal of Biological Chemistry. 271 (1996) 12897-12902.

Eytan, G.D., Regev, R., Oren, G., Hurwitz, C.D., and Assaraf, Y.G. Efficiency of P-glycoprotein-mediated exclusion of rhodamine dyes from multidrug-resistant cells is determined by their passive transmembrane movement rate. European Journal of Biochemistry. 248 (1997) 104-112.

Fagerholm, U., Lindahl, A., and Lennernas, H. Regional intestinal permeability in rats of compounds with different physicochemical properties and transport mechanisms. Journal of Pharmacy and Pharmacology. 49 (1997) 687-690.

Floren, L.C., Bekersky, I., Benet, L.Z., Mekki, Q., Dressler, D., Lee, J.W., Roberts, J.P., and Hebert, M.F. Tacrolimus oral bioavailability doubles with coadministration of ketoconazole. Clinical Pharmacology and Therapeutics. 62 (1997) 41-49.

Florence, A.T. and Attwood, D. Physicochemical Principles of Pharmacy. 2nd ed. Chapman and Hall, New York (1988) pp. 485.

Ford, J.M. and Hait, W.N. Pharmacology of drugs that alter multidrug resistance in cancer. Pharmacological Reviews. 42 (1990) 155-199.

Gan, Z., Jim, T.F., Li, M., Yuer, Z., Wang, S., and Wu, C. Enzymatic biodegradation of poly(ethylene oxide-b-epsilon-caprolactone) diblock copolymer and its potential biomedical applications. Macromolecules. 32 (1999) 590-594.

Gao, Z. and Eisenberg, A. A model of micellization for block copolymers in solutions. Macromolecules. 26 (1993) 7353-7360.

Garrigues, A., Escargueil, A.E., and Orlowski, S. The multidrug transporter, P-glycoprotein, actively mediates cholesterol redistribution in the cell membrane. Proceedings of the National Academy of Sciences of the United States of America. 99 (2002) 10347-10352.

Ghetie, M., Marches, R., Kufert, S., and Vitetta, E.S. An anti-CD19 antibody inibits the interaction between P-glycoprotein (P-gp) and CD19, causes P-gp to translocate out of lipid rafts, and chemosensitizes a multidrug-resistant (MDR) lymphoma cell line. Blood. 104 (2004) 178-183.

Giocondi, M.C., Mamdouh, Z., and Le Grimellec, C. Benzyl alcohol differently affects fluid phase endocytosis and exocytosis in renal epithelial cells. Biochimica et Biophysica Acta. 1234 (1995) 197-202.

Goldstein, D.B. The effects of drugs on membrane fluidity. Annual Review of Pharmacology and Toxicology. 24 (1984) 43-64.

Gollapudi, S., Kim, C.H., Tran, B.N., Sangha, S., and Gupta, S. Probenecid reverses multidrug resistance in multidrug resistance-associated protein-overexpressing HL60/AR and H69/AR cells but not in P-glycoprotein-overexpressing HL60/Tax and P388/ADR cells. Cancer Chemotherapy and Pharmacology. 40 (1997) 150-158.

Gottesman, M.M. and Pastan, I. Biochemistry of multidrug resistance mediated by the multidrug transporter. Annual Review of Biochemistry. 62 (1993) 385-427.

Griffin, W.C. Calculation of HLB values of non-ionic surfactants. Journal of the Society of Cosmetic Chemists. (1954) 249-256.

Grundy, J.S., Eliot, L.A., and Foster, R.T. Extrahepatic first-pass metabolism of nifedipine in the rat. Biopharmaceutics and Drug Disposition. 18 (1997) 509-522.

Gutmann, H., Fricker, G., Török, M., Michael, S., Beglinger, C., and Drewe, J. Evidence for different ABC-transporters in Caco-2 cells modulating drug uptake. Pharmaceutical Research. 16 (1999) 402-407.

Halmos, T., Santarromana, M., Antonakis, K., and Scherman, D. Synthesis of glucose-

chlorambucil derivatives and their recognition by the human GLUT1 glucose transporter. European Journal of Pharmacology. 318 (1996) 477-484.

Halperin, A. Polymeric micelles: a star model. Macromolecules. 20 (1987) 2943-2946.

Haseto, S., Ouchi, H., Isoda, T., Mizuma, T., Hayashi, M., and Awazu, S. Transport of low and high molecular peptides across rabbit Peyer's patches. Pharmaceutical Research. 11 (1994) 361-364.

Helenius, A. and Simons, K. Solubilization of membranes by detergents. Biochimica et Biophysica Acta. 415 (1975) 29-79.

Hidalgo, I.J., Bhatnagar, P., Lee, C.P., Miller, J., Cucullino, G., and Smith, P.L. Structural requirements for interaction with the oligopeptide transporter in Caco-2 cells. Pharmaceutical Research. 12 (1995) 317-319.

Hidalgo, I.J. and Jibin, L. Carrier-mediated transport and efflux mechanisms in Caco-2 cells. Advanced Drug Delivery Reviews. 22 (1996) 53-66.

Hidalgo, I.J., Raub, T.J., and Borchardt, R.T. Characterization of the human colon carcinoma cell line (Caco-2) as a model system for intestinal epithelial permeability. Gastroenterology. 96 (1989) 736-749.

Higgins, C.F. ABC transporters: from microorganisms to man. Annual Review of Cell Biology. 8 (1992) 67-113.

Higgins, C.F. and Gottesman, M.M. Is the multidrug transporter a flippase? Trends in Biochemical Sciences. 17 (1992) 18-21.

Hirohashi, T., Suzuki, H., Chu, X.-Y., Tamai, I., Tsuji, A., and Sugiyama, Y. Function and expression of multidrug resistance-associated protein family in human colon adenocarcinoma cells (Caco-2). Journal of Pharmacology and Experimental Therapeutics. 292 (2000) 265-270.

Ho, N.F.H., Raub, T.J., Burton, P.S., Barsuhn, C.L., Adson, A., Audus, K.L., and Borchardt, R.T. Quantitative approaches to delineate passive transport mechanisms in cell culture monolayers. Drugs and the Pharmaceutical Sciences: Transport Processes in Pharmaceutical Systems. 102 (2000) 219-316.

Hochman, J.H., Chiba, M., Nishime, J., Yamazaki, M., and Lin, J.H. Influence of P-glycoprotein on the transport and metabolism of indinavir in caco-2 cells expressing cytochrome P-450 3A4. Journal of Pharmacology and Experimental Therapeutics. 292 (2000) 310-318.

Hodes, M.E., Palmer, C.G., and Livengood, D. Action of synthetic surfactants on membranes of tumor cells. II. Titration experiments. Experimental Cell Research. 24 (1961) 298-310.

Homolya, L., Hollo, Z., Germann, U.A., Pastan, I., Gottesman, M.M., and Sarkadi, B.

Fluorescent cellular indicators are extruded by the multidrug resistance protein. Journal of Biological Chemistry. 268 (1993) 21493-21496.

Hosoya, K.I., Kim, K.J., and Lee, V.H. Age-dependent expression of P-glycoprotein gp170 in Caco-2 cell monolayers. Pharmaceutical Research. 13 (1996) 885-890.

Hugger, E.D., Audus, K.L., and Borchardt, R.T. Effects of poly(ethylene glycol) on efflux transporter activity in Caco-2 cell monolayers. Journal of Pharmaceutical Sciences. 91 (2002a) 1980-1990.

Hugger, E.D., Novak, B.L., Burton, P.S., Audus, K.L., and Borchardt, R.T. A comparison of commonly used polyethoxylated pharmaceutical excipients on their ability to inhibit P-glycoprotein activity in vitro. Journal of Pharmaceutical Sciences. 91 (2002b) 1991-2002.

Hunter, J. and Hirst, B.H. Intestinal secretion of drugs. The role of P-glycoprotein and related drug efflux systems in limiting oral drug absorption. Advanced Drug Delivery Reviews. 25 (1997) 129-157.

Hunter, J., Hirst, B.H., and Simmons, N.L. Epithelial secretion of vinblastine by human intestinal adenocarcinoma cell (HCT-8 and T84) layers expressing P-glycoprotein. British Journal of Cancer. 64 (1991a) 437-444.

Hunter, J., Hirst, B.H., and Simmons, N.L. Transepithelial vinblastine secretion mediated by P-glycoprotein is inhibited by forskolin derivatives. Biochemical and Biophysical Research Communications. 181 (1991b) 671-676.

Hunter, J., Hirst, B.H., and Simmons, N.L. Drug absorption limited by P-glycoprotein-mediated secretory drug transport in human intestinal epithelial Caco-2 cell layers. Pharmaceutical Research. 10 (1993a) 743-749.

Hunter, J., Jepson, M.A., Tsuruo, T., Simmons, N.L., and Hirst, B.H. Functional expression of P-glycoprotein in apical membranes of human intestinal Caco-2 cells. Kinetics of vinblastine secretion and interaction with modulators. Journal of Biological Chemistry. 268 (1993b) 14991-14997.

Hyde, R.J., Cass, C.E., Young, J.D., and Baldwin, S.A. The ENT family of eukaryote nucleoside and nucleobase transporters: recent advances in the investigation of structure/function relationships and the identification of novel isoforms. Molecular Membrane Biology. 18 (2001) 53-63.

Imanidis, G., Hartner, K.C., and Mazer, N.A. Intestinal permeation and metabolism of a model peptide (leuprolide) and mechanisms of permeation enhancement by non-ionic surfactants. International Journal of Pharmaceutics. 120 (1995) 41-50.

Inui, K., Yamamoto, M., and Saito, H. Transepithelial transport of oral cephalosporins by monolayers of intestinal epithelial cell line Caco-2: specific transport systems in apical and basolateral membranes. Journal of Pharmacology and Experimental Therapeutics. 261 (1992) 195-201.

Isoda, T., Watanabe, E., Haga, M., Haseto, S., Awazu, S., and Hayashi, M. Increase of polypeptide transport by lectin conjugation across rabbit Peyer's patches. European Journal of Pharmaceutics and Biopharmaceutics. 44 (1997) 133-136.

Jackson, J.K., Winternitz, C.I., and Burt, H.M. Mechanism of hemolysis of human erythrocytes exposed to monosodium urate monohydrate crystals. Preliminary characterization of membrane pores. Biochimica et Biophysica Acta. 1281 (1996) 45-52.

Jedlitschky, G., Leier, I., Buchholz, U., Barnouin, K., Kurz, G., and Keppler, D. Transport of glutathione, glucuronate, and sulfate conjugates by the MRP gene-encoded conjugate export pump. Cancer Research. 56 (1996) 988-994.

Jedrzejczak, M., Koceva-Chyla, A., Gwozdzinski, K., and Jozwiak, Z. Changes in plasma membrane fluidity of immortal rodent cells induced by anticancer drugs doxorubicin, aclarubicin, and mitoxantrone. Cell Biology International. 23 (1999) 497-506.

Jenkins, P.G., Howard, K.A., Blackhall, N.W., Thomas, N.W., Davis, S.S., and O'Hagan, D.T. Microparticulate absorption from the rat intestine. Journal of Controlled Release. 29 (1994) 339-350.

Jones, M. and Leroux, J. Polymeric micelles - a new generation of colloidal drug carriers. European Journal of Pharmaceutics and Biopharmaceutics. 48 (1999) 101-111.

Jones, M.N. Surfactants in membrane solubilisation. International Journal of Pharmaceutics. 177 (1999) 137-159.

Juliano, R.L. and Ling, V. A surface glycoprotein modulating drug permeability in Chinese hamster ovary cell mutants. Biochimica et Biophysica Acta. 455 (1976) 152-162.

Kabanov, A.V., Batrakova, E.V., Melik-Nubarov, N.S., Fedoseev, N.A., Dorodnich, T.U., Alakhov, V.Y., Chekhonin, V.P., Nazarova, I.R., and Kabanov, V.A. A new class of drug carriers: micelles of poly(oxyethylene)-poly(oxypropylene) block copolymers as microcontainers for drug targeting from blood in brain. Journal of Controlled Release. 22 (1992) 141-158.

Kabanov, A.V., Chekhonin, V.P., Alakhov, V.Y.u., Batrakova, E.V., Lebedev, A.S., Melik-Nubarov, N.S., Arzhakov, S.A., Levashov, A.V., Morozov, G.V., Severin, E.S., and et, a.l. The neuroleptic activity of haloperidol increases after its solubilization in surfactant micelles. Micelles as microcontainers for drug targeting. FEBS Letters. 258 (1989) 343-345.

Kabanov, A.V., Nazarova, I.R., Astafieva, I.V., Batrakova, E.V., Alakhov, V.Y., Yaroslavov, A.A., and Kabanov, V.A. Micelle formation and solubilization of fluorescent probes in Poly(oxyethylene-*b*-oxypropylene-*b*-oxyethylene) solutions. Macromolecules. 28 (1995) 2303-2314.

Kabanov, A.V., Batrakova, E.V., and Alakhov, V.Y. Pluronic block copolymers as novel polymer therapeutics for drug and gene delivery. Journal of Controlled Release. 82

(2002a) 189-212.

Kabanov, A.V., Batrakova, E.V., and Alakhov, V.Y. Pluronic block copolymers for overcoming drug resistance in cancer. Advanced Drug Delivery Reviews. 54 (2002b) 759-779.

Kabanov, A.V., Batrakova, E.V., Li, S., and Alakhov, V.Y. Selective energy depletion and sensitization of multiple drug-resistant cancer cells by Pluronic block copolymer. Macromolecular Symposia. 172 (2001) 103-112.

Kabanov, A.V., Batrakova, E.V., and Miller, D.W. Pluronic block copolymers as modulators of drug efflux transporter activity in the blood-brain barrier. Advanced Drug Delivery Reviews. 55 (2003) 151-164.

Kakizawa, Y. and Kataoka, K. Block copolymer micelles for delivery of gene and related compounds. Advanced Drug Delivery Reviews. 54 (2002) 203-222.

Kataoka, K., Matsumoto, T., Yokoyama, M., Okano, T., Sakurai, Y., Fukushima, S., Okamoto, K., and Kwon, G.S. Doxorubicin-loaded poly(ethylene glycol)-poly(beta-benzyl-L-aspartate) copolymer micelles: their pharmaceutical characteristics and biological significance. Journal of Controlled Release. 64 (2000) 143-153.

Katayose, S. and Kataoka, K. Remarkable increase in nuclease resistance of plasmid DNA through supramolecular assembly with poly(ethylene glycol)-poly(L-lysine) block copolymer. Journal of Pharmaceutical Sciences. 87 (1998) 160-163.

Keller, R.P., Altermatt, H.J., Donatsch, P., Zihlmann, H., Laissue, J.A., and Hiestand, P.C. Pharmacologic interactions between the resistance-modifying cyclosporine SDZ PSC 833 and etoposide (VP 16-213) enhance in vivo cytostatic activity and toxicity. International Journal of Cancer. 51 (1992) 433-438.

Kim, C., Lee, S.C., Shin, J.H., Yoon, J.-S., Kwon, I.C., and Jeong, S.Y. Amphiphilic diblock copolymers based on poly(2-ethyl-2-oxazoline) and poly(1,3-trimethylene carbonate): Synthesis and micellar characteristics. Macromolecules. 33 (2000) 7448-7452.

Kim, R.B., Fromm, M.F., Wandel, C., Leake, B., Wood, A.J.J., Roden, D.M., and Wilkinson, G.R. The drug transporter P-glycoprotein limits oral absorption and brain entry of HIV-1 protease inhibitors. Journal of Clinical Investigation. 101 (1998) 289-294.

Kim, S.C., Kim, D.W., Shim, Y.H., Bang, J.S., Oh, H.S., Kim, S.W., and Seo, M.H. In vivo evaluation of polymeric micellar paclitaxel formulation: toxicity and efficacy. Journal of Controlled Release. 72 (2001) 191-202.

Kim, S.Y. and Lee, Y.M. Taxol-loaded block copolymer nanospheres composed of methoxy poly(ethylene glycol) and poly(epsilon-caprolactone) as novel anticancer drug carriers. Biomaterials. 22 (2001) 1697-1704.

Kim, S.Y., Lee, Y.M., Shin, H.J., and Kang, J.S. Indomethacin-loaded methoxypoly(ethylene

glycol)/poly(caprolactone) diblock copolymer nanosphere: pharmacokinetic characteristics of indomethacin in the normal Sprague-Dawley rats. Biomaterials. 22 (2001) 2049-2056.

Kim, S.Y., Shin, I.G., and Lee, Y.M. Amphiphilic diblock copolymeric nanospheres composed of methoxy poly(ethylene glycol) and glycolide: properties, cytotoxicity and drug release behaviour. Biomaterials. 20 (1999) 1033-1042.

Kim, S.Y., Shin, I.G., Lee, Y.M., Cho, C.S., and Sung, Y.K. Methoxy poly(ethylene glycol) and epsilon-caprolactone amphiphilic block copolymeric micelle containing indomethacin. II. Micelle formation and drug release behaviours. Journal of Controlled Release. 51 (1998) 13-22.

Klein, I., Sarkadi, B., and Varadi, A. An inventory of the human ABC proteins. Biochimica et Biophysica Acta. 1461 (1999) 237-262.

Kowalski, A., Duda, A., and Penczek, S. Kinetics and mechanism of cyclic esters polymerization initiated with tin(II) octoate. 3. Polymerization of L,L-dilactide. Macromolecules. 33 (2000) 7359-7370.

Kozlov, M., Melik-Nubarov, N.S., Batrakova, E.V., and Kabanov, A.V. Relationship between pluronic block copolymer structure, critical micellization concentration and partitioning coefficients of low molecular mass solutes. Macromolecules. 33 (2000) 3305-3313.

Kricheldorf, H.R., Kreiser-Saunders, I., and Stricker, A. Polylactones 48. SnOct2-Initiated Polymerizations of Lactide: A Mechanistic Study. Macromolecules. 33 (2000) 702-709.

Krishna, R. and Mayer, L.D. Multidrug resistance (MDR) in cancer. Mechanisms, reversal using modulators of MDR and the role of MDR modulators in influencing the pharmacokinetics of anticancer drugs. European Journal of Pharmaceutical Sciences. 11 (2000) 265-283.

Kwon, G., Naito, M., Kataoka, K., Yokoyama, M., Sakurai, Y., and Okano, T. Block copolymer micelles as vehicles for hydrophobic drugs. Colloids and Surfaces B: Biointerfaces. 2 (1994) 429-434.

Kwon, G., Naito, M., Yokoyama, M., Okano, T., Sakurai, Y., and Kataoka, K. Block copolymer micelles for drug delivery: loading and release of doxorubicin. Journal of Controlled Release. 48 (1997) 195-201.

Kwon, G., Suwa, S., Yokoyama, M., Okano, T., Sakurai, Y., and Kataoka, K. Enhanced tumor accumulation and prolonged circulation times of micelle-forming poly(ethylene oxide-asparate) block copolymer-adriamycin conjugates. Journal of Controlled Release. 29 (1994) 17-23.

Kwon, G.S., Naito, M., Yokoyama, M., Okano, T., Sakurai, Y., and Kataoka, K. Physical entrapment of adriamycin in AB block copolymer micelles. Pharmaceutical Research. 12

(1995) 192-195.

Laffont, C.M., Toutain, P.-L., Alvinerie, M., and Bousquet-Melou, A. Intestinal secretion is a major route for parent ivermectin elimination in the rat. Drug Metabolism and Disposition. 30 (2002) 626-630.

Lampen, A., Zhang, Y., Hackbarth, I., Benet, L.Z., Sewing, K.-F., and Christians, U. Metabolism and transport of the macrolide immunosuppressant sirolimus in the small intestine. Journal of Pharmacology and Experimental Therapeutics. 285 (1998) 1104-1112.

Lampidis, T.J., Castello, C., del Giglio, A., Pressman, B.C., Viallet, P., Trevorrow, K.W., Valet, G.K., Tapiero, H., and Savaraj, N. Relevance of the chemical charge of rhodamine dyes to multiple drug resistance. Biochemical Pharmacology. 38 (1989) 4267-4271.

Lampidis, T.J., Kolonias, D., Podona, T., Israel, M., Safa, A.R., Lothstein, L., Savaraj, N., Tapiero, H., and Priebe, W. Circumvention of P-GP MDR as a Function of Anthracycline Lipophilicity and Charge. Biochemistry. 36 (1997) 2679-2685.

Lande, M.B., Donovan, J.M., and Zeidel, M.L. The relationship between membrane fluidity and permeabilities to water, solutes, ammonia, and protons. Journal of General Physiology. 106 (1995) 67-84.

Lapierre, L.A. The molecular sturcture of the tight junction. Advanced Drug Delivery Reviews. 41 (2000) 255-264.

Larhed, A.W., Artursson, P., and Bjork, E. The influence of intestinal mucus components on the diffusion of drugs. Pharmaceutical Research. 15 (1998) 66-71.

Larhed, A.W., Artursson, P., Grsjoe, J., and Bjoerk, E. Diffusion of drugs in native and purified gastrointestinal mucus. Journal of Pharmaceutical Sciences. 86 (1997) 660-665.

Larrivee, B. and Averill, D.A. Modulation of adriamycin cytotoxicity and transport in drug-sensitive and multidrug-resistant Chinese hamster ovary cells by hyperthermia and cyclosporin A. Cancer Chemotherapy and Pharmacology. 45 (2000) 219-230.

Lavasanifar, A., Samuel, J., and Kwon, G.S. Poly(ethylene oxide)-block-poly(L-amino acid) micelles for drug delivery. Advanced Drug Delivery Reviews. 54 (2002) 169-190.

Lavie, Y., Fiucci, G., and Liscovitch, M. Up-regulation of caveolae and caveolar constituents in multidrug-resistant cancer cells. Journal of Biological Chemistry. 273 (1998) 32380-32383.

Lee, J., Cho, E.C., and Cho, K. Incorporation and release behavior of hydrophobic drug in functionalized poly(d,l-lactide)-block-poly(ethylene oxide) micelles. Journal of Controlled Release. 94 (2004) 323-335.

Lee, S.C., Kim, C., Kwon, I.C., Chung, H., and Jeong, S.Y. Polymeric micelles of poly(2-

ethyl-2-oxazoline)-block-poly(epsilon-caprolactone) copolymer as a carrier for paclitaxel. Journal of Controlled Release. 89 (2003) 437-446.

Leroux, J.C., Roux, E., Le Garrec, D., Hong, K., and Drummond, D.C. N-isopropylacrylamide copolymers for the preparation of pH-sensitive liposomes and polymeric micelles. Journal of Controlled Release. 72 (2001) 71-84.

Li, Y. and Kwon, G.S. Methotrexate esters of poly(ethylene oxide)-block-poly(2-hydroxyethyl-L-aspartamide). Part I: Effects of the level of methotrexate conjugation on the stability of micelles and on drug release. Pharmaceutical Research. 17 (2000) 607-611.

Lieb, W.R. and Stein, W.D. Non-Stokesian nature of transverse diffusion within human red cell membranes. Journal of Membrane Biology. 92 (1986) 111-119.

Liggins, R.T. and Burt, H.M. Polyether-polyester diblock copolymers for the preparation of paclitaxel loaded polymeric micelle formulations. Advanced Drug Delivery Reviews. 54 (2002) 191-202.

Liggins, R.T., Hunter, W.L., and Burt, H.M. Solid-state characterization of paclitaxel. Journal of Pharmaceutical Sciences. 86 (1997) 1458-1463.

Litman, T., Zeuthen, T., Skovsgaard, T., and Stein, W.D. Competitive, non-competitive and cooperative interactions between substrates of P-glycoprotein as measured by its ATPase activity. Biochimica et Biophysica Acta. 1361 (1997) 169-176.

Liu, J., Xiao, Y., and Allen, C. Polymer-drug compatibility: A guide to the development of delivery systems for the anticancer agent, ellipticine. Journal of Pharmaceutical Sciences. 93 (2004) 132-143.

Liu, R. and Sharom, F.J. Site-directed fluorescence labeling of P-Glycoprotein on cysteine residues in the nucleotide binding domains. Biochemistry. 35 (1996) 11865-11873.

Lo, Y.L., Hsu, C.Y., and Huang, J.D. Comparison of effects of surfactants with other MDR reversing agents on intracellular uptake of epirubicin in Caco-2 cell line. Anticancer Research. 18 (1998) 3005-3009.

Lo, Y. Relationships between the hydrophilic-lipophilic balance values of pharmaceutical excipients and their multidrug resistance modulating effect in Caco-2 cells and rat intestines. Journal of Controlled Release. 90 (2003) 37-48.

Loo, T.W. and Clarke, D.M. Determining the structure and mechanism of the human multidrug resistance P-glycoprotein using cysteine-scanning mutagenesis and thiol-modification techniques. Biochimica et Biophysica Acta. 1461 (1999) 315-325.

Loo, T.W., Bartlett, M.C., and Clarke, D.M. Methanethiosulfonate derivatives of rhodamine and verapamil activate human P-glycoprotein at different sites. Journal of Biological Chemistry. 278 (2003a) 50136-50141.

Loo, T.W., Bartlett, M.C., and Clarke, D.M. Simultaneous binding of two different drugs in the binding pocket of the human multidrug resistance P-glycoprotein. Journal of Biological Chemistry. 278 (2003b) 39706-39710.

Loo, T.W., Bartlett, M.C., and Clarke, D.M. Substrate-induced ocnformational changes in the transmembrane segments of human P-glycoprotein. direct evidence for the substrate-induced fit mechanism for drug binding. Journal of Biological Chemistry. 278 (2003c) 13603-13606.

Loo, T.W., Bartlett, M.C., and Clarke, D.M. Disulfide cross-linking analysis shows that transmembrane segments 5 and 8 of human P-glycoprotein are close together on the cytoplasmic side of the membrane. Journal of Biological Chemistry. 279 (2004) 7692-7697.

Loo, T.W. and Clarke, D.M. The transmembrane domains of the human multidrug resistance P-glycoprotein are sufficient to mediate drug binding and trafficking to the cell surface. Journal of Biological Chemistry. 274 (1999) 24759-24765.

Loo, T.W. and Clarke, D.M. Defining the drug-binding site in the human multidrug resistance P-glycoprotein using a methanethiosulfonate analog of verapamil, MTS-verapamil. Journal of Biological Chemistry. 276 (2001a) 14972-14979.

Loo, T.W. and Clarke, D.M. Determining the dimensions of the drug-binding domain of human P-glycoprotein using thiol cross-linking compounds as molecular rulers. Journal of Biological Chemistry. 276 (2001b) 36877-36880.

Lopez, O., Cocera, M., and de la Maza, A. Influence of the level of ceramides on the permeability of stratum corneum lipid liposomes caused by a C14-alkyl betaine/sodium dodecyl sulfate mixture. Colloids and Surfaces, A: Physicochemical and Engineering Aspects. 157 (1999) 167-176.

Lu, P., Liu, R., and Sharom, F.J. Drug transport by reconstituted P-glycoprotein in proteoliposomes: effect of substrates and modulators, and dependence on bilayer phase state. European Journal of Biochemistry. 268 (2001) 1687-1697.

Luker, G.D., Pica, C.M., Kumar, A.S., Covey, D.F., and Piwnica-Worms, D. Effects of cholesterol and enantiomeric cholesterol on P-Glycoprotein localization and function in low-density membrane domains. Biochemistry. 39 (2000) 7651-7661.

Luo, L., Tam, J., Maysinger, D., and Eisenberg, A. Cellular internalization of poly(ethylene oxide)-b-poly(caprolactone) diblock copolymer micelles. Bioconjugate Chemistry. 13 (2002) 1259-1265.

Macheras, P., Reppas, C., and Dressman, J.B. Biopharmaceutics of orally administered drugs. Ellis Horwood Limited, Great Britain (1995) pp. 281.

Meerum Terwogt, J.M., Beijnen, J.H., ten Bokkel Huinink, W.W., Rosing, H., and Schellens, J.H. Co-administration of cyclosporin enables oral therapy with paclitaxel. Lancet. 352

(1998) 285.

Mellman, I. Endocytosis and molecular sorting. Annual Review of Cell and Developmental Biology. 12 (1996) 575-625.

Miller, D.W., Batrakova, E.V., and Kabanov, A.V. Inhibition of multidrug resistance-associated protein (MRP) functional activity with pluronic block copolymers. Pharmaceutical Research. 16 (1999) 396-401.

Miller, D.W., Batrakova, E.V., Waltner, T.O., Alakhov, V.Y.u., and Kabanov, A.V. Interactions of pluronic block copolymers with brain microvessel endothelial cells: evidence of two potential pathways for drug absorption. Bioconjugate Chemistry. 8 (1997) 649-657.

Morita, A., Siddiqui, B., Erickson, R.H., and Kim, Y.S. Glycoproteins and glycolipids of rat small intestinal microvillus and basolateral membranes. Digestive Diseases and Sciences. 34 (1989) 596-605.

Nagarajan, R. and Ganesh, K. Block copolymer self-assembly in selective solvents: spherical micelles with segregated cores. Journal of Chemical Physics. 90 (1989) 5843-5856.

Nagarajan, R. and Ganesh, K. Comparison of solubilization of hydrocarbons in (PEO-PPO) diblock versus (PEO-PPO-PEO) triblock copolymer micelles. Journal of Colloid and Interface Science. 184 (1996) 489-499.

Nerurkar, M.M., Burton, P.S., and Borchardt, R.T. The use of surfactants to enhance the permeability of peptides through Caco-2 cells by inhibition of an apically polarized efflux system. Pharmaceutical Research. 13 (1996) 528-534.

Nerurkar, M.M., Ho, N.F., Burton, P.S., Vidmar, T.J., and Borchardt, R.T. Mechanistic roles of neutral surfactants on concurrent polarized and passive membrane transport of a model peptide in Caco-2 cells. Journal of Pharmaceutical Sciences. 86 (1997) 813-821.

Neyfakh, A.A. Use of fluorescent dyes as molecular probes for the study of multidrug resistance. Experimental Cell Research. 174 (1988) 168-176.

Nishiyama, N., Okazaki, S., Cabral, H., Miyamoto, M., Kato, Y., Sugiyama, Y., Nishio, K., Matsumura, Y., and Kataoka, K. Novel cisplatin-incorporated polymeric micelles can eradicate solid tumors in mice. Cancer Research. 63 (2003) 8977-8983.

Nonaka, K., Kazama, S., Goto, A., Fukuda, H., Yoshioka, H., and Yoshioka, H. Spin probe study on the interaction of chitosan-derived polymer surfactants with lipid membrane. Journal of Colloid and Interface Science. 246 (2002) 288-295.

Oh, D.M. and Amidon, G.L. Overview of membrane transport. Pharmaceutical Biotechnology. 12 (1999) 1-27.

Oh, D.M., Han, H.K., and Amidon, G.L. Drug transport and targeting. Intestinal transport.

Pharmaceutical Biotechnology. 12 (1999) 59-88.

Olson, A.L. and Pessin, J.E. Structure, function, and regulation of the mammalian facilitative glucose transporter gene family. Annual Review of Nutrition. 16 (1996) 235-256.

Paradis, R., Noel, C., and Page, M. Use of Pluronic micelles to overcome multidrug resistance. International Journal of Oncology. 5 (1994) 1305-1308.

Pauli-Magnus, C., Von Richter, O., Burk, O., Ziegler, A., Mettang, T., Eichelbaum, M., and Fromm, M.F. Characterization of the major metabolites of verapamil as substrates and inhibitors of P-glycoprotein. Journal of Pharmacology and Experimental Therapeutics. 293 (2000) 376-382.

Petrova, Ts., Manolova, N., Rashkov, I., Li, S., and Vert, M. Synthesis and characterization of poly(oxyethylene)-poly(caprolactone) multiblock copolymers. Polymer International. 45 (1998) 419-426.

Pinto, M., Robine-Leon, S., Appay, M., Kedinger, M., Triadou, N., Dussaulx, E., Lacroix, B., Simon-Assmann, P., Haffen, K., Fogh, J., and Zweibaum, A. Enterocyte-like differentiation and polarization of the human colon carcinoma cell line caco-2 in culture. Biologie Cellulaire. 47 (1983) 323-330.

Polli, J.W., Jarrett, J.L., Studenberg, S.D., Humphreys, J.E., Dennis, S.W., Brouwer, K.R., and Woolley, J.L. Role of p-glycoprotein on the CNS disposition of amprenavir (141W94), an HIV protease inhibitor. Pharmaceutical Research. 16 (1999) 1206-1212.

Polli, J.W., Wring, S.A., Humphreys, J.E., Huang, L., Morgan, J.B., Webster, L.O., and Serabjit-Singh, C.S. Rational use of in vitro P-glycoprotein assays in drug discovery. Journal of Pharmacology and Experimental Therapeutics. 299 (2001) 620-628.

Qu, Q., Russell, P.L., and Sharom, F.J. Stoichiometry and affinity of nucleotide binding to P-Glycoprotein during the catalytic cycle. Biochemistry. 42 (2003) 1170-1177.

Rao, V.V., Dahlheimer, J.L., Bardgett, M.E., Snyder, A.Z., Finch, R.A., Sartorelli, A.C., and Piwnica-Worms, D. Choroid plexus epithelial expression of MDR1 P-glycoprotein and multidrug resistance-associated protein contribute to the blood-cerebrospinal-fluid drug-permeability barrier. Proceedings of the National Academy of Sciences of the United States of America. 96 (1999) 3900-3905.

Rapoport, N., Marin, A.P., and Timoshin, A.A. Effect of a polymeric surfactant on electron transport in HL-60 cells. Archives of Biochemistry and Biophysics. 384 (2000) 100-108.

Raub, T.J., Barsuhn, C.L., Williams, L.R., Decker, D.E., Sawada, G.A., and Ho, N.F. Use of a biophysical-kinetic model to understand the roles of protein binding and membrane partitioning on passive diffusion of highly lipophilic molecules across cellular barriers. Journal of Drug Targeting. 1 (1993) 269-286.

Raviv, Y., Pollard, H.B., Bruggemann, E.P., Pastan, I., and Gottesman, M.M. Photosensitized

labeling of a functional multidrug transporter in living drug-resistant tumor cells. Journal of Biological Chemistry. 265 (1990) 3975-3980.

Rege, B.D., Kao, J.P.Y., and Polli, J.E. Effects of nonionic surfactants on membrane transporters in Caco-2 cell monolayers. European Journal of Pharmaceutical Sciences. 16 (2002) 237-246.

Regev, R., Assaraf, Y.G., and Eytan, G.D. Membrane fluidization by ether, other anesthetics, and certain agents abolishes P-glycoprotein ATPase activity and modulates efflux from multidrug-resistant cells. European Journal of Biochemistry. 259 (1999) 18-24.

Riou, M., Guegnard, F., Le Vern, Y., and Kerboeuf, D. Modulation of the multidrug resistance (MDR) system in the nematode Haemonchus contortus by changing cholesterol content: effects on resistance to anthelmintics. Journal of Antimicrobial Chemotherapy. 52 (2003) 180-187.

Robert, J. and Jarry, C. Multidrug resistance reversal agents. Journal of Medicinal Chemistry. 46 (2003) 4805-4817.

Romsicki, Y. and Sharom, F.J. The membrane lipid environment modulates drug interactions with the P-glycoprotein multidrug transporter. Biochemistry. 38 (1999) 6887-6896.

Romsicki, Y. and Sharom, F.J. Phospholipid flippase activity of the reconstituted P-glycoprotein multidrug transporter. Biochemistry. 40 (2001) 6937-6947.

Rosenberg, M.F., Velarde, G., Ford, R.C., Martin, C., Berridge, G., Kerr, I.D., Callaghan, R., Schmidlin, A., Wooding, C., Linton, K.J., and Higgins, C.F. Repacking of the transmembrane domains of P-glycoprotein during the transport ATPase cycle. EMBO Journal. 20 (2001) 5615-5625.

Rothnie, A., Theron, D., Soceneantu, L., Martin, C., Traikia, M., Berridge, G., Higgins, C.F., Devaux, P.F., and Callaghan, R. The importance of cholesterol in maintenance of P-glycoprotein activity and its membrane perturbing influence. European Biophysics Journal. 30 (2001) 430-442.

Saengkhae, C., Loetchutinat, C., and Garnier-Suillerot, A. Kinetic analysis of rhodamines efflux mediated by the multidrug resistance protein (MRP1). Biophysical Journal. 85 (2003) 2006-2014.

Sakai, M., Imai, T., Ohtake, H., and Otagiri, M. Cytotoxicity of absorption enhancers in Caco-2 cell monolayers. Journal of Pharmacy and Pharmacology. 50 (1998) 1101-1108.

Sarver, J.G., Klis, W.A., Byers, J.P., and Erhardt, P.W. Microplate screening of the differential effects of test agents on Hoechst 33342, rhodamine 123, and rhodamine 6G accumulation in breast cancer cells that overexpress P-glycoprotein. Journal of Biomolecular Screening. 7 (2002) 29-34.

Sauna, Z.E. and Ambudkar, S.V. Evidence for a requirement for ATP hydrolysis at two

distinct steps during a single turnover of the catalytic cycle of human P-glycoprotein. Proceedings of the National Academy of Sciences of the United States of America. 97 (2000) 2515-2520.

Sauna, Z.E. and Ambudkar, S.V. Characterization of the catalytic cycle of ATP hydrolysis by human P-glycoprotein. The two ATP hydrolysis events in a single catalytic cycle are kinetically similar but affect different functional outcomes. Journal of Biological Chemistry. 276 (2001) 11653-11661.

Savolainen, J., Edwards, J.E., Morgan, M.E., McNamara, P.J., and Anderson, B.D. Effects of a P-glycoprotein inhibitor on brain and plasma concentrations of anti-human immunodeficiency virus drugs administered in combination in rats. Drug Metabolism and Disposition. 30 (2002) 479-482.

Sawada, G.A., Ho, N.F.H., Williams, L.R., Barsuhn, C.L., and Raub, T.J. Transcellular permeability of chlorpromazine demonstrating the roles of protein binding and membrane partitioning. Pharmaceutical Research. 11 (1994) 665-673.

Scala, S., Akhmed, N., Rao, U.S., Paull, K., Lan, L.-B., Dickstein, B., Lee, J.-S., Elgemeie, G.H., Stein, W.D., and Bates, S.E. P-glycoprotein substrates and antagonists cluster into two distinct groups. Molecular Pharmacology. 51 (1997) 1024-1033.

Schinkel, A.H. and Jonker, J.W. Mammalian drug efflux transporters of the ATP binding cassette (ABC) family: an overview. Advanced Drug Delivery Reviews. 55 (2003) 3-29.

Schinkel, A.H., Kemp, S., Dolle, M., Rudenko, G., and Wagenaar, E. N-Glycosylation and deletion mutants of the human MDR1 P-glycoprotein. Journal of Biological Chemistry. 268 (1993) 7474-7481.

Schmiedlin-Ren, P., Thummel, K.E., Fisher, J.M., Paine, M.F., Lown, K.S., and Watkins, P.B. Expression of enzymically active CYP3A4 by Caco-2 cells grown on extracellular matrix-coated permeable supports in the presence of 1-alpha,25-dihydroxyvitamin D3. Molecular Pharmacology. 51 (1997) 741-754.

Schuurhuis, G.J., Broxterman, H.J., Pinedo, H.M., van Heijningen, T.H., van Kalken, C.K., Vermorken, J.B., Spoelstra, E.C., and Lankelma, J. The polyoxyethylene castor oil Cremophor EL modifies multidrug resistance. British Journal of Cancer. 62 (1990) 591-594.

See, Y.P., Carlsen, S.A., Till, J.E., and Ling, V. Increased drug permeability in Chinese hamster ovary cells in the presence of cyanide. Biochimica et Biophysica Acta. 373 (1974) 242-252.

Seelig, A. and Landwojtowicz, E. Structure-activity relationship of P-glycoprotein substrates and modifiers. European Journal of Pharmaceutical Sciences. 12 (2000) 31-40.

Seelig, A. A general pattern for substrate recognition by P-glycoprotein. European Journal of Biochemistry. 251 (1998) 252-261.

Segal, M.B. The choroid plexuses and the barriers between the blood and the cerebrospinal fluid. Cellular and Molecular Neurobiology. 20 (2000) 183-196.

Sehested, M., Skovsgaard, T., Jensen, P.B., Demant, E.J.F., Friche, E., and Bindslev, N. Transport of the multidrug resistance modulators verapamil and azidopine in wild type and daunorubicin resistant Ehrlich ascites tumor cells. British Journal of Cancer. 62 (1990) 37-41.

Severcan, F., Kazanci, N., and Zorlu, F. Tamoxifen increases membrane fluidity at high concentrations. Bioscience reports. 20 (2000) 177-184.

Seydel, J.K. Function, composition, and organization of membranes. Methods and Principles in Medicinal Chemistry. 15 (2002) 2-33.

Shapiro, A.B., Corder, A.B., and Ling, V. P-glycoprotein-mediated Hoechst 33342 transport out of the lipid bilayer. European Journal of Biochemistry. 250 (1997) 115-121.

Shapiro, A.B. and Ling, V. Positively cooperative sites for drug transport by P-glycoprotein with distinct drug specificities. European Journal of Biochemistry. 250 (1997) 130-137.

Shapiro, A.B. and Ling, V. The mechanism of ATP-dependent multidrug transport by P-glycoprotein. Acta Physiologica Scandinavica, Supplementum. 163 (1998) 227-234.

Shargel, L. and Yu, A.B.C. Applied Biopharmaceutics and Pharmacokinetics. 3rd ed. Appleton and Lange, Connecticut (1993) pp. 625.

Sharom, F.J. The P-glycoprotein efflux pump: how does it transport drugs? Journal of Membrane Biology. 160 (1997a) 161-175.

Sharom, F.J. The P-glycoprotein multidrug transporter: interactions with membrane lipids, and their modulation of activity. Biochemical Society Transactions. 25 (1997b) 1088-1096.

Sharom, F.J., Yu, X., Chu, J.W., and Doige, C.A. Characterization of the ATPase activity of P-glycoprotein from multidrug-resistant Chinese hamster ovary cells. Biochemical Journal. 308 (1995) 381-390.

Shepard, R.L., Winter, M.A., Hsaio, S.C., Pearce, H.L., Beck, W.T., and Dantzig, A.H. Effect of modulators on the ATPase activity and vanadate nucleotide trapping of human P-glycoprotein. Biochemical Pharmacology. 56 (1998) 719-727.

Sheppard, D.N. and Welsh, M.J. Structure and function of the CFTR chloride channel. Physiological Reviews. 79 (1999) S23-S45.

Shiau, Y.F., Fernandez, P., Jackson, M.J., and McMonagle, S. Mechanisms maintaining a low-pH microclimate in the intestine. American journal of physiology. 248 (1985) G608-617.

Shin, I.G., Kim, S.Y., Lee, Y.M., Cho, C.S., and Sung, Y.K. Methoxy poly(ethylene glycol)/epsilon-caprolactone amphiphilic block copolymeric micelle containing indomethacin. I. Preparation and characterization. Journal of Controlled Release. 51 (1998) 1-11.

Shono, Y., Nishihara, H., Matsuda, Y., Furukawa, S., Okada, N., Fujita, T., and Yamamoto, A. Modulation of intestinal P-glycoprotein function by Cremophor EL and other surfactants by an in vitro diffusion chamber method using the isolated rat intestinal membranes. Journal of Pharmaceutical Sciences. 93 (2004) 877-885.

Sikic, B.I. Pharmacologic approaches to reversing multidrug resistance. Seminars in Hematology. 34 (1997) 40-47.

Singer, S.J. and Nicolson, G.L. Fluid mosaic model of the structure of cell membranes. Science. 175 (1972) 720-731.

Sinicrope, F.A., Dudeja, P.K., Bissonnette, B.M., Safa, A.R., and Brasitus, T.A. Modulation of P-glycoprotein-mediated drug transport by alterations in lipid fluidity of rat liver canalicular membrane vesicles. Journal of Biological Chemistry. 267 (1992) 24995-25002.

Song, D., Wientjes, M.G., and Au, J.L.S. Bladder tissue pharmacokinetics of intravesical taxol. Cancer Chemotherapy and Pharmacology. 40 (1997) 285-292.

Soo, P.L., Luo, L., Maysinger, D., and Eisenberg, A. Incorporation and release of hydrophobic probes in biocompatible polycaprolactone-block-poly(ethylene oxide) micelles: Implications for drug delivery. Langmuir. 18 (2002) 9996-10004.

Sparreboom, A., van Asperen, J., Mayer, U., Schinkel, A.H., Smit, J.W., Meijer, D.K., Borst, P., Nooijen, W.J., Beijnen, J.H., and van Tellingen, O. Limited oral bioavailability and active epithelial excretion of paclitaxel (Taxol) caused by P-glycoprotein in the intestine. Proceedings of the National Academy of Sciences of the United States of America. 94 (1997) 2031-2035.

Steffansen, B., Nielsen, C.U., Brodin, B., Eriksson, A.H., Andersen, R., and Frokjaer, S. Intestinal solute carriers: an overview of trends and strategies for improving oral drug absorption. European Journal of Pharmaceutical Sciences. 21 (2004) 3-16.

Stein, W.D. Transport and Diffusion Across Cell Membranes. Academic Press Inc., London (1986) pp. 685.

Storey, R.F. and Sherman, J.W. Kinetics and mechanism of the stannous octoate-catalyzed bulk polymerization of epsilon-caprolactone. Macromolecules. 35 (2002) 1504-1512.

Sugiyama, Y., Kusuhara, H., and Suzuki, H. Kinetic and biochemical analysis of carrier-mediated efflux of drugs through the blood-brain and blood-cerebrospinal fluid barriers: importance in the drug delivery to the brain. Journal of Controlled Release. 62 (1999) 179-186.

Sun, H., Dai, H., Shaik, N., and Elmquist, W.F. Drug efflux transporters in the CNS. Advanced Drug Delivery Reviews. 55 (2003) 83-105.

Suzuki, T., Matsuzaki, T., and Takata, K. Polarized distribution of Na+-dependent glucose cotransporter SGLT1 in epithelial cells. Acta Histochemica et Cytochemica. 33 (2000) 159-162.

Swenson, E.S. and Curatolo, W.J. Means to enhance penetration. 2. Intestinal permeability enhancement for proteins, peptides and other polar drugs: mechanisms and potential toxicity. Advanced Drug Delivery Reviews. 8 (1992) 39-92.

Swenson, E.S., Milisen, W.B., and Curatolo, W. Intestinal permeability enhancement: efficacy, acute local toxicity, and reversibility. Pharmaceutical Research. 11 (1994a) 1132-1142.

Swenson, E.S., Milisen, W.B., and Curatolo, W. Intestinal permeability enhancement: structure-activity and structure-toxicity relationships for nonylphenoxypolyoxyethylene surfactant permeability enhancers. Pharmaceutical Research. 11 (1994b) 1501-1504.

Synold, T.W., Dussault, I., and Forman, B.M. The orphan nuclear receptor SXR coordinately regulates drug metabolism and efflux. Nature Medicine. 7 (2001) 584-590.

Taipalensuu, J., Tornblom, H., Lindberg, G., Einarsson, C., Sjoqvist, F., Melhus, H., Garberg, P., Sjostrom, B., Lundgren, B., and Artursson, P. Correlation of gene expression of ten drug efflux proteins of the ATP-binding cassette transporter family in normal human jejunum and in human intestinal epithelial Caco-2 cell monolayers. Journal of Pharmacology and Experimental Therapeutics. 299 (2001) 164-170.

Thiebaut, F., Tsuruo, T., Hamada, H., Gottesman, M.M., Pastan, I., and Willingham, M.C. Immunohistochemical localization in normal tissues of different epitopes in the multidrug transport protein P170: evidence for localization in brain capillaries and crossreactivity of one antibody with a muscle protein. Journal of Histochemistry and Cytochemistry. 37 (1989) 159-164.

Thiebaut, F., Tsuruo, T., Hamada, H., Gottesman, M.M., Pastan, I., and Willingham, M.C. Cellular localization of the multidrug-resistance gene product P-glycoprotein in normal human tissues. Proceedings of the National Academy of Sciences of the United States of America. 84 (1987) 7735-7738.

Thomson, A.B.R. and Wild, G. The influence of the intestinal unstirred water layers on the understanding of the mechanisms of lipid absorption. Intestinal Lipid Metabolism. (2001) 135-152.

Thummel, K.E., Kunze, K.L., and Shen, D.D. Enzyme-catalyzed processes of first-pass hepatic and intestinal drug extraction. Advanced Drug Delivery Reviews. 27 (1997) 99-127.

Thummel, K.E., O'Shea, D., Paine, M.F., Shen, D.D., Kunze, K.L., Perkins, J.D., and

Wilkinson, G.R. Oral first-pass elimination of midazolam involves both gastrointestinal and hepatic CYP3A-mediated metabolism. Clinical Pharmacology and Therapeutics. 59 (1996) 491-502.

Tomonaga, M., Oka, M., Narasaki, F., Fukuda, M., Nakano, R., Takatani, H., Ikeda, K., Terashi, K., Matsuo, I., Soda, H., Cowan, K.H., and Kohno, S. The multidrug resistance-associated protein gene confers drug resistance in human gastric and colon cancers. Japanese Journal of Cancer Research. 87 (1996) 1263-1270.

Torchilin, V.P. Structure and design of polymeric surfactant-based drug delivery systems. Journal of Controlled Release. 73 (2001) 137-172.

Troost, J., Albermann, N., Emil Haefeli, W., and Weiss, J. Cholesterol modulates P-glycoprotein activity in human peripheral blood mononuclear cells. Biochemical and Biophysical Research Communications. 316 (2004) 705-711.

Troutman, M.D. and Thakker, D.R. Novel experimental parameters to quantify the modulation of absorptive and secretory transport of compounds by P-glycoprotein in cell culture models of intestinal epithelium. Pharmaceutical Research. 20 (2003a) 1210-1224.

Troutman, M.D. and Thakker, D.R. Rhodamine 123 requires carrier-mediated influx for its activity as a P-glycoprotein substrate in caco-2 cells. Pharmaceutical Research. 20 (2003b) 1192-1199.

Tsuji, A. and Tamai, I. Carrier-mediated intestinal transport of drugs. Pharmaceutical Research. 13 (1996) 963-977.

Twentyman, P.R., Rhodes, T., and Rayner, S. A comparison of rhodamine 123 accumulation and efflux in cells with P-glycoprotein-mediated and MRP-associated multidrug resistance phenotypes. European Journal of Cancer. 30A (1994) 1360-1369.

Van Asperen, J., van Tellingen, O., Sparreboom, A., Schinkel, A.H., Borst, P., Nooijen, W.J., and Beijnen, J.H. Enhanced oral bioavailability of paclitaxel in mice treated with the P-glycoprotein blocker SDZ PSC 833. British Journal of Cancer. 76 (1997) 1181-1183.

Van Asperen, J., van Tellingen, O., van der Valk, M.A., Rozenhart, M., and Beijnen, J.H. Enhanced oral absorption and decreased elimination of paclitaxel in mice cotreated with cyclosporin A. Clinical Cancer Research. 4 (1998) 2293-2297.

Van Asperen, J., Van Tellingen, O., and Beijnen, J.H. The role of mdr1a P-glycoprotein in the biliary and intestinal secretion of doxorubicin and vinblastine in mice. Drug Metabolism and Disposition. 28 (2000) 264-267.

van der Sandt, I.C.J., Blom-Roosemalen, M.C.M., de Boer, A.G., and Breimer, D.D. Specificity of doxorubicin versus rhodamine-123 in assessing P-glycoprotein functionality in the LLC-PK1, LLC-PK1:MDR1 and Caco-2 cell lines. European Journal of Pharmaceutical Sciences. 11 (2000) 207-214.

Vinardell, M.P. and Infante, M.R. The relationship between the chain length of non-ionic surfactants and their hemolytic action on human erythrocytes. Comparative Biochemistry and Physiology. Part C, Pharmacology, Toxicology and Endocrinology. 124 (1999) 117-20.

Wacher, V.J., Salphati, L., and Benet, L.Z. Active secretion and enterocytic drug metabolism barriers to drug absorption. Advanced Drug Delivery Reviews. 46 (2001) 89-102.

Wacher, V.J., Wu, C.-Y., and Benet, L.Z. Overlapping substrate specificities and tissue distribution of cytochrome P450 3A and P-glycoprotein: implications for drug delivery and activity in cancer chemotherapy. Molecular Carcinogenesis. 13 (1995) 129-134.

Ward, P.D., Tippin, T.K., and Thakker, D.R. Enhancing paracellular permeability by modulating epithelial tight junctions. Pharmaceutical Science and Technolology Today. 3 (2000) 346-358.

Washington, N., Washington, C., and Wilson, C. Physiological pharmaceutics: Barriers to drug absorption. 2nd ed. Taylor and Francis, London (2001) pp. 312.

Watkins, P.B. The barrier function of CYP3A4 and P-glycoprotein in the small bowel. Advanced Drug Delivery Reviews. 27 (1997) 161-170.

Werner, U., Kissel, T., and Reers, M. Effects of permeation enhancers on the transport of a peptidomimetic thrombin inhibitor (CRC 220) in a human intestinal cell line (Caco-2). Pharmaceutical Research. 13 (1996) 1219-1227.

Wijnholds, J., De Lange, E.C.M., Scheffer, G.L., Van den Berg, D.-J., Mol, C.A.A.M., Van der Valk, M., Schinkel, A.H., Scheper, R.J., Breimer, D.D., and Borst, P. Multidrug resistance protein 1 protects the choroid plexus epithelium and contributes to the blood-cerebrospinal fluid barrier. Journal of Clinical Investigation. 105 (2000) 279-285.

Wijnholds, J., Scheffer, G.L., Van der Valk, M., Van der Valk, P., Beijnen, J.H., Scheper, R.J., and Borst, P. Multidrug resistance protein 1 protects the oropharyngeal mucosal layer and the testicular tubules against drug-induced damage. Journal of Experimental Medicine. 188 (1998) 797-808.

Woodcock, D.M., Jefferson, S., Linsenmeyer, M.E., Crowther, P.J., Chojnowski, G.M., Williams, B., and Bertoncello, I. Reversal of the multidrug resistance phenotype with cremophor EL, a common vehicle for water-insoluble vitamins and drugs. Cancer Research. 50 (1990) 4199-4203.

Woodcock, D.M., Linsenmeyer, M.E., Chojnowski, G., Kriegler, A.B., Nink, V., Webster, L.K., and Sawyer, W.H. Reversal of multidrug resistance by surfactants. British Journal of Cancer. 66 (1992) 62-68.

Wu, C.-Y., Benet, L.Z., Hebert, M.F., Gupta, S.K., Rowland, M., Gomez, D.Y., and Wacher, V.J. Differentiation of absorption and first-pass gut and hepatic metabolism in humans: studies with cyclosporine. Clinical Pharmacology and Therapeutics. 58 (1995) 492-497.

Xia, W.J. and Onyuksel, H. Mechanistic studies on surfactant-induced membrane permeability enhancement. Pharmaceutical Research. 17 (2000) 612-618.

Xiang, T.X. and Anderson, B.D. Phospholipid surface density determines the partitioning and permeability of acetic acid in DMPC:cholesterol bilayers. Journal of Membrane Biology. 148 (1995) 157-167.

Xiang, T.X. and Anderson, B.D. Permeability of acetic acid across gel and liquid-crystalline lipid bilayers conforms to free-surface-area theory. Biophysical Journal. 72 (1997) 223-237.

Xiang, T.X. and Anderson, B.D. Influence of chain ordering on the selectivity of dipalmitoylphosphatidylcholine bilayer membranes for permeant size and shape. Biophysical Journal. 75 (1998) 2658-2671.

Yamaguchi, H., Yano, I., Saito, H., and Inui, K.-I. Pharmacokinetic role of P-glycoprotein in oral bioavailability and intestinal secretion of grepafloxacin in vivo. Journal of Pharmacology and Experimental Therapeutics. 300 (2002) 1063-1069.

Yamazaki, T., Sato, Y., Hanai, M., Mochimaru, J., Tsujino, I., Sawada, U., and Horie, T. Non-ionic detergent Tween 80 modulates VP-16 resistance in classical multidrug resistant K562 cells via enhancement of VP-16 influx. Cancer Letters. 149 (2000) 153-161.

Yang, C.Y., Dantzig, A.H., and Pidgeon, C. Intestinal peptide transport systems and oral drug availability. Pharmaceutical Research. 16 (1999) 1331-1343.

Yao, S.Y.M., Ng, A.M.L., Sundaram, M., Cass, C.E., Baldwin, S.A., and Young, J.D. Transport of antiviral 3'-deoxy-nucleoside drugs by recombinant human and rat equilibrative, nitrobenzylthioinosine (NBMPR)-insensitive (ENT2) nucleoside transporter proteins produced in Xenopus oocytes. Molecular Membrane Biology. 18 (2001) 161-167.

Yokoyama, M. Block copolymers as drug carriers. Critical Reviews in Therapeutic Drug Carrier Systems. 9 (1992) 213-248.

Yokoyama, M., Fukushima, S., Uehara, R., Okamoto, K., Kataoka, K., Sakurai, Y., and Okano, T. Characterization of physical entrapment and chemical conjugation of adriamycin in polymeric micelles and their design for in vivo delivery to a solid tumor. Journal of Controlled Release. 50 (1998a) 79-92.

Yokoyama, M., Satoh, A., Sakurai, Y., Okano, T., Matsumura, Y., Kakizoe, T., and Kataoka, K. Incorporation of water-insoluble anticancer drug into polymeric micelles and control of their particle size. Journal of Controlled Release. 55 (1998b) 219-29.

Yoo, H.S. and Park, T.G. Biodegradable polymeric micelles composed of doxorubicin conjugated PLGA-PEG block copolymer. Journal of Controlled Release. 70 (2001) 63-70.

Yu, B.G., Okano, T., Kataoka, K., and Kwon, G. Polymeric micelles for drug delivery: solubilization and haemolytic activity of amphotericin B. Journal of Controlled Release.

53 (1998) 131-136.

Yu, H., Cook, T.J., and Sinko, P.J. Evidence for diminished functional expression of intestinal transporters in Caco-2 cell monolayers at high passages. Pharmaceutical Research. 14 (1997) 757-762.

Yu, L., Bridgers, A., Polli, J., Vickers, A., Long, S., Roy, A., Winnike, R., and Coffin, M. Vitamin E-TPGS increases absorption flux of an HIV protease inhibitor by enhancing its solubility and permeability. Pharmaceutical Research. 16 (1999) 1812-1817.

Yu, Y. and Eisenberg, A. Synthesis of biodegradable and biocompatible amphiphilic ethylene oxide/epsilon-caprolactone block copolymer by sequential anionic ring-opening polymerization. Polymeric Materials Science and Engineering. 79 (1998) 288-289.

Yuan, M., Wang, Y., Li, X., Xiong, C., and Deng, X. Polymerization of lactides and lactones. 10. Synthesis, characterization, and application of amino-terminated poly(ethylene glycol)-co-poly(epsilon-caprolactone) block copolymer. Macromolecules. 33 (2000) 1613-1617.

Zacherl, J., Hamilton, G., Thalhammer, T., Riegler, M., Cosentini, E.P., Ellinger, A., Bischof, G., Schweitzer, M., Teleky, B., and Koperna, T. Inhibition of P-glycoprotein-mediated vinblastine transport across HCT-8 intestinal carcinoma monolayers by verapamil, cyclosporine A and SDZ PSC 833 in dependence on extracellular pH. Cancer Chemotherapy and Pharmacology. 34 (1994) 125-132.

Zaman, G.J.R., Lankelma, J., van Tellingen, O., Beijnen, J., Dekker, H., Paulusma, C., Elferink, R.P.J.O., Baas, F., and Borst, P. Role of glutathione in the export of compounds from cells by the multidrug-resistance-associated protein. Proceedings of the National Academy of Sciences of the United States of America. 92 (1995) 7690-7694.

Zelphati, O. and Szoka, F.C. Jr. Intracellular distribution and mechanism of delivery of oligonucleotides mediated by cationic lipids. Pharmaceutical Research. 13 (1996) 1367-1372.

Zhang, X., Jackson, J.K., and Burt, H.M. Determination of surfactant critical micelle concentration by a novel fluorescence depolarization technique. Journal of Biochemical and Biophysical Methods. 31 (1996a) 145-150.

Zhang, X., Jackson, J.K., and Burt, H.M. Development of amphiphilic diblock copolymers as micellar carriers of taxol. International Journal of Pharmaceutics. 132 (1996b) 195-206.

Zheng, Y., Qiu, Y., Lu, M.F., Hoffman, D., and Reiland, T.L. Permeability and absorption of leuprolide from various intestinal regions in rabbits and rats. International Journal of Pharmaceutics. 185 (1999) 83-92.

Zhou, S., Deng, X., and Yang, H. Biodegradable poly(epsilon-caprolactone)-poly(ethylene glycol) block copolymers: characterization and their use as drug carriers for a controlled delivery system. Biomaterials. 24 (2003) 3563-3570.

Zhu, Z., Xiong, C., Zhang, L., and Deng, X. Synthesis and characterization of poly(epsilon-caprolactone)-poly(ethylene glycol) block copolymer. Journal of Polymer Science, Part A: Polymer Chemistry. 35 (1997) 709-714.